ALEX(01)-TR-77-02

12 B.S.

CONTINUATION OF THE SEISMIC RESEARCH OBSERVATORIES EVALUATION

TECHNICAL REPORT NO.2

VELA NETWORK EVALUATION AND AUTOMATIC PROCESSING RESEARCH

Prepared by
Alan C. Strauss and Leonard C. Weltman

TEXAS INSTRUMENTS INCORPORATED
Equipment Group
Post Office Box 6015
Dallas, Texas 75222

Prepared for

AIR FORCE TECHNICAL APPLICATIONS CENTER
Alexandria, Virginia 22314

Sponsored by

ADVANCED RESEARCH PROJECTS AGENCY
Nuclear Monitoring Research Office
ARPA Program Code No. 7F10
ARPA Order No. 2551

16 November 1977

Acknowledgment: This research was supported by the Advanced Research Projects Agency, Nuclear Monitoring Research Office, under Project VELA-UNIFORM, and accomplished under the technical direction of the Air Force Technical Applications Center under Contract Number F08606-77-C-0004.

APPROVED FOR PUBLIC RELEASE, DISTRIBUTION UNLIMITED

(14) TI-ALEX(01)-TR-77-02

(12)

(6) CONTINUATION OF THE SEISMIC RESEARCH OBSERVATORIES EVALUATION

(9) TECHNICAL REPORT NO.2

VELA NETWORK EVALUATION AND AUTOMATIC PROCESSING RESEARCH

Prepared by

(10) Alan C. Strauss and Leonard C. Weltman

TEXAS INSTRUMENTS INCORPORATED
Equipment Group
Post Office Box 6015
Dallas, Texas 75222

(15) F08606-77-C-0004,
ARPA Order-2551

Prepared for

AIR FORCE TECHNICAL APPLICATIONS CENTER
Alexandria, Virginia 22314

Sponsored by

ADVANCED RESEARCH PROJECTS AGENCY
Nuclear Monitoring Research Office
ARPA Program Code No. 7F10
ARPA Order No. 2551

(11) 16 November 1977 (12) 284p

Acknowledgment: This research was supported by the Advanced Research Projects Agency, Nuclear Monitoring Research Office, under Project VELA-UNIFORM, and accomplished under the technical direction of the Air Force Technical Applications Center under Contract Number F08606-77-C-0004.

405 076 JOB

UNCLASSIFIED

SECURITY CLASSIFICATION OF THIS PAGE (When Data Entered)

REPORT DOCUMENTATION PAGE		READ INSTRUCTIONS BEFORE COMPLETING FORM
1. REPORT NUMBER	2. GOVT ACCESSION NO.	3. RECIPIENT'S CATALOG NUMBER
4. TITLE (and Subtitle) CONTINUATION OF THE SEISMIC RESEARCH OBSERVATORIES EVALUATION		5. TYPE OF REPORT & PERIOD COVERED Technical 6. PERFORMING ORG. REPORT NUMBER ALEX(01)-TR-77-02
7. AUTHOR(s) Alan C. Strauss and Leonard C. Weltman		8. CONTRACT OR GRANT NUMBER(s) F08606-77-C-0004
9. PERFORMING ORGANIZATION NAME AND ADDRESS Texas Instruments Incorporated Equipment Group Dallas, Texas 75222		10. PROGRAM ELEMENT, PROJECT, TASK AREA & WORK UNIT NUMBERS VELA T/7705/B/ETR
11. CONTROLLING OFFICE NAME AND ADDRESS Advanced Research Projects Agency 1400 Wilson Boulevard Arlington, Virginia 22209		12. REPORT DATE 16 November 1977 13. NUMBER OF PAGES 282
14. MONITORING AGENCY NAME & ADDRESS (if different from Controlling Office) Air Force Technical Applications Center VELA Seismological Center Alexandria, Virginia 22314		15. SECURITY CLASS. (of this report) UNCLASSIFIED 15a. DECLASSIFICATION/DOWNGRADING SCHEDULE

16. DISTRIBUTION STATEMENT (of this Report)

APPROVED FOR PUBLIC RELEASE, DISTRIBUTION UNLIMITED

17. DISTRIBUTION STATEMENT (of the abstract entered in Block 20, if different from Report)

18. SUPPLEMENTARY NOTES

ARPA Order No. 2551

19. KEY WORDS (Continue on reverse side if necessary and identify by block number)

20. ABSTRACT (Continue on reverse side if necessary and identify by block number)

This report presents the results of a continued evaluation of the Seismic Research Observatory stations performed by Texas Instruments Incorporated at the Seismic Data Analysis Center in Alexandria, Virginia. During the time period this evaluation was carried out, data were available from six stations - Albuquerque, New Mexico (ANMO); Guam, Marianas Islands (GUMO); Mashhad, Iran (MAIO); Narrogin, Western Australia (NWAO); Taipei, Taiwan (TATO); and Wellington (South Karori), New Zealand (SNZO).

Next page

DD FORM 1 JAN 73 1473 EDITION OF 1 NOV 65 IS OBSOLETE

UNCLASSIFIED

SECURITY CLASSIFICATION OF THIS PAGE (When Data Entered)

20. Abstract (continued)

cont.

The major areas of investigation in the evaluation were:

- (1) Analysis of RMS noise levels, RMS noise trends, and noise spectral content;
- (2) Estimation of the quality of performance of the short-period automatic event detector;
- (3) Estimation of the detection capability of the individual stations on a regionalized basis;
- (4) Estimation of the discrimination capability of the individual stations; and
- (5) Estimation of the detection capability of the stations functioning as a network.

In the course of processing and analyzing data for these areas of investigation, estimates were made of the data quality, station reliability, and probability of mixed events. Conclusions regarding the above areas of interest and plans for further work are also presented in this report.

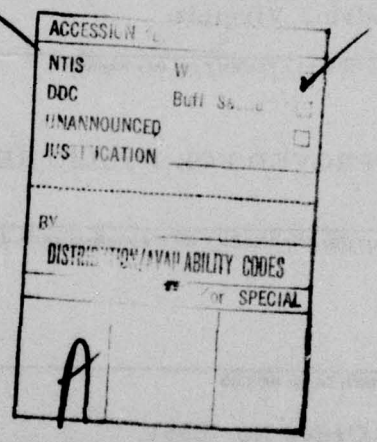

Neither the Advanced Research Projects Agency nor the Air Force Technical Applications Center will be responsible for information contained herein which has been supplied by other organizations or contractors, and this document is subject to later revision as may be necessary. The views and conclusions presented are those of the authors and should not be interpreted as the Advanced Research Projects Agency, the Air Force Technical Applications Center, or the U.S. Government.

ABSTRACT

This report presents the results of a continued evaluation of the Seismic Research Observatory stations performed by Texas Instruments Incorporated at the Seismic Data Analysis Center in Alexandria, Virginia. During the time period this evaluation was carried out, data were available from six stations - Albuquerque, New Mexico (ANMO); Guam, Marianas Islands (GUMO); Mashhad, Iran (MAIO), Narrogin, Western Australia (NWAO); Taipei, Taiwan (TATO); and Wellington (South Karori), New Zealand (SNZO).

The major areas of investigation in the evaluation were:

- Analysis of RMS noise levels, RMS noise trends, and noise spectral content.
- Estimation of the quality of performance of the short-period automatic event detector.
- Estimation of the detection capability of the individual stations on a regionalized basis.
- Estimation of the discrimination capability of the individual stations.
- Estimation of the detection capability of the stations functioning as a network.

In the course of processing and analyzing data for these areas of investigation, estimates were made of the data quality, station reliability, and probability of mixed events. Conclusions regarding the above areas of interest and plans for further work are also presented in this report.

TABLE OF CONTENTS

TABLE OF CONTENTS
(continued)

TABLE OF CONTENTS
(continued)

LIST OF FIGURES

LIST OF FIGURES
(continued)

LIST OF FIGURES
(continued)

LIST OF FIGURES
(continued)

LIST OF FIGURES
(continued)

LIST OF FIGURES
(continued)

LIST OF FIGURES
(continued)

LIST OF FIGURES
(continued)

LIST OF TABLES

LIST OF TABLES
(continued)

SECTION I
INTRODUCTION

A. THE SEISMIC RESEARCH OBSERVATORY SYSTEM

It has been noted (Robinson, 1967) that seismic data recorded by surface-sited instruments is degraded or obscured to a significant degree by wind-induced earth tilts. Theoretical data and tests indicated that this wind-induced noise component decreases rapidly with depth. Therefore, it is possible to enhance the seismic data quality by locating the seismic sensor at a depth of approximately 100 meters. The Seismic Research Observatories form the first network of single sites to implement this observation.

The Seismic Research Observatories data acquisition and recording system has been described in detail previously (Strauss, 1976). Therefore, only a brief description of the system is presented here.

Broadband seismic energy is recorded by force-balance type seismometers which produce an output proportional to earth acceleration over the frequency range of 0.02 to 1.0 Hz. Both long-period and short-period data are produced from each sensor by selectively filtering the broadband output. The long-period data are digitized and recorded continuously on an 800 bit per inch magnetic tape. The vertical component of short-period motion is input to an automatic detector, which permits recording of vertical-component short-period motion only when certain operator-specified conditions are satisfied. Each magnetic tape can hold up to fourteen days of digital seismic data. When full, these magnetic tapes are shipped to the Albuquerque Seismological Center at Kirtland Air Force Base in New Mexico. Copies of these tapes are sent to the Seismic Data Analysis Center at Alexandria, Virginia.

The long-period data are sampled once per second and quantized at 5 computer counts per millimicron of ground motion. Short-period data are sampled 20 times per second and quantized at 2000 computer counts per millimicron of ground motion with the following exceptions. Beginning 1 May 1976 at Guam, 14 April 1976 at Wellington, New Zealand, and 13 May 1976 at Taipei, Taiwan, the short-period data were quantized at 2 computer counts per millimicron of ground motion to prevent data clipping.

B. THE EVALUATION TASK

This report presents the results of a continued evaluation of the Seismic Research Observatories. The specific goals of this evaluation are:

- To estimate the data quality and reliability of each station
- To investigate the short-period and long-period noise field characteristics of each station
- To investigate the design of the short-period automatic detector and to make recommendations to improve this design
- To estimate the detection capability of each station on a regionalized basis
- To estimate the discrimination capability of each station on a regionalized basis
- To investigate the performance of the stations as a network.

The approach to reaching these evaluation goals is as follows. First, a suitable suite of seismic events and noise samples was constructed from available event lists. The procedure for selecting this event suite is described in Section II. This section also describes the manner in which the events and noise samples were processed and gives estimates derived from processing experience of the quality of the Seismic Research Observatory

data and reliability of the individual stations. Section III discusses the short-period automatic detector resident at each station. The discussion of this topic covers the present design of the automatic detector, design problems found during the course of evaluation of short-period data, and steps which may be taken to alleviate these problems.

In Section IV, the local noise field characteristics at each evaluated SRO station are presented. The local noise field is characterized by its RMS noise levels, monthly RMS noise level trends, peak noise amplitudes, and spectral content of the noise. Section V presents the detection capability of each station in terms of the entire area of interest and in terms of specified regions within the area of interest. In the course of estimating detection capability, the effect which mixed events and system malfunctions have on these estimates are discussed. Section VI considers the question of discriminating between earthquakes and presumed nuclear explosions. The technique used in this section is the $M_s - m_b$ discriminant. Section VII presents a first look at the detection capability of the stations functioning as a network. Network detection capability estimates are made from the station noise characteristics and from the detection statistics of the individual stations. Section VIII summarizes the results of this evaluation and suggests future avenues of investigation to improve these results. Section IX lists the references cited in the text of the report.

SECTION II
THE DATA BASE

A. DATA AVAILABILITY

The Seismic Research Observatory network, when fully operational, will consist of at least the ten stations listed in Table II-1 and shown in Figure II-1. (The shaded area of Figure II-1 shows the area in which events used in this evaluation occurred.) During the contract period covered by this report, data were available from six of these ten stations: Albuquerque, New Mexico (ANMO), Mashhad, Iran (MAIO), Guam, Marianas Islands (GUMO), Narrogin, Western Australia (NWAO), Taipei, Taiwan (TATO), and Wellington (South Karori), New Zealand (SNZO).

Figure II-2 shows diagrammatically the availability of data for each evaluated station from the start-up date of each to the end of 1976. The vertical dashed lines in Figure II-2 enclose the time frame from which data were selected for use in performing this evaluation. ANMO, MAIO, and NWAO show near-continuous data availability from their start-up dates to the end of this time frame. GUMO and SNZO each show two major breaks in data availability during this time frame. Of the six stations, the least data were available from TATO, which became operational 13 May 1976, was down for six days in July 1976, and went down for the rest of the year on 20 September 1976. (TATO did not produce more data until 18 July 1977.) For this reason, the evaluation time frame for TATO is 13 May 1976 to 20 September 1976.

B. FORMATION OF THE DATA BASE

In this evaluation of the Seismic Research Observatory stations, the detection and discrimination capabilities of each station are to be presented

TABLE II-1

SEISMIC RESEARCH OBSERVATORY LOCATIONS

Station Number	Station Name	Station Designator	Coordinates	
			Latitude	Longitude
30	Albuquerque, New Mexico*	ANMO	34°56'30"N	106°27'30"W
31	Ankara, Turkey **	ANTO	39°54'N	32°47'E
32	Bogota, Columbia	BOCO	4°35'46.0N	74°02'57.0"W
33	Chiang Mai, Thailand	CHTO	18°47'24.0"N	98°58'37.0"E
35	Guam, Marianas Islands*	GUMO	18°35'16"N	144°51'58.6"E
36	Mashhad, Iran*	MAIO	36°18'00N	59°29'40.2"E
38	Narrogin, Western Australia*	NWAO	32°55'42"S	117°14'9"E
40	Shillong, India**	SHIO	25°34'N	91°53'E
41	Taipei, Taiwan*	TATO	24°58'33.6"N	121°29'19.8"E
42	South Karori, New Zealand*	SNZO	41°18'37"S	174°42'16.7"E

* Evaluated in this report

** Coordinates approximate

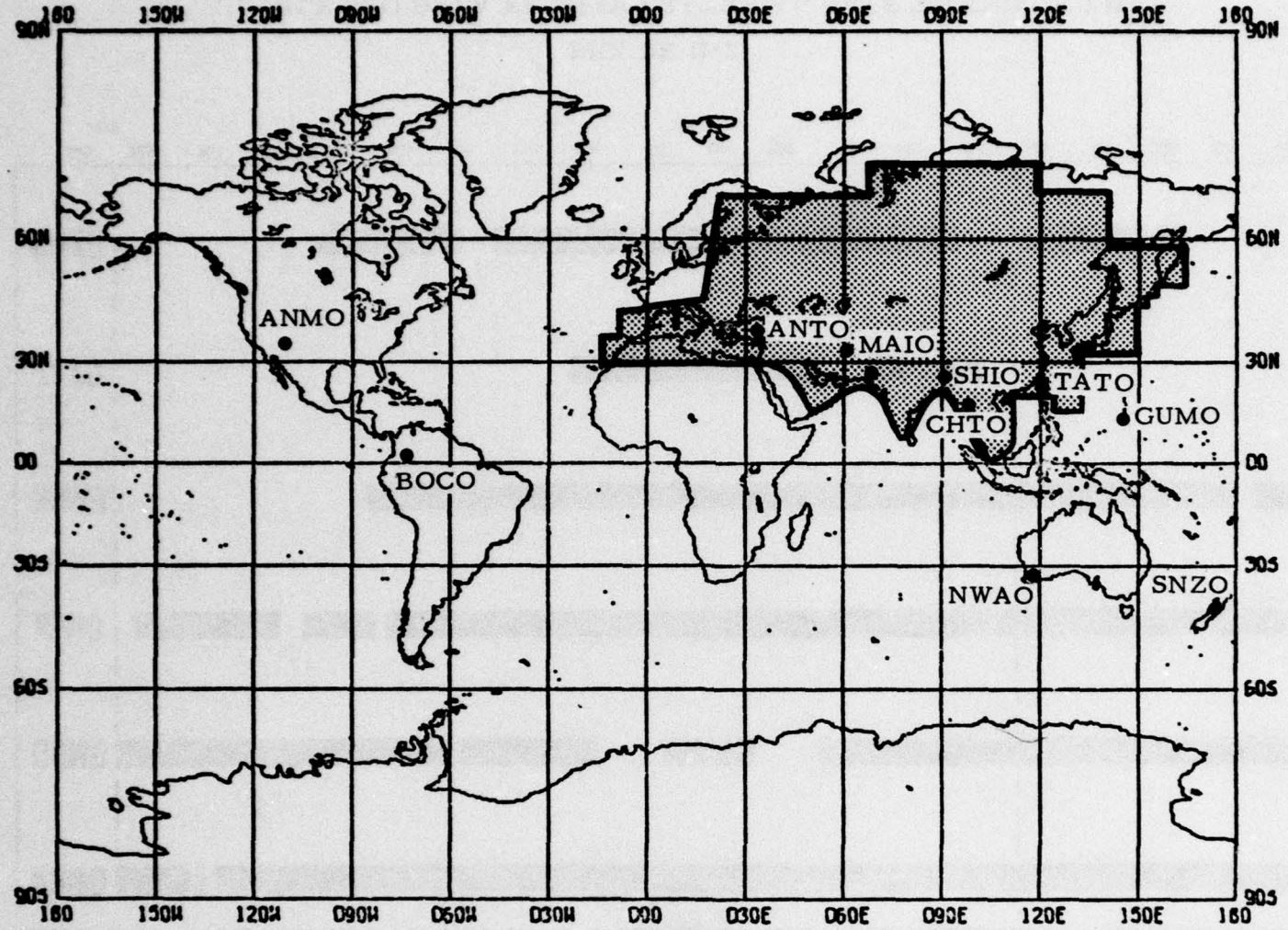

MILLER MODIFIED MERCATOR PROJECTION
MAP SCALE: 0.02000 INCHES/DEGREE LONGITUDE

FIGURE II-1

LOCATIONS OF SRO STATIONS

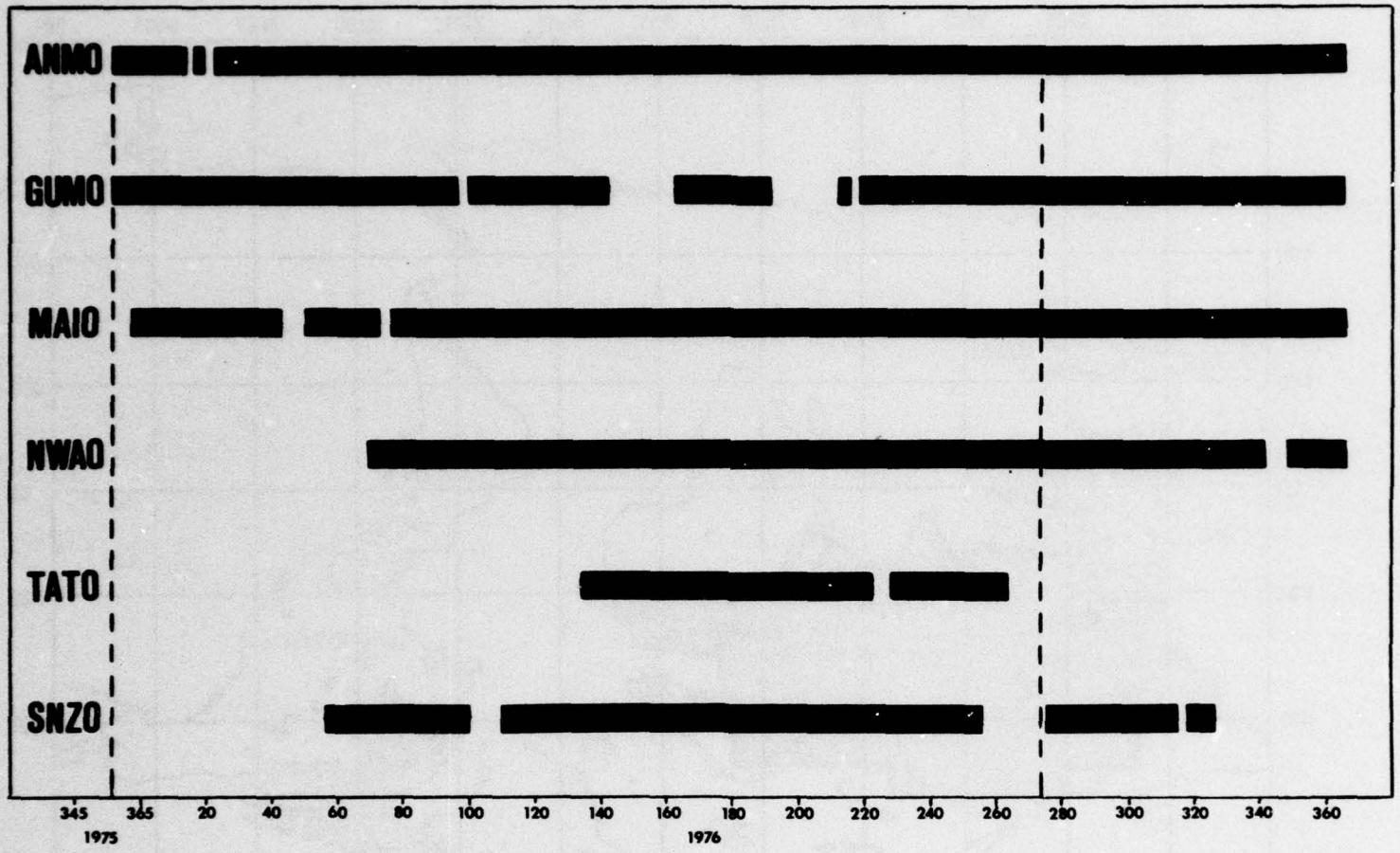

FIGURE II-2

AVAILABLE SRO DATA FROM OPERATIONAL DATE TO END OF 1976

on a regionalized basis. The general area of interest for this evaluation was identified as Eurasia. This cutback from the world-wide area used in the preliminary Seismic Research Observatory evaluation (Strauss, 1976) was made to keep the size of the data base within reasonable bounds. Since Eurasia is and always has been the main area of interest from an evaluation standpoint, this cutback can be made without any significant loss of information.

The first step in forming the evaluation data base was to select all seismic events with Eurasian epicenters as listed by the Norwegian Seismic Array (NORSAR) bulletins. (At the time of formation of the data base, this was the only available event list.) The time frame selected was from 22 December 1975, when the first station became operational, to 30 September 1976, when the NORSAR bulletins ceased being issued. This selection yielded a Eurasian event list of 2697 events. Since this was far too great a volume of data to be processed and analyzed in the available time, it was necessary to reduce this list to manageable proportions.

The event list was reduced in the following manner. First, the events were grouped by seismic region as defined by Flinn and Engdahl (Flinn and Engdahl, 1965). Those seismic regions containing fewer than 80 events were immediately rejected and their contained events dropped from the event list. Next, the events in the remaining regions were grouped by their sub-regions, again as defined by Flinn and Engdahl. Those sub-regions which contained only a few events and which were separated from the main body of events in that region were then rejected and their contained events deleted from the event list.

Table II-2 lists the region numbers and corresponding sub-region numbers for the data base. Flinn and Engdahl's region 19 was sub-divided into regions 1 and 2, corresponding to the Kurile Islands and northern Japan, respectively. This sub-division was made to centralize the grouping

TABLE II-2

DATA BASE REGIONALIZATION

Region # As Used in This Report	Flinn & Engdahl's Report #	General Area	Flinn & Engdahl's Geographic Subregions
1	19	Kuriles-Kamchatka	217, 218, 219, 221, 222, 225
2	19	N. Japan	224, 227, 228, 229, 230
3	20	S. Japan	232, 233, 234, 235, 237, 238
4	21	S.E. China	242, 243, 244, 245, 246, 247
5	25	Burma	294, 296, 297, 298
6	26	N. India	302, 303, 304, 305, 306, 307, 308, 309, 310, 311, 313, 315, 317, 318, 319
7	27	Tibet	320, 321, 322, 323, 324
8	28	Central Asia	326, 327, 328, 329, 330, 331, 332, 334
9	29	Iran-Ural Mountains	335, 336, 337, 338, 339, 340, 342, 343, 344, 345, 346, 347, 348, 349, 350, 351, 353, 354
10	30	Greece-Turkey	357, 358, 359, 360, 361, 362, 363, 364, 365, 366, 368, 369, 370, 371, 373, 375
11	31	W. Mediterranean	381, 382, 383, 390, 391, 392, 398, 399, 400
12	41	E. China	657, 658, 660, 661, 662, 663, 664, 665, 666
13	47	S. Pakistan	709, 710, 711, 712
14	48	N. Pakistan-Afghanistan	713, 714, 715, 716, 717, 718, 719, 720
15	49	N. Russia-Siberia	724, 726
16	3	Nevada Test Site	37, 41

of events. The regions were re-numbered simply to make them sequential and will be referred to by these new numbers throughout this report. (Not all of these regions are used in the discussion of regionalized results of Sections V and VI since mixed events and system malfunctions in some cases reduced the number of events in a region below the point where reasonable results could be determined.) The region boundaries are shown in Figure II-3.

At this point, the data base still contained approximately 2300 events. To further reduce this number, events were systematically deleted (every other event, two out of three, as needed) from heavily event-populated regions until no region contained more than 150 events. This procedure resulted in the final data base of 1472 events. The event parameters of the data base are given in Appendix A.

It should be noted that the manner in which the data base was created produces a data base which is essentially a random sampling of Eurasian seismic events. No effort was made to exclude obviously mixed events, so that mixed event statistics derived from this data base should accurately reflect the frequency of occurrence of mixed events. The frequency of occurence of system malfunctions resulting in the inability of the analyst to study a desired segment of seismic data will yield representative estimates of station reliability.

The short-period data base used in this evaluation is simply a subset of the above-described data base. All members of this subset have station-epicenter separations of less than 103 degrees. This restriction was placed on the short-period data base since detection of the P wave beyond 103^{o} from the event epicenter is limited by a shadow zone. At some stations this restriction severely limited the size of the data base, since these stations are located far from the general area of interest. Table II-3 presents the mean epicentral distances from each station to each region. (These values

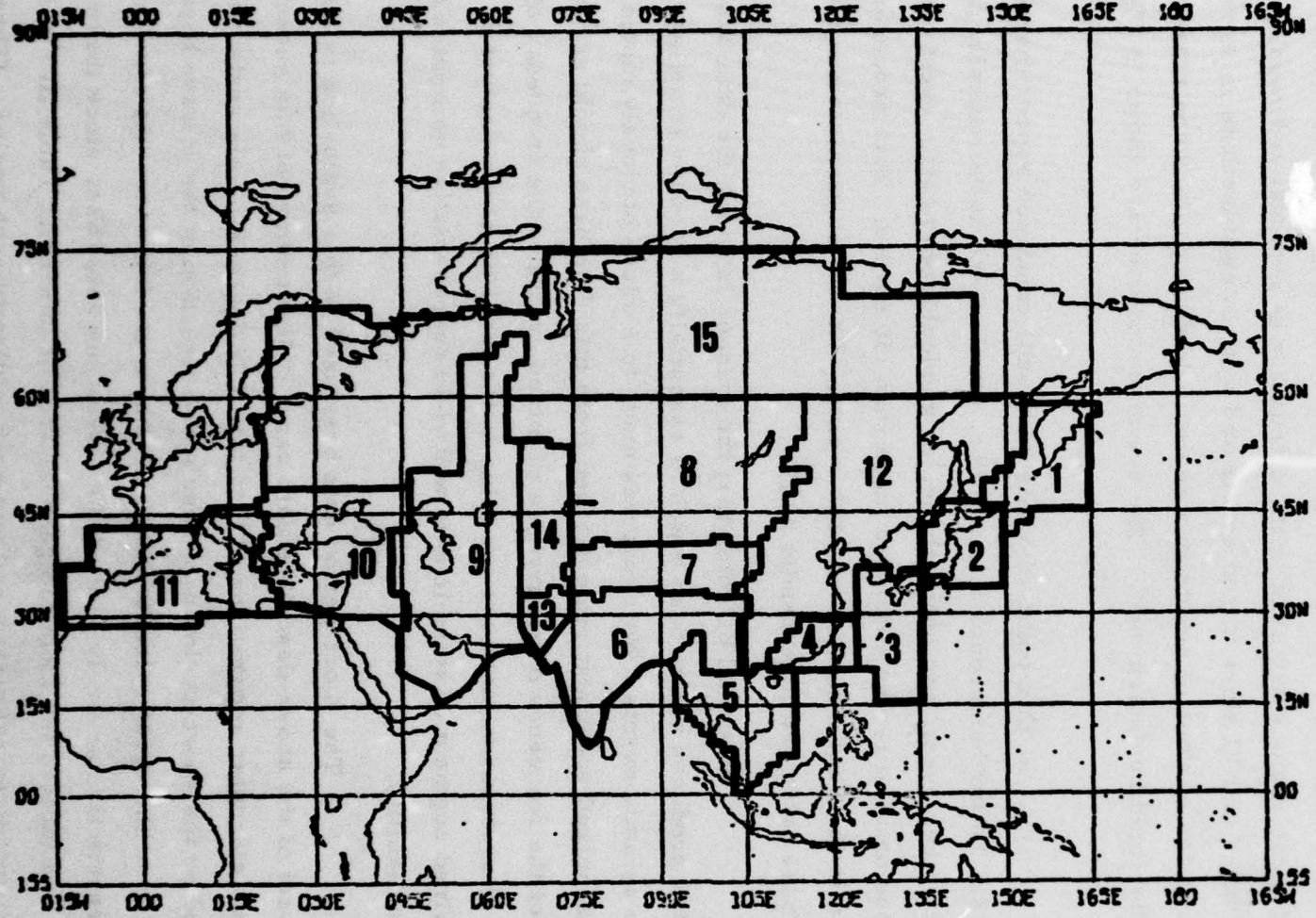

MILLER MODIFIED MERCATOR PROJECTION
MAP SCALE: 0.03429 INCHES/DEGREE LONGITUDE

FIGURE II-3

LOCATION OF SELECTED SEISMIC REGIONS

TABLE II-3

MEAN EPICENTRAL DISTANCES
(degrees)

Region	ANMO		GUMO		MAIO		NWAO		TATO		SNZO	
	Mean	S.D.	Mean	S.D.	Mean	S.D.	Mean	S.D.	Mean	S.D.	Mean	S.D.
ALL	91.9	16.3	62.7	30.5	38.5	22.1	87.4	17.3	43.9	24.5	120.4	27.6
1	72.1	5.3	34.2	5.8	65.7	2.4	86.8	5.1	34.7	4.8	90.9	3.4
2	82.6	2.9	25.8	3.0	62.6	1.4	75.9	3.1	22.3	2.8	85.9	2.4
5	116.6	2.8	47.1	1.6	33.4	2.5	60.9	2.5	22.7	1.8	98.0	1.7
6	111.7	5.2	54.0	9.5	25.1	8.6	69.0	4.9	26.8	8.1	108.0	7.3
7	105.8	2.1	57.4	8.6	21.7	8.8	76.3	5.5	30.0	9.6	116.4	5.7
8	95.7	0.4	63.5	0.6	19.4	0.5	88.5	0.2	40.0	0.3	122.7	0.2
9	108.2	4.4	80.8	5.4	7.1	2.7	88.5	3.3	54.6	5.4	131.5	4.3
10	94.9	2.4	99.5	8.7	24.4	4.8	107.8	6.7	75.2	6.1	152.3	7.3
11	90.8	2.2	105.8	3.0	31.3	1.4	115.2	2.4	82.6	1.4	160.4	2.0
12	93.9	2.3	34.4	2.2	46.4	1.6	72.7	2.2	14.9	2.2	95.2	2.0
14	109.1	---	66.6	0.3	11.4	0.3	79.8	0.2	41.8	0.3	120.1	0.0
16	8.1	0.4	88.9	0.3	105.6	---	137.1	0.4	---	---	101.5	0.3

S.D. = Standard Deviation

are derived from the station-epicenter separations of the events occurring in each region.) In particular, note that station SNZO is more than 103 degrees from the majority of the regions. Therefore, very little can be expected from the short-period data recorded at this station.

The description of the noise sample data base is given in detail in Section IV of this report. In brief, the short-period noise samples were selected from time gates immediately preceding the observed signal which triggered the automatic detector. Long-period noise samples were selected from time gates during which no signals were expected to be arriving at the stations as determined from the NORSAR event bulletins.

C. DATA PROCESSING

1. Long-Period Data Processing

The long-period signal and noise data used in this evaluation were processed in two stages--a basic processing stage and an analysis processing stage. The basic processing stage is illustrated by Figure II-4. For long-period data, the basic processing stage exists in two forms. In the first form, the seismic events and noise samples selected for analysis are first processed by an edit program, which searches the field tape for the desired edit start time, reads in the desired data, resamples the data to a 2-second sample rate, quality checks the data, computes the trace means, and writes the data on an edit tape. At this point, the three components of motion are in their recorded vertical, north, east (V, N, E) configuration. Next, the data is read from the edit tape by a program which removes the trace means, rotates the data from its V, N, E configuration to a vertical, transverse, radial (V, T, R) configuration, and writes the result on a second tape. Finally, this rotated data is read by a third program which bandpass filters (0.023-0.059 Hz passband) and plots the data.

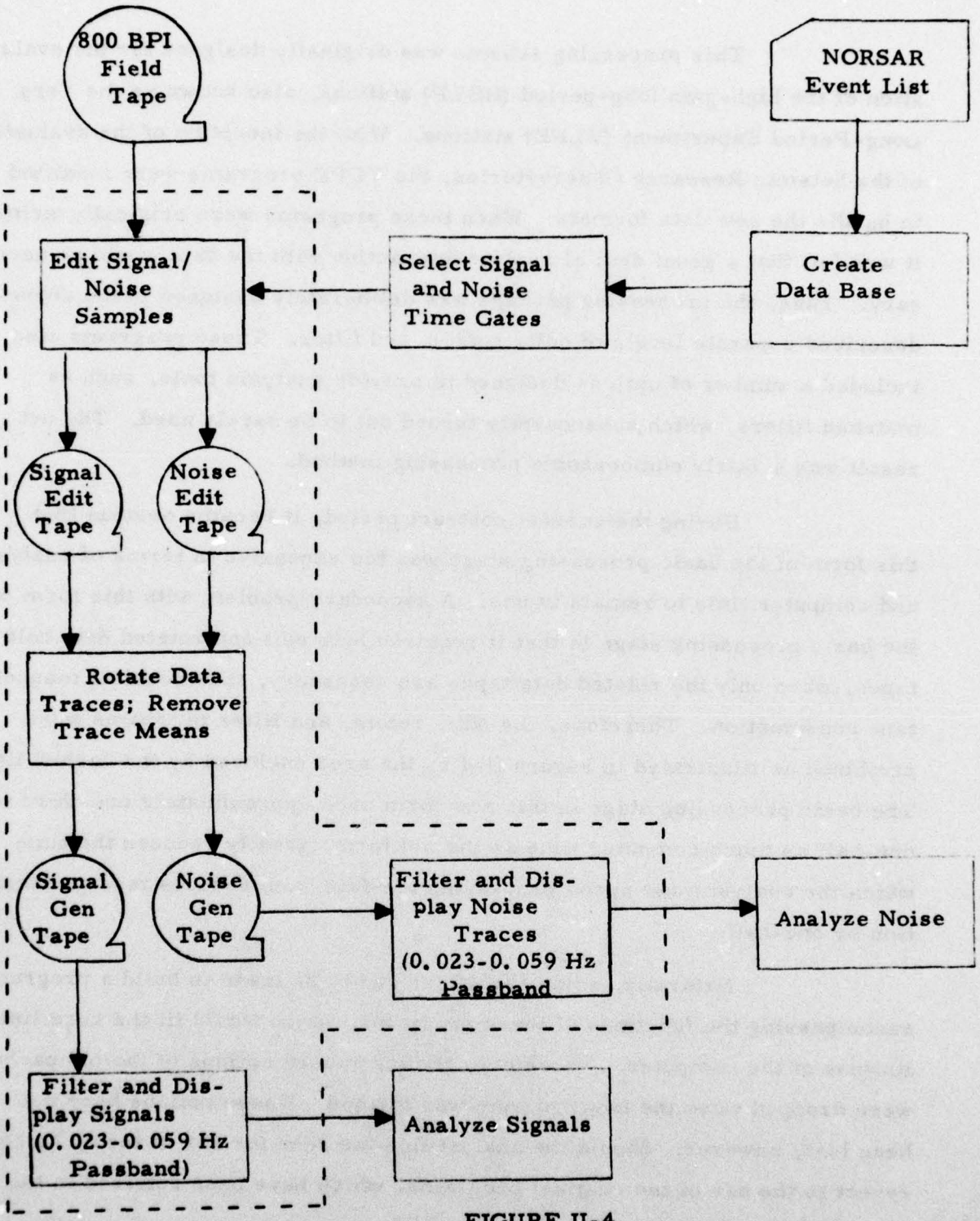

FIGURE II-4

LONG-PERIOD DATA PROCESSING FLOW CHART (IBM 360/44 DATA PROCESSING)

This processing scheme was originally designed for the evaluation of the high-gain long-period (HGLP) stations, also known as the Very Long-Period Experiment (VLPE) stations. With the inception of the evaluation of the Seismic Research Observatories, the VLPE programs were modified to handle the new data formats. When these programs were originally written, it was felt that a great deal of analyst interaction with the data would be necessary. Thus, the processing package was deliberately designed in the above-described separate levels of edit, rotate, and filter. These programs also included a number of options designed to provide analysis tools, such as matched filters, which subsequently turned out to be rarely used. The net result was a fairly cumbersome processing method.

During the current contract period, it became obvious that this form of the basic processing stage was too expensive in terms of analyst and computer time to remain in use. A secondary problem with this form of the basic processing stage is that it requires both edit and rotated data hold tapes, when only the rotated data tapes are necessary, thus doubling magnetic tape consumption. Therefore, the edit, rotate, and filter programs were combined as illustrated in Figure II-4 by the area enclosed by the dashed line. The basic processing stage in this new form uses approximately one-third to one-half as much computer time as the old form, greatly reduces the time which the analyst must spend processing the data, and reduces tape consumption by one-half.

Naturally, some sacrifices had to be made to build a program, encompassing the functions of three programs, which would fit the core limitations of the computer. Therefore, the least-used options of the old package were dropped when the new program was formed. These options have not been lost, however. Should the analyst find the need for any of them, he can revert to the use of the original programs, which have been retained in the form of Fortran card decks and listings.

The new program was thoroughly checked before it replaced the old programs. The method of checking was to perform a hexadecimal dump of a portion of a field tape. These data were manually decoded from hexadecimal to decimal and the appropriate trace means subtracted. The data were next manually rotated from their V, N, E configuration to the V, T, R configuration. Finally, the results were compared to the equivalent data output from the new program. The two sets of data were found to agree in all particulars. As a final check, several events were processed using the old programs and the new program. The results were compared and found to be identical.

One other benefit of the new basic processing stage was found after it was put in use. In the old edit program, if a parity error was encountered while the program was searching for the edit start time, the program would be unable to proceed and the analyst was forced to declare a malfunction (tape error) for that event. To avoid this problem, when the new program encounters a parity error, it increments a parity counter and proceeds. The total number of parity errors is printed out after the edit start time is found. This approach has greatly reduced the number of declared malfunctions. Documentation for this new basic processing stage has been completed during the current contract period (Schmidt, 1977).

The long-period analysis processing stage is described in detail in Section IV for noise analysis, in Section V for signal detection, and in Section VI for signal discrimination. Therefore, this stage will be only briefly described here.

Once the long-period noise samples have been processed through the basic processing stage, they are visually checked for unreported events and system malfunctions such as spikes or glitches. Each noise sample passing this visual check is then processed by the analysis program, which computes RMS noise amplitudes, measures the peak 25-second noise amplitude of

the sample, and computes the power spectrum of each component of the sample. All computed values are output on punched cards, which form the input to the programs which plot RMS noise amplitudes, RMS noise trends, spectral content of the noise, and maximum 25-second noise amplitudes.

The signal analysis stage is primarily visual, as the analyst searches each record for detection of the event under consideration while simultaneously checking for data quality. One program used by the analyst in this stage is the maximum likelihood curve fitting program (Ringdal, 1974) which is used in estimating station detection capability. A second program used in the signal analysis is the surface wave magnitude (M_s) measurement program. This program computes the surface wave magnitude for each waveform in the signal gate and then searches this series of M_s values for the largest 20, 25, and 30 second M_s values.

2. Short-Period Data Processing

Unlike the long-period data processing, the short-period data processing was performed in a single stage. This processing was carried out on the PDP-15 computer using the Interactive Seismic Processing System (ISPS) package (Ringdal, Shaub, and Black, 1975). The processing method is shown in Figure II-5.

The short-period record headers on the 1600 BPI copy of the SRO field tape are first dumped to reveal when the automatic detector permitted the recording of short-period data. The data base is then searched to find those events for which short-period data were recorded. These events are then edited, resampled to 10 points per second, and written on the disk pack. The analyst can then filter the data, (0.5-4.0 Hz passband) make Calcomp plots, and measure such parameters as RMS noise amplitudes and peak one-second noise amplitudes. When the analyst is finished with the data from one tape, the disk data files are overwritten with data from the next tape and analysis is resumed.

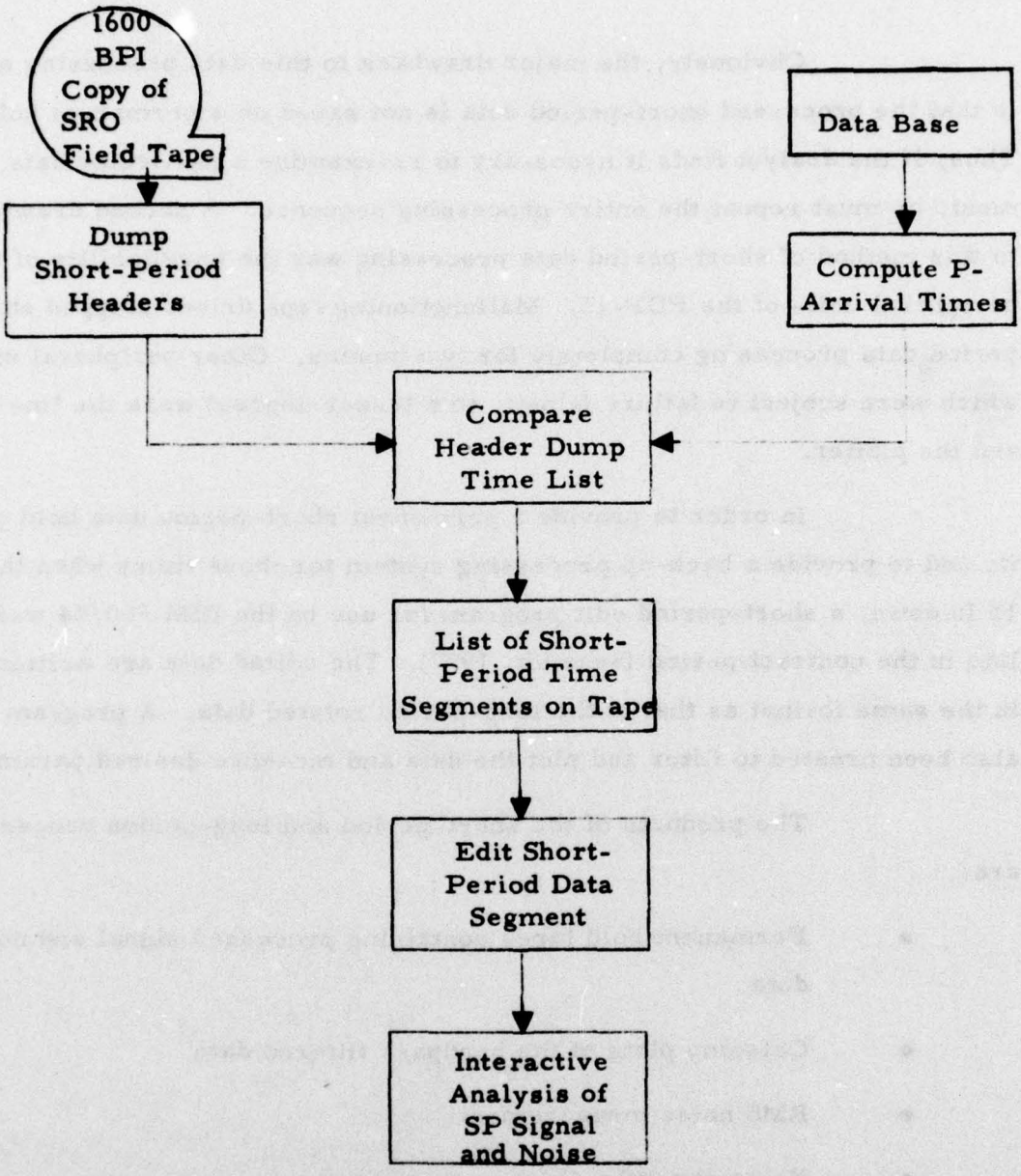

FIGURE II-5

SHORT-PERIOD DATA PROCESSING FLOW CHART
(PDP-15 DATA PROCESSING)

Obviously, the major drawback to this data processing approach is that the processed short-period data is not saved on a permanent hold tape. Thus, if the analyst finds it necessary to re-examine a particular data segment, he must repeat the entire processing sequence. A second drawback to this method of short-period data processing was the unreliability of the peripheral units of the PDP-15. Malfunctioning tape drives stopped short-period data processing completely for two months. Other peripheral units which were subject to failure (albeit, to a lesser degree) were the line printer and the plotter.

In order to provide a permanent short-period data hold capability and to provide a back-up processing system for those times when the PDP-15 is down, a short-period edit program for use on the IBM 360/44 was created late in the contract period (Schmidt, 1977). The edited data are written on tape in the same format as that of the long-period rotated data. A program has also been created to filter and plot the data and measure desired parameters.

The products of the short-period and long-period processing are:

- Permanent hold tapes containing processed signal and noise data
- Calcomp plots of the bandpass filtered data
- RMS noise measurements
- Noise spectra
- Maximum 1 second (SP) and 25 second (LP) noise amplitudes
- Detection statistics
- Surface wave magnitudes computed at 20, 25, and 30 second periods.

D. PROCESSING SUMMARY

Table II-4 summarizes the processing results of the work performed during the current contract period on the Seismic Research Observatories evaluation task. In this table, the 'SP' and 'LP' under the heading 'DATA TYPE' refer to short-period data and long-period data respectively. The heading 'DETECTED' refers to the number of events which were visually detected on a bandpass filtered (0.023-0.059 Hz passband for LP and 0.5-4.0 Hz passband for SP) plot under the detection criteria of Section V. The heading 'NOT DETECTED' refers to the number of events for which only seismic noise was observed in the signal gate. The heading 'MIXED' refers to the number of events which were not detectable due to the presence of some other signal in the signal gate. The heading 'NO SP DATA RECORDED' refers to the number of events not detected by the short-period automatic detector. The heading 'SYSTEM FAILURE-NO DATA RECORDED' refers to the number of events for which no data were recorded since the system had gone down (failed). The heading 'MALFUNCTION' refers to the number of events for which the detection status could not be determined due to malfunctions (spikes, glitches, and the like) in the signal gate. The heading '$\Delta < 103^{\circ}$' refers to the number of events for which short-period data were not processed due to their epicentral distances being greater than 103°.

It was not possible to process all of the events in the data base at all of the stations under evaluation. Conversion of the long-period processing package and the subsequent checking out of the new processing program made substantial inroads into the time available for data processing. Short-period data processing was delayed by hardware failures on the PDP-15. Even with these difficulties, however, a substantial amount of data was processed and analysed during the current contract period.

TABLE II-4

SUMMARY OF SRO EVENT PROCESSING

Station	Data Type	De-tected	Not de-tected	Mixed	No SP Data Recorded	No Data Recorded	Mal-function	$\Delta > 103^{\circ}$	Total
ANMO	SP	110	92	11	668	83	7	430	1401
	LP	144	563	353	---	101	57	---	1218
GUMO	SP	2	48	0	733	235	14	255	1287
	LP	152	495	256	---	303	90	---	1296
MAIO	SP	285	118	28	777	49	107	7	1371
	LP	323	420	343	---	65	33	---	1184
NWAO	SP	11	15	5	584	0	0	245	860
	LP	69	579	251	---	7	83	---	989
TATO	SP	19	35	8	552	39	0	0	653
	LP	151	222	212	---	39	29	---	
SNZO	SP	0	71	0	217	16	2	451	757
	LP	29	417	168	---	71	82	---	767

The quality of the data recorded at the Seismic Research Observatories was very good in most cases. The types of malfunctions which degrade the data quality were described in detail in the preliminary evaluation of the Seismic Research Observatories (Strauss, 1976). The overall frequency of occurrence of these malfunctions can be estimated from Table II-4. Long-period data were degraded by malfunctions three to eight percent of the time. With the exception of data recorded at MAIO, the short-period data is degraded by malfunctions one percent of the time or less. The relatively high malfunction rate of MAIO short-period data is primarily due to a type of malfunction first encountered during the current contract period. This malfunction appears on the short-period record as a 1.7 Hz (approximate) waveform. The waveform rises out of the noise field with an onset time of approximately three seconds. This waveform reaches peak amplitudes (measured zero-to-peak) of four to five millimicrons and may continue for several hours. (The effect of this on the short-period automatic detector is discussed in Section III.)

Estimates of station reliability can be made from the values given in Table II-4. The two factors which detract from the reliability of the station are the number of times it was not possible to examine the data since no data was recorded and the number of times it was not possible to examine the data due to system malfunctions. Thus, the reliability estimates presented here are calculated from:

$$\text{Reliability} = 1 - \left[P(\text{no data recorded}) + P(\text{malfunction})\right]$$

where the two probabilities are estimated empirically from the data of Table II-4.

The reliability estimates are presented in Table II-5. The relatively low reliability of GUMO is primarily due to station down time, when no data was recorded (see Figure II-2).

TABLE II-5

STATION RELIABILITY ESTIMATES

Station	Reliability	
	Short-Period	Long-Period
ANMO	0.91	0.87
GUMO	0.76	0.70
MAIO	0.89	0.92
NWAO	1.00	0.91
TATO	0.94	0.90
SNZO	0.94	0.80

With the large data base processed in this evaluation, it was possible to form estimates of the probability that an event of interest will be masked by some other event (a 'mixed' event). From the data of Table II-4, one can see that the probability that any short-period event will be mixed is very small. At MAIO, the worst case, the short-period data is mixed in two percent of all events studied. This low probability of mixing for short-period data is due to the length of the signal coda, which is quite short relative to the average time between signals.

The long-period data presents quite a different picture. Due to their relatively long signal coda, there is a significant probability of mixing for long-period data. Table II-6 presents estimates of the probability of mixing derived from the processed data base. To provide more robust statistics, the data were computed for selected ranges in m_b rather than for each individual m_b. These values are surprisingly constant from station to station and from m_b range to m_b range.

TABLE II-6

LONG-PERIOD MIXED EVENT PROBABILITY ESTIMATES

m_b Range	ANMO	Probability That Desired Event is Mixed*				
		GUMO	MAIO	NWAO	TATO	SNZO
3.1-3.5	0.35	0.30	0.30	0.30	0.40	0.30
3.6-4.0	0.35	0.30	0.35	0.30	0.45	0.25
4.1-4.5	0.30	0.30	0.35	0.35	0.35	0.30
4.6-5.0	0.30	0.25	0.25	0.25	0.20	0.30

* All probability estimates are rounded off to nearest five-hundredths.

SECTION III

THE SHORT-PERIOD AUTOMATIC DETECTOR

A. DISCUSSION

This section reviews the design of the short-period automatic detector currently in operation at the Seismic Research Observatory stations and discusses problems of this detector discovered during the course of this evaluation.

The prime reason for incorporating a short-period automatic detector at the Seismic Research Observatory stations was to minimize the amount of short-period data recorded during which no short-period seismic events could be observed and thus maximize the recording life of each magnetic tape. This would minimize expenditures for the purchasing and transportation of magnetic tapes and the amount of data lost during tape changes without seriously decreasing the number of short-period seismic events recorded. Since the single component of short-period motion is sampled twenty times per second while the three components of long-period motion are each sampled once per second, the bulk of each tape (87%) would be filled with short-period data if short-period data were recorded continuously. In this continuous recording mode, the recording life of a 2400 foot, 800 BPI magnetic tape would be approximately four days. With the automatic detector in operation, this has been extended to up to sixteen days.

The design of any automatic detector should take into account the following points:

- Maximum detection probability consistent with the largest tolerable false alarm rate

- Stable false alarm rate over a wide range of ambient noise levels
- Minimum number of detections declared from the same event while retaining the ability to detect possible secondary phase arrivals within the coda
- Minimum time necessary to re-establish equilibrium after parameter value changes
- Low sensitivity to degraded data quality (Swindell and Snell, 1977).

In this evaluation of the automatic detector design, data output by the automatic detector will be assessed in terms of the above points.

At any point in the operation of the automatic detector, one of four events must occur:

- Signal in time gate, detection declared
- No signal in time gate, no detection declared
- Signal in time gate, no detection declared (type 1 error)
- No signal in time gate, detection declared (type 2 error).

The third and fourth of these four events are, of course, the two possible types of detector errors. With only data which has been processed by the automatic detector available, it is not possible to assess the frequency of occurrence of the type 1 errors. It would be necessary to have continuous data and data for the same time frame which has been processed by the automatic detector to determine how often the automatic detector fails to detect an analyst-detectable signal. It is possible to at least qualitatively assess the performance of the automatic detector in terms of the type 2 error, i.e., false alarms.

B. DESIGN OF THE PRESENT SHORT-PERIOD AUTOMATIC DETECTOR

Each Seismic Research Observatory station is equipped with a short-period automatic event detector (hereafter referred to as the SRO automatic detector) which is intended to discriminate between seismic noise and short-period seismic events. The design of the SRO automatic detector is based on a study carried out by the Charles Stark Draper Laboratory (Eterno, et al., 1974).

The design concept of the SRO automatic detector is illustrated by Figure III-1. The short-period analog data from the sensor unit is first digitized at a rate of twenty points per second. At the SRO automatic detector input, each datum is converted to a twelve bit integer quantity. The digitized data next passes through a band-limiting four pole-pair Butterworth filter with two zeros at zero frequency. (This filter is constructed by cascading four recursive single pole-pair filters. A single-zero filter is placed in front of the first and fourth cascaded filters.) The lower cutoff of this filter is 0.5 Hz, the upper cutoff is 2.0 Hz, the filter response within the passband is flat to within $\pm$ 1 dB, and the rejection rate outside the passband is more than 25 dB.

The data are then rectified and passed to the short-term averager (STA). Utilizing a single-pole recursive stage, one-second exponentially-weighted short-term averages are constantly generated. The short-term averager imparts an absolute gain of approximately 13 dB to the data. The short-term averages are combined to form a long-term average (LTA). Long-term averages may be formed over operator-selected time intervals of 10, 20, 30, or 40 seconds. The approximate 13 dB gain imparted by the short-term averager allows greater accuracy in calculating the long-term average. However, once the calculation is complete, the long-term average is rescaled to unitize the gain at zero frequency.

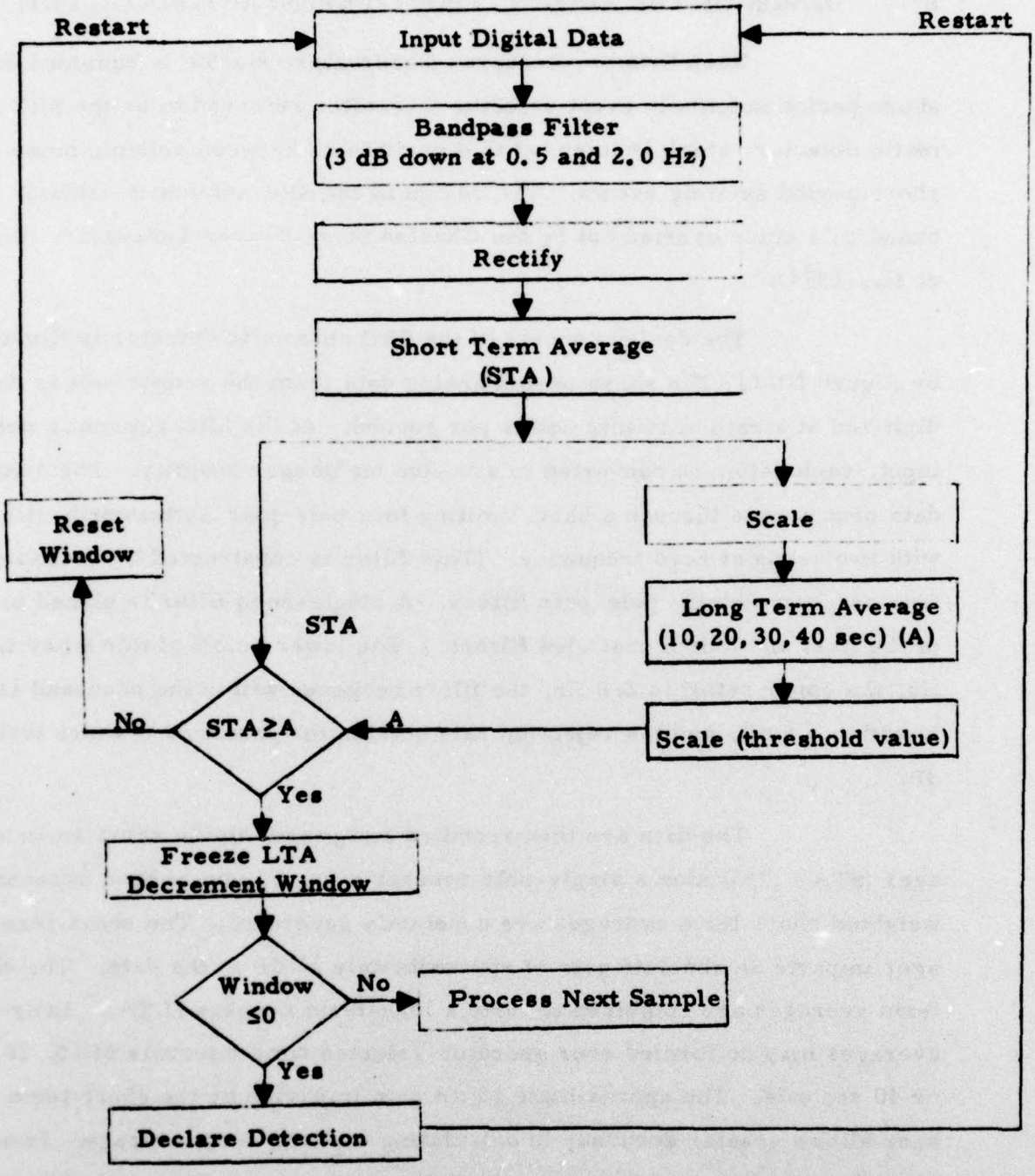

FIGURE III-1

SHORT-PERIOD DETECTOR CONCEPT

The SRO automatic detector tests for detections by continuously comparing the short-term average with the long-term average. The long-term average is first scaled upward by an operator-selected threshold constant (the 'turn-on' threshold). This scaling is intended to minimize false alarms. If the short-term average rises above the scaled long-term average, the long-term average is 'frozen' at its current value. If the short-term average then remains above the frozen value of the long-term average for one second (twenty samples) a detection is declared and the short-period data, which has been held in a separate memory buffer, is written on the magnetic tape. If the short-term average drops below the frozen long-term average before the one second time gate is over, no detection is declared and the long-term average is 'unfrozen' and updated.

Once a detection has been declared, the frozen long-term average is scaled upward by a second operator-selected threshold constant (the 'turn-off' threshold). When the short-term average drops below the rescaled long-term average, the event is considered to be over and the current buffer of short-period data completes the magnetic tape record. Scaling the frozen long-term average by the turn-off threshold is intended to minimize the recording of the sometimes persistent coda that can follow the initial arrival of a short-period event.

Thus, the operator can 'tune' the SRO automatic detector via four adjustable constants: the long-term averager time constant, the detection turn-on threshold, the detection turn-off threshold, and the digital gain factor. In addition, the operator can override the SRO automatic detector and record short-period continuously.

Set procedures exist for setting the proper digital gain factor. However, selection of the other constants is largely a matter of trial-and-error. The operator zeros in on optimum values after selecting initial values within experimentally determined ranges.

C. PROBLEMS WITH THE CURRENT DESIGN OF THE SRO AUTOMATIC DETECTOR

During the course of processing and analyzing short-period data to be used in the estimation of the short-period detection capability of the Seismic Research Observatory stations, several persistent problems were found in the present design of the SRO automatic detector.

The first problem found in the automatic detector design is illustrated by Figure III-2. The monotonic waveform (1.7 Hz frequency approximately) seen emerging from the noise in the upper trace has been repeatedly found to be the triggering agent of the SRO automatic detector at ANMO and MAIO. The source of this waveform at ANMO is apparently a large centrifuge operated at Kirtland Air Force Base, while at MAIO it is apparently a rock crusher. The center trace of Figure III-2 shows the data as it would appear to the SRO automatic detector after application of the 0.5-2.0 Hz passband filter. This filter has cleaned up the seismic noise preceeding the 1.7 Hz filter while leaving this waveform essentially uneffected. The SRO automatic detector detects the rise in the short-term average due to the onset of this waveform and starts declaring detections. Since this waveform at times persists for hours, hundreds of false alarms can be rapidly written on tape.

The lower trace of Figure III-2 presents the same data after application of a 0.5-1.5 Hz passband filter. Note that the 1.7 Hz waveform has been completely removed from the data. The scale factor for this trace indicates that the remaining waveforms are simply seismic noise. Tests of this filter on seismic signals buried in this 1.7 Hz waveform indicate that the 1.7 Hz waveform can be removed without significantly degrading the signal. Therefore, the detection false alarm rate can be substantially reduced at stations displaying this 1.7 Hz waveform by changing the passband filter limits of the SRO automatic detector from 0.5-2.0 Hz to 0.5-1.5 Hz.

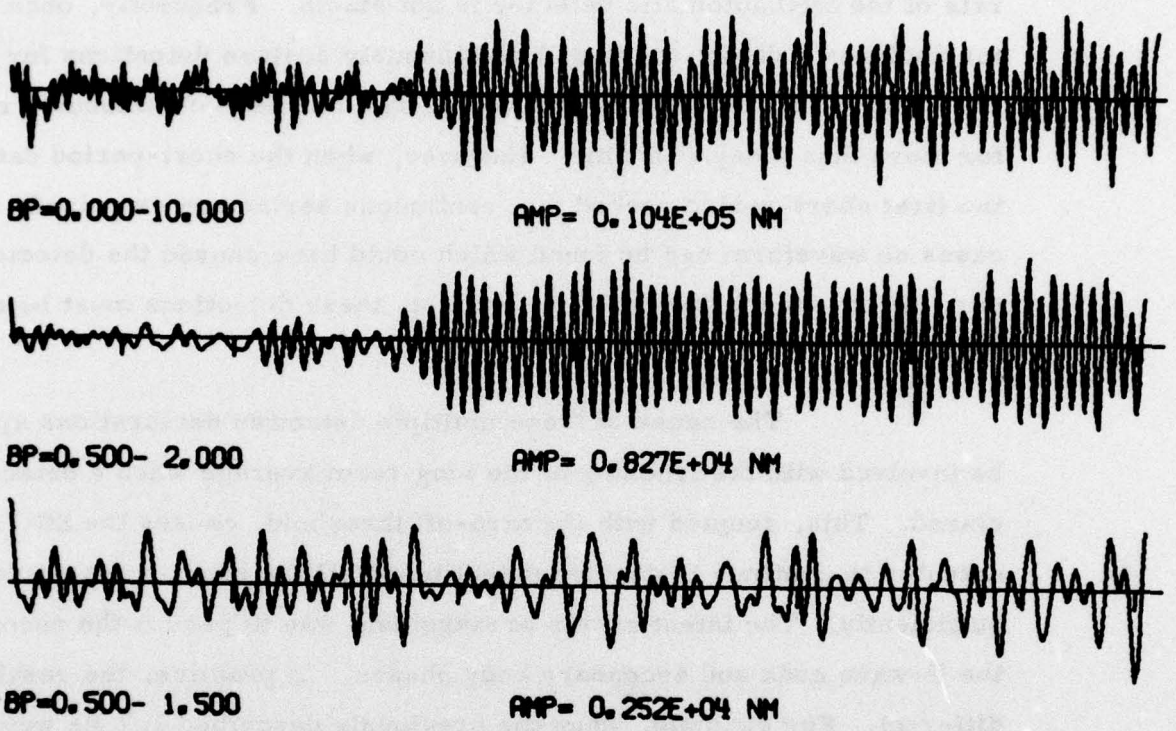

FIGURE III-2

SHORT-PERIOD NOISE SAMPLE SHOWING
ONSET OF 1.7 Hz WAVEFORM

The next design problem to be discussed is that the false alarm rate of the SRO automatic detector is not stable. Frequently, once the detector declares a detection, it will continuously declare detections for hours. In the worst case, at SNZO, short-period data has been continuously recorded for more than a day at a time. However, when the short-period data following the first short-period record of a continuous series are examined, in many cases no waveform can be found which could have caused the detector to trigger. From the standpoint of the analyst, these detections must be called false alarms.

The cause of these multiple detection declarations appears to be involved with the freezing of the long-term average when a detection is declared. This, coupled with the turn-off threshold, causes the SRO automatic detector to continue to declare detections until the short-term average drops sufficiently. The intent of this arrangement was to permit the recording of the P-wave coda and secondary body phases. In practice, the result is quite different. For example, when the previously described 1.7 Hz waveform triggers the detector, the frozen long-term average and turn-off threshold ensure that short-period data recording will be continuous from that point until this waveform drops back into the noise.

If the short-period noise level was to abruptly rise and hold its new level, a long series of detections would be made. This could happen if the turn-on threshold was set too low and the station was sited near a coastline, where an approaching storm could provide the increase in noise level. This may be the cause of the long series of continuously declared detections at SNZO, where visual examination of the data has revealed no reason for the declared detections.

Examples of the instability of the SRO automatic detector can be seen in Tables III-1 and III-2. Table III-1 presents the detection statistics for a 10-day period in 1976. In this period, the automatic detector at GUMO

TABLE III-1

PERFORMANCE OF AUTOMATIC DETECTOR FOR AN ARBITRARY 10-DAY PERIOD IN 1976

Date	Number of Detections					
	ANMO	GUMO	MAIO	NWAO	TATO	SNZO
06/21/76	6	36	11	23	9	7
06/22/76	19	53	9	0	1	1
06/23/76	14	11	9	3	4	1
06/24/76	16	0	6	1	2	2
06/25/76	16	4	20	6	0	2
06/26/76	4	8	15	3	0	0
06/27/76	8	18	11	4	2	3
06/28/76	15	64	12	3	1	2
06/29/76	13	62	6	4	2	6
06/30/76	15	22	5	3	7	4

Date	Percentage of Time Recorded					
	ANMO	GUMO	MAIO	NWAO	TATO	SNZO
06/21/76	59	10	12	1	2	67
06/22/76	6	33	9	0	9	>1
06/23/76	3	42	23	>1	1	>1
06/24/76	4	0	7	>1	>1	>1
06/25/76	6	3	14	20	0	89
06/26/76	1	1	32	3	0	100
06/27/76	2	2	26	2	>1	64
06/28/76	3	9	22	1	96	>1
06/29/76	3	49	11	>1	5	42
06/30/76	3	2	54	>1	1	41

TABLE III-2

PERFORMANCE OF AUTOMATIC DETECTOR FOR AN ARBITRARY 9-DAY PERIOD IN 1977

Date	Number of Detections					
	ANMO	GUMO	MAIO	NWAO	TATO	SNZO
07/23/77	7	3	12	3	16	0
07/24/77	12	4	12	4	20	0
07/25/77	14	4	13	3	14	0
07/26/77	11	4	15	3	13	0
07/27/77	14	10	10	5	15	0
07/28/77	28	7	12	3	21	0
07/29/77	67	9	17	5	22	0
07/30/77	13	11	19	2	16	0
07/31/77	13	8	6	2	11	0

Date	Percentage of Time Recorded					
	ANMO	GUMO	MAIO	NWAO	TATO	SNZO
07/23/77	1	2	3	>1	1	0
07/24/77	5	1	11	1	4	0
07/25/77	3	>1	3	>1	1	0
07/26/77	2	>1	4	>1	1	0
07/27/77	2	1	6	>1	1	0
07/28/77	5	1	4	>1	2	0
07/29/77	13	6	10	7	4	0
07/30/77	2	1	6	>1	7	0
07/31/77	1	97	3	>1	1	0

reported many more detections than did the other stations. This, coupled with the high short-period noise levels recorded at GUMO (Section IV) leads the authors to believe that many of these reported detections are false alarms. This table also shows that the percentage of short-period data recorded (where 100 percent indicates continuous recording) varies widely from day to day and from station to station. For example, compare days 6/21/76 and 6/27/76 at ANMO. Although the number of detections declared are about the same for the two days, the percentage of recorded data differs greatly (59 percent as opposed to 2 percent).

Since software and parameter setting changes have been made following this time period, Table III-2 was constructed to illustrate the automatic detector performance approximately one year later. The data in this table indicate greater stability in detector performance. However, several points should be noted. On 7/29/77 ANMO shows 67 detections, a value far greater than those at the other stations. Also, at GUMO on 7/31/77, 97 percent of the short-period data were recorded, an amount that appears far too large in view of the amounts of short-period data recorded at the other stations on that day. Finally, the lack of short-period data at SNZO indicates that perhaps changes in parameter settings went to the opposite extreme from those of a year previously. It would appear that the detection thresholds were set too high to permit any detections.

Next to be described are two sources of false alarms which, while less common than those previously described, must be recognized and corrected. Figure III-3 shows in the upper trace an unfiltered short-period record from SNZO and in the lower trace the same record after filtering by a 0.5 to 2.0 Hz filter. This record was the first in a series of continuous detection declarations. Therefore, the reason this record was declared a detection by the SRO automatic detector must be the waveform produced by filtering the spike. This type of false alarm can be eliminated by placing a spike-correction algorithm at the front end of the SRO automatic detector.

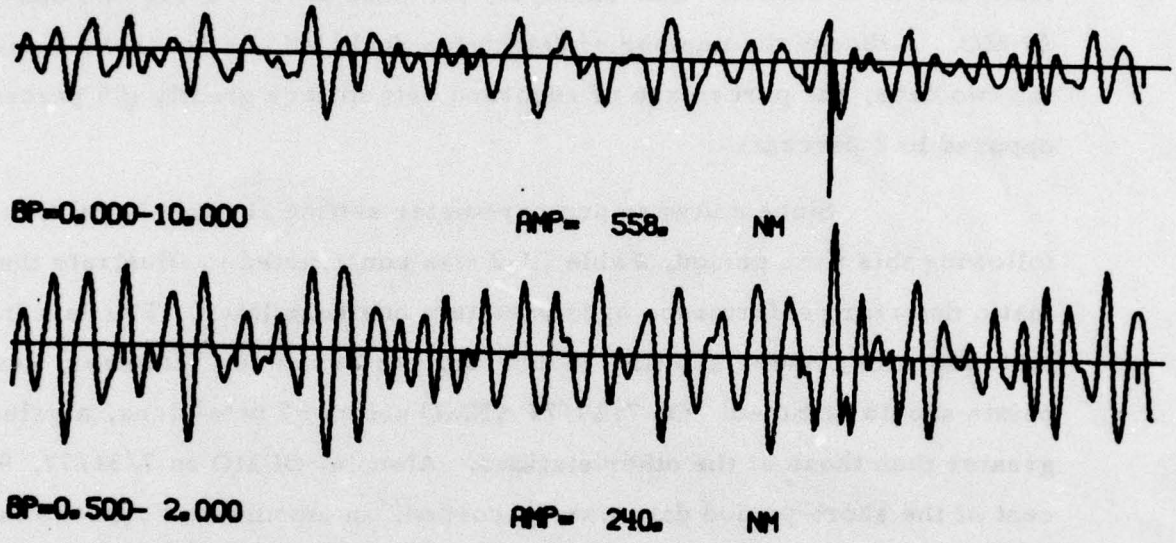

FIGURE III-3

SHORT-PERIOD NOISE SAMPLE CONTAINING SPIKE

Figure III-4 shows the second of these false alarm sources. The waveform causing the SRO automatic detector to declare a detection is a glitch of unknown source; it does not resemble any of the recorded waveforms which the author has been able to associate with known seismic events. In particular, it displays no recognizable coda following the initial pulse. This waveform triggered the automatic detector by exceeding the turn-on threshold for more than twenty sample points. However, if it had been required that the short-term average exceed the scaled long-term average for more than twenty points (say, thirty points) this false alarm would not have been declared.

In summation, the following changes in the design of the SRO automatic detector should be made:

- Change the bandpass filter limits from 0.5-2.0 Hz to 0.5-1.5 Hz, or notch out a very narrow band about 1.7 Hz.
- Alter the frozen long-term turn-off threshold combination so that fewer detection declarations following the first of a continuous series are made.
- Put a spike-correction algorithm at the front end of the SRO automatic detector.
- Increase the number of contiguous points for which the short-term average must exceed the scaled long-term average in order for a detection to be declared from 20 points to at least 30 points.

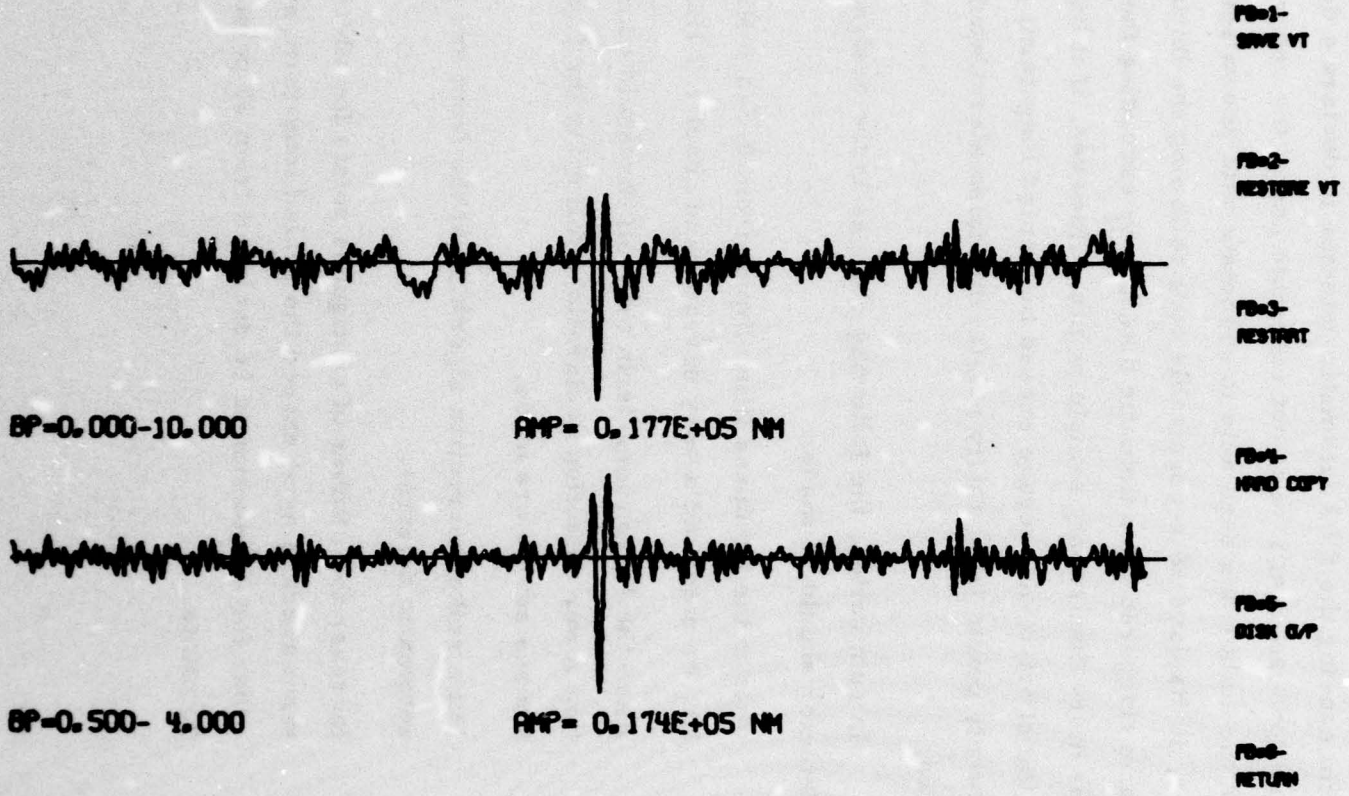

FIGURE III-4

SHORT-PERIOD NOISE SAMPLE CONTAINING GLITCH

SECTION IV
NOISE ANALYSIS

A. DISCUSSION

The goal of this section is to describe the characteristics of the noise field at each Seismic Research Observatory under evaluation. The preliminary Seismic Research Observatory evaluation (Strauss, 1976) presented a first look at short-period and long-period RMS noise levels and at long-period average noise spectra. The long-period noise was corrected for instrument response while the short-period results were not, since instrument response correction capability is not part of the PDP-15 interactive processing system.

In this continuation of the Seismic Research Observatories evaluation, one change in and one addition to the noise analysis have been made. First, both short-period and long-period RMS noise and spectra content results are presented without instrument response corrections. This change was made since it is recognized that the analyst is primarily concerned with the noise as he will see it, i.e., after it has passed through the sensing, filtering, and recording instrumentation. A long-period noise analysis with instrument response corrections is presented in Appendix B for the interested reader.

The addition to the noise analysis is the measurement of maximum noise amplitudes, which are made at 1-second periods for short-period data and 25-second periods for long-period data. These measurements were made at the suggestion of Dr. Filson of the Advanced Research Projects Agency. They will be used in the analysis of Seismic Research Observatories network detection capability (Section VII).

The definition of seismic noise used in this report is most clearly stated by Enders A. Robinson (Robinson, 1967):

> Any ground motion that is not caused by an explosion or an earthquake is usually regarded as ambient seismic noise. The predominant components of such seismic noise are surface-generated microseisms that originate from meteorological, hydrodynamic, or cultural sources. Such microseisms chiefly propagate along the surface of the earth as Rayleigh waves.

B. VERTICAL-COMPONENT SHORT-PERIOD NOISE

Short-period noise analysis was performed on the PDP-15 computer using the Interactive Seismic Processing System (Ringdal, Shaub, and Black, 1975). Subject to data availability and time constraints, a minimum of two noise samples per day from each station were processed. These noise samples were obtained in one of two ways. First, while processing short-period events of the data base, a set of noise samples was obtained by selecting the time gate prior to the observed P-wave arrival. A second set of short-period edits was made to produce noise samples for days on which the data base did not have any events. Each of these edits started at the first point of a data segment output by the automatic detector. This start time was picked to avoid making noise measurements in signal coda. Due to the manner in which the automatic detector operates, the length of the time gate prior to the P-wave arrival (and, hence, the length of the noise sample) was usually about 20 seconds.

After the noise gate was selected, each sample was filtered by a 0.5-4.0 Hz bandpass filter. RMS noise was then computed by the equation

$$\text{RMS Noise} = \left[\frac{\sum_{i=1}^{n} (x_i)^2}{n} \right]^{\frac{1}{2}}$$

where n=number of data points

X_i = the i^{th} data point.

All available RMS noise values for each day were averaged to provide a more stable RMS noise estimate and converted to millimicrons. The resulting RMS noise values are plotted against Julian day in Figures IV-1 to IV-3 and the monthly RMS noise trends derived from these values are plotted in Figures IV-4 to IV-6.

The ANMO short-period RMS noise shows little change with time. The higher values between days 240 and 250 are probably due to the 1.7 Hz waveform described in Section III. When the noise samples were selected, those which obviously contained this waveform were rejected. Apparently, some accepted samples contained a significant amount of this waveform.

The GUMO short-period noise values up to approximately day 115 reflect the almost continuous data clipping caused by the 2000 computer count per millimicron quantization. Starting at approximately day 125, the data was quantized at 2 computer counts per millimicron and valid estimates of GUMO RMS noise appear. These values show that the noise field changes rapidly from day to day, maintaining high levels throughout. The MAIO short-period RMS noise values, like the ANMO values, show little trend with time. However, they do show greater day-to-day variation. The NWAO and SNZO RMS noise values both show an upward trend with increasing time, while the TATO noise values cover too limited a time frame to reveal any clear trend.

Table IV-1 lists the mean short-period RMS noise values. These data reveal a correlation between the mean RMS noise level at a station and the distance between that station and the nearest coastline. The lowest RMS noise values are recorded at ANMO and MAIO, which are the most

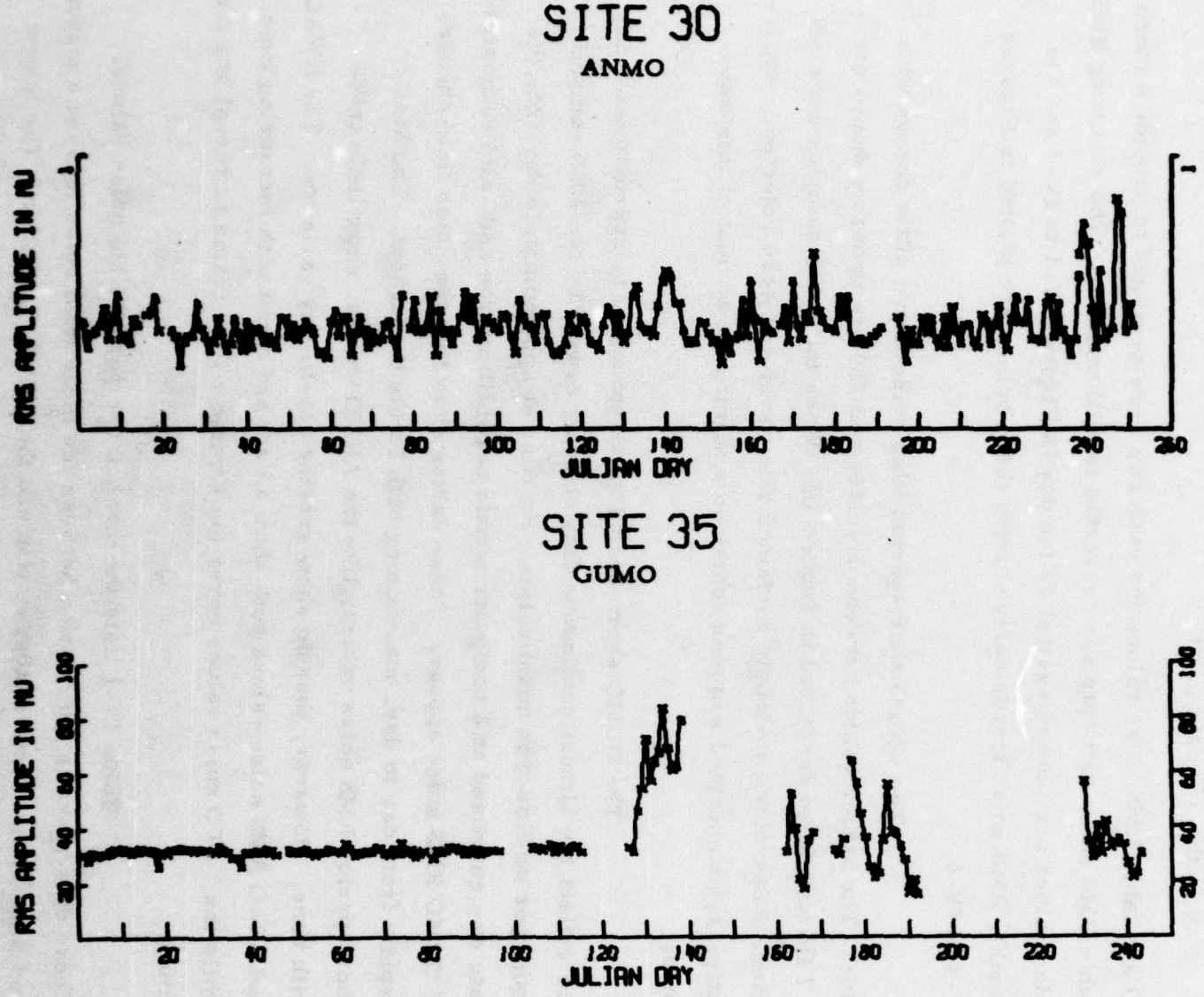

FIGURE IV-1

ANMO AND GUMO SHORT-PERIOD RMS NOISE

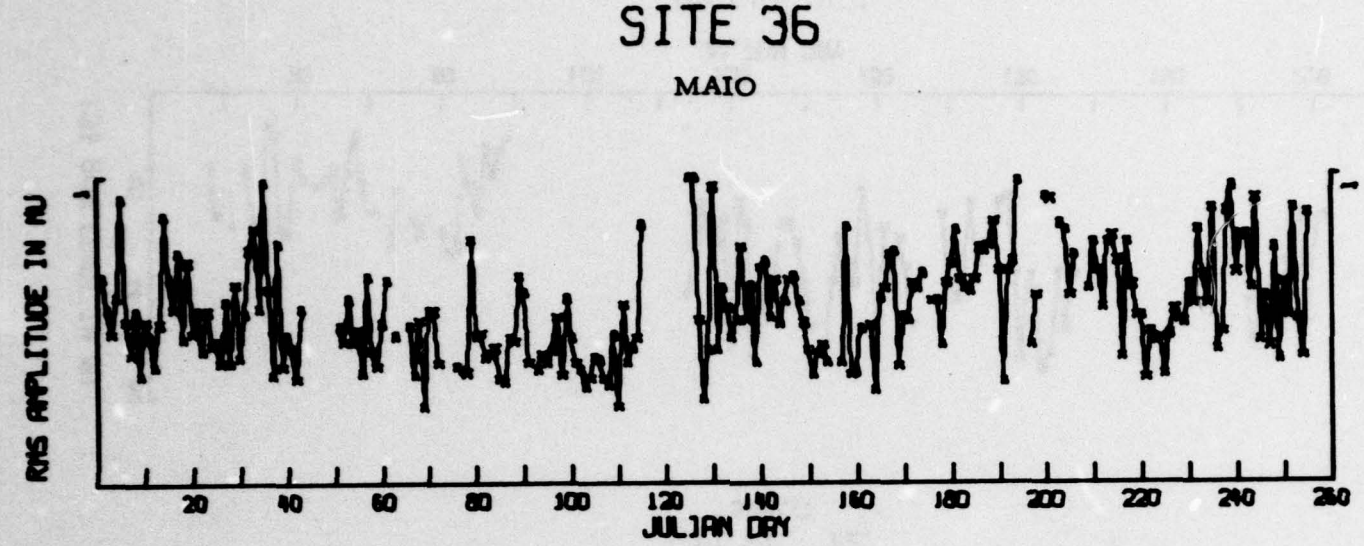

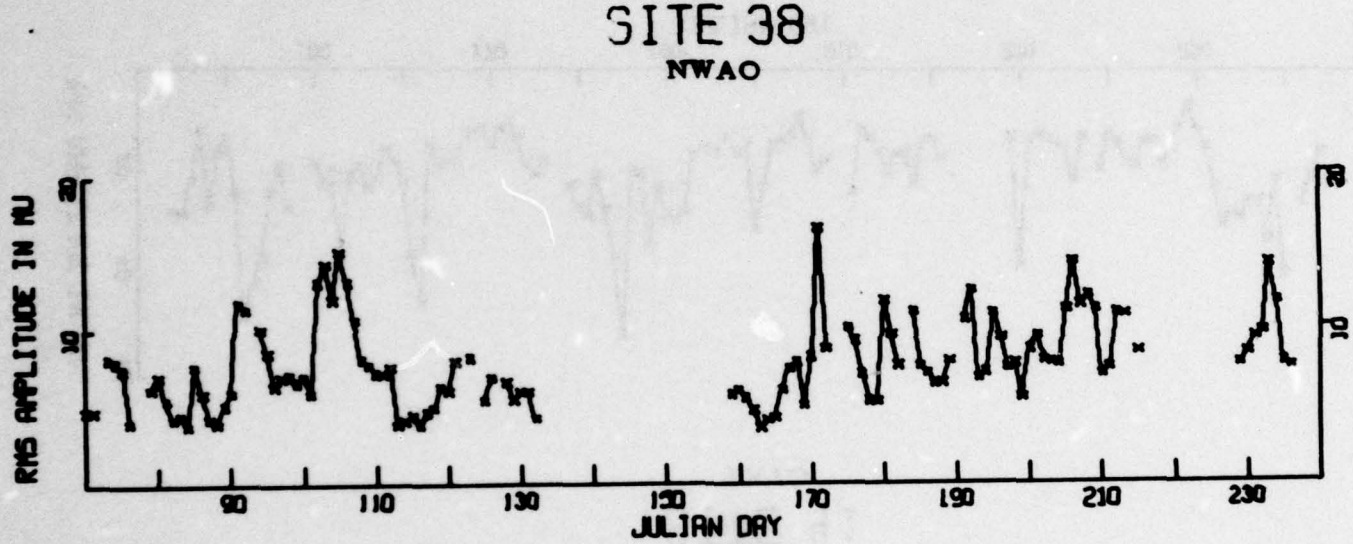

FIGURE IV-2

MAIO AND NWAO SHORT-PERIOD RMS NOISE

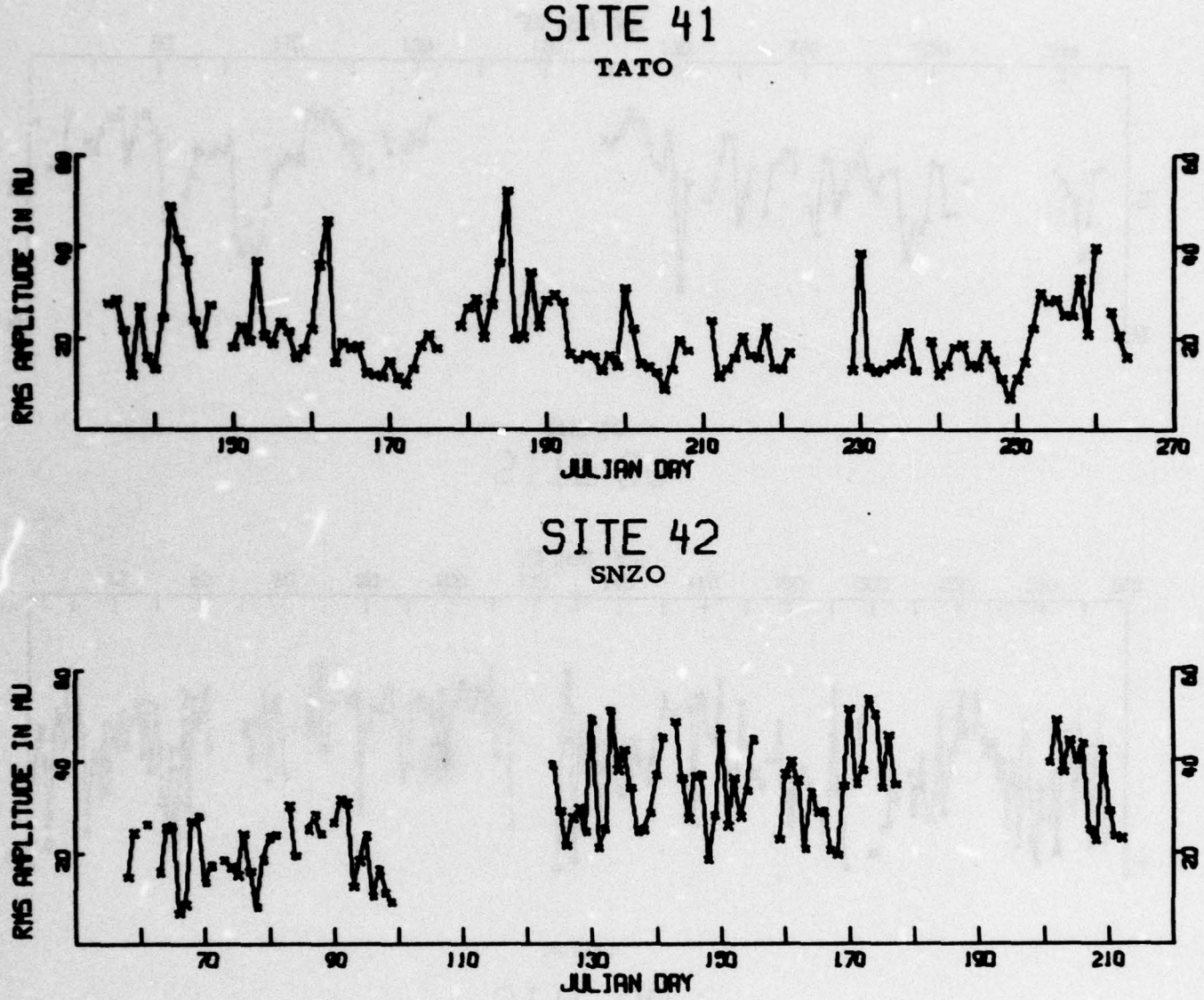

FIGURE IV-3

TATO AND SNZO SHORT-PERIOD RMS NOISE

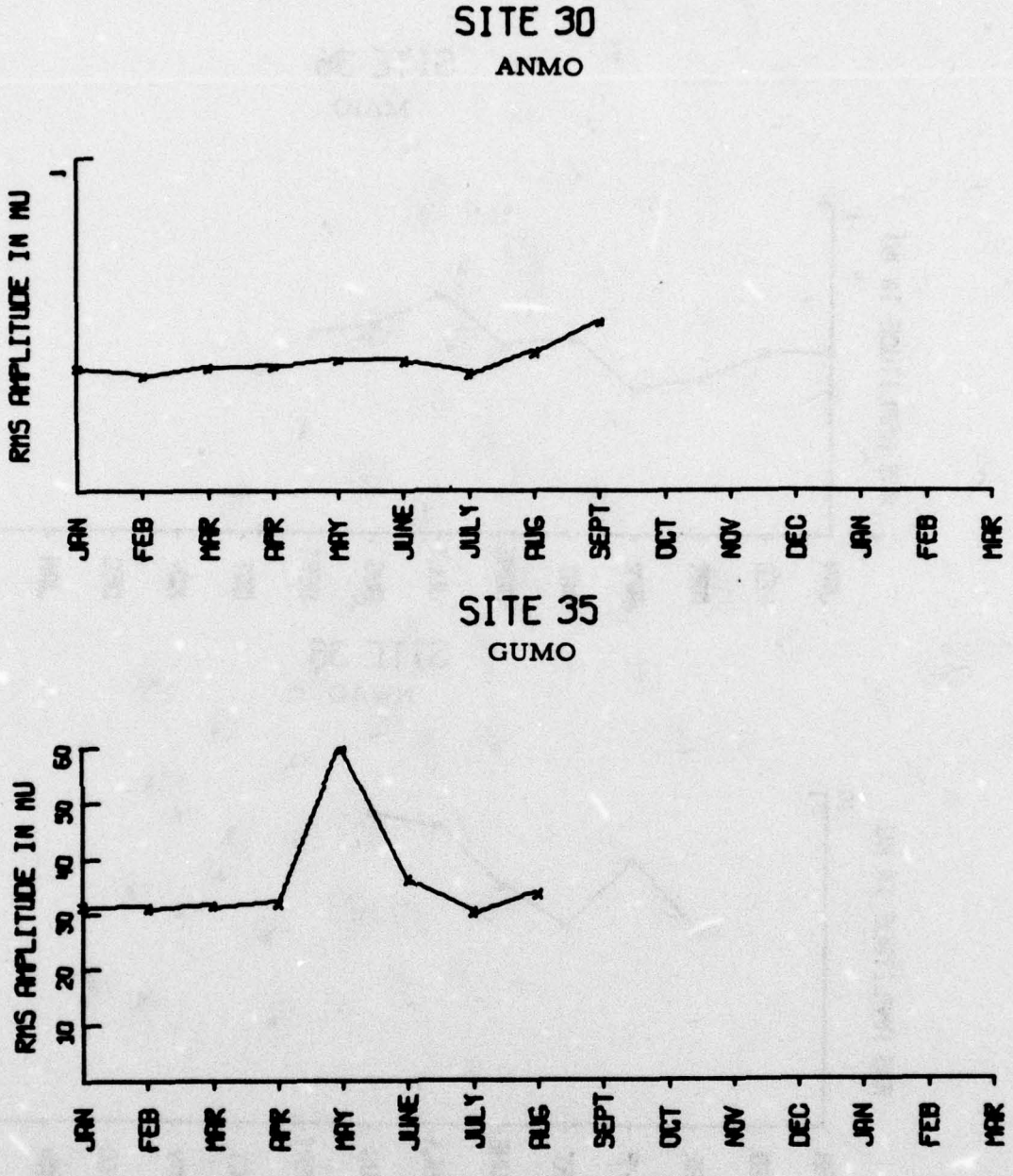

FIGURE IV-4

ANMO AND GUMO SHORT-PERIOD RMS NOISE TRENDS

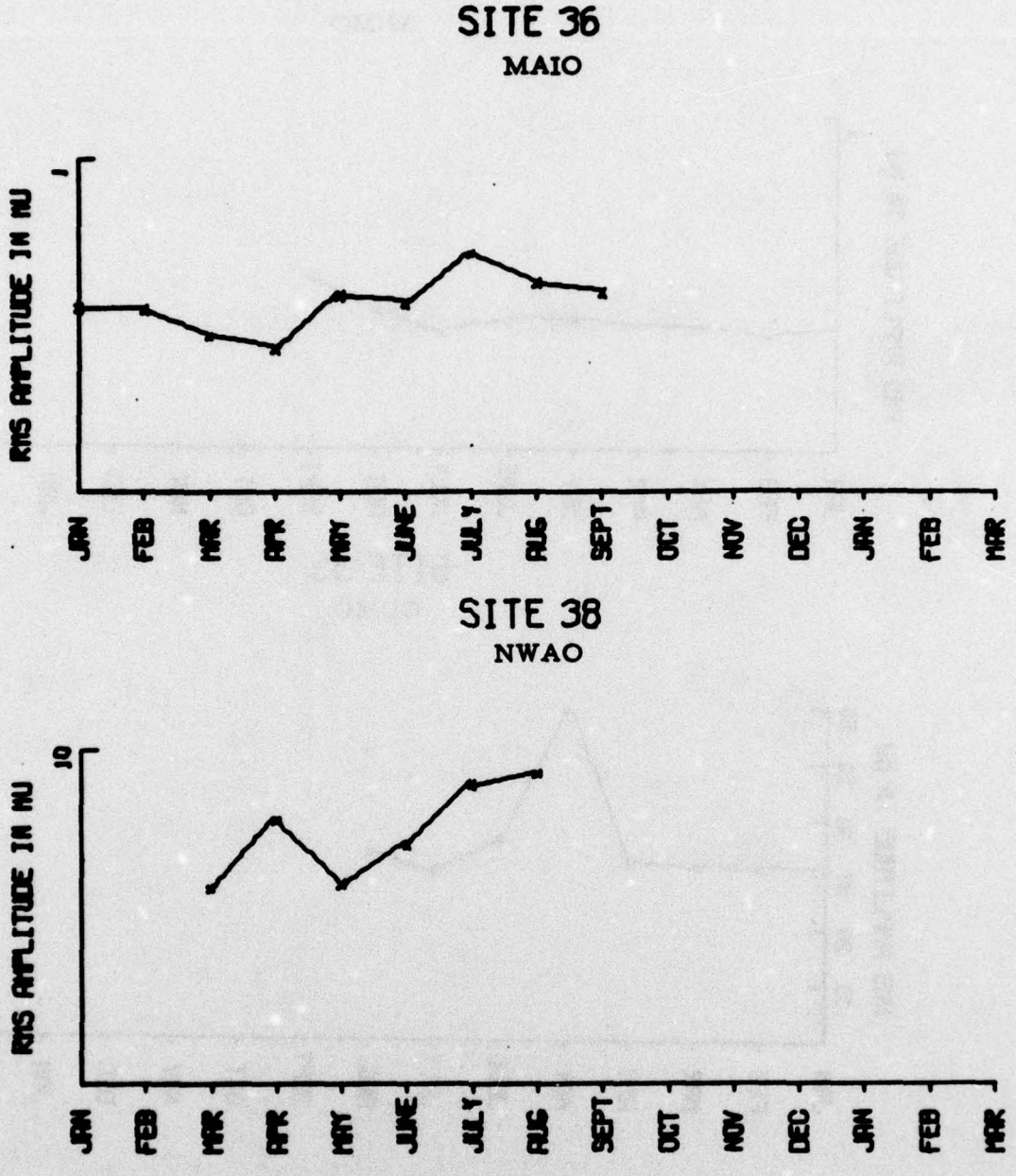

FIGURE IV-5

MAIO AND NWAO SHORT-PERIOD RMS NOISE TRENDS

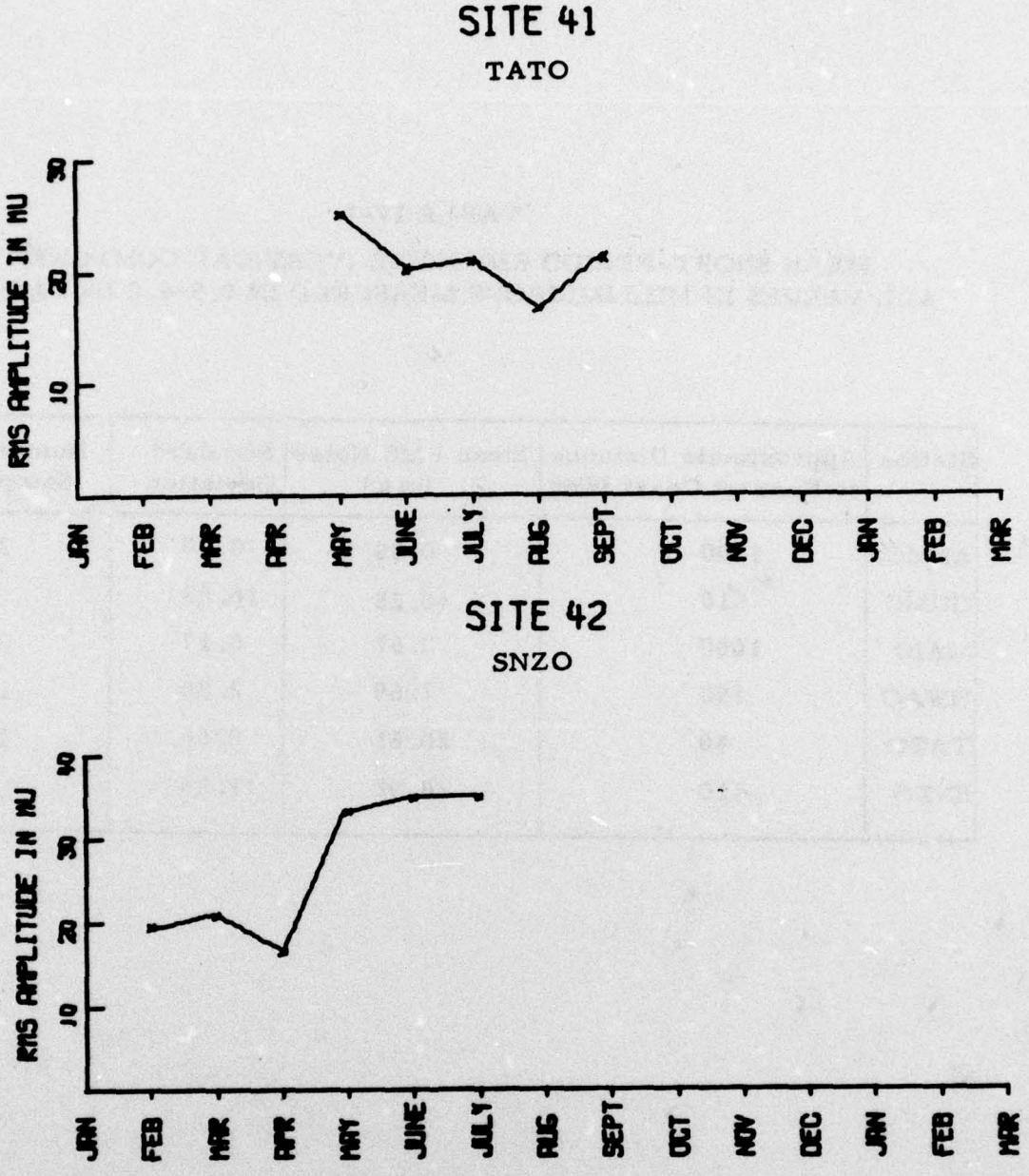

FIGURE IV-6

TATO AND SNZO SHORT-PERIOD RMS NOISE TRENDS

TABLE IV-1

MEAN SHORT-PERIOD RMS NOISE (VERTICAL COMPONENT) ALL VALUES IN MILLIMICRONS MEASURED IN 0.5-4.0 Hz PASSBAND

Station	Approximate Distance to Nearest Coast (Km)	Mean RMS Noise (mμ)	Standard Deviation	Number of Samples
ANMO	1100	0.38	0.09	244
GUMO	<10	40.25	16.83	53
MAIO	1000	0.57	0.17	222
NWAO	150	7.69	2.80	116
TATO	40	20.61	8.66	116
SNZO	<10	28.92	11.05	98

distant of the evaluated stations from the nearest coastline. Next in order of increasing RMS noise and decreasing distance to the nearest coastline is NWAO, followed by TATO. Although both GUMO and SNZO are essentially at the coastline, their mean short-period RMS noise values are substantially different. (Both are higher than the other stations.) This difference at these two stations may be due to the fact that the coastline nearest SNZO is that of the Cook inlet, which is somewhat sheltered from the open ocean, while GUMO lacks any such shelter from the ocean.

This correlation between mean short-period RMS noise and station-coastline separation suggests that, above an RMS 'baseline' of about 0.5 millimicrons, short-period noise is predominantly due to ocean wave energy injected to the land at the coastline.

During the course of the evaluation, it was requested that peak noise amplitudes be measured at one-second period for the short-period data. To perform this task, it was necessary to add a module to the parameter measurement section of the Interactive Seismic Processing System on the PDP-15 used in short-period data analysis. Once this was programmed, installed, and tested, measurement of short-period noise amplitudes was initiated. The noise amplitudes were measured as maximum zero-to-peak displacement of 1-second period waveforms in the gate preceding the signal waveform detected by the short-period automatic detector. This noise gate was normally approximately 20 seconds in length. The statistics of these measurements are reported in Table IV-2 in terms of the mean and standard deviation of the logarithm of the measured values. Note that exponentiating these means yields the geometric mean of the data.

C. THREE-COMPONENT LONG-PERIOD NOISE

The goals of the long-period noise analysis were to estimate the long-period RMS noise levels, the peak 25 second noise amplitudes, and

TABLE IV-2

SHORT-PERIOD NOISE
LOG_{10} [PEAK ONE-SECOND NOISE AMPLITUDE] STATISTICS

Station	Mean Log_{10} (AMP)	Standard Deviation Log_{10} (AMP)	Number of Samples
ANMO	-0.05740	0.16278	51
GUMO	1.85473	0.14499	27
MAIO	0.05679	0.15088	75
NWAO	0.95440	0.19597	38
TATO	1.49354	0.16769	27
SNZO	1.79363	0.17075	50

the spectral content of the noise field for each of the three components of motion (V, N, and E) at each station under evaluation. For each station, the evaluation time frame was from the date at which the station began recording data (or 1 January 1976, whichever was later) to 30 September 1976.

Noise samples were selected by reviewing the NORSAR event bulletins for daily time intervals during which no seismic events would be expected to be recorded at a given station. A 4096-second noise sample was then processed as described in Section II. All noise samples were kept in the recorded V, N, E configuration. Plots of each noise sample were examined for unreported signals and for system malfunctions such as spikes. Due to constraints on computer and analyst time, if either a signal or malfunction rendered the noise sample unusable, that noise sample was discarded and no replacement was attempted. If neither seismic signals nor malfunctions were observed, the entire 4096-second sample was included in the noise data base. In some cases, only part of the noise sample was unusable due to a signal or malfunction. When this occurred, 2048 seconds of the sample were included in the noise data base.

Those noise samples which passed this visual inspection were then input to a program which performs the following functions:

- Compute RMS noise values uncorrected for instrument response in the 0.023-0.059 Hz passband
- Compute RMS noise values corrected for instrument response using Parseval's formula in the 0.023-0.059 Hz passband
- Measure zero-to-peak 25-second noise amplitudes
- Compute the power spectrum for each trace of the noise sample and smooth to 128 frequencies.

All measured and computed values are output on punched cards to facilitate input to succeeding plot programs. The 25-second noise amplitudes are measured as the maximum 25-second noise amplitude of the entire noise sample.

The long-period RMS noise values in millimicrons (uncorrected for instrument response) for the vertical, north, and east components of motion are plotted versus Julian day in Figures IV-7 to IV-12. These values were measured in the 0.023-0.059 Hz passband. In these figures, values for consecutive days are connected by solid lines. Gaps of one or two days in length are generally due to bad noise samples. Longer gaps are generally due to down-time at the station, resulting in data not being available for analysis. The mean values and associated standard deviations for these RMS noise values are listed in Table IV-3.

Figures IV-7, IV-8, and IV-9 for ANMO, GUMO, and MAIO cover the same time period. For ANMO and MAIO, the great majority of the larger excursions from the mean occur during the days 1 to 90. In contrast, at GUMO the larger excursions from the mean are scattered throughout the time period covered. The implication of this observation is that cold weather and winter storms increase the noise level at ANMO and MAIO. Since GUMO is located much farther south than these two stations, it does not suffer from this problem.

Since the stations were not operational, no noise data exists for stations NWAO, TATO, and SNZO for the early months of 1976. Figures IV-10, IV-11, and IV-12 for these stations shows no particular pattern in the RMS noise level excursions from the mean for the months in which data were available.

Table IV-3 presents the mean long-period RMS noise amplitude for the stations under evaluation. The long-period noise does not show the strong correlation between noise level and station-nearest coastline separation

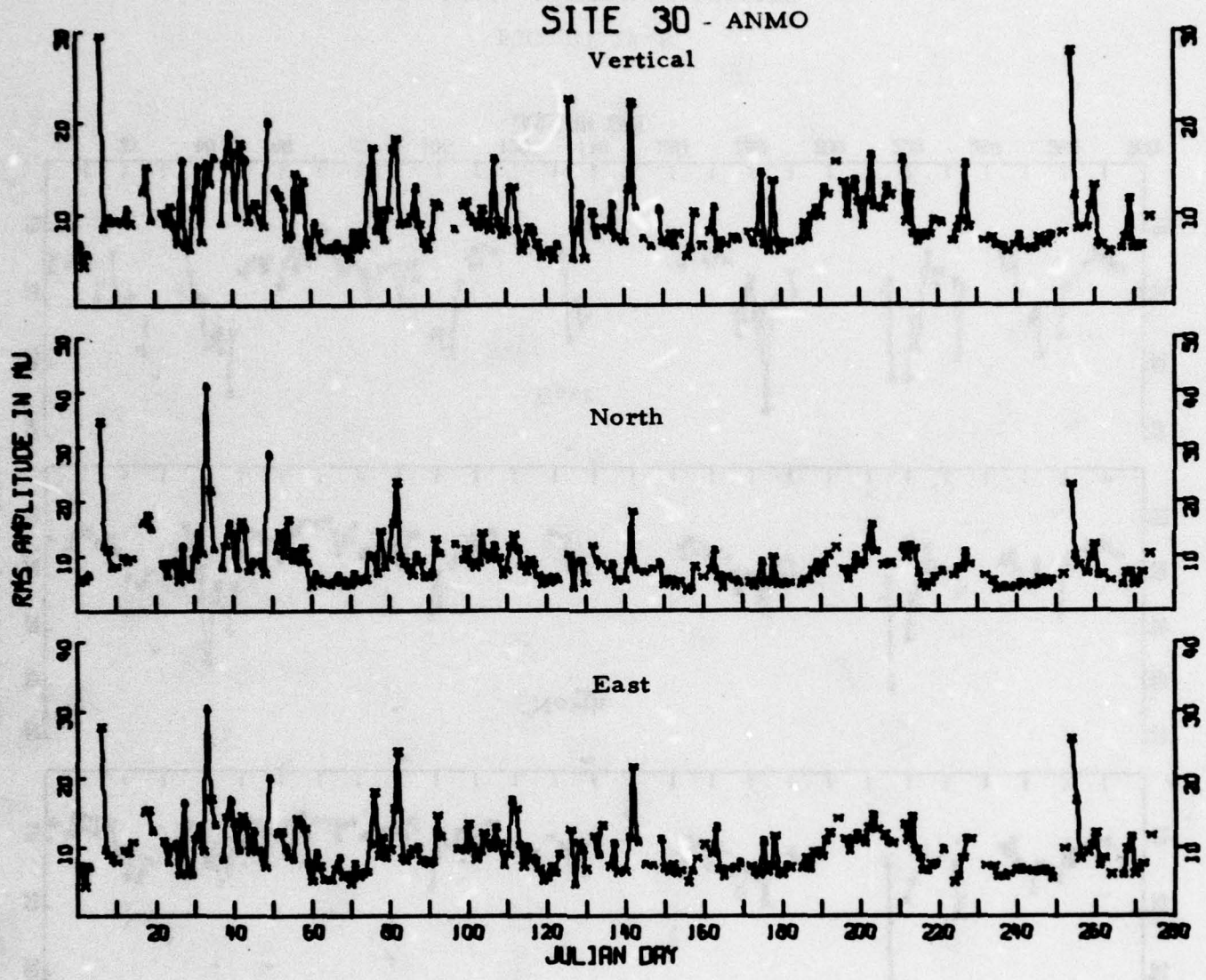

FIGURE IV-7

ANMO LONG-PERIOD RMS NOISE

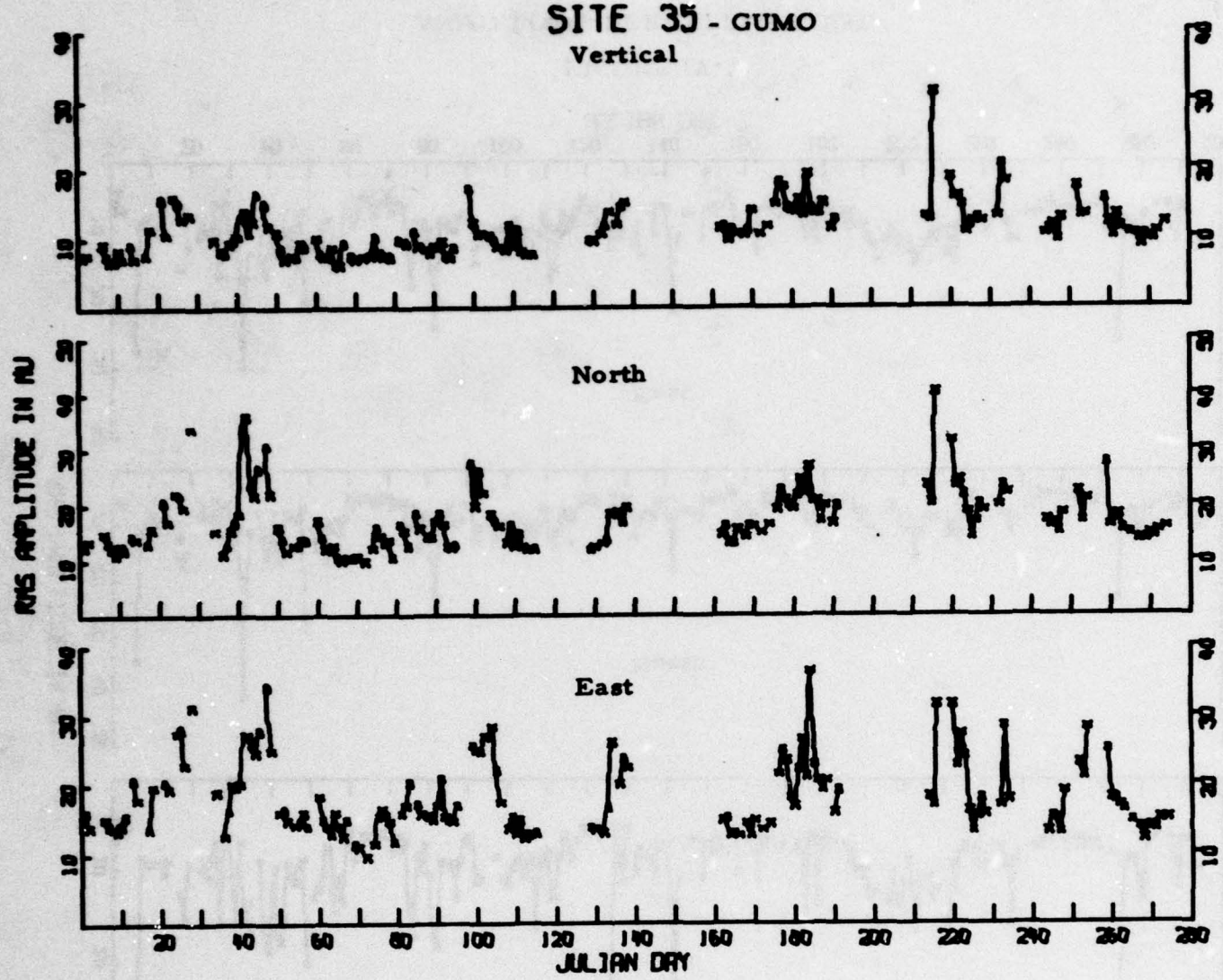

FIGURE IV-8

GUMO LONG-PERIOD RMS NOISE

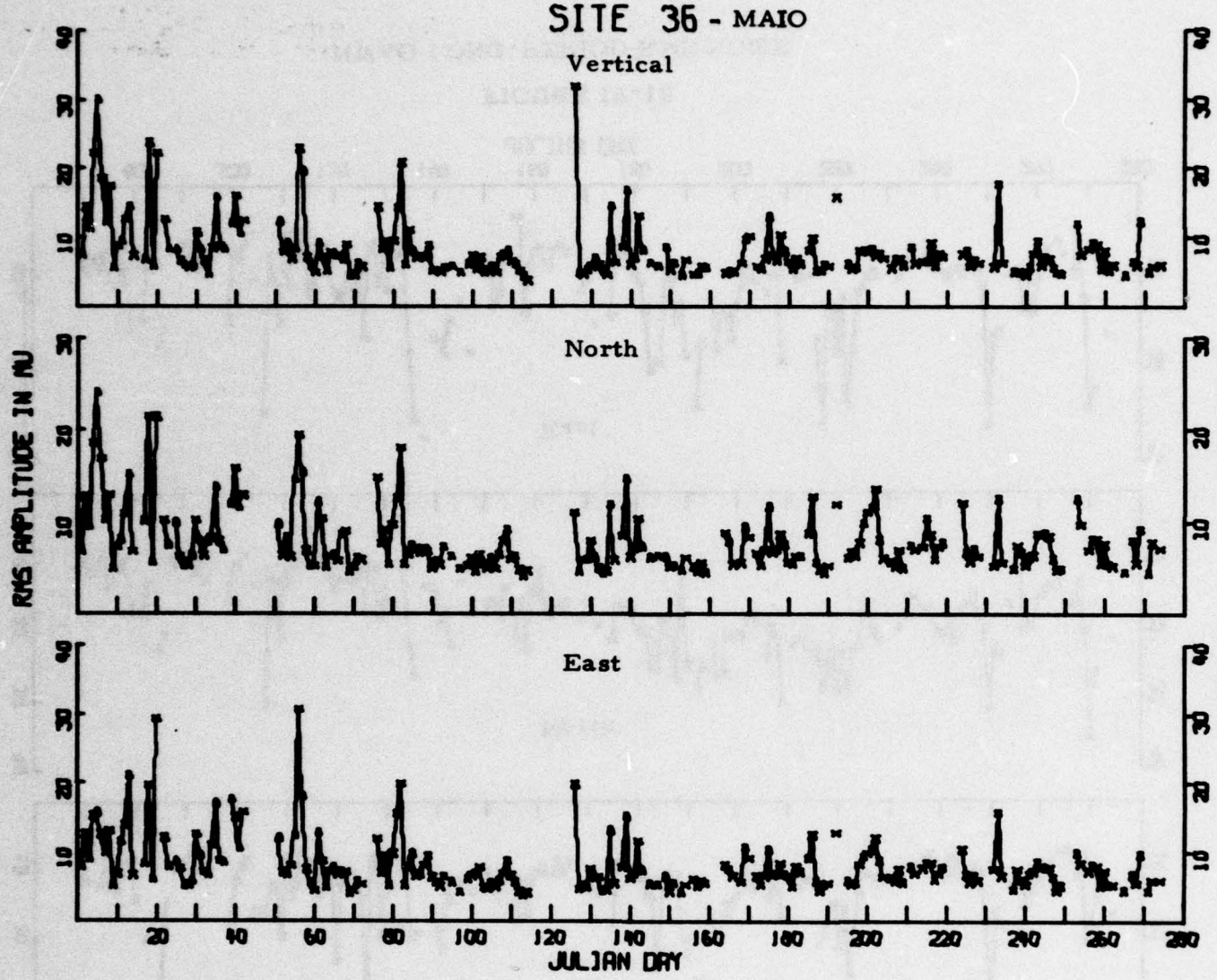

FIGURE IV-9

MAIO LONG-PERIOD RMS NOISE

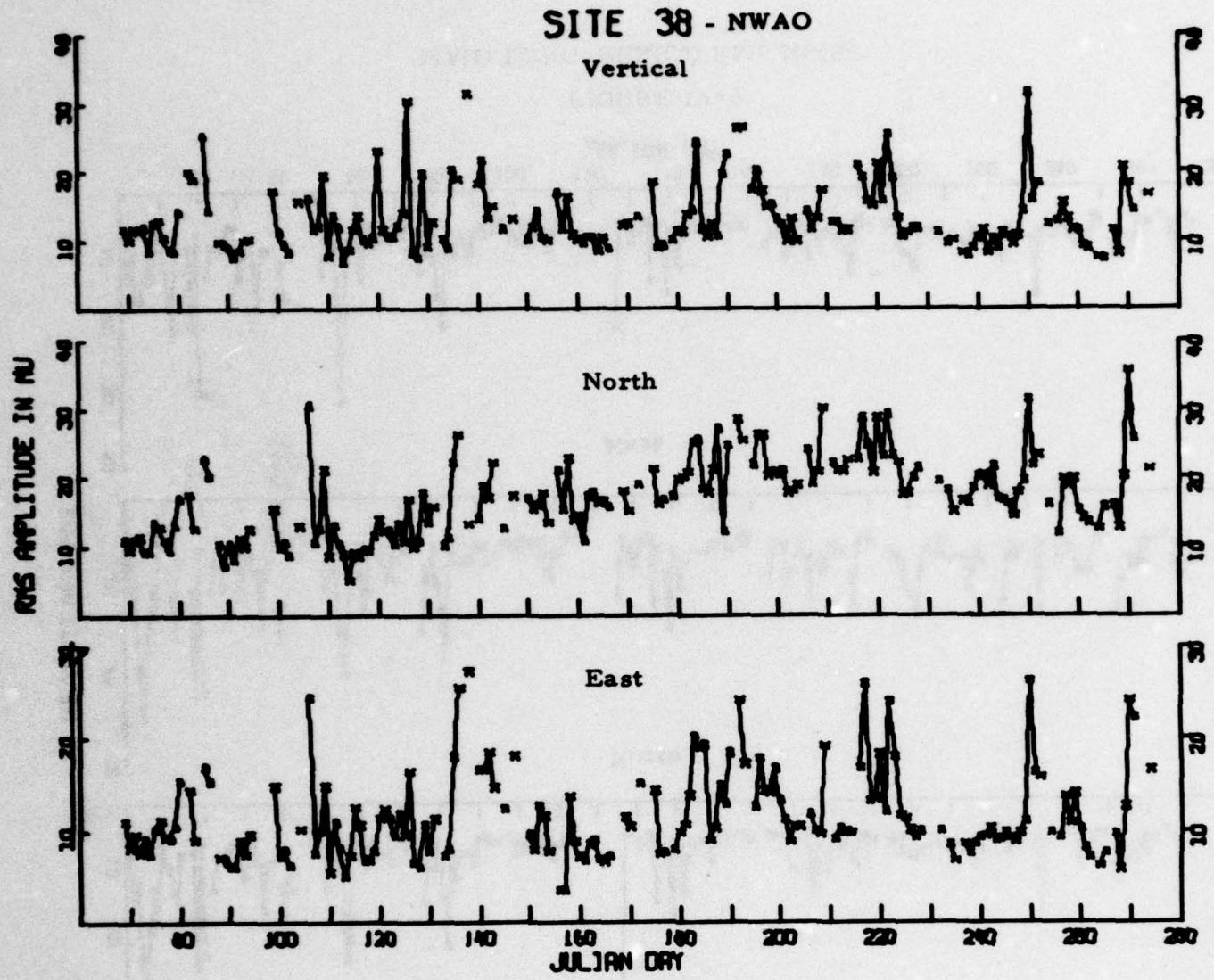

FIGURE IV-10

NWAO LONG-PERIOD RMS NOISE

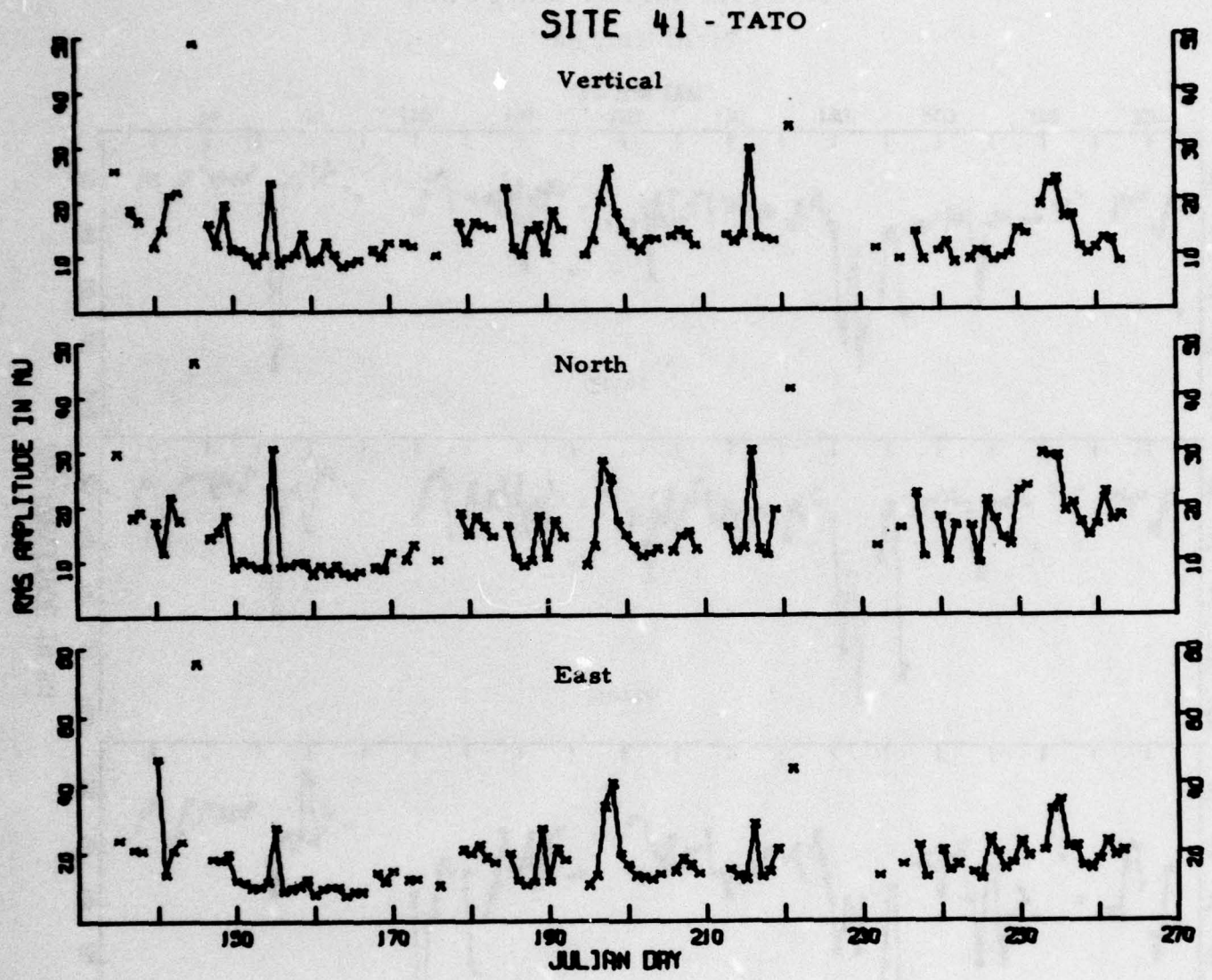

FIGURE IV-11

TATO LONG-PERIOD RMS NOISE

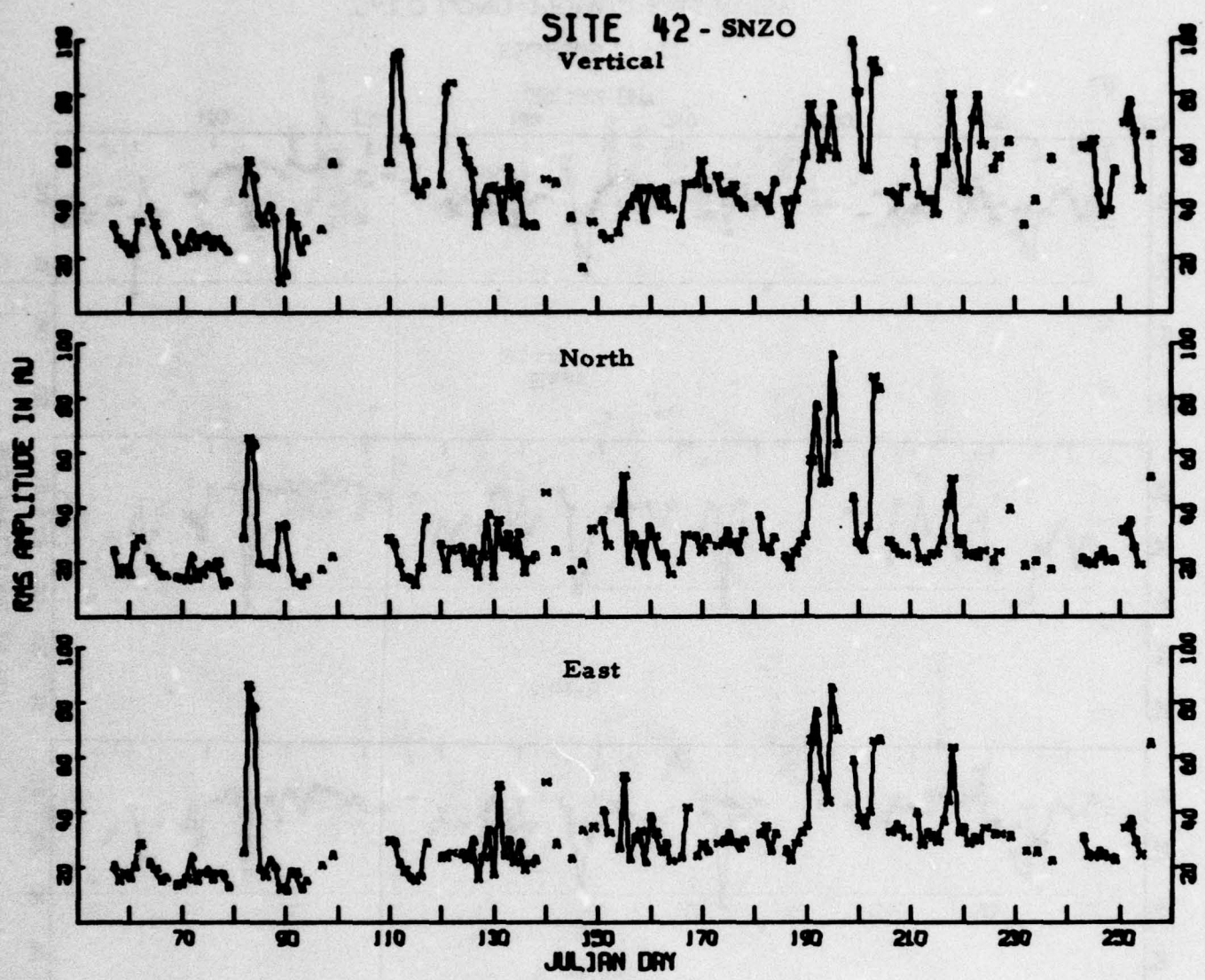

FIGURE IV-12

SNZO LONG-PERIOD RMS NOISE

TABLE IV-3

MEAN LONG-PERIOD RMS NOISE AMPLITUDES IN MILLIMICRONS

Station	Mean RMS Noise Amplitudes						No. of Samples
	Vertical		North		East		
	Mean	S. D.	Mean	S. D.	Mean	S. D.	
ANMO	9.56	3.83	8.66	4.65	9.76	3.87	221
GUMO	11.25	3.45	17.20	5.34	18.23	5.34	151
MAIO	8.20	4.37	7.89	3.45	8.19	4.00	207
NWAO	13.44	4.85	17.29	5.67	11.61	4.79	167
TATO	14.22	6.04	15.65	7.14	18.12	9.56	95
SNZO	45.92	17.28	27.26	14.22	30.17	14.41	148

S. D. = Standard Deviation

that was found for the short-period noise. The stations can be grouped by noise level, however. Stations ANMO and MAIO form the group with lower noise levels and stations GUMO, NWAO, and TATO form the goup with higher noise levels. Considering the locations of these stations, this suggests that the somewhat higher noise levels at GUMO, NWAO, and TATO are due to wave energy injected at the coastline. (Station SNZO was not included in this grouping, since the noise levels at this station seem too high to be due to seismic noise.)

Figures IV-13 to IV-18 show the monthly noise level trends for the stations under evaluation. Stations ANMO and MAIO show a downward trend in noise level from January 1976 to September 1976. It seems reasonable to ascribe this trend to the decrease in storm activity with the passing of the winter months and associated winter storms. Station GUMO shows a general upward trend in noise level during the same time period. Considering the location of the station, it seems possible that this increase in seismic noise is due to wave energy generated by tropical storms. Stations NWAO and SNZO show a general upward trend in noise levels from their start-up dates to September 1976, dropping off slightly after peaking in July 1976. Since these stations are in the southern hemisphere, this represents an increase in noise level with the onset of the winter months. Again, this increased winter noise can be associated with increased storm activity. Disregarding the noise level for May 1976, station TATO shows an upward trend in noise level in the same manner as station GUMO. Thus, this increase can be ascribed to increased tropical storm activity in the late summer months.

Figures IV-19 to IV-24 show the average RMS amplitude spectra for the noise at each station under evaluation. These spectra are uncorrected for instrument response. They were determined by averaging the individual spectra computed from the noise samples and converting them to RMS amplitudes using Parseval's formula:

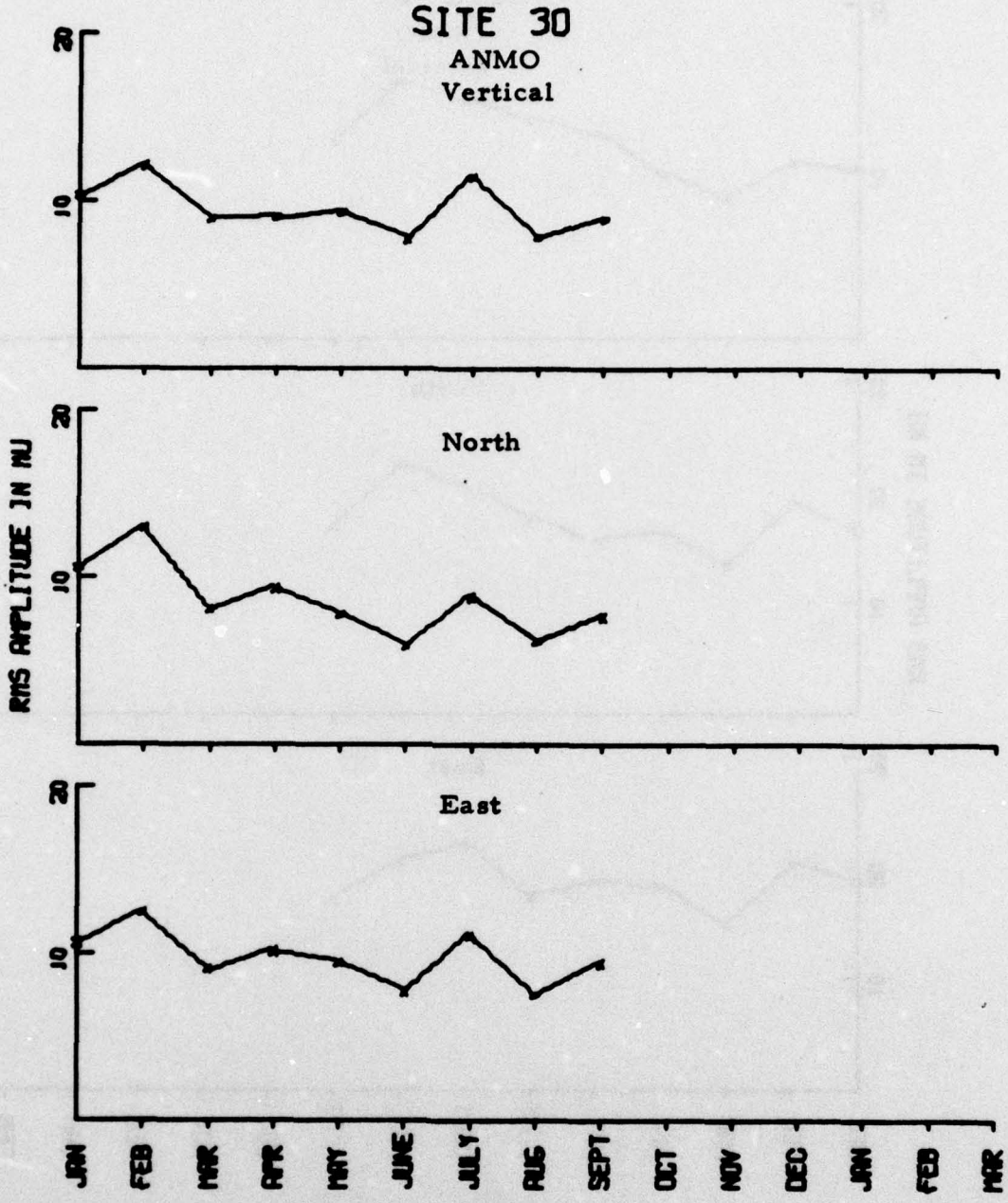

FIGURE IV-13

ANMO LONG-PERIOD RMS NOISE TRENDS

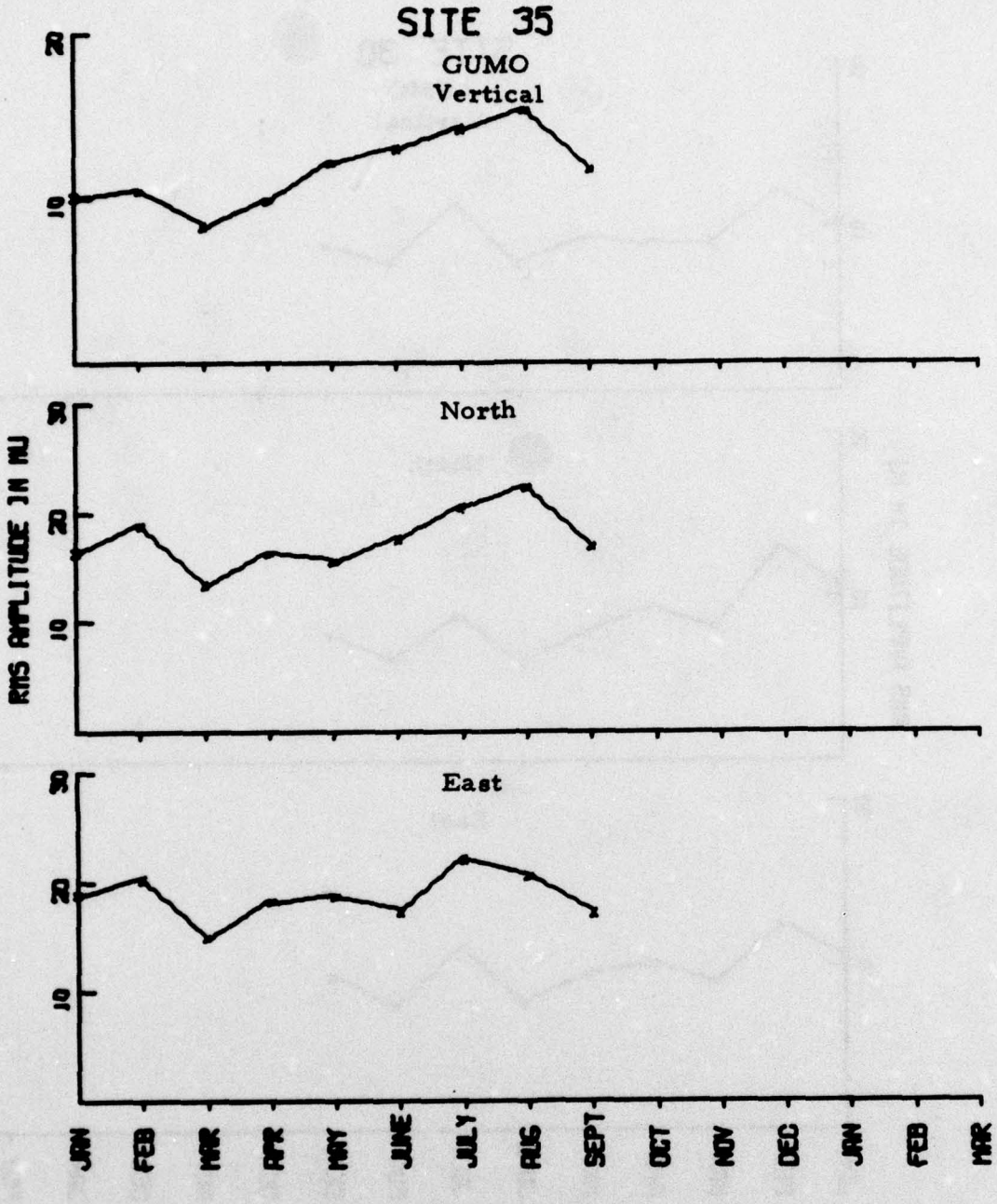

FIGURE IV-14

GUMO LONG-PERIOD RMS NOISE TRENDS

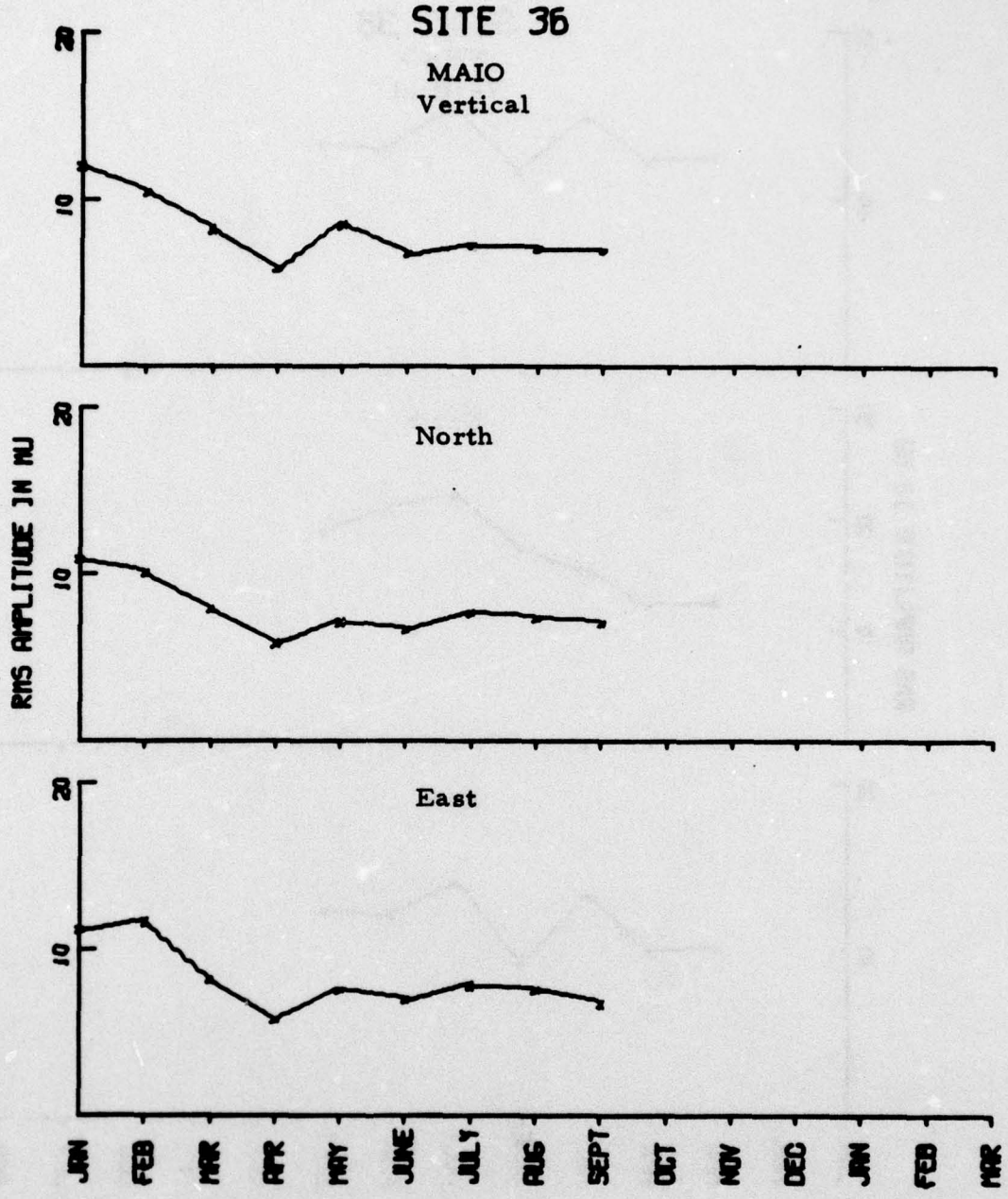

FIGURE IV-15

MAIO LONG-PERIOD RMS NOISE TRENDS

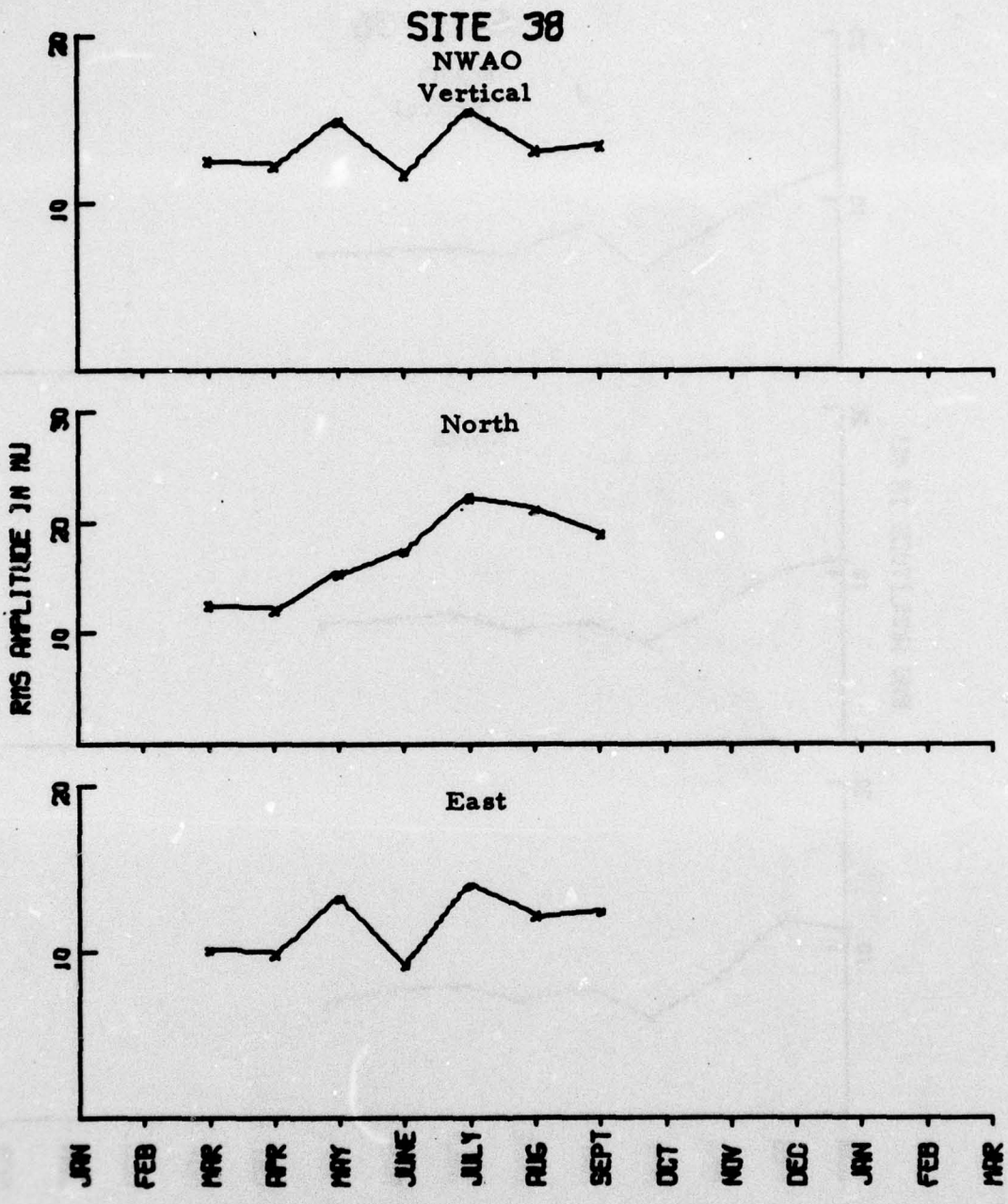

FIGURE IV-16

NWAO LONG-PERIOD RMS NOISE TRENDS

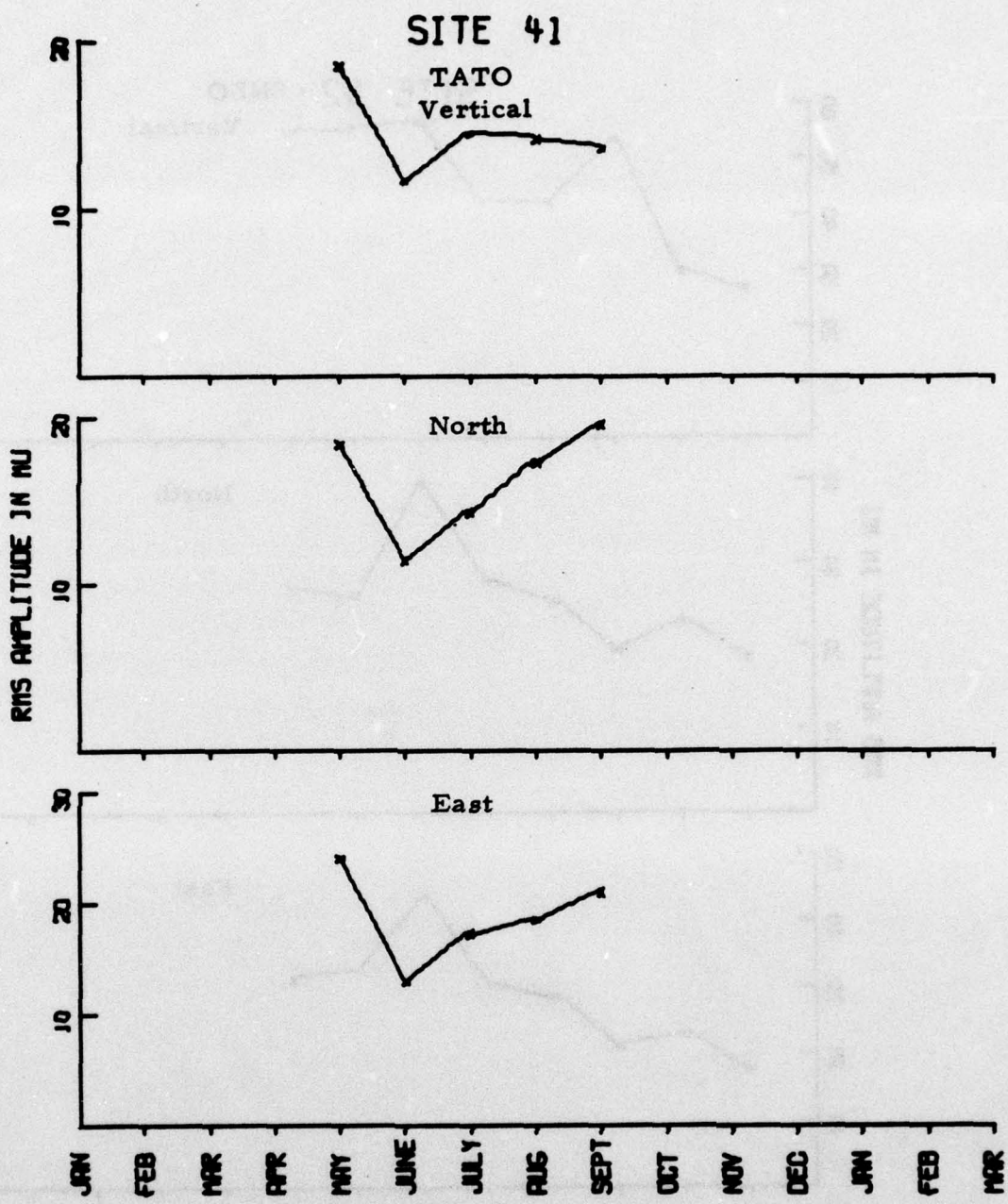

FIGURE IV-17

TATO LONG-PERIOD RMS NOISE TRENDS

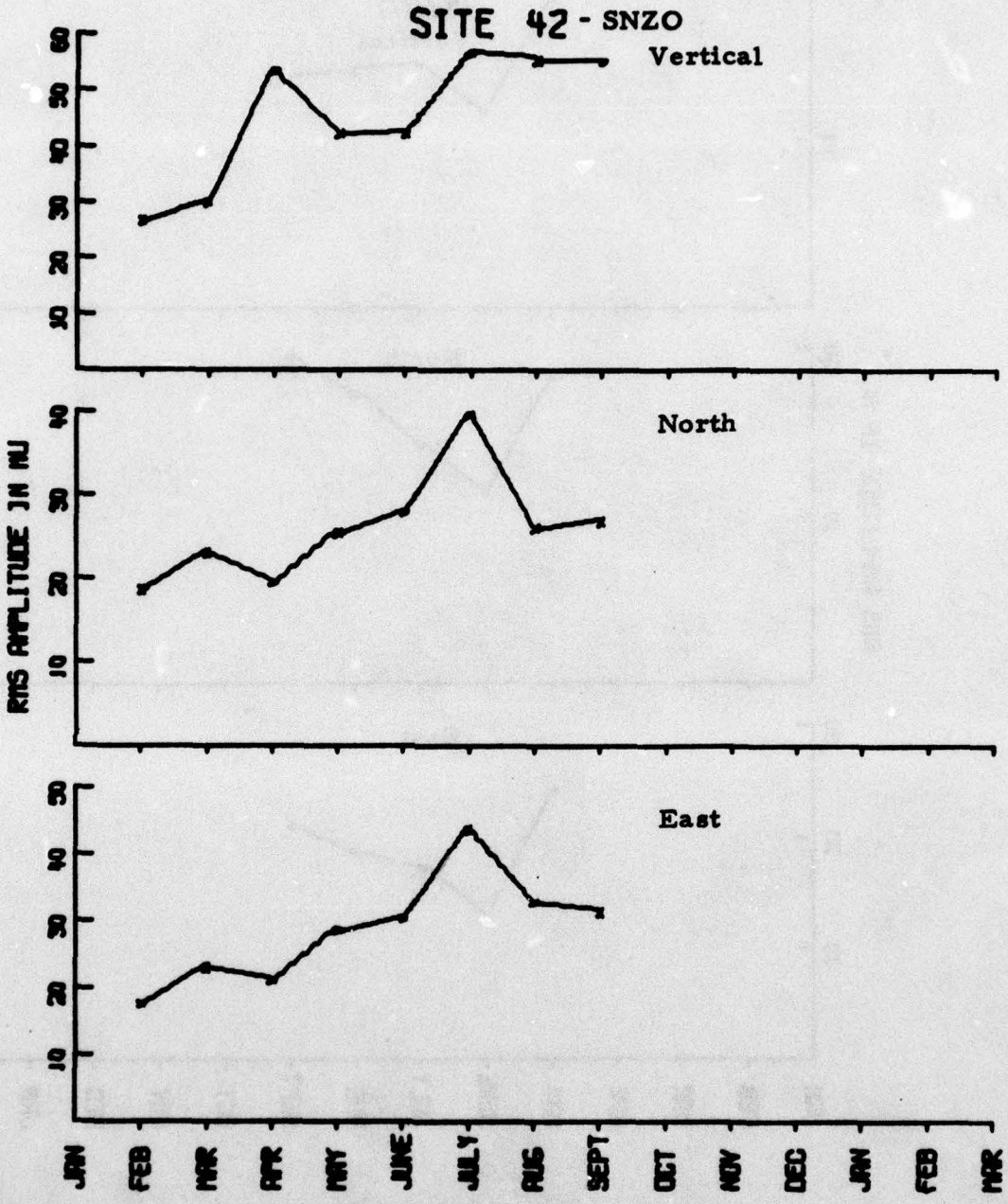

FIGURE IV-18

SNZO LONG-PERIOD RMS NOISE TRENDS

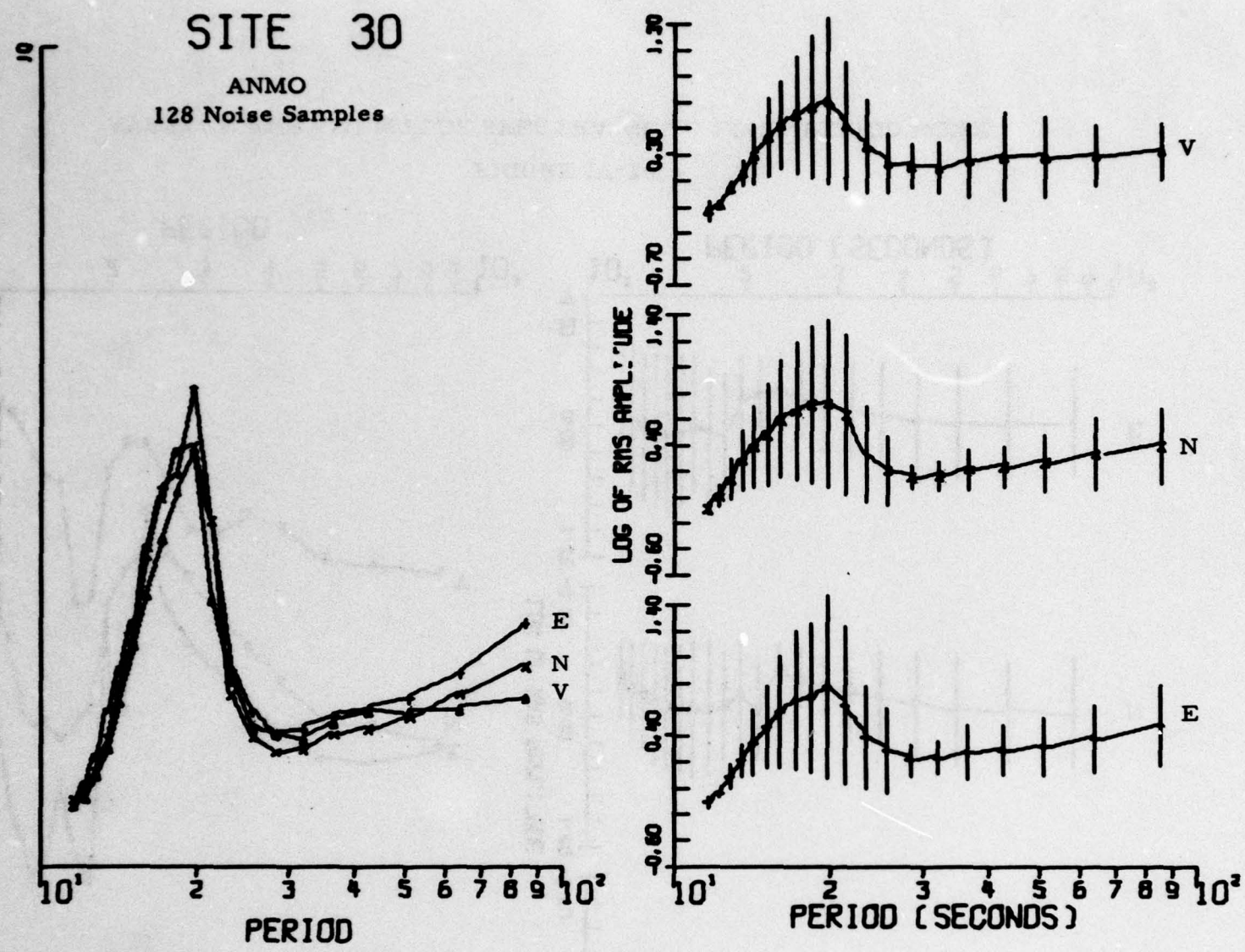

FIGURE IV-19

AVERAGE RMS AMPLITUDE SPECTRA-ANMO LONG-PERIOD NOISE

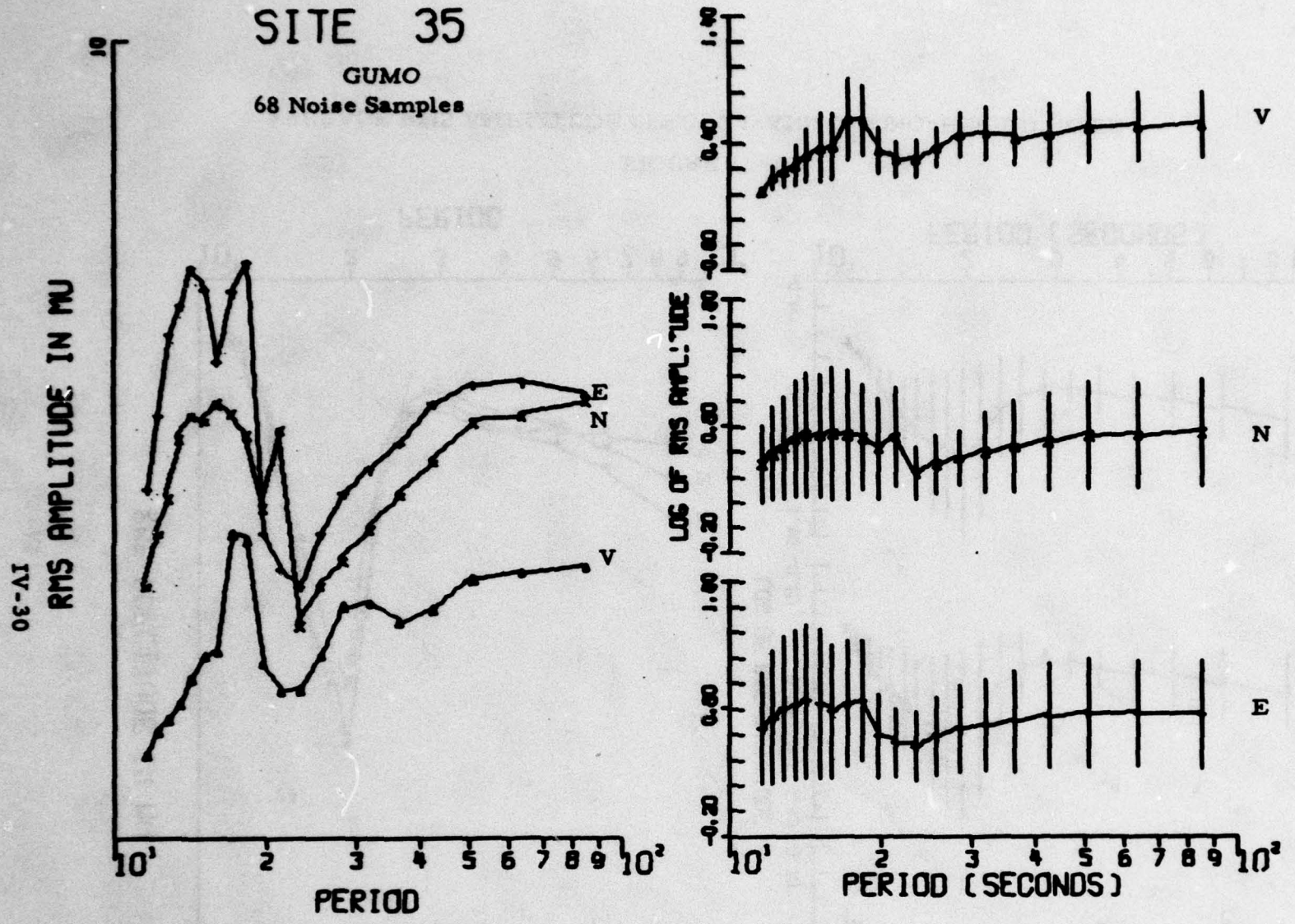

FIGURE IV-20

AVERAGE RMS AMPLITUDE SPECTRA-GUMO LONG-PERIOD NOISE

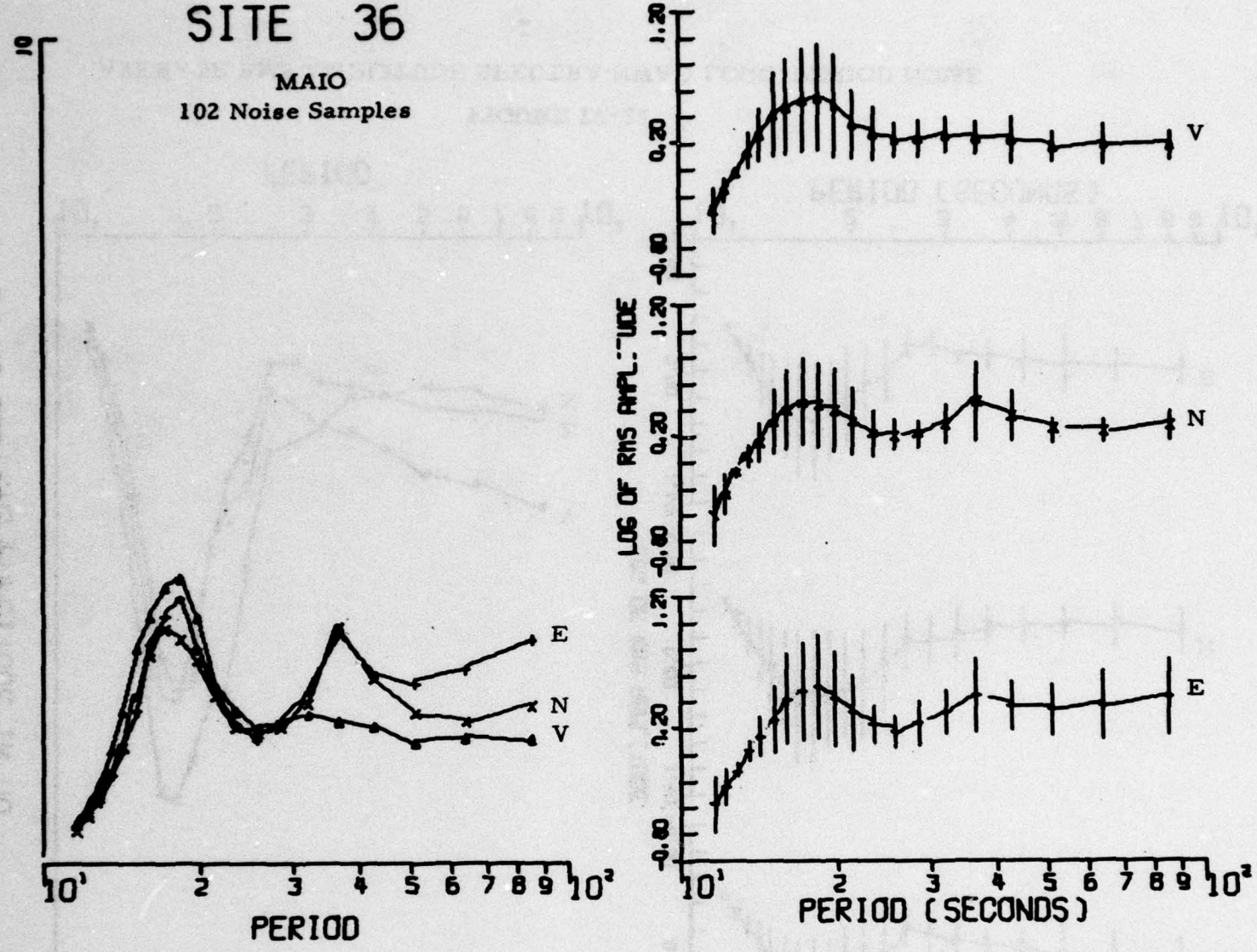

FIGURE IV-21

AVERAGE RMS AMPLITUDE SPECTRA-MAIO LONG-PERIOD NOISE

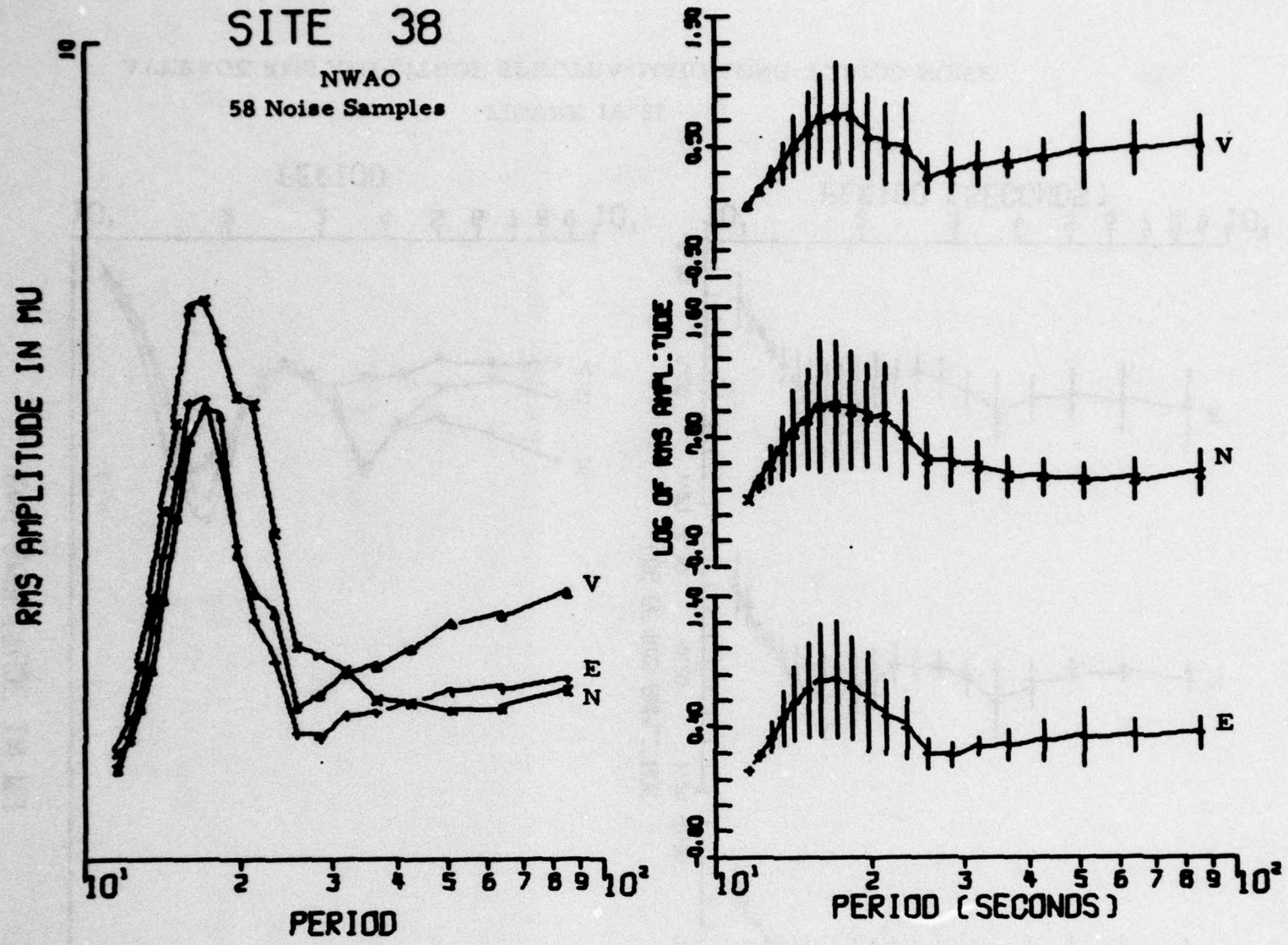

FIGURE IV-22

AVERAGE RMS AMPLITUDE SPECTRA-NWAO LONG-PERIOD NOISE

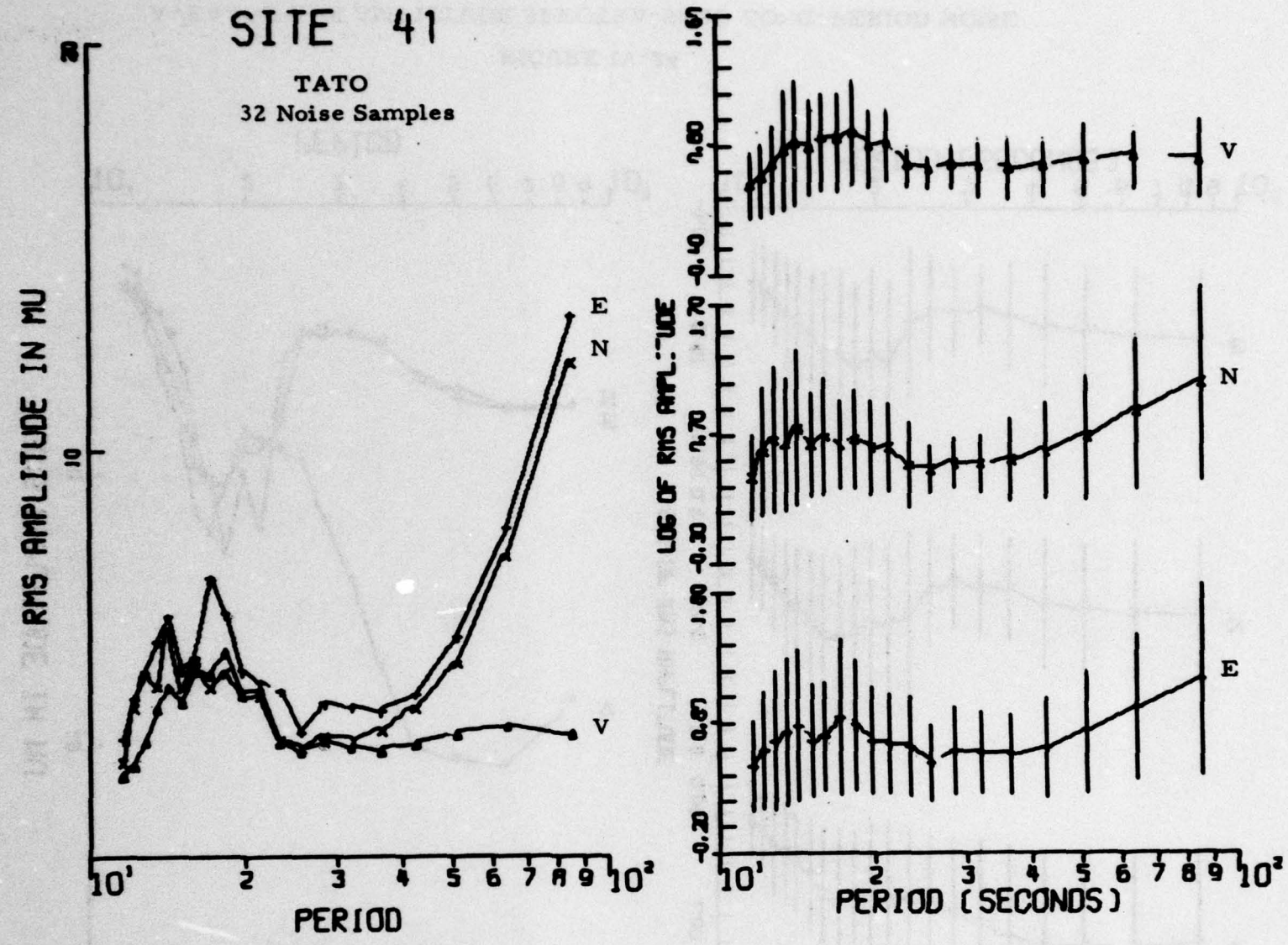

FIGURE IV-23

AVERAGE RMS AMPLITUDE SPECTRA-TATO LONG-PERIOD NOISE

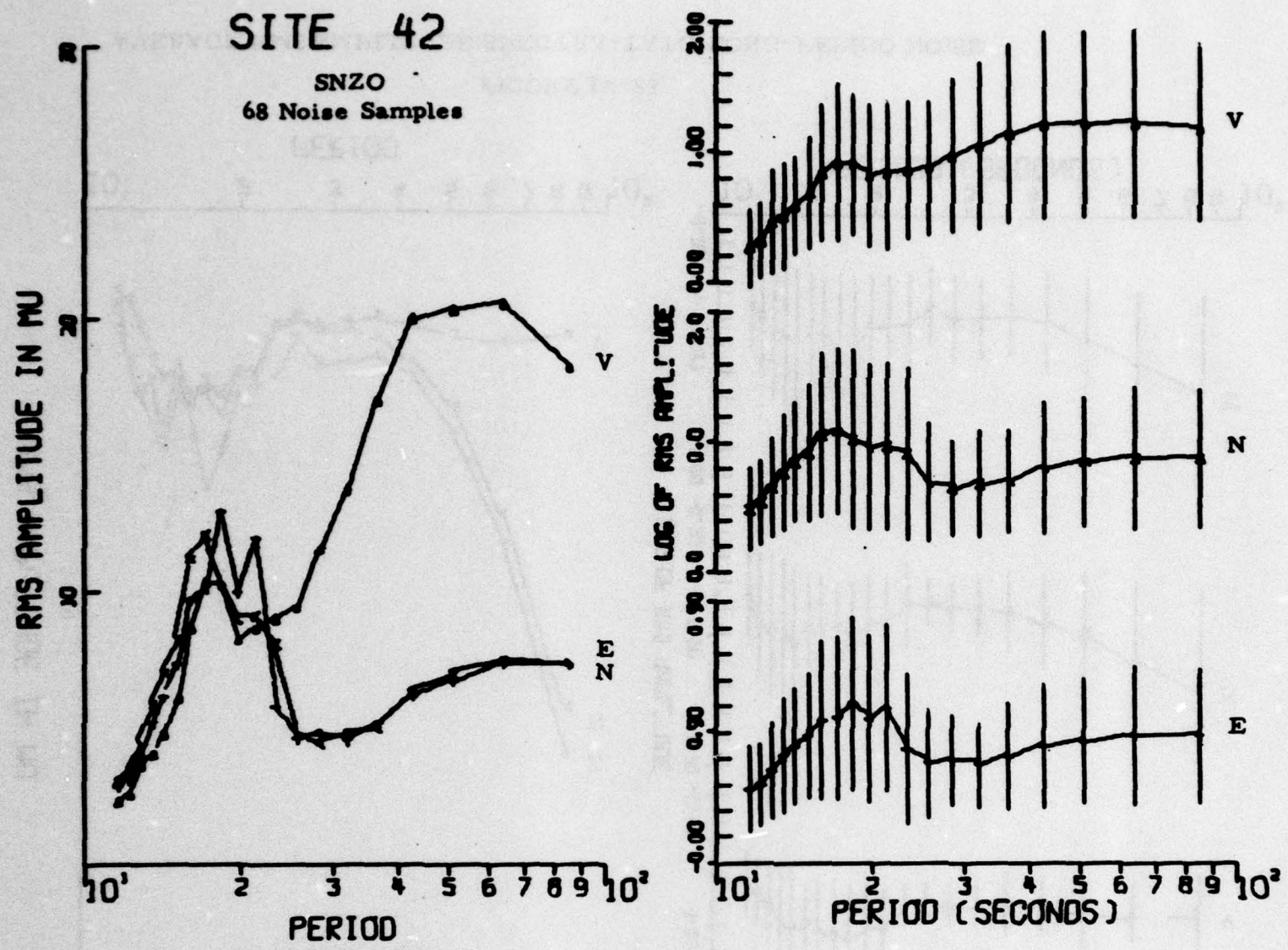

FIGURE IV-24

AVERAGE RMS AMPLITUDE SPECTRA-SNZO LONG-PERIOD NOISE

$$RMS_a^b = \sqrt{f \sum_{i=a}^{b} |A(f_i)|^2 * C(f_i)^2}$$

where Δf = the elemental frequency interval (f=0.001953 Hz)

$|A(f_i)|^2$ = the discrete Fourier transform spectral density estimate at frequency f_i,

$C(f_i)$ = the instrument response correction at frequency f_i,

a = the initial frequency index, and

b = the final frequency index.

Since the RMS amplitude at each discrete frequency was desired, in this case a=b. Also, since no instrument response corrections were made, $C(f_i)=1$ for all frequencies.

The left-hand side of each figure shows the average RMS noise amplitude spectra for each component of motion. These spectra were computed for the period range of 11.6 to 85.3 seconds so that the analyst can inspect the noise levels in and around the signal periods. The right-hand side of each figure shows the log mean spectra with vertical bars representing plus and minus one standard deviation. These are presented to give a qualitative idea of the day-to-day variability of the noise from period to period.

The following comments can be made about the individual figures:

- Figure IV-19---ANMO noise: The three components show nearly identical spectral content and level of the local noise field. The noise field has its greatest day-to-day variability between 14 and 25 seconds period.
- Figure IV-20---GUMO noise: The three components show markedly different spectral content and level of the local noise field from one component to the next. The horizontal components

show higher noise levels and day-to-day variability then does the vertical component.

- Figure IV-21 - MAIO noise: At periods below 30 seconds, the three components show nearly identical spectral content and level of the local noise field. The horizontal components show a secondary peak at 37 seconds nearly as large as the microseismic peak. The noise field has its greatest variability between 14 and 23 seconds period for all components and at 37 seconds period for the horizontal components.

- Figure IV-22 - NWAO noise: The three components of noise recorded at this station show more variation in spectral content and level of the noise from one to the next than do the three components of noise recorded at ANMO or MAIO. The noise field has its greatest day-to-day variability between 13 and 23 seconds period.

- Figure IV-23 - TATO noise: At periods below 35 seconds, the three components show similar spectral content and level of the noise. The component-to-component variation appears no greater than that observed at NWAO. Above 35 seconds, the horizontal components show rapidly increasing noise levels while the vertical component remains fairly constant. The day-to-day variation appears to be quite large at all frequencies.

- Figure IV-24 - SNZO noise: At periods below 20 seconds, the three components show similar spectral content and level of the noise. The component-to-component variation appears no greater than that observed at NWAO and TATO. At periods above 20 seconds, the vertical component noise increases rapidly, causing

the high RMS noise values observed in Table IV-3. The day-to-day variation appears to be quite large at all frequencies.

The above comments lead the author to believe that oceanic wave energy plays a large part in determining the level, spectral content, and variability of the local long-period noise field for stations near the coast. Stations ANMO and GUMO of the six evaluated show low noise levels, very similar noise spectra for the three components, and day-to-day noise variations which are large only near the microseismic peak. As the station-coastline separation decreases, the noise levels rise, the differences among the spectra of the three components increase, and the day-to-day variability of the noise rises. While the effect of oceanic wave energy on the long-period noise field is not as severe as it is on the short-period noise field, it is in the author's opinion significant enough to affect the detection capability of the station. The spectral horizontal components at longer periods appear to be abnormally high when compared to those of other stations. This is apparently due to the seismometer being underwater.

The level and spectral content of the vertical component of the SNZO noise field do not appear reasonable. The filtering of the broadband data to produce the long-period data cut down the 64-second data by approximately 9 dB relative to the 25-second data. However, Figure IV-24 shows that after this filtering, the 64-second data are approximately 7 dB above the 25-second data. These high noise levels at longer periods have been ascribed to electronic noise on the vertical component.

When the average noise spectra for GUMO were plotted, it was noticed that they were quite different from those prepared for the preliminary Seismic Research Observatories evaluation, which were made by averaging the spectra of noise samples recorded during the period January to April, 1976. Figure IV-25 was created to investigate this difference. Each plot of this figure shows the average spectra for noise samples recorded during one

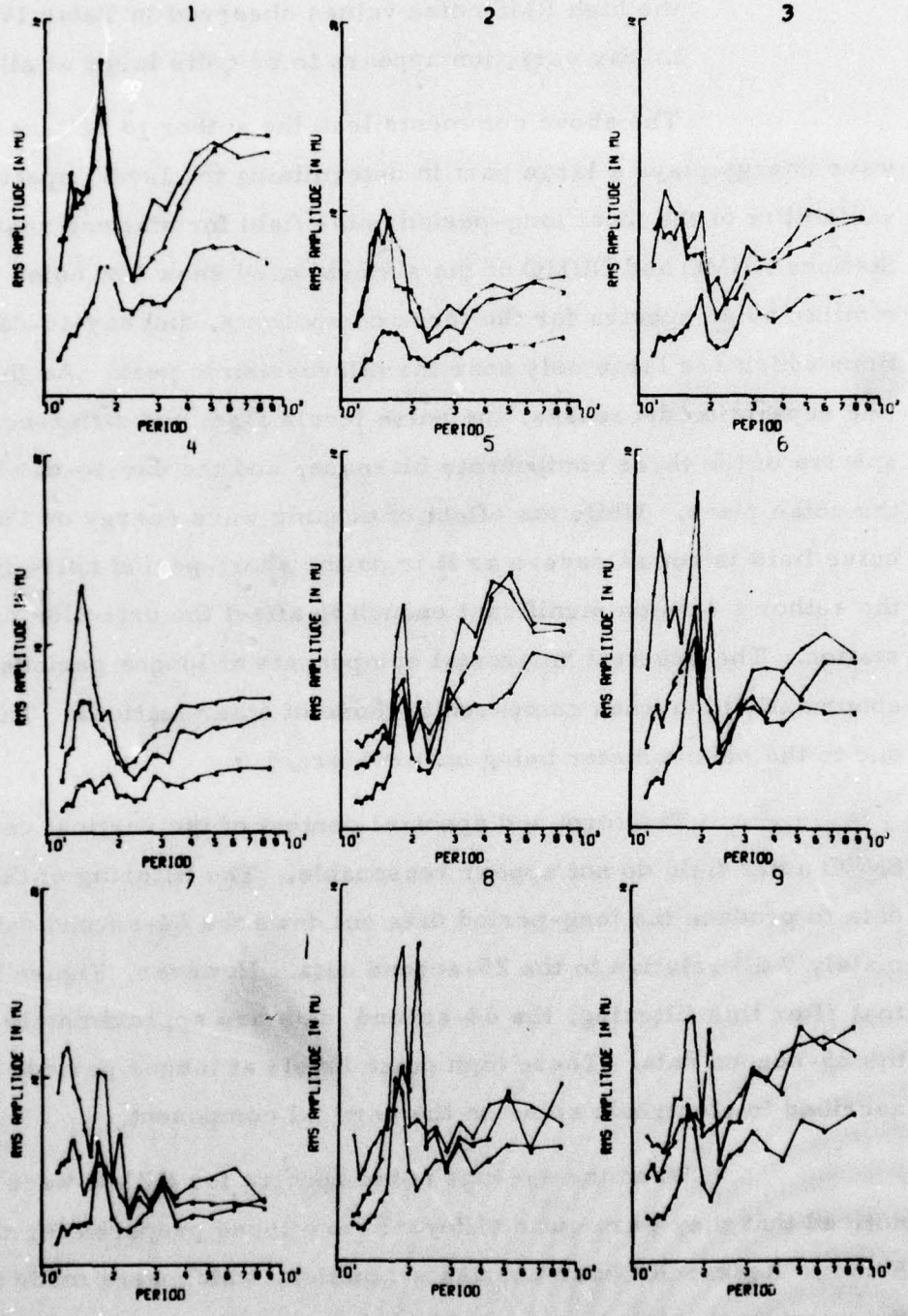

FIGURE IV-25

GUMO MONTHLY AVERAGE RMS AMPLITUDE SPECTRA

month of 1976. (The number at the top of each plot indicates the month.) Although the noise spectra for the first four months show marked variations from one to the next, they form a group distinctly different from the noise spectra for the succeeding months. These months show much greater variations in noise level and spectral content than do the first four months. Thus, it is not surprising that the nine-month average presented in this report differs so much from the four-month average presented last year.

Peak 25-second noise amplitudes were measured on all noise samples during the course of the noise analysis. Each value measured represents the absolute value of the largest zero-to-peak excursion of a waveform of period 25 seconds plus-or-minus one second. Table IV-4 lists the mean and standard deviation of the logarithms of the measured peak amplitudes for each station. They are presented in this form since it is in this form that they are used in the evaluation of the Seismic Research Observatory network (Section VII).

TABLE IV-4

MAXIMUM 25 SECOND NOISE AMPLITUDES
MEAN LOG_{10} (AMPLITUDE)

Station	Vertical		North		East		No. of Samples
	Mean	S. D.	Mean	S. D.	Mean	S. D.	
ANMO	1.38	0.16	1.35	0.19	1.42	0.16	222
GUMO	1.62	0.16	1.73	0.15	1.73	0.17	70
MAIO	1.36	0.17	1.36	0.16	1.37	0.16	207
NWAO	1.54	0.15	1.59	0.15	1.43	0.17	167
TATO	1.59	0.15	1.63	0.18	1.68	0.19	95
SNZO	2.10	0.16	1.84	0.17	1.88	0.16	145

SECTION V

SRO DETECTION CAPABILITY

A. DISCUSSION

In past evaluation tasks, detection statistics were derived from an event population for every member of which a clear detection/non-detection decision could be made; i. e., the analyst could state that he either saw the sought-for signal or he saw seismic noise. Unfortunately, the world does not always present the analyst with such a clear-cut case. Mixed events, system failures resulting in no data being recorded, and malfunctions all tend to obscure the detection capability picture.

The term 'mixed event' refers to the case where the sought-for signal is obscured or completely masked by a second signal. This can happen either when the two signals arrive at the station at essentially the same time or when a larger signal arrives before the signal under analysis, burying this signal in its coda. The term 'system failure' refers to the total shutting down of the station so that no data is recorded. The term 'malfunction' refers to any partial failure of the system, from sensor unit to reception of data at the Seismic Data Analysis Center, which causes degradation of the seismic data.

The problem of mixed events is often difficult for the analyst to resolve and is probably the major source of false alarms. (The term 'false alarm' in this case means declaring a detection when in fact the observed signal is from an event other than that under analysis.) When a signal is observed in the time gate of the event under analysis, the analyst first checks the waveforms on the three components of motion to see that their

inter-relationships are correct. If still in doubt, the analyst checks available event lists to see whether any other reported event could have arrived in the signal gate. In general, the analyst declares a detection if a dispersed signal is observed having the correct inter-relationships between the Love and Rayleigh waves and if no other event has been reported which could be mistaken for the event under analysis.

Since mixed events and (secondarily) events for which no data were recorded or which contained malfunctions are a fairly common problem, the Seismic Research Observatory detection capability estimates are calculated in two ways. The first of these is termed the absolute detection capability estimate. When computing this estimate, all mixed events, events for which no data were recorded, and events containing malfunctions are counted as non-detections when forming the detection statistics. This approach gives a real-world detection capability estimate.

The second of these estimates is termed the conditional detection capability estimate. When computing this estimate, all mixed events, events for which no data were recorded, and events containing malfunctions are rejected from the detection statistics. This approach gives an ideal detection capability estimate. The value of this ideal estimate is that it shows the detection capability improvement possible if the reliability of the instrumentation can be improved and if methods of separating mixed events can be found.

The number used to represent detection capability is the 50 percent detection threshold, denoted by 'm_{b50}'. The 50 percent detection threshold is the body wave magnitude for which the probability of detection is 0.5. It is computed by fitting the Gaussian probability function to the detection statistics by maximum likelihood method (Ringdal, 1974).

It must be kept in mind that, since the data base was derived from the NORSAR event bulletins, all detection capability estimates are in terms of NORSAR m_b units. This fact is important, since NORSAR m_b units are not the same as those from other earthquake parameters sources such as the National Earthquake Information Service (NEIS) event list.

Depending on the quantity of data available, one of three levels of confidence is placed on each 50 percent detection threshold. If a 50 percent detection threshold is given to two decimal places (e.g., $m_{b50} = 4.56$), sufficient detection statistics were available to compute a reliable detection capability estimate. If a 50 percent detection threshold is enclosed in parentheses and given to only one decimal place, (e.g., $m_{b50} = (4.6)$) the detection statistics were sparse and the detection capability estimate can be considered to be only a first approximation. Finally, if a 50 percent detection threshold is expressed as greater than some value (e.g., $m_{b50} > 5.0$), the detection statistics were too sparse to allow fitting of the Gaussian probability curve. In most cases, this is due to a lack of detected events. When this occurred, the value given is the m_b of the largest non-detected event.

B. SHORT-PERIOD DETECTION CAPABILITY ESTIMATES

The criteria for determining whether an event was detected on the recorded vertical short-period component are as follows:

- The waveform is at least 12 dB above the surrounding noise waveforms
- The waveform is impulsive, not emergent
- The waveform begins within ± 20 seconds of the predicted arrival time.

The requirement that the maximum waveform amplitude be at least 12 dB above the surrounding noise waveforms is set high because

the amplitude change is of overriding importance when searching for P-waves on a single component of motion. It must be remembered that the analyst does not have available the information which three components of short-period motion provide, i.e., the approximate arrival azimuth provided by the direction of motion of the first arrival and the approximate epicentral distance provided by the P-S arrival time separation. (S is rarely observed on the vertical component.) Therefore, the analyst must rely on an abrupt amplitude change to feel confident that the waveform under consideration is a P-wave. Occasionally, it is possible to pick a P-wave when this criterion is not satisfied. This occurs when a change in frequency and amplitude are simultaneously observed. Typically, this change in frequency is from two Hertz to one Hertz.

The impulsive waveform requirement is made in order that the analyst be able to determine the P-wave arrival time. Without this, the analyst cannot be confident of fulfilling the third criterion. This third criterion, the ± 20 second P-wave arrival gate, is an implicit recognition that the origin time and/or epicenter coordinates may be in error, resulting in a deviation of the actual arrival time from the predicted arrival time. Also, it must be noted that the predicted arrival time is based on the assumption that the event occurred at normal (33 km) depth. Departures from this normal depth will also cause departures from the predicted arrival time.

The third detection criterion is not absolute. It is possible that errors in computation of origin time, location, and depth may all combine to place the actual P-wave arrival outside the ± 20 second gate. In cases where a P-wave was observed outside the gate and no other event could be found in the NORSAR bulletins which would have arrived at that time, a detection was declared. This was, however, a rare occurrence.

Short-period 50 percent detection thresholds were first computed by station for all regions as a unit using three sub-sets of the detection

statistics. The first sub-set ('ALL REGIONS A') consists of all short-period events with epicentral distances less than 103 degrees. This produces the previously defined absolute detection capability estimate for each station. The second sub-set ('ALL REGIONS B') produces the previously defined conditional detection capability estimate. Note that this estimate contains the non-detections caused by the failure of the automatic detector to trigger. These detection capability estimates represent the short-period detection capability of the stations as they are currently constituted. The third sub-set ('ALL REGIONS C') contains only those short-period events for which data were recorded. (The non-detections in this subset were found primarily in 'false alarm' records output by the automatic detector.) These detection capability estimates were calculated in an attempt to estimate the effect of the automatic detector on detection capability. The detection capability estimates for the individual regions were computed in the same fashion as they were for 'ALL REGIONS B', i.e., those events not detected by the automatic detector were counted as non-detections in the detection statistics.

The detection statistics and fitted maximum likelihood curves for the short-period data are shown in Figures V-1 to V-8. Each of the 'sub-figures' in Figures V-1 to V-8 represents one short-period detection capability estimate. The upper portion of each 'sub-figure' is a histogram giving the detection statistics as a function of body-wave magnitude for that particular case. The lower portion shows the percentage of events detected at each body-wave magnitude (represented by asterisks), the fitted maximum likelihood curve (represented by a solid line), and the 90 percent confidence limits for this curve (represented by dashed lines). The values for 'MB5O' and 'MB90' shown on the figures are the 50 and 90 percent detection thresholds as picked from the maximum likelihood curve. The value shown for 'SIGMA' is the standard deviation of Gaussian probability function obtained by maximum likelihood method.

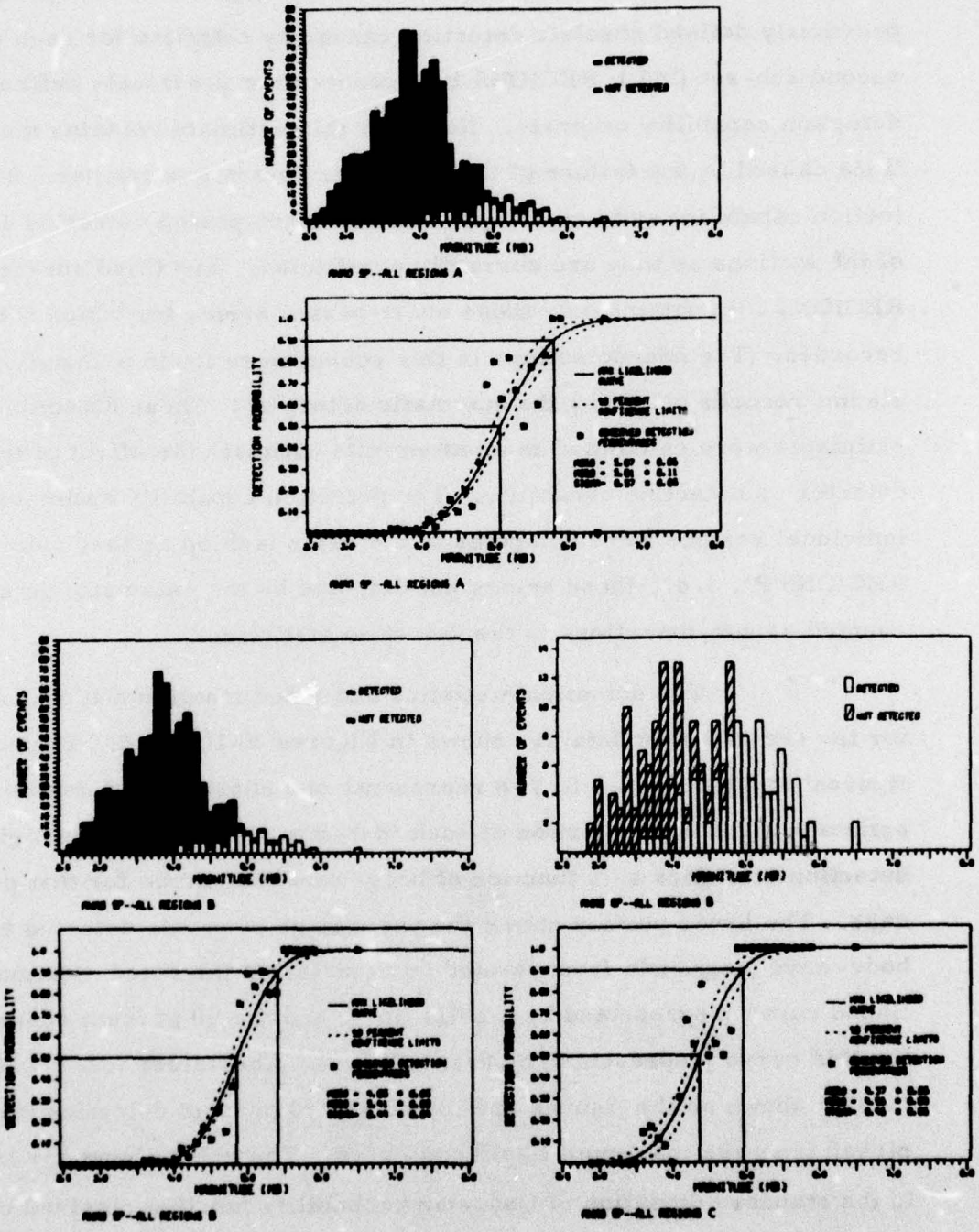

FIGURE V-1

ANMO SHORT-PERIOD DETECTION STATISTICS
ALL REGIONS A, B, AND C

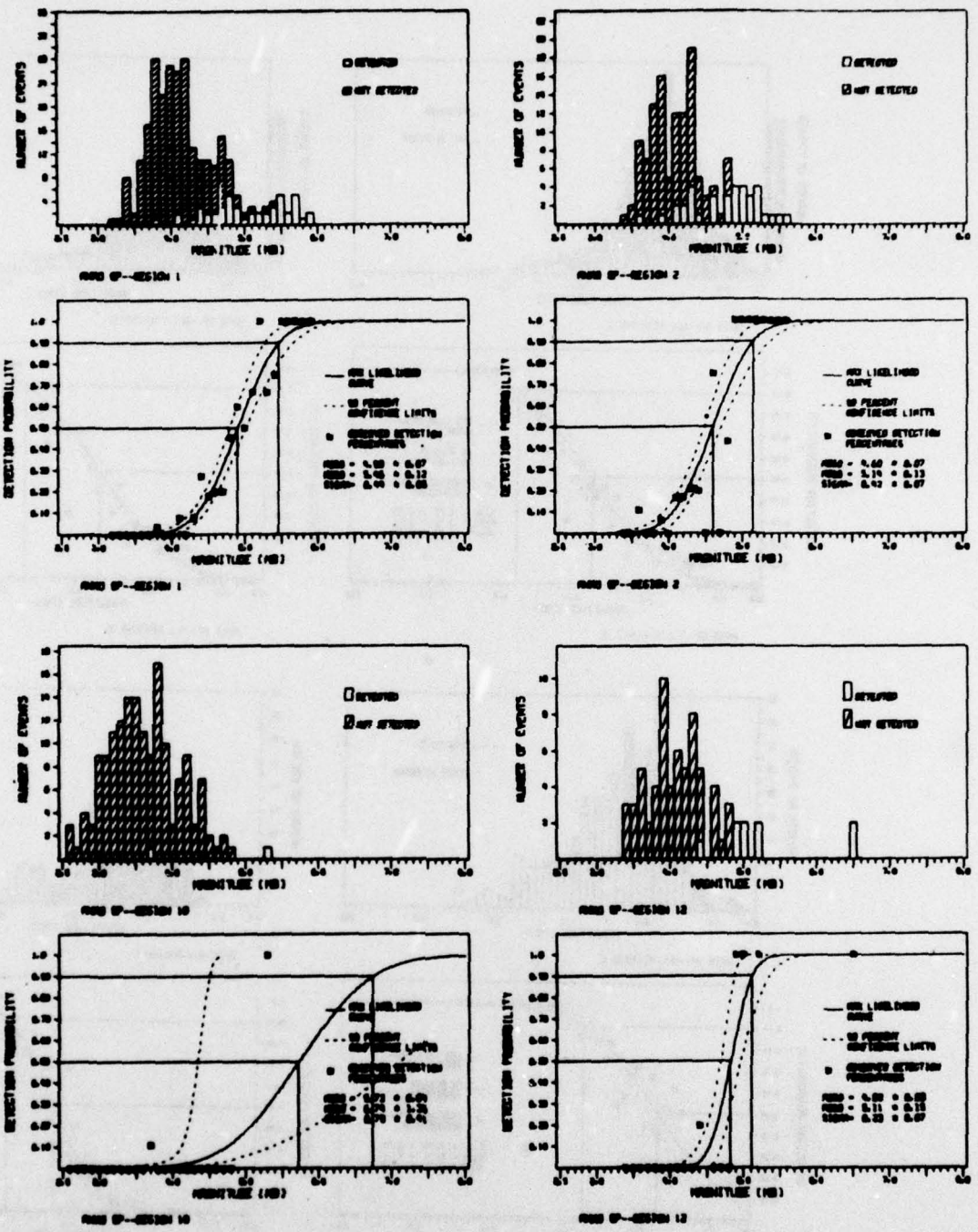

FIGURE V-2

ANMO SHORT-PERIOD DETECTION STATISTICS
REGIONS 1, 2, 10, AND 12

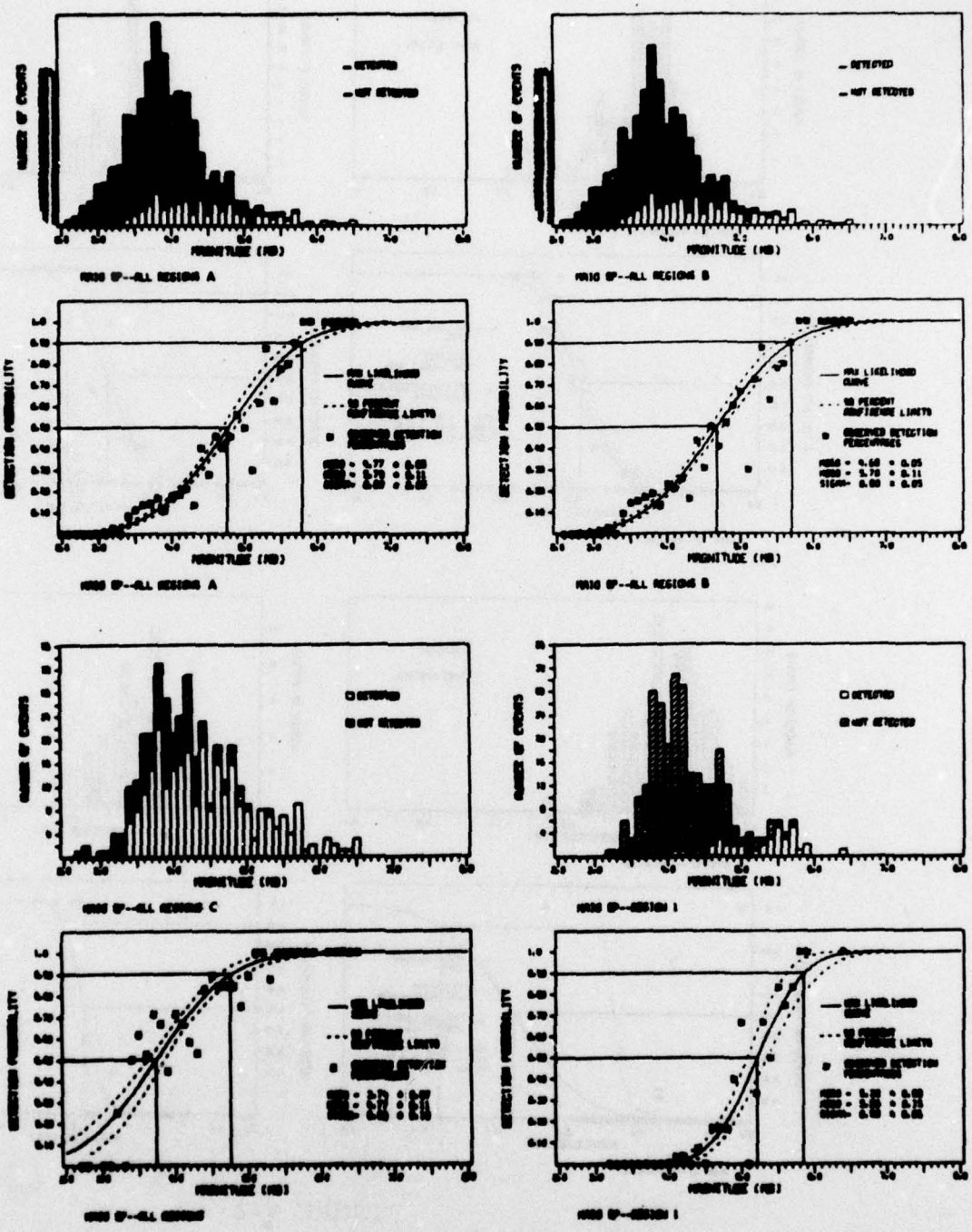

FIGURE V-3

MAIO SHORT PERIOD DETECTION STATISTICS
ALL REGIONS A, B, C AND REGION 1

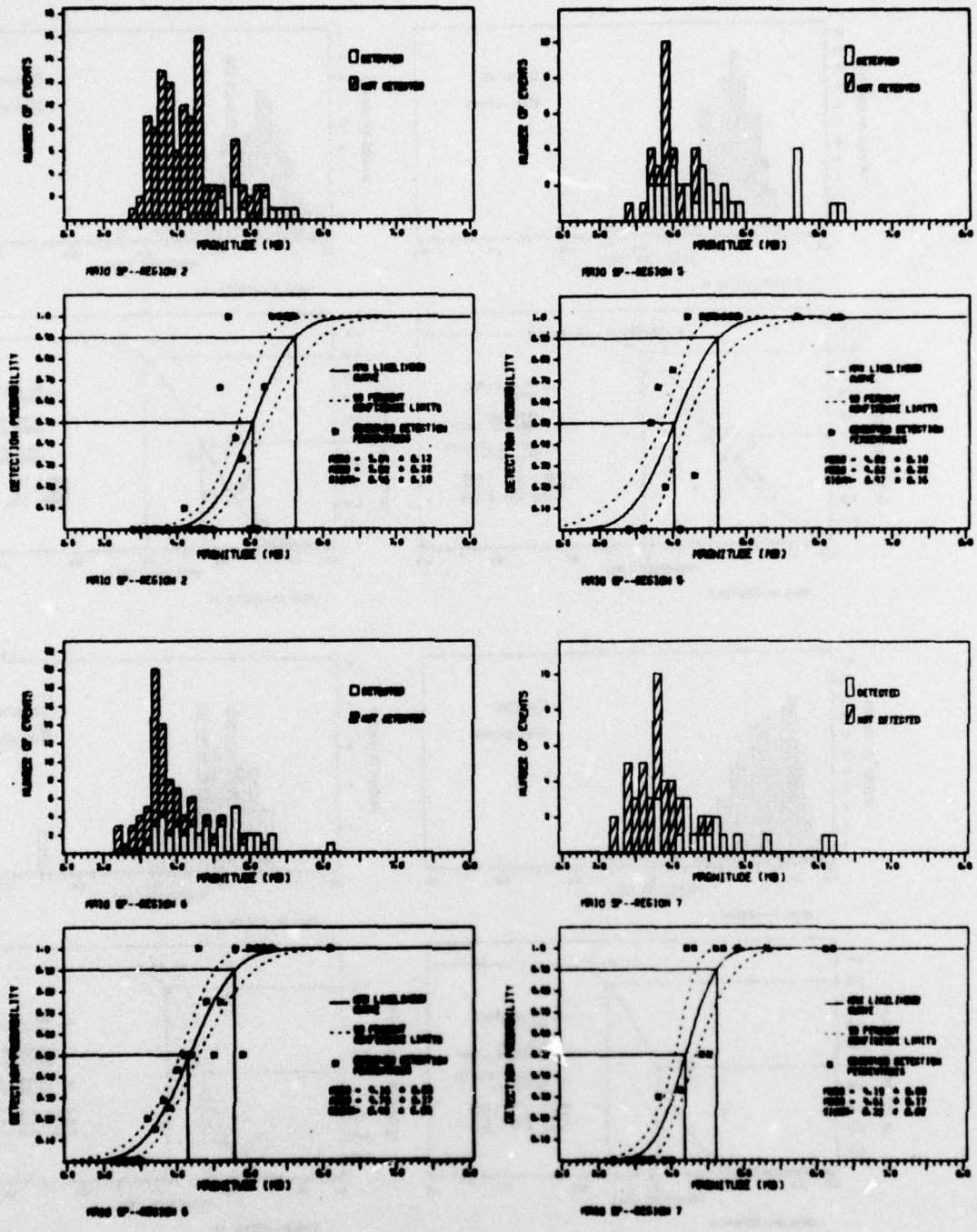

FIGURE V-4

MAIO SHORT-PERIOD DETECTION STATISTICS
REGIONS 2, 5, 6, AND 7

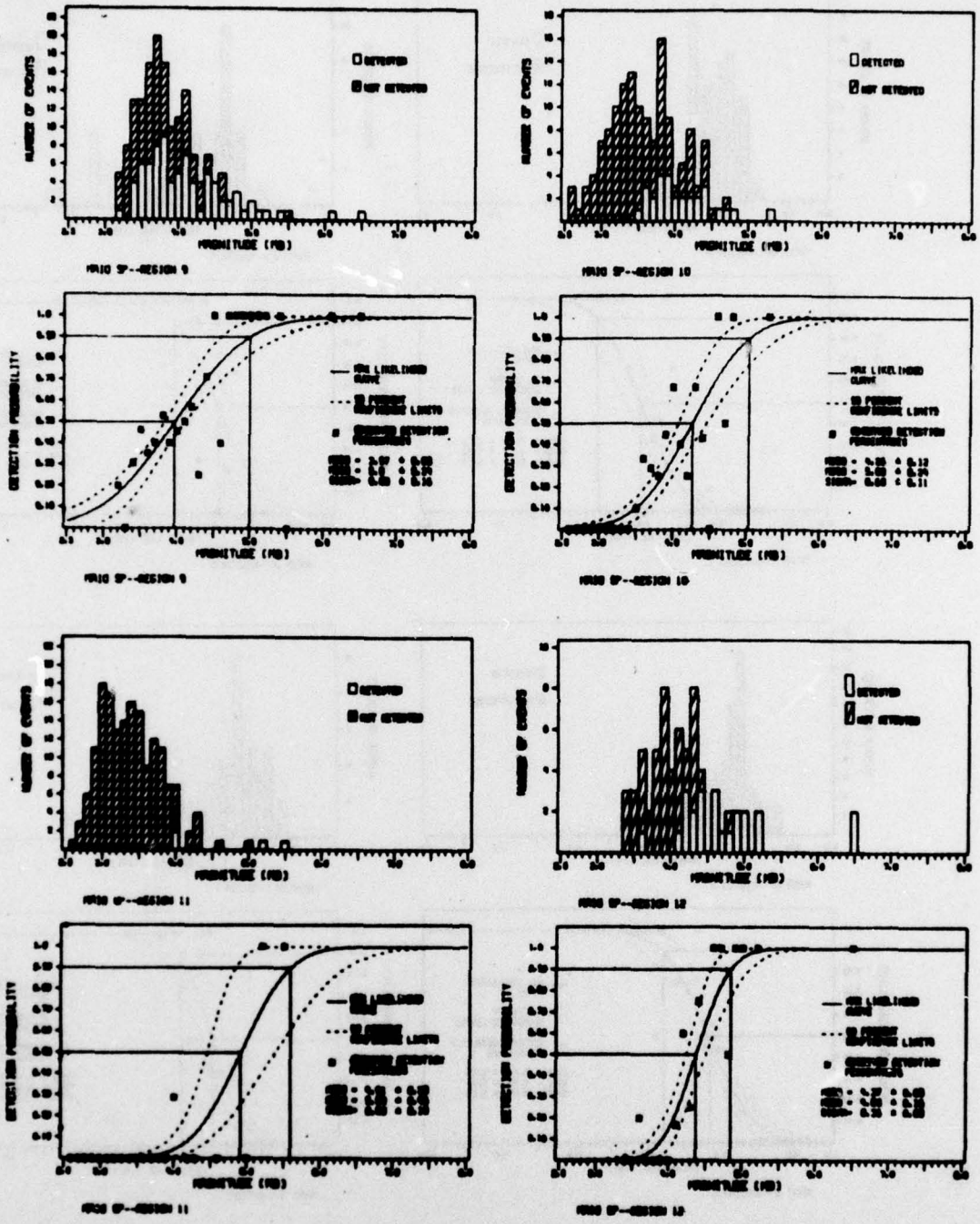

FIGURE V-5

MAIO SHORT-PERIOD DETECTION STATISTICS
REGIONS 9, 10, 11, AND 12

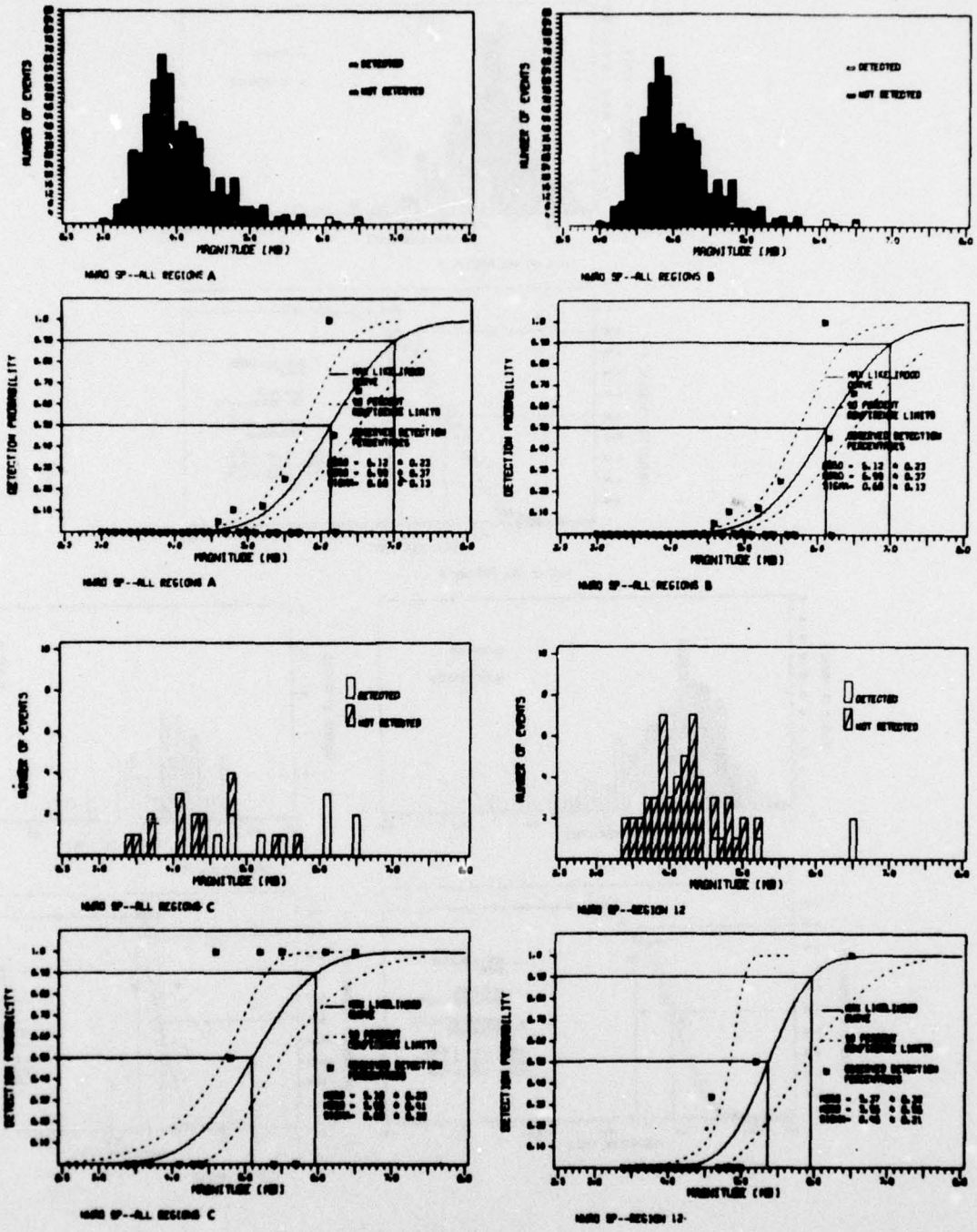

FIGURE V-6

NWAO SHORT-PERIOD DETECTION STATISTICS
ALL REGIONS A, B, C AND REGION 12

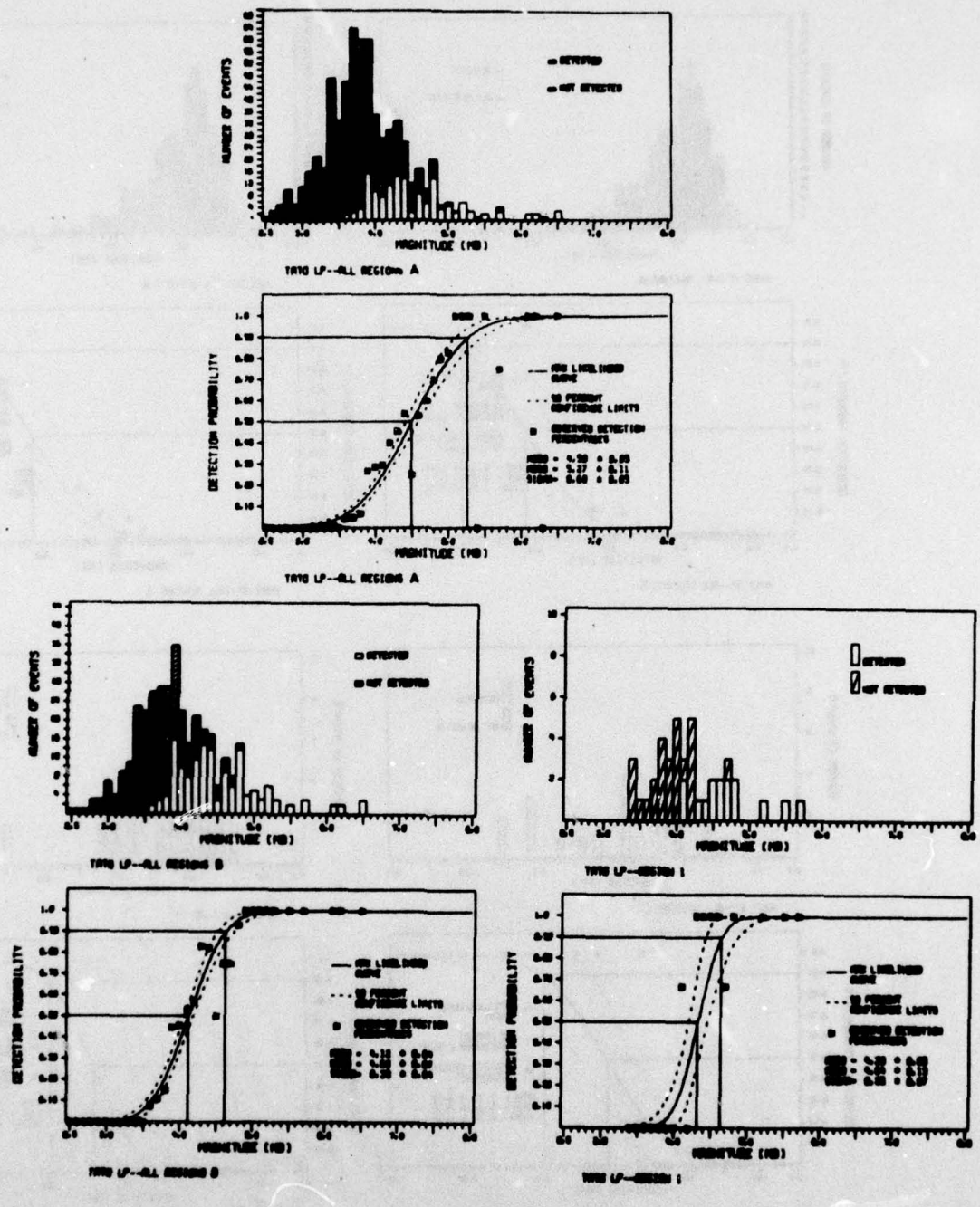

FIGURE V-7

TATO SHORT-PERIOD DETECTION STATISTICS
ALL REGIONS A, B, AND C

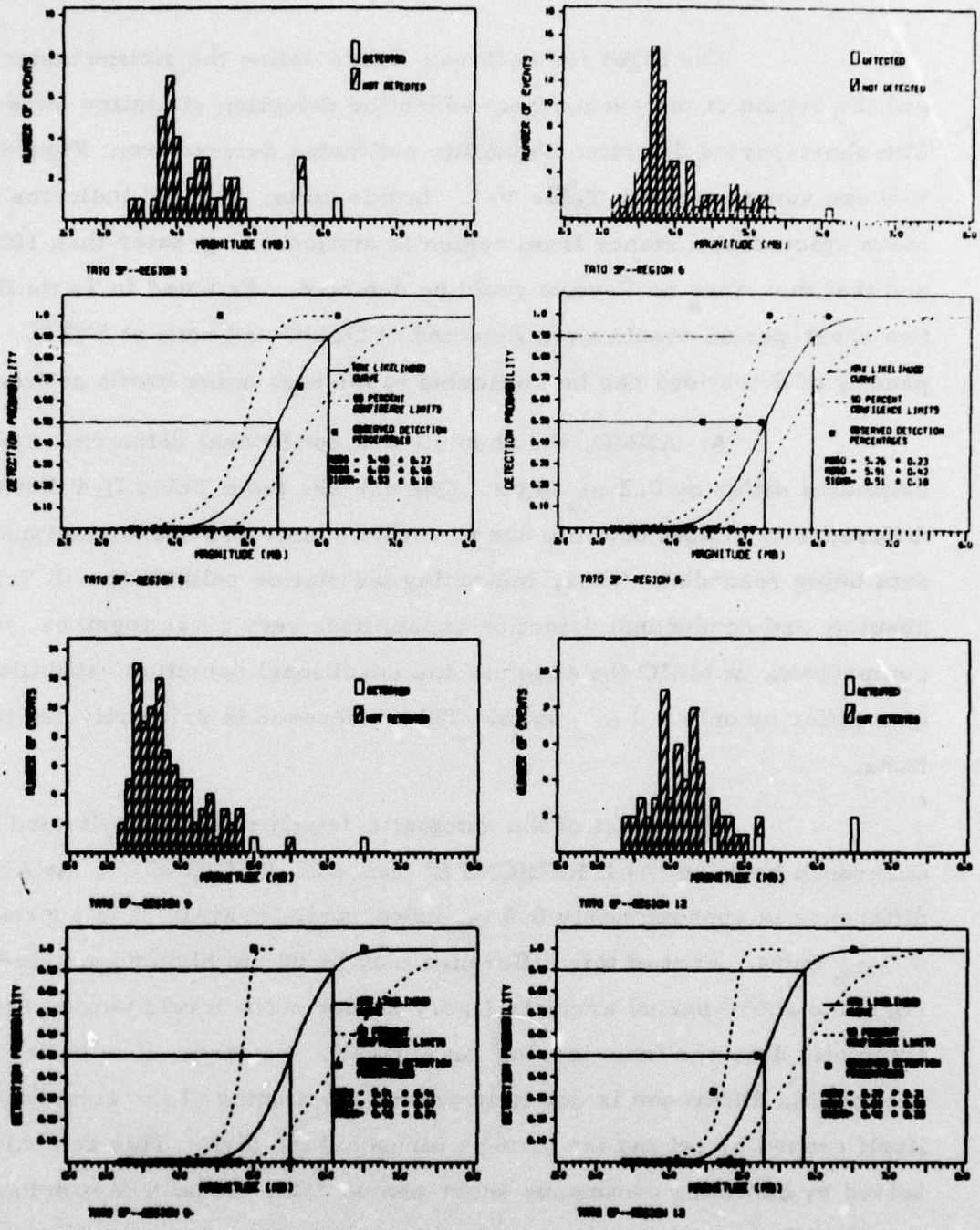

FIGURE V-8

TATO SHORT-PERIOD DETECTION STATISTICS
REGIONS 5, 6, 9, 12

The titles for each sub-figure define the station under evaluation and the region of the events from which the detection statistics were derived. The short-period detection capability estimates derived from Figures V-1 to V-8 are summarized in Table V-1. In this table, '$\Delta > 103$' indicates that the mean epicentral distance from region to station was greater than 103 degrees and that therefore no P-wave could be detected. As noted in Table II-4, only two short-period events were detected at GUMO and none at SNZO. This paucity of detections can be attributed to the high noise levels at these stations.

At ANMO, the absolute and conditional detection capability estimates differ by 0.2 m_b units. One can see from Table II-4 that this difference is almost entirely due to events counted as non-detections due to no data being recorded. Thus, improving the station reliability will bring the absolute and conditional detection capabilities very close together. In comparison, at MAIO the absolute and conditional detection capability estimates differ by only 0.1 m_b units. This difference is primarily due to malfunctions.

The effect of the automatic detector can be estimated by the difference between 'ALL REGIONS B' and 'ALL REGIONS C'. At ANMO this difference is approximately 0.5 m_b units, while at MAIO it is approximately 0.9 m_b units. Part of this difference may be due to higher noise levels masking some short-period arrivals (i.e., higher noise levels would prevent the automatic detector from 'seeing' an arrival). However, it is believed that part of this difference is due to improper functioning of the automatic detector itself caused by setting the turn-on threshold too high. This can only be resolved by obtaining continuous short-period data, visually examining this data for detections, and finally running this data through the automatic detector to determine which events it can detect.

The individual region detection capability estimates of Table V-1 are determined in the same fashion as the estimates for 'ALL REGIONS B'.

TABLE V-1

SRO SP DETECTION CAPABILITY

Region	50 Percent Detection Threshold					
	ANMO	GUMO	MAIO	NWAO	TATO	SNZO
All Regions A	5.07	>6.0	4.77	(6.1)	(5.7)	>6.5
All Regions B	4.85	>6.0	4.68	(6.1)	(5.5)	>6.5
All Regions C	4.37	>6.0	3.74	(5.1)	(4.9)	>5.7
1	4.90	>6.4	5.22	>5.7	>5.7	>5.7
2	4.60	>5.6	5.04	>5.6	>5.0	>5.6
5	Δ>103	>5.7	(4.0)	>6.2	(5.4)	>6.2
6	Δ>103	>6.0	4.16	>5.3	(5.3)	Δ>103
7	Δ>103	>6.0	(4.2)	>5.2	>5.3	Δ>103
9	Δ>103	>6.5	(4.0)	>6.0	(5.5)	Δ>103
10	(5.7)	---	(4.3)	Δ>103	>5.3	Δ>103
11	>4.6	Δ>103	(4.9)	Δ>103	----	Δ>103
12	(4.8)	---	(4.4)	(5.4)	(5.3)	>6.5

All Regions A — Mixed, no data recorded, no short-period data recorded, and malfunctions are counted as non-detections.

All Regions B — Mixed, no data recorded, and malfunctions rejected from detection statistics

All Regions C — Mixed, no data recorded, no short-period data recorded, and malfunctions rejected from detection statistics.

Individual region estimates were computed in the same fashion as "All Regions B".

50 percent detection thresholds are in NORSAR m_b units.

Thus, these detection capability estimates represent the detection capability of the stations as they now function. With few exceptions, the detection statistics were too sparse to permit determination of reliable detection capability estimates. If good estimates are desired, a great deal more short-period data (at most stations, double or more the amount already processed) must be processed and analysed.

C. LONG-PERIOD DETECTION CAPABILITY ESTIMATES

Estimates of long-period Seismic Research Observatory detection capability are presented for each of the six stations evaluated in this report. The criteria for determining whether detection has been achieved for a given event are:

- The presence of dispersion in the signal gate
- The presence of a peak in the dispersed wave train 3 dB or more above any peak outside the dispersed wave train and inside a time gate starting 600 seconds before the predicted Love wave arrival time and ending 600 seconds after the estimated Rayleigh wave end time.
- The occurrence of signal onset within ± 180 seconds of the predicted signal onset time
- Detection of the event on at least two components.

Occasionally, an event is considered to be detected which does not satisfy all three. Signal peaks are occasionally less than 3 dB above the noise peaks and still recognized as signals from their dispersion characteristics. Also, at a given station it is sometimes possible to find specific features of a seismic waveform from a given region, which enable the analyst to detect the event even though not all detection criteria have been satisfied. An interesting example of this is discussed in the preliminary Seismic Research

Observatory report (Strauss, 1976). The last criterion is intended to reduce the number of false alarms, i.e., calling an event detected when it is not.

The long-period detection statistics and derived maximum likelihood curves are presented in Figures V-9 to V-24. The 50 percent detection thresholds were first computed by station for all regions as a unit using two subsets of the detection statistics. The first subset ('ALL REGIONS A') is used to estimate the previously defined absolute detection capability estimate. In this case, mixed events, events for which no data were recorded, and events for which the data contained malfunctions were counted as non-detections. The second subset ('ALL REGIONS B') is used to estimate the previously defined conditional detection capability estimate. In this case, mixed events, events for which no data were recorded, and events for which the data contained malfunctions were rejected from the detection statistics. The estimates for the individual regions are conditional detection capability estimates determined in the same fashion as 'ALL REGIONS B'.

Figures V-9 to V-24 are laid out in the same manner as Figures V-1 to V-8 for the short-period detection capability estimates. Each of the 'sub-figures' represents one long-period detection capability estimate, where the upper portion shows a histogram of the detection statistics and the lower portion shows the maximum likelihood curve fitted to these statistics.

The long-period detection capability estimates derived from these figures are summarized in Table V-2.

The differences between the absolute and conditional detection capability estimates fall into three groups. At NWAO and SNZO, this difference is approximately 0.3 m_b units. At NWAO, this is primarily due to mixed events, while at SNZO system failures resulting in no data being recorded and malfunctions have roughly as much effect as do the mixed events. (See Table II-4.) At ANMO, MAIO, and TATO, the difference between the

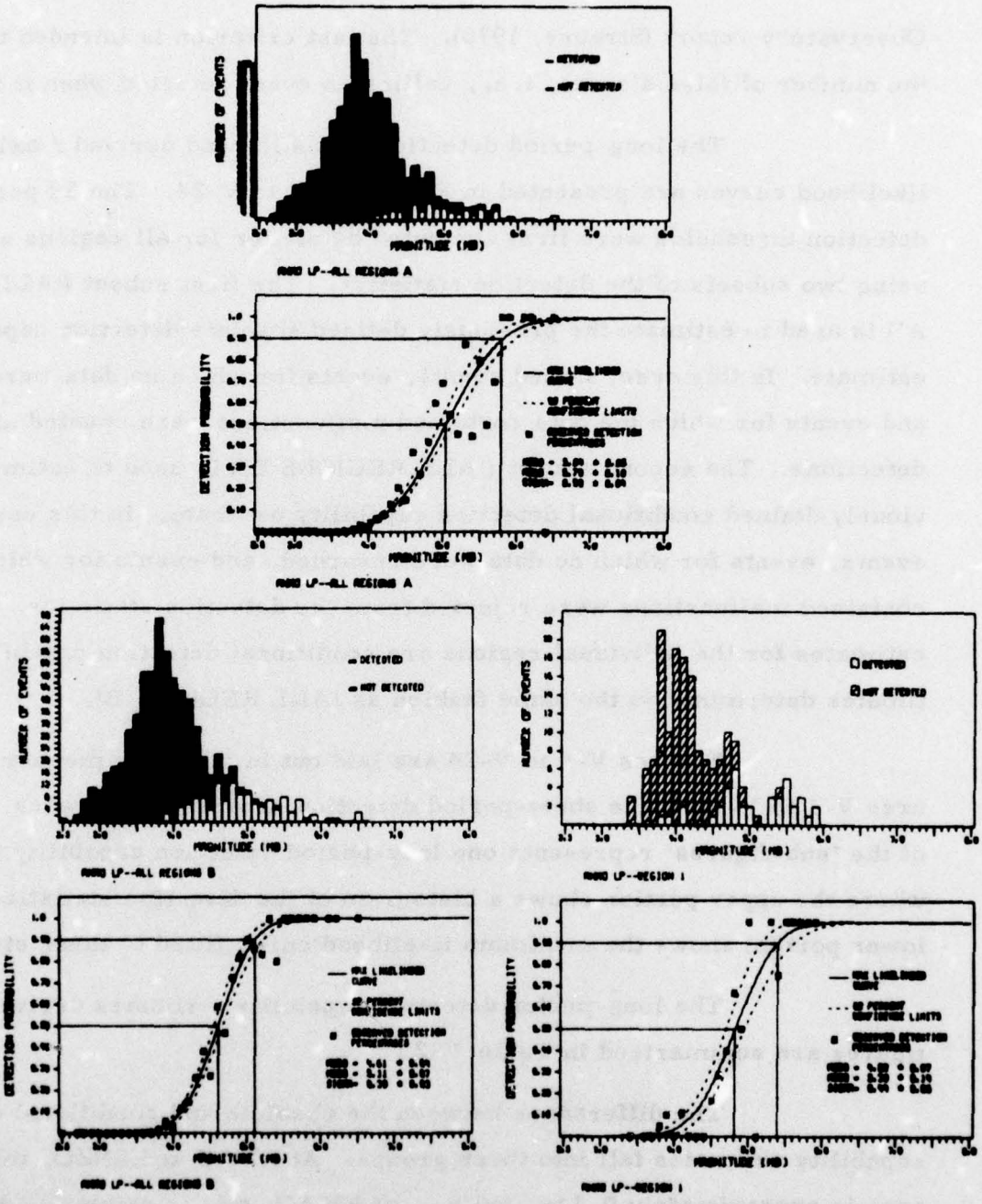

FIGURE V-9

ANMO LONG PERIOD DETECTION STATISTICS
ALL REGIONS A AND B---REGION 1

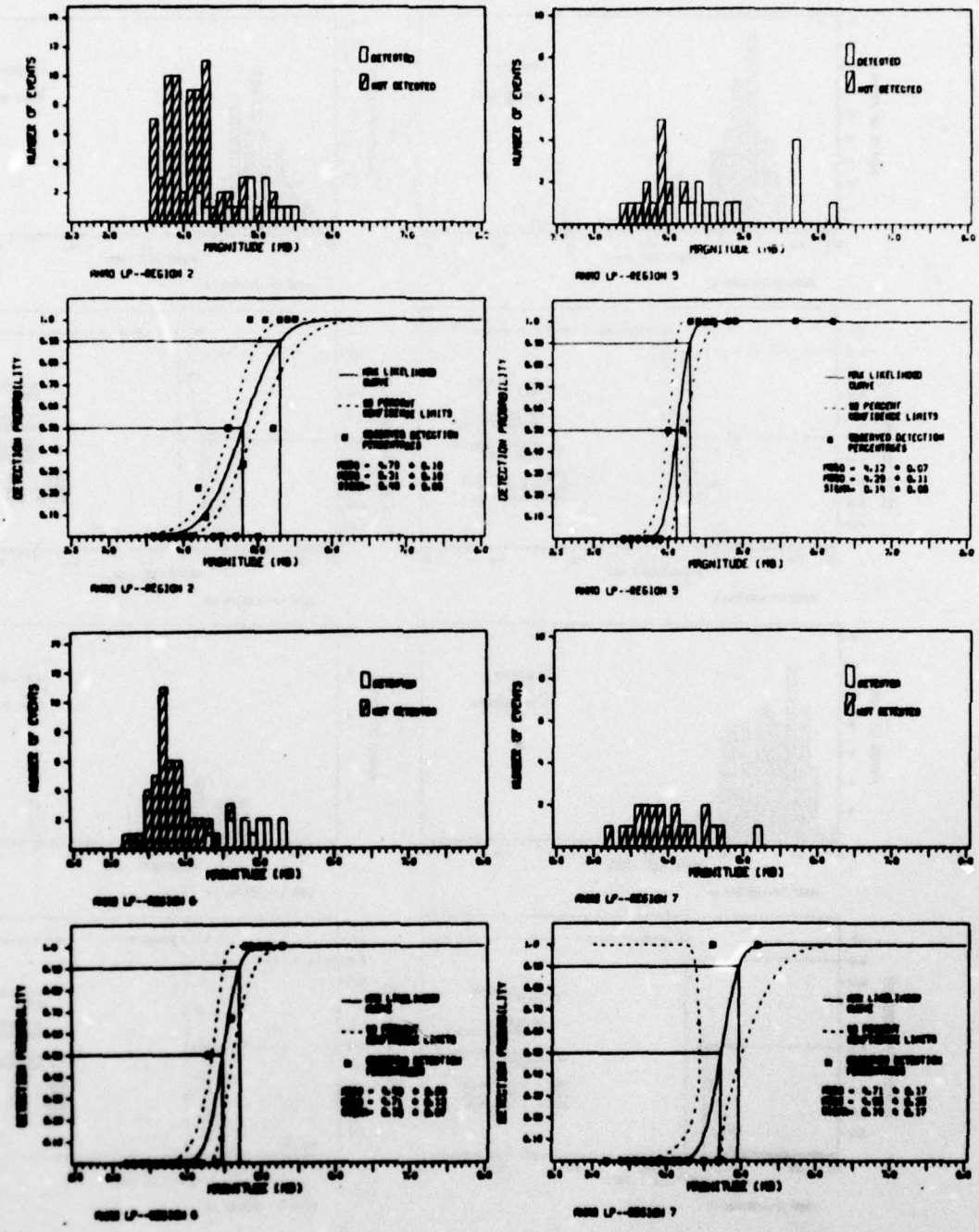

FIGURE V-10

ANMO LONG-PERIOD DETECTION STATISTICS
REGIONS 2, 5, 6, AND 7

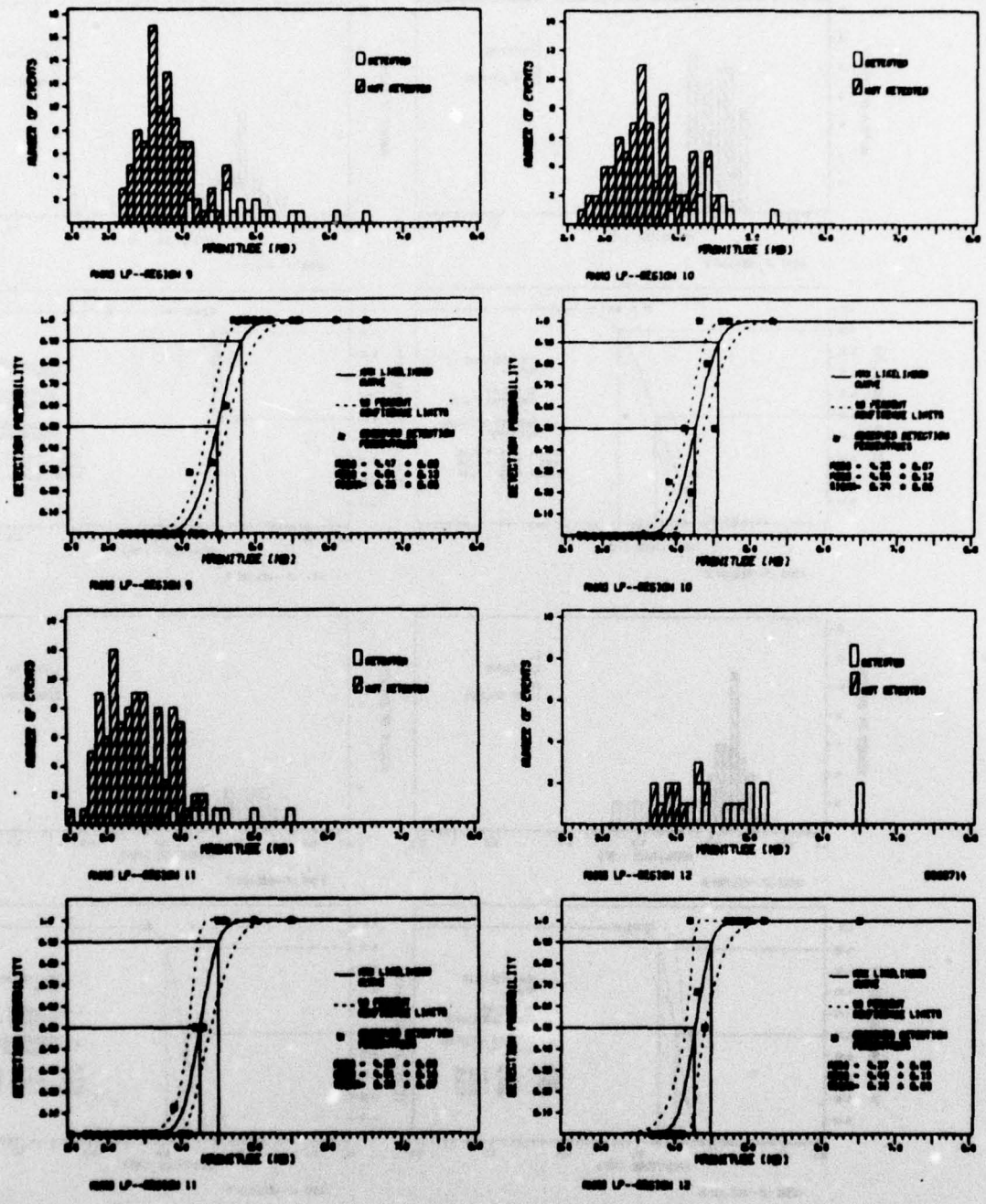

FIGURE V-11

ANMO LONG-PERIOD DETECTION STATISTICS
REGIONS 9, 10, 11, AND 12

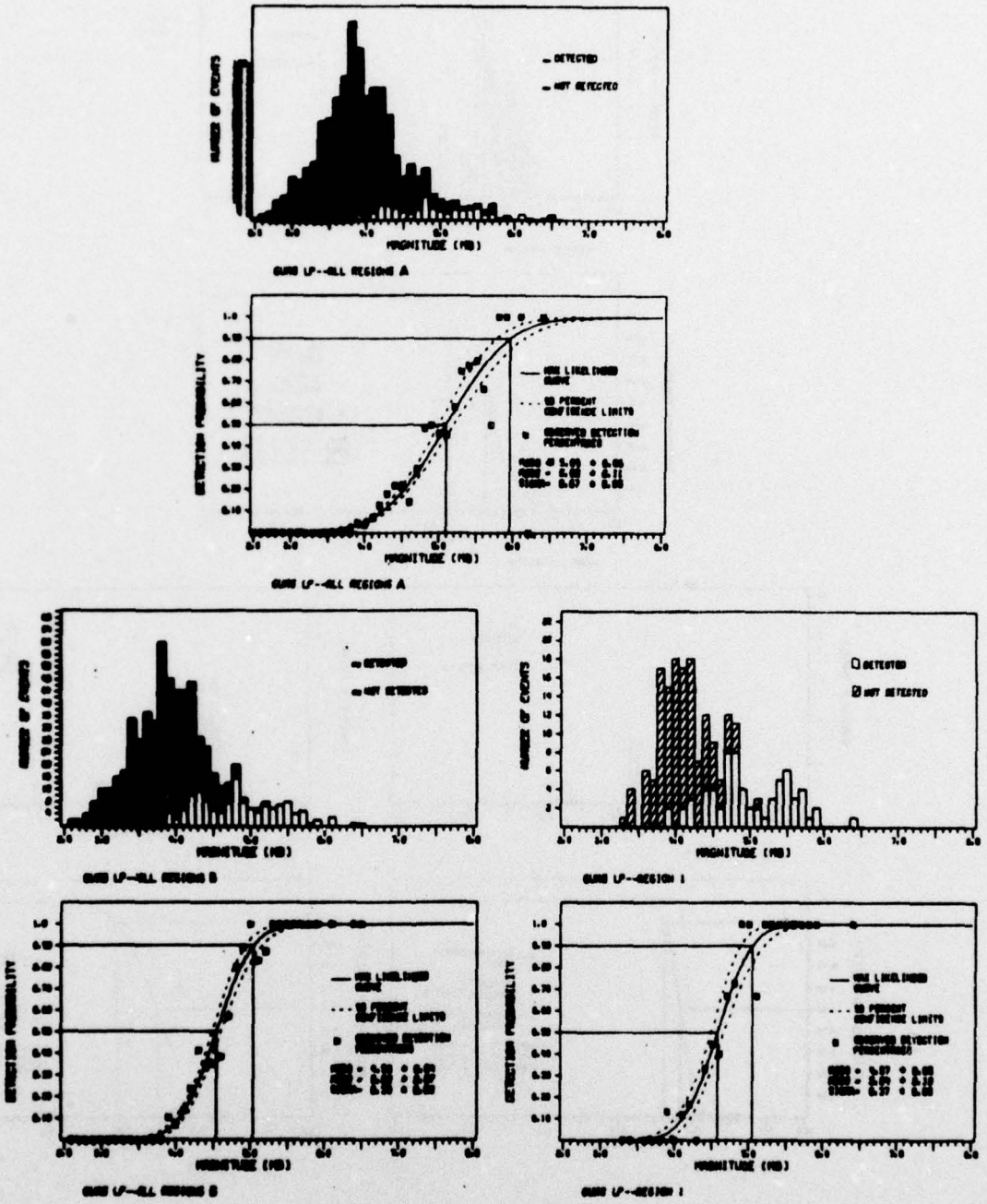

FIGURE V-12

GUMO LONG-PERIOD DETECTION STATISTICS
ALL REGIONS A AND B--REGION 1

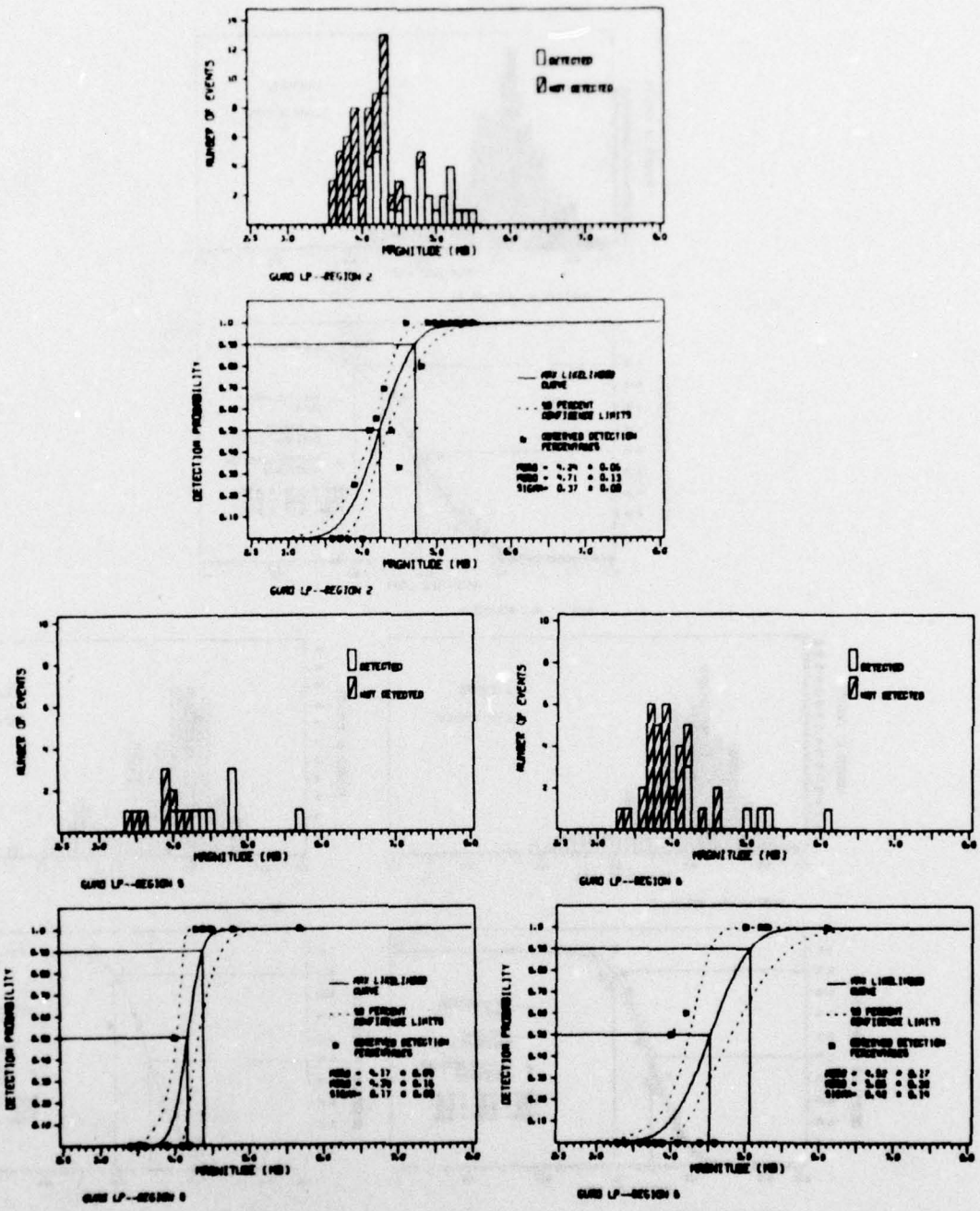

FIGURE V-13

GUMO LONG-PERIOD DETECTION STATISTICS
REGIONS 2, 5, AND 6

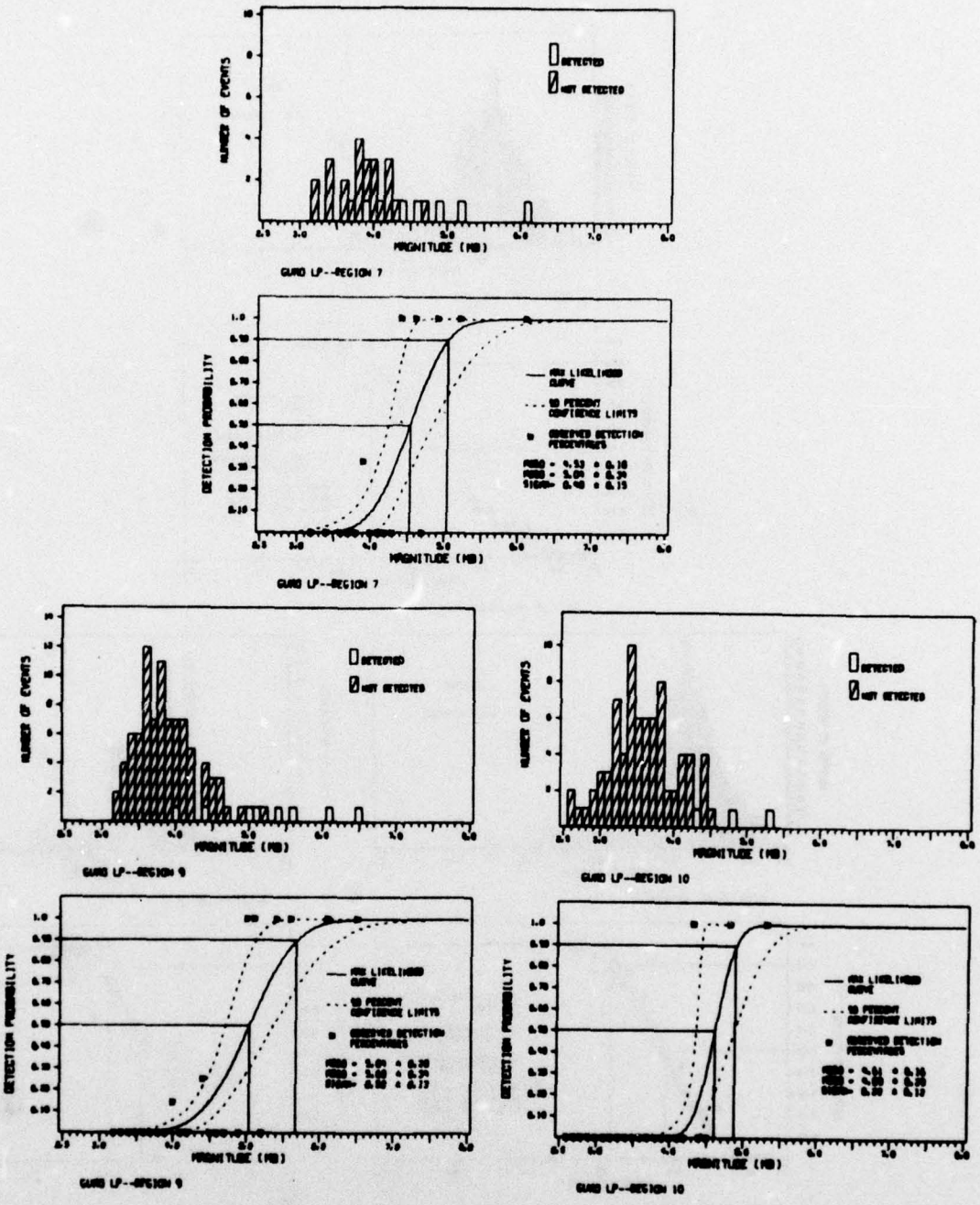

FIGURE V-14

GUMO LONG-PERIOD DETECTION STATISTICS
REGIONS 7, 9, AND 10

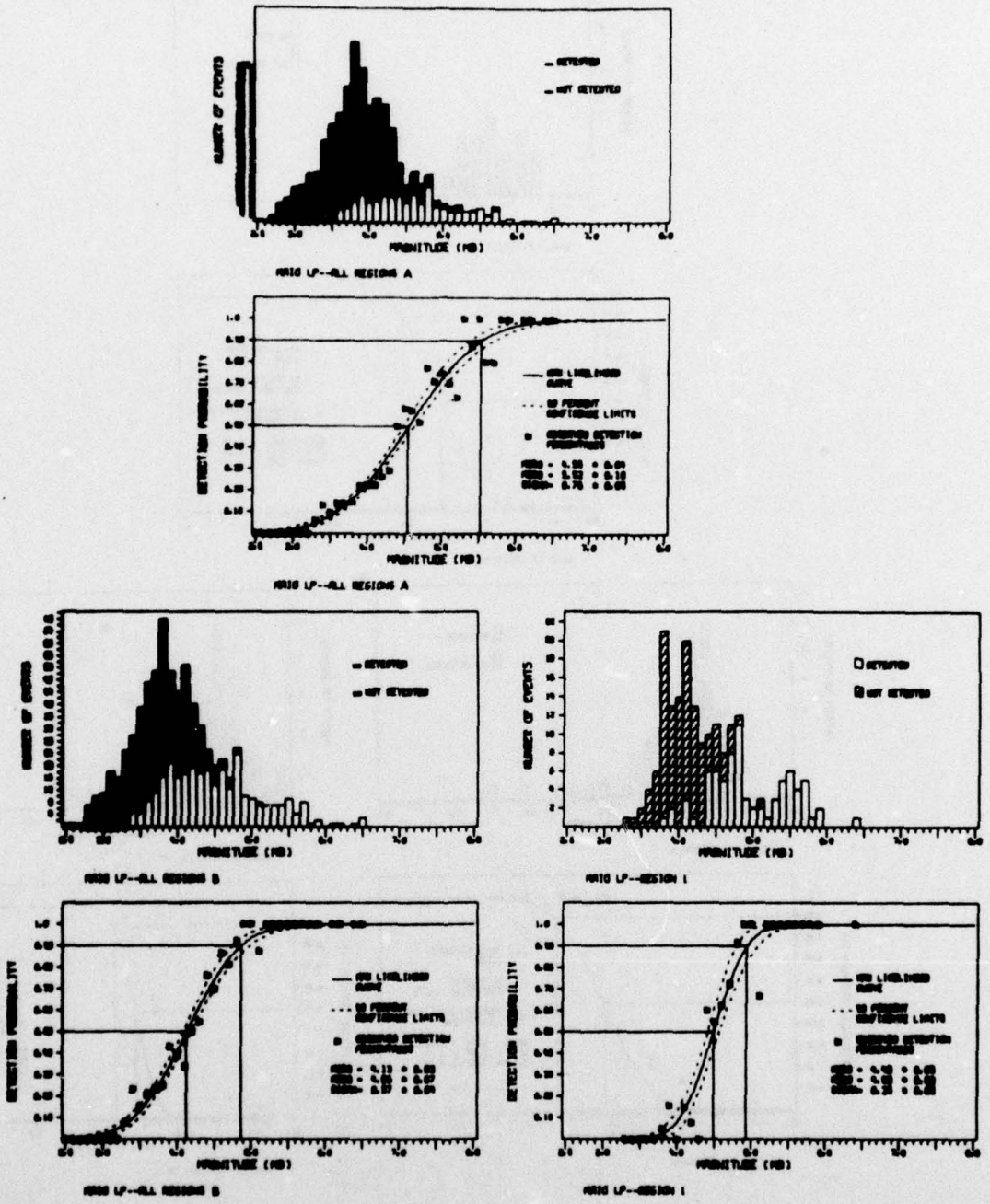

FIGURE V-15

MAIO LONG-PERIOD DETECTION STATISTICS
ALL REGIONS A AND B--REGION 1

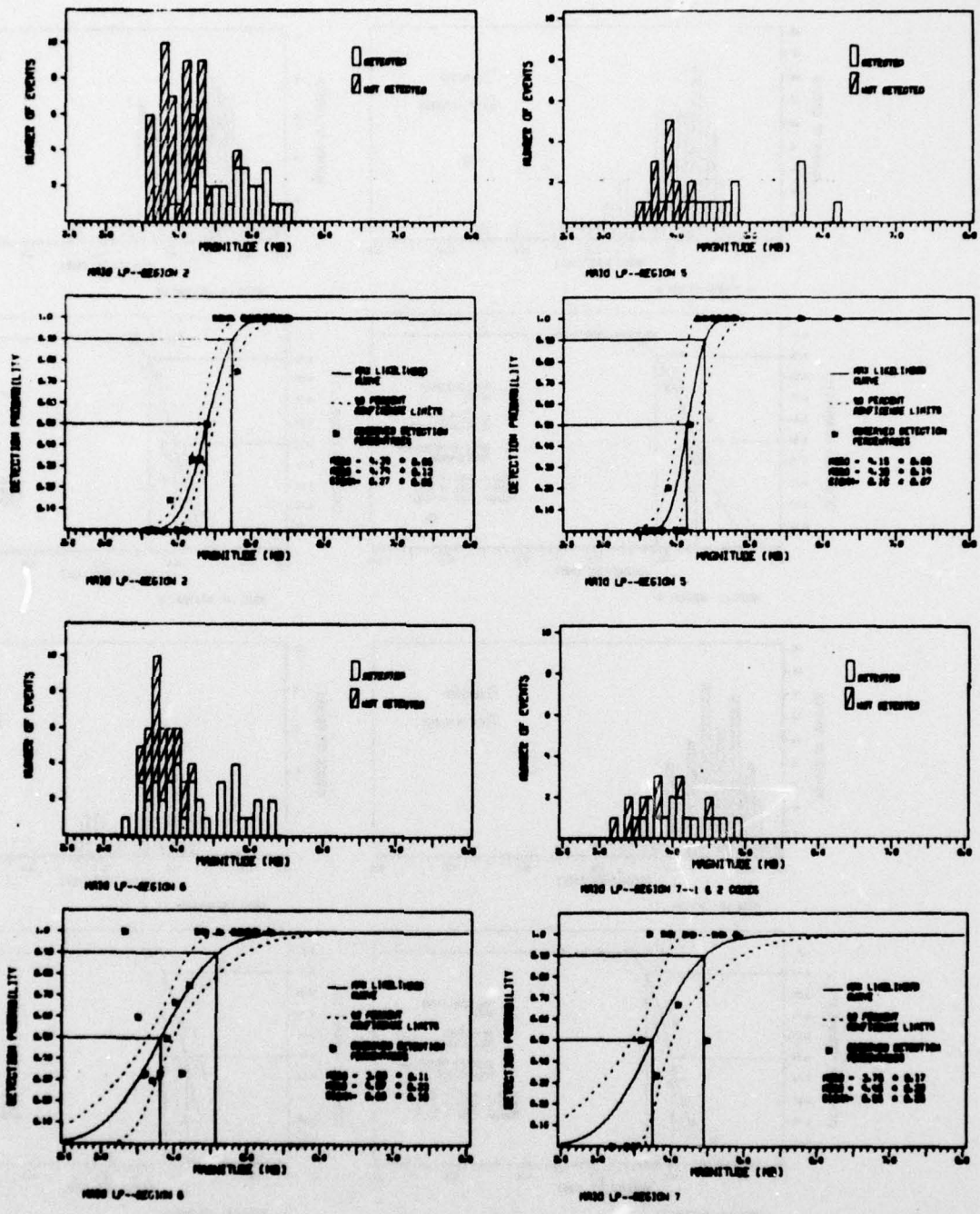

FIGURE V-16

MAIO LONG-PERIOD DETECTION STATISTICS
REGIONS 2, 5, 6, AND 7

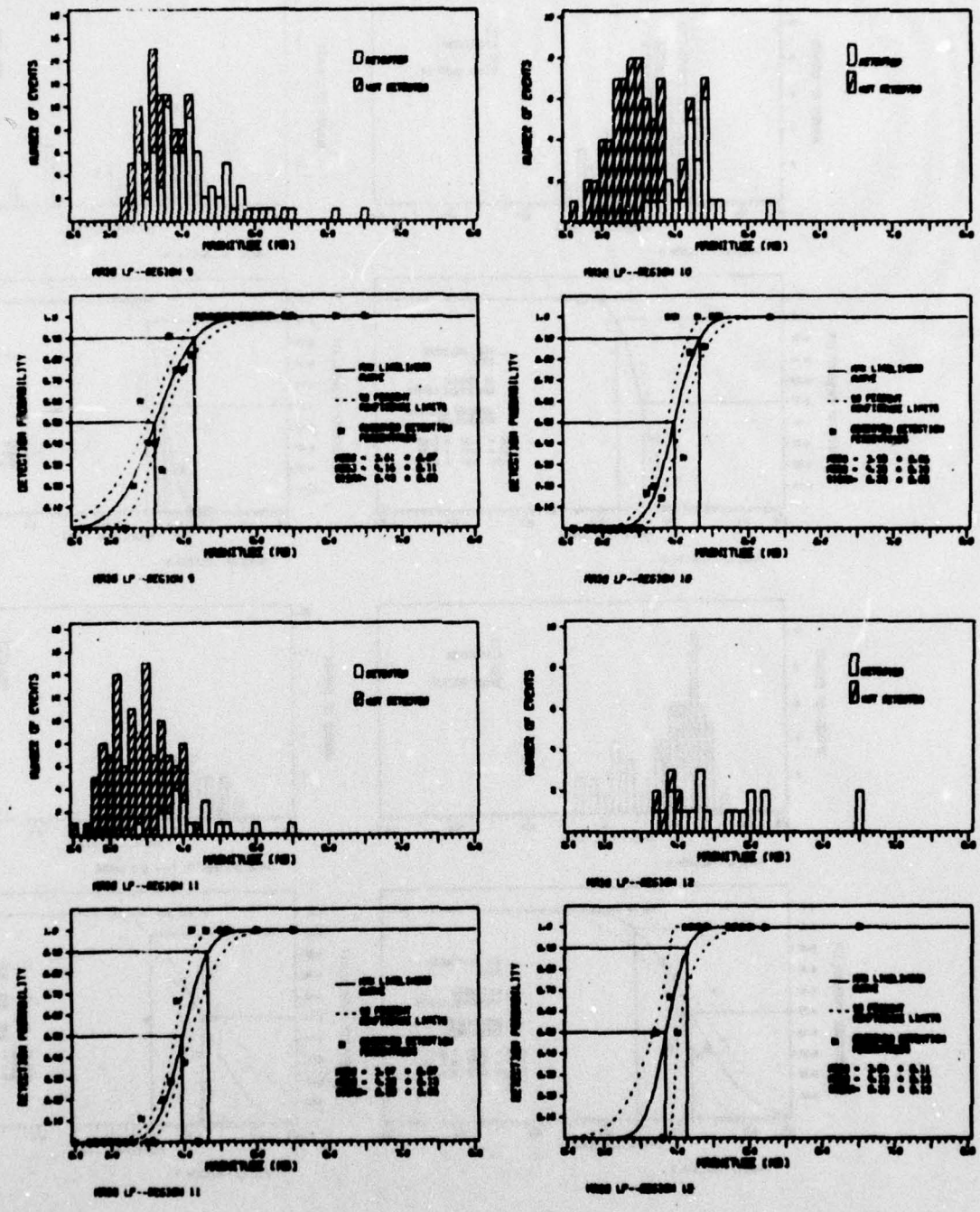

FIGURE V-17

MAIO LONG-PERIOD DETECTION STATISTICS
REGIONS 9, 10, 11, AND 12

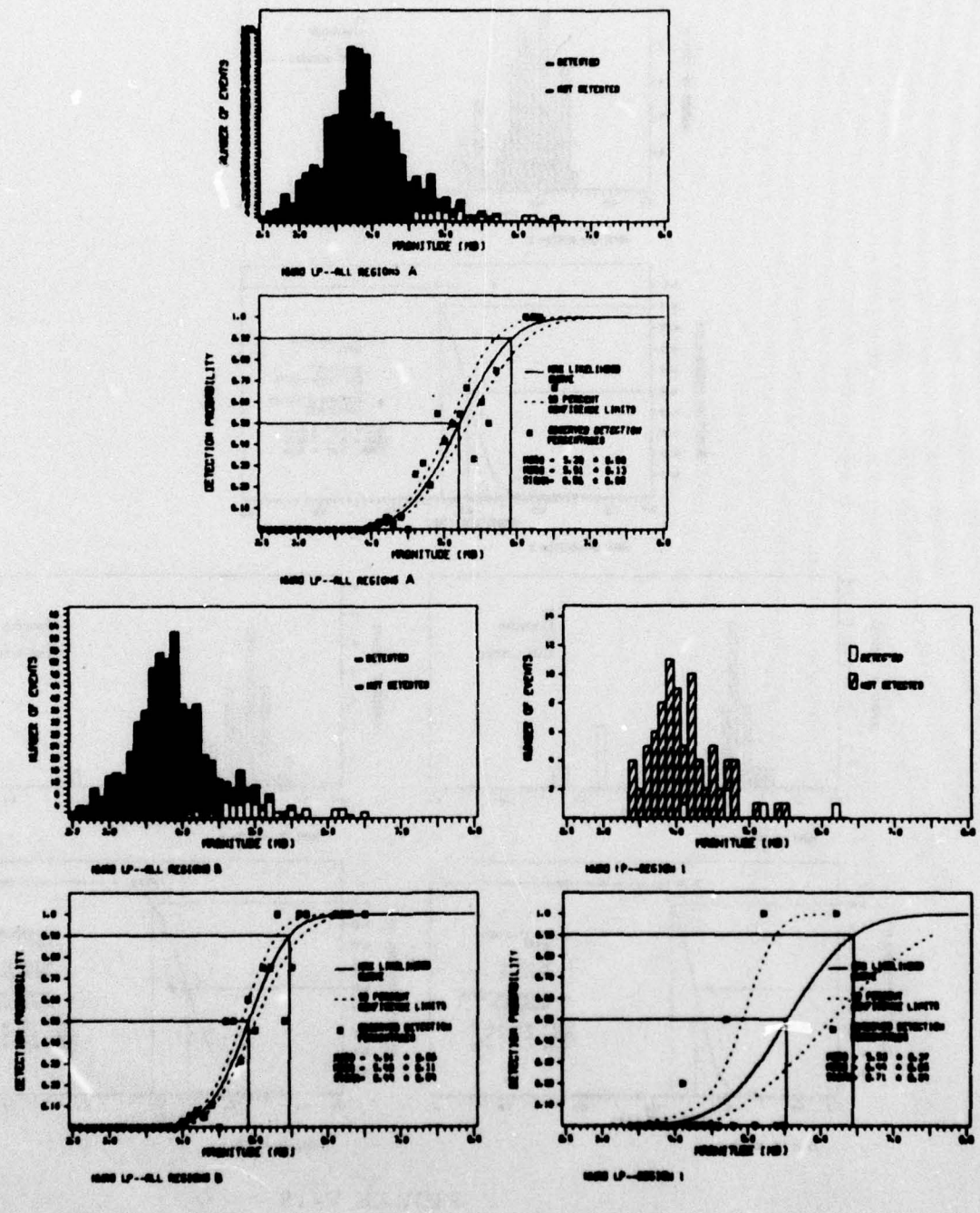

FIGURE V-18

NWAO LONG-PERIOD DETECTION STATISTICS
ALL REGIONS A AND B--REGION 1

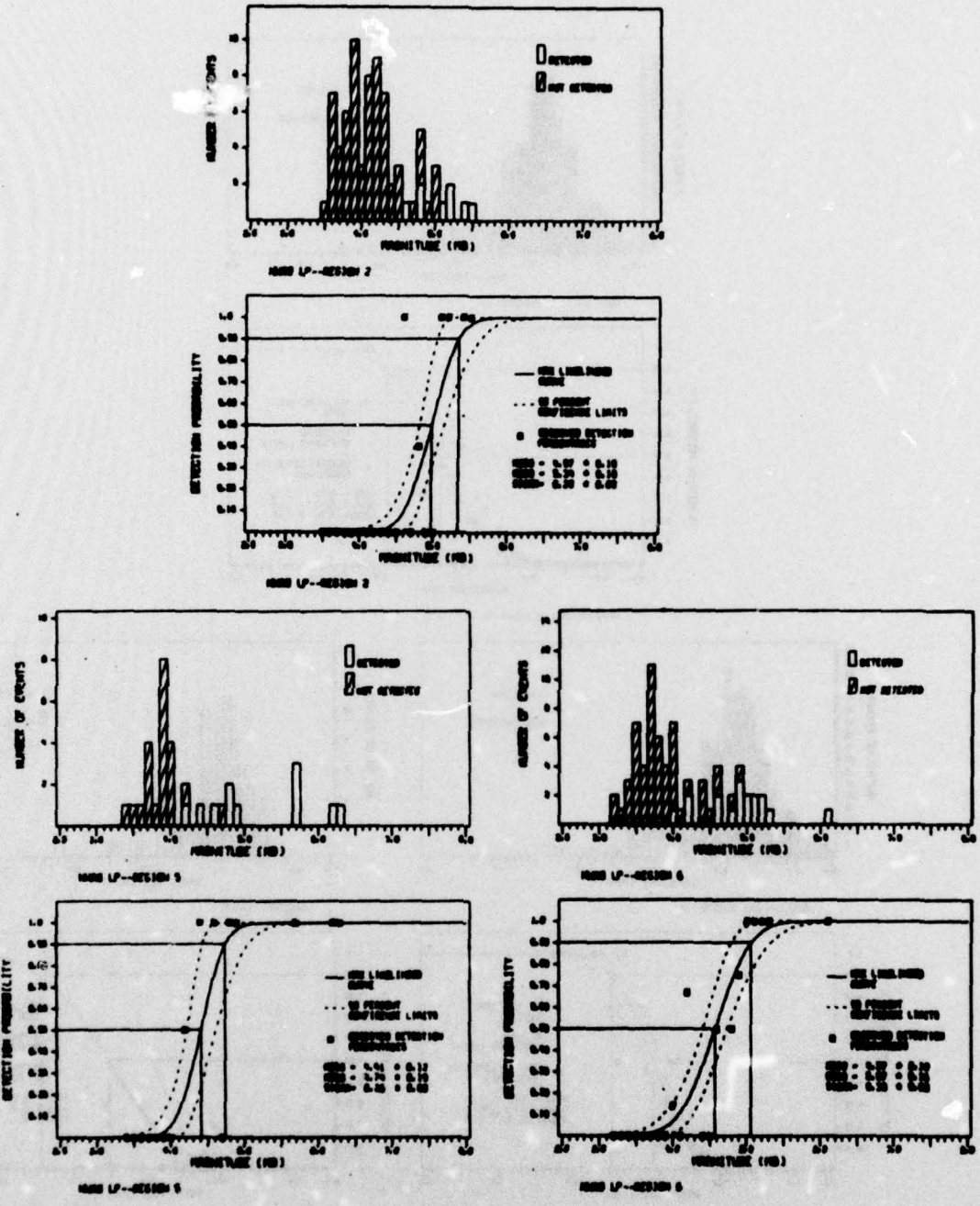

FIGURE V-19

NWAO LONG-PERIOD DETECTION STATISTICS
REGIONS 2, 5, AND 6

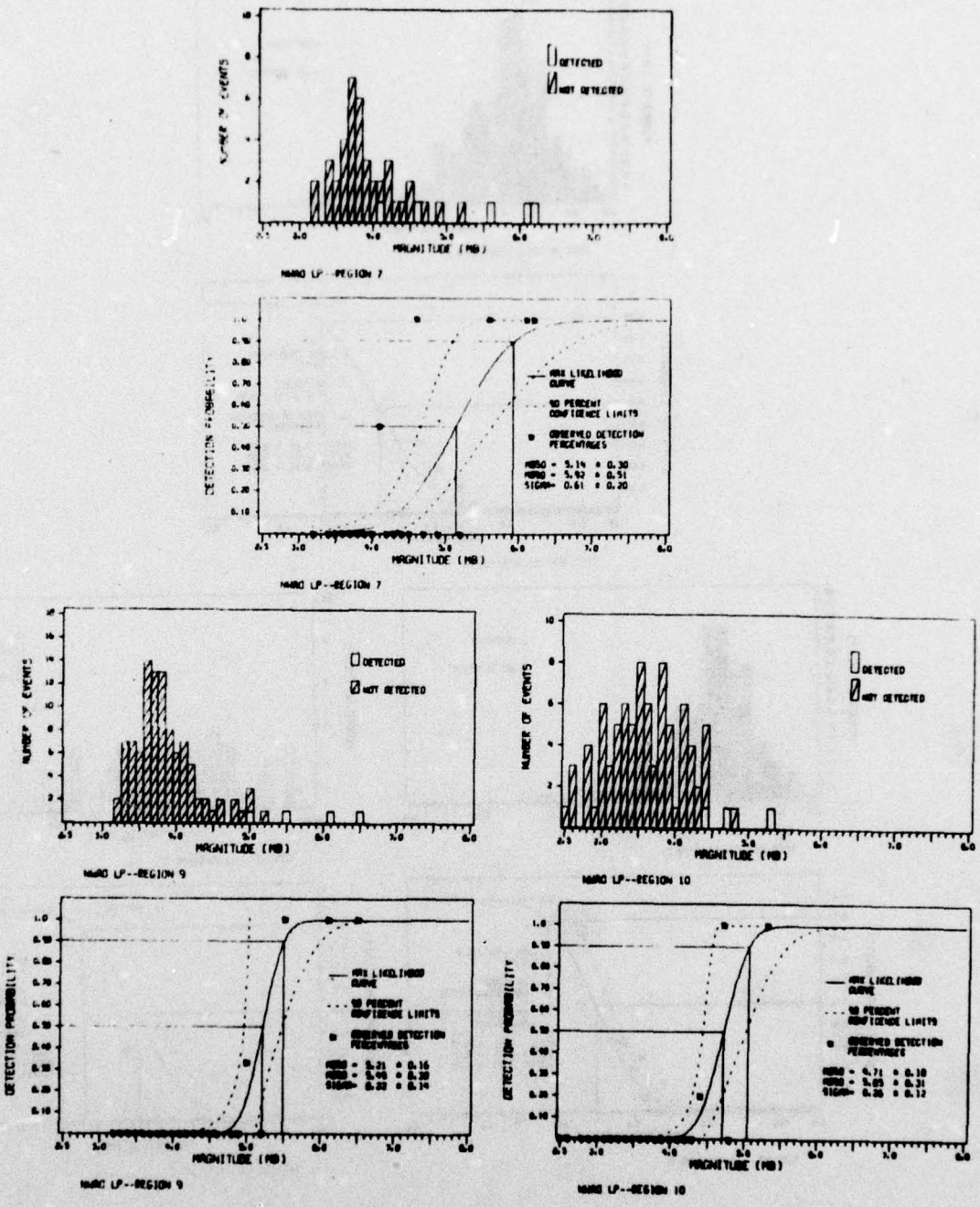

FIGURE V-20

NWAO LONG-PERIOD DETECTION STATISTICS
REGIONS 7, 9, AND 10

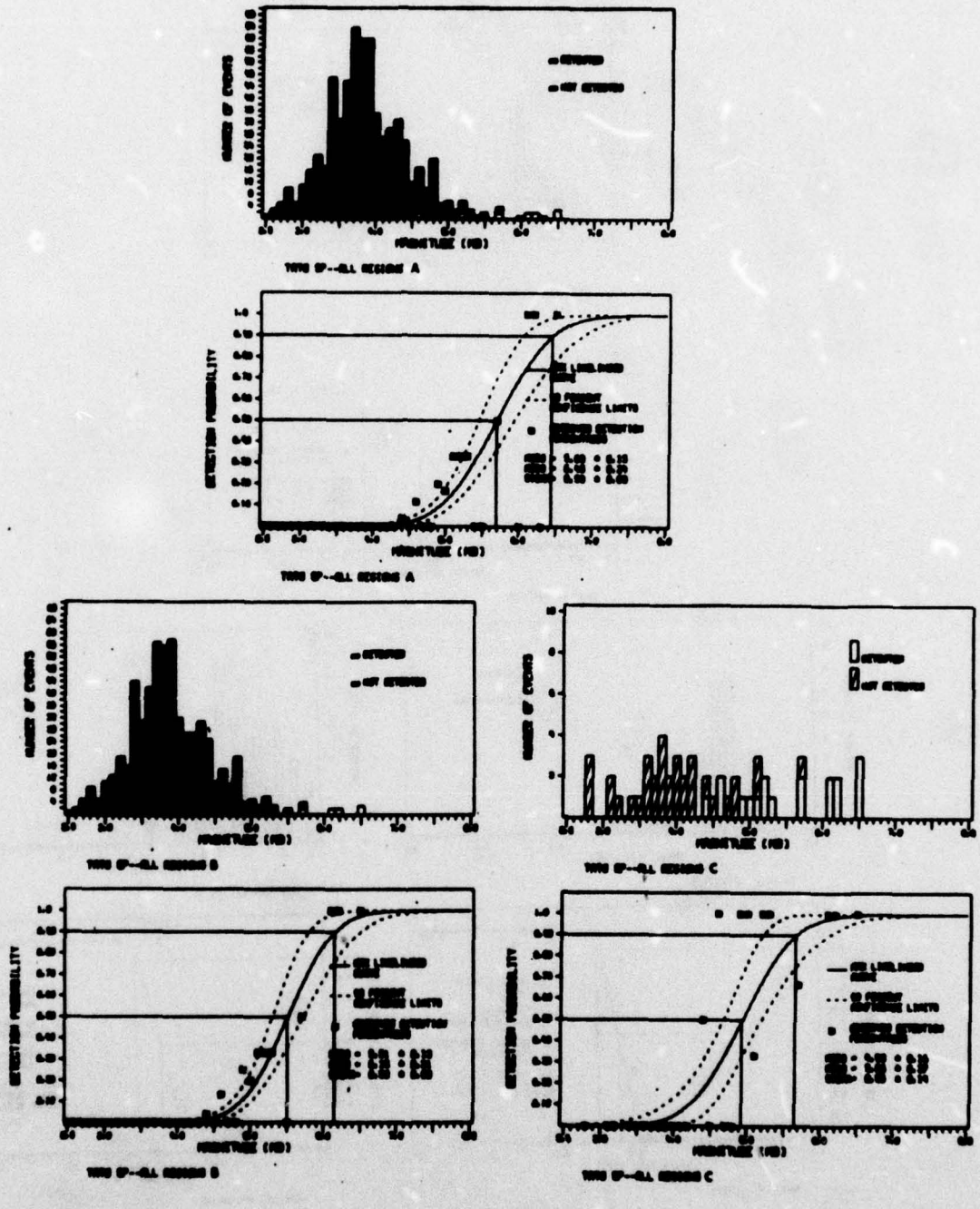

FIGURE V-21

TATO LONG-PERIOD DETECTION STATISTICS
ALL REGIONS A AND B--REGION 1

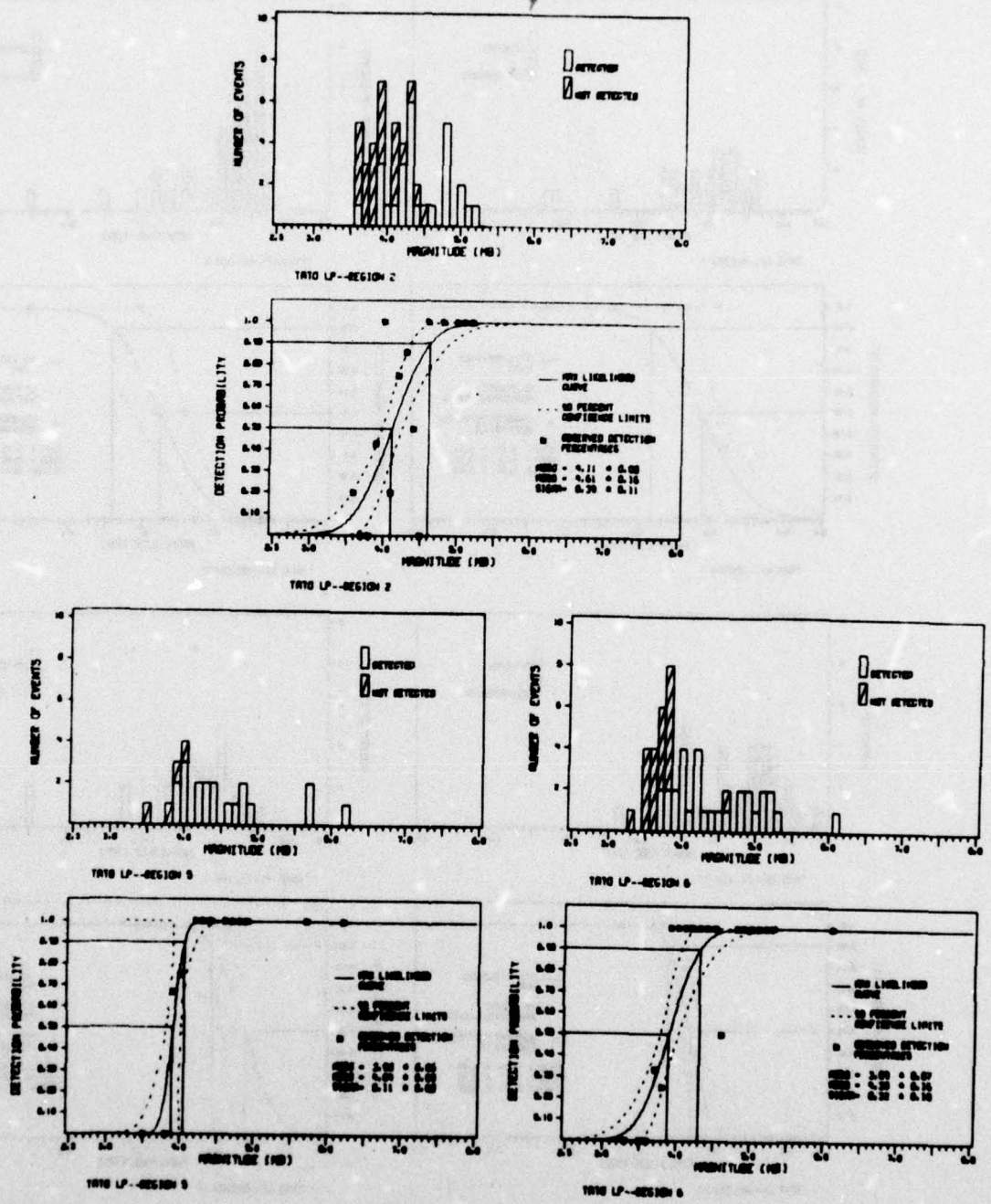

FIGURE V-22

TATO LONG-PERIOD DETECTION STATISTICS
REGIONS 2, 5, AND 6

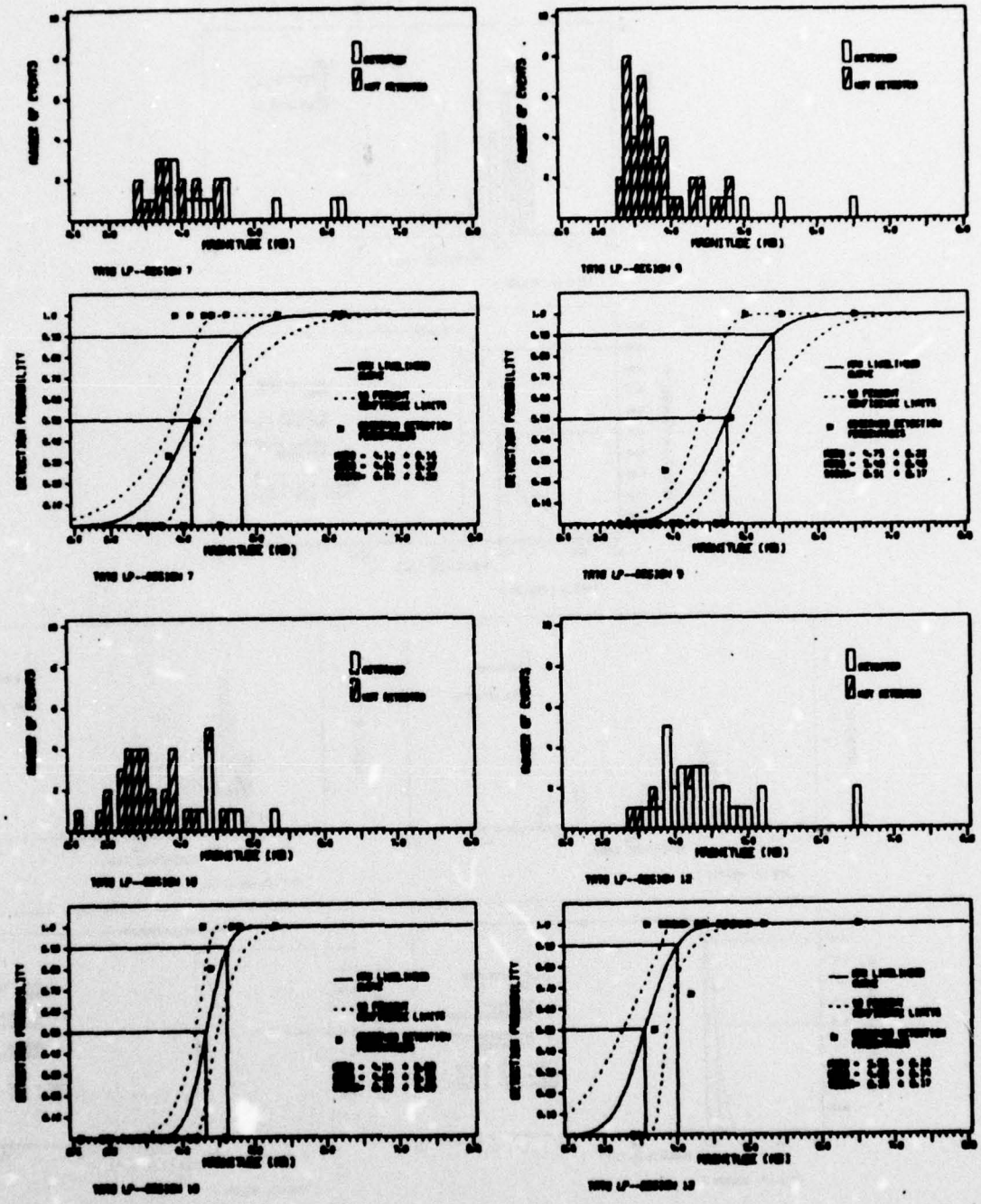

FIGURE V-23

TATO LONG-PERIOD DETECTION STATISTICS
REGIONS 7, 9, 10, AND 12

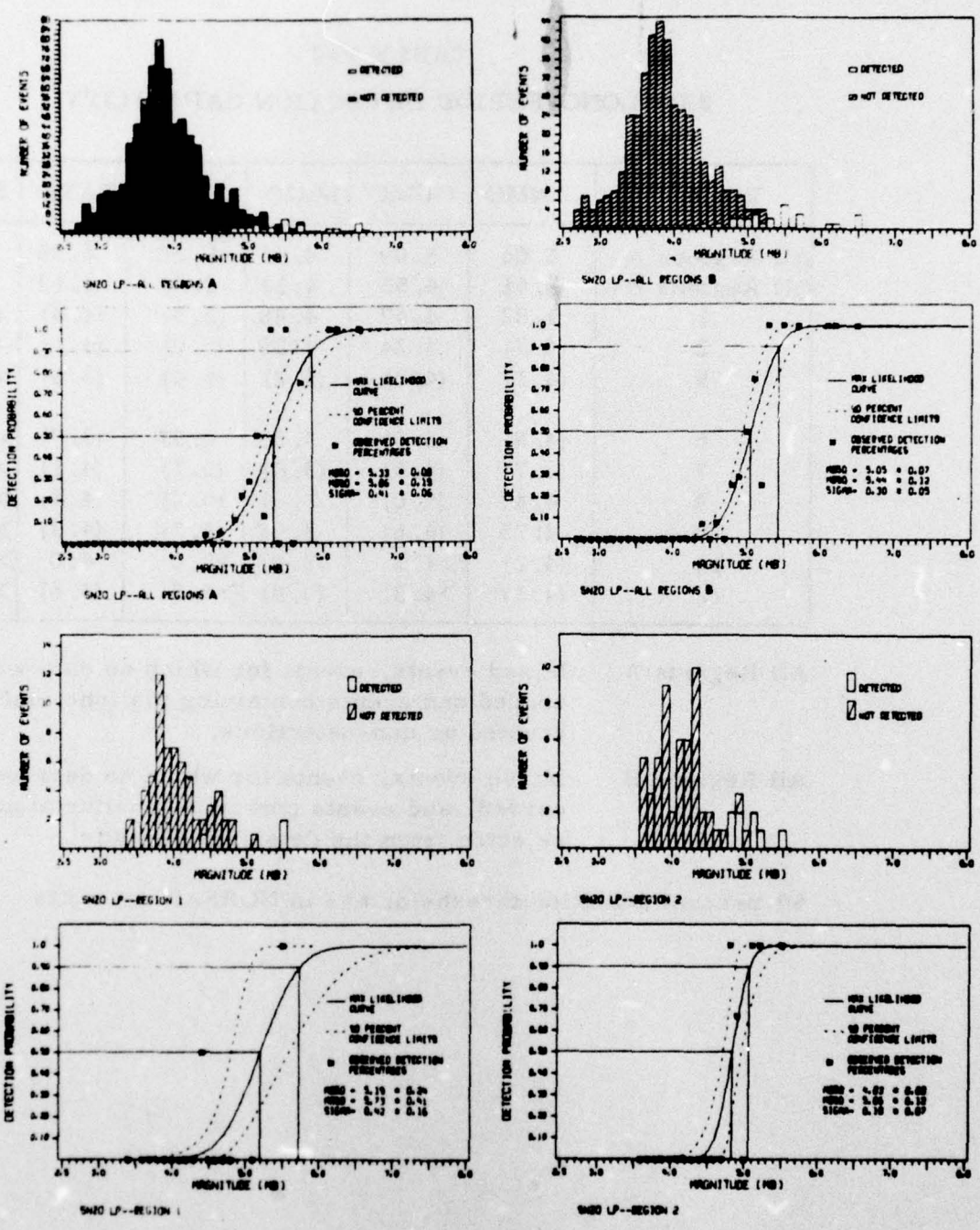

FIGURE V-24

SNZO LONG-PERIOD DETECTION STATISTICS
ALL REGIONS A AND B--REGIONS 1 AND 2

TABLE V-2

SRO LONG-PERIOD DETECTION CAPABILITY

Region	ANMO	GUMO	MAIO	NWAO	TATO	SNZO
All Regions A	5.04	5.09	4.55	5.20	4.50	5.33
All Regions B	4.61	4.53	4.13	4.91	4.12	5.05
1	4.82	4.57	4.48	(5.5)	(4.3)	(5.2)
2	(4.8)	4.24	4.39	(5.0)	(4.1)	(4.8)
5	(4.1)	(4.2)	(4.2)	(4.4)	(3.9)	>4.4
6	(4.5)	(4.5)	3.80	4.57	(3.9)	>4.9
7	(4.7)	(4.5)	(3.8)	(5.1)	(4.1)	>5.2
9	4.47	(5.0)	3.61	(5.2)	(4.8)	>5.2
10	4.25	(4.6)	3.98	(4.7)	(4.3)	>4.7
11	(4.2)	>4.3	3.97	>5.0	4.0	>4.5
12	(4.3)	>4.3	(3.8)	>4.5	(3.6)	>4.9

All Regions A Mixed events, events for which no data were recorded and events containing malfunctions are counted as non-detections.

All Regions B Mixed events, events for which no data were recorded, and events containing malfunctions are rejected from the detection statistic.

50 percent detection thresholds are in NORSAR m_b units.

absolute and conditional detection capabilities is approximately 0.4 m_b units. In each case, this difference is due more to mixed events than to system failures or malfunctions. At GUMO, the difference between the absolute and conditional detection capability estimates is greater than 0.5 m_b units. The increase in this difference over that of the previous group of stations is due to the increased system failure rate (resulting in no data being recorded) of GUMO. The remainder of the difference is primarily due to mixed events.

SECTION VI

EARTHQUAKE-PRESUMED EXPLOSION DISCRIMINATION

A. DISCUSSION

This section considers the question of discriminating between earthquakes and presumed nuclear explosions using long-period data. The discrimination method used is the surface wave magnitude (M_s) versus body wave magnitude (m_b) plot. This plot of M_s versus m_b is expected to function as an earthquake-presumed nuclear explosion discriminant since, for a given m_b, an explosion produces much lower Rayleigh and Love waves than does an earthquake. (Theoretically, an explosion should generate no Love waves, since the source is completely compressional. However, some Love wave energy is radiated from tectonic strain release (Sun, 1977) subsequent to the explosion.) Therefore, a plot of M_s versus m_b can be expected to show a separation of the data points into an earthquake population and an explosion population.

The data base for this discrimination study is comprised of all events which were visually detected on bandpass-filtered (0.023-0.059 Hz passband) plots.

B. COMPUTATION OF SURFACE WAVE MAGNITUDES

In earlier evaluation tasks, the signal amplitude and period values used in computing surface wave magnitudes (M_s) were measured manually on the filtered signal plots at various periods. The computation of M_s then used the equation:

$$M_s = \text{Log}_{10}\left[\frac{A*SF}{T*Q*G}\right] + \text{Log}_{10}\Delta + 1.12$$

where:

A = peak-to-peak amplitude measured in inches on the plot

SF = plot scale factor in computer counts per inch

T = period in seconds of the measured amplitude

Q = quantization factor = 5 computer counts per millimicron

G = instrument response correction factor, and

Δ = epicentral distance in degrees.

This approach has several disadvantages. First, the analyst is apt to have difficulties finding the largest peak at each desired period--it is sometimes necessary to measure the periods of a number of waveforms before finding the desired period. Next, having found the waveform for which M_s is to be measured, the analyst may make a measurement error. Finally, errors are apt to occur either in transcribing the measured values or in calculating the surface-wave magnitude from these values.

In order to avoid these problems and make the process of obtaining M_s values less tiresome, a program was written to perform the measurements and calculations automatically. This program operates by first finding the times of all zero crossings in a given time gate and the maximum absolute amplitude in millimicrons between each pair of adjacent zero crossings. The waveform period is then simply

$$T = 2 * \left[\text{Time of Zero}_{i+1} - \text{Time of Zero}_{i}\right]$$

The program reads the epicentral distance from the event header. The quantization factor and instrument response corrections are built into the program. (The instrument response corrections are derived from the instrument response curve of Figure VI-1.)

The program uses the above information to compute a surface-wave magnitude for each amplitude-period pair. These M_s values with their

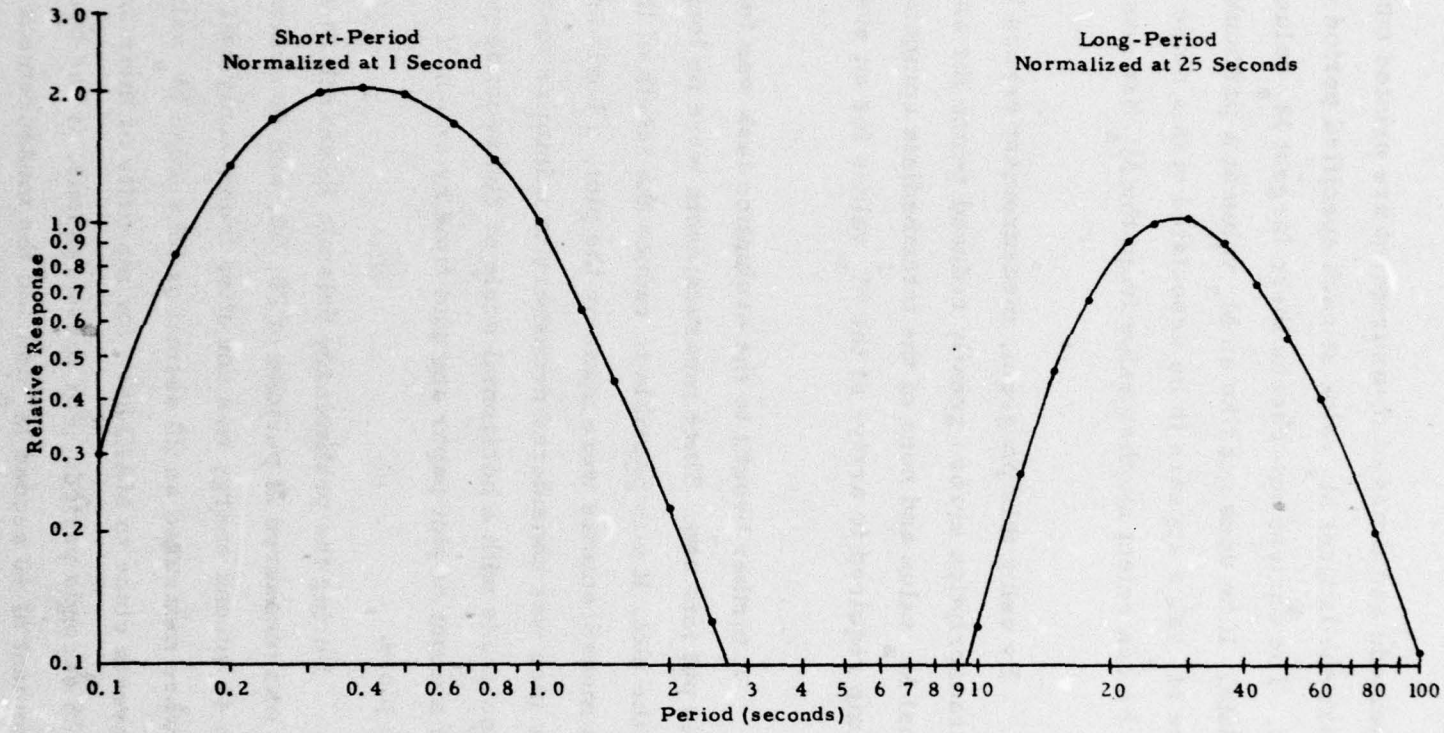

FIGURE VI-1

NORMALIZED INSTRUMENT RESPONSE CURVES

associated periods and times of measurement are printed out. Finally the program picks the largest M_s value at each specified period of interest and prints it out. The analyst now checks these largest M_s values against the plot of the data. If he does not like an M_s value at a particular period (for example, the M_s value appears to be associated with a noise pulse in the signal gate) he can select another value from the M_s list generated by the program.

By using this program, measurement errors have been eliminated and transcription errors greatly reduced (since the analyst only writes down the final M_s value and none of the intermediate computational values). Also, the time required to arrive at the M_s values for an event has been reduced.

A further benefit to the evaluation task was found once this program was put into use. Since measurements were no longer being made directly on the plot, it was possible to reduce the length of the plots by one-half. When measurements were made on the plot, a horizontal scale of 100 seconds per inch was considered necessary to minimize measurement errors. Plots are now made with a horizontal scale of 200 seconds per inch. This reduced the amount of plot paper and plot time by one-half and produced more manageable plots.

During the preliminary Seismic Research Observatories evaluation, M_s was measured at periods of 20, 30, and 40 seconds. However, measurable 40 second energy was not often found--only half as many 40 second M_s values were measured as 20 second or 30 second M_s values. It was also noted that events close to MAIO have the majority of their energy concentrated at or near 25 seconds period. For these reasons, it has been decided to drop the measurement of 40 second M_s and add the measurement of 25 second M_s.

C. DISCRIMINATION RESULTS

Table VI-1 lists those events of the data base which may be termed presumed nuclear explosions. They were selected on the basis of their epicentral locations and body wave magnitudes. Thus, the events from Region 16 were selected because their epicenters are at the Nevada Test Site and their body wave magnitudes are much larger than known earthquakes in the area. The events from Region 8 were selected because their epicenters are at the eastern Kazakh test site and their body wave magnitudes are larger than most earthquakes from that area. The one event from Region 10 has its epicenter in an area of low seismicity where peaceful nuclear devices are known to have been used.

The numbers in the columns under the heading 'Processing Results' refer to the detection status of the events as recorded at each station. A dash indicates that the event was not processed at that station--in most cases because the station was not operational. The number 1 indicates that the event was detected, 2 indicates that it was not detected, 3 indicates that it was mixed with another event, 4 indicates no data were recorded for that event, and 5 indicates that a system malfunction obscured the data. These codes indicate that five of the eighteen events listed in Table VI-1 cannot be used in the discrimination study, since they were not detected at any of the stations.

Figures VI-2 to VI-50 show the M_s - m_b plots for the Seismic Research Observatories surface wave magnitudes measured at periods of 25 seconds. The values are plotted by station with one plot encompassing data from all regions followed by individual plots for data from each region. Each regional plot also shows the data points for the presumed nuclear explosions. The symbols used in these plots are:

O - earthquake with depth less than 60 km or depth unknown

TABLE VI-1

PRESUMED NUCLEAR EXPLOSION EVENT LIST WITH DETECTION STATUS

Event	Region	m_b	Detection Status*					
			ANMO	GUMO	MAIO	NWAO	TATO	SNZO
13	8	6.3	1	1	---	---	---	---
91	16	5.9	1	1	1	---	---	---
171	8	5.0	4	3	3	---	---	---
401	16	5.9	1	1	4	---	---	---
410	16	5.6	1	3	4	---	---	---
485	16	5.4	1	1	1	1	---	1
500	16	5.9	1	1	4	1	---	1
522	16	5.7	1	1	1	1	---	2
523	16	5.6	1	3	1	1	---	2
537	8	4.8	1	1	1	1	---	2
675	8	4.9	2	2	2	2	---	2
676	8	5.4	2	2	2	2	---	2
839	8	4.6	2	5	1	2	2	2
958	8	5.3	2	4	3	3	3	3
1062	8	6.2	1	1	1	2	1	2
1152	8	4.9	3	4	3	5	4	3
1200	10	6.7	3	4	1	3	1	3
1368	8	6.0	---	2	---	2	1	---

* Meaning of Detection Status Codes

1 - event detected according to detection criteria of Section V

2 - event not detected

3 - mixed event

4 - system failure resulting in no data being recorded

5 - malfunction (spike, glitch or the like) in signal gate.

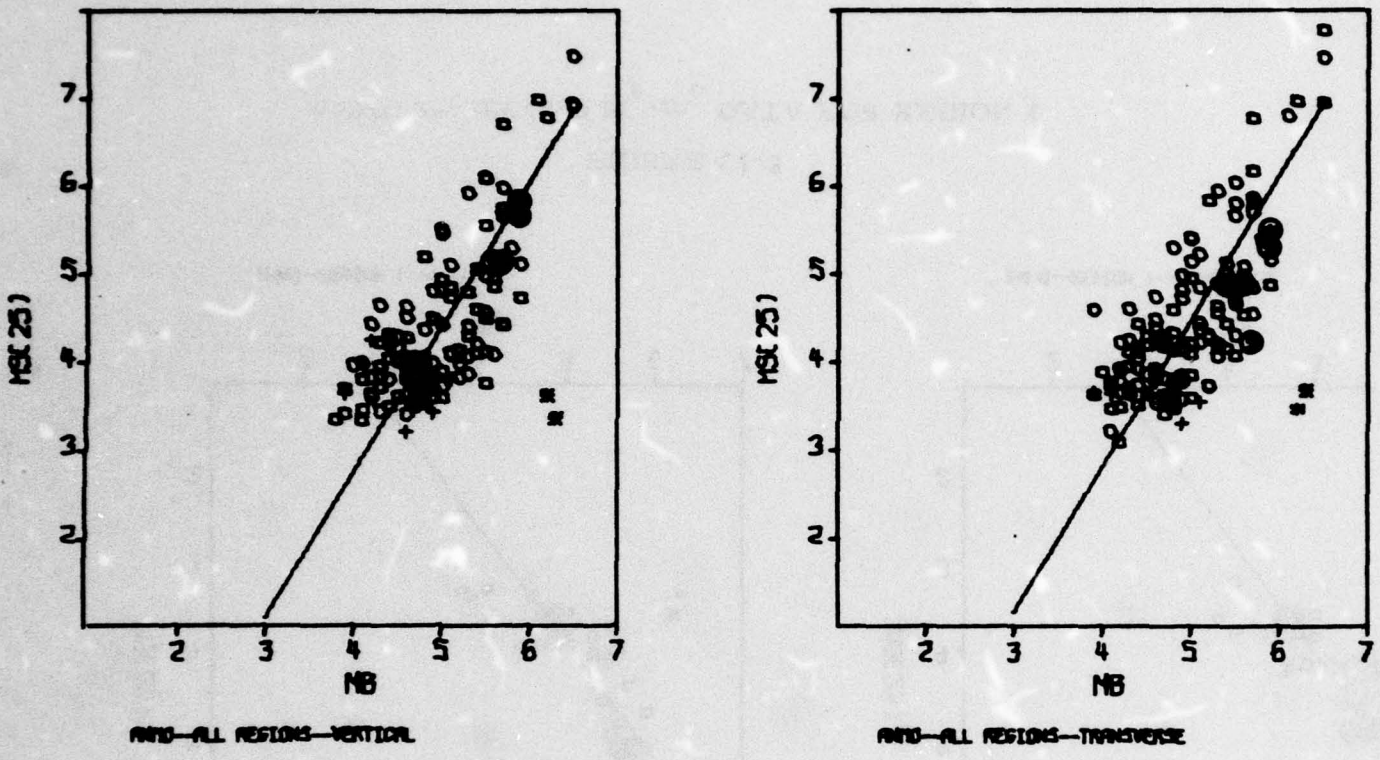

FIGURE VI-2

ANMO 25-SECOND M_s-m_b DATA FOR ALL REGIONS

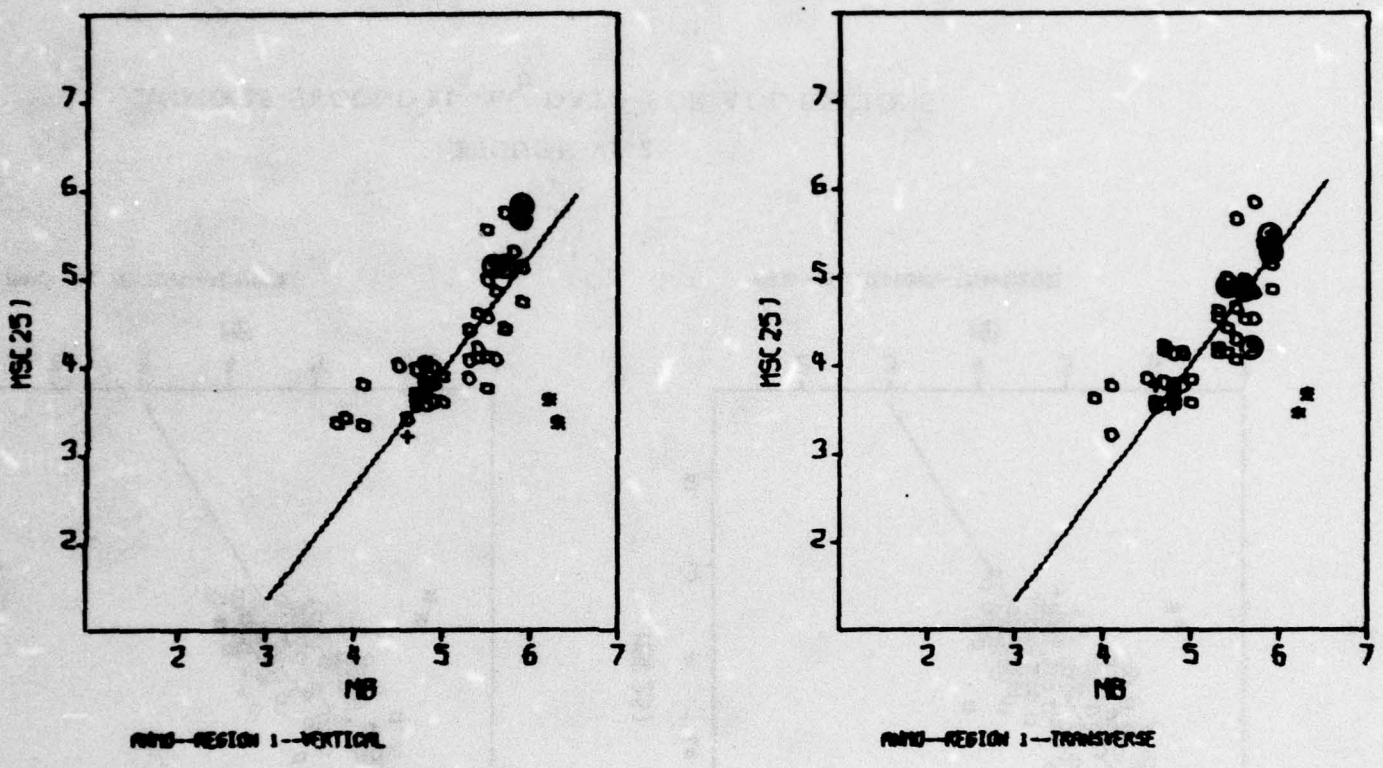

FIGURE VI-3

ANMO 25-SECOND M_s-m_b DATA FOR REGION 1

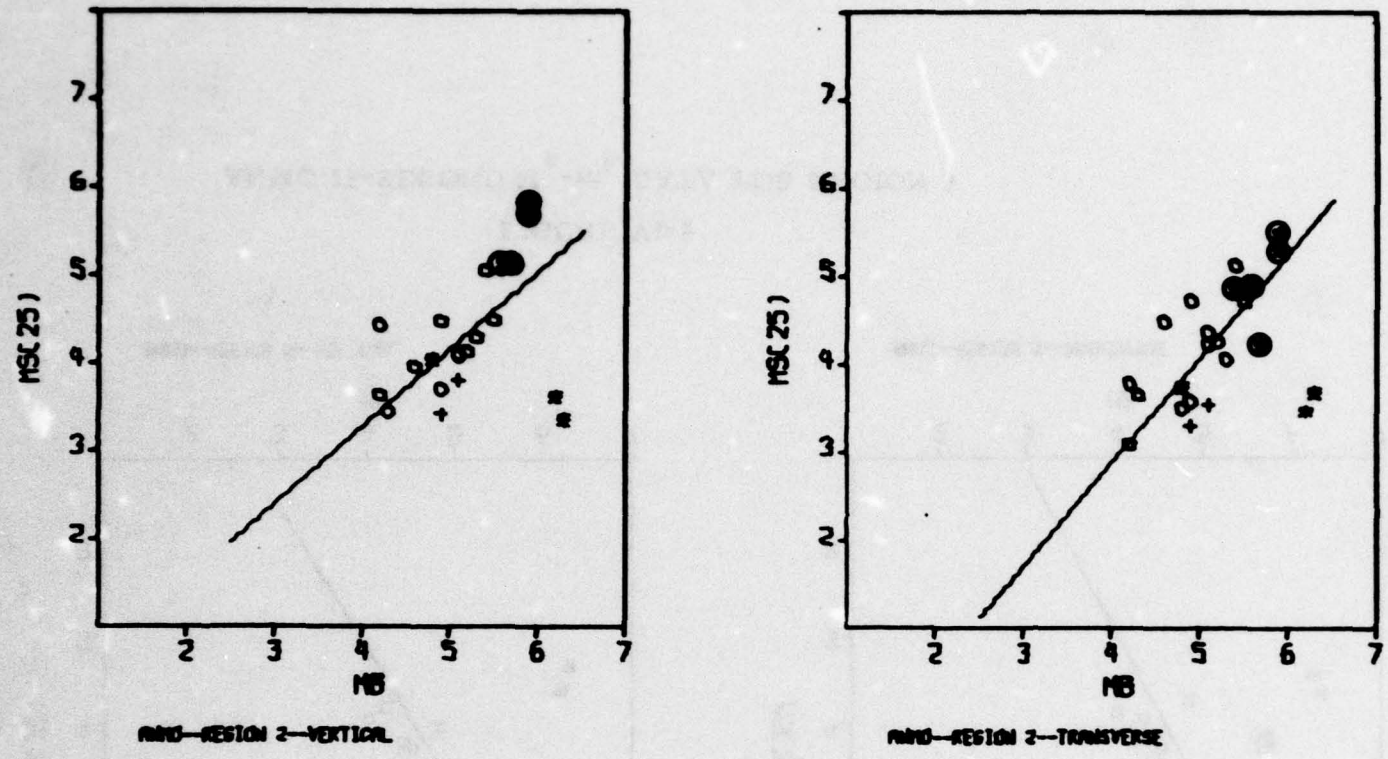

FIGURE VI-4

ANMO 25-SECOND M_s-m_b DATA FOR REGION 2

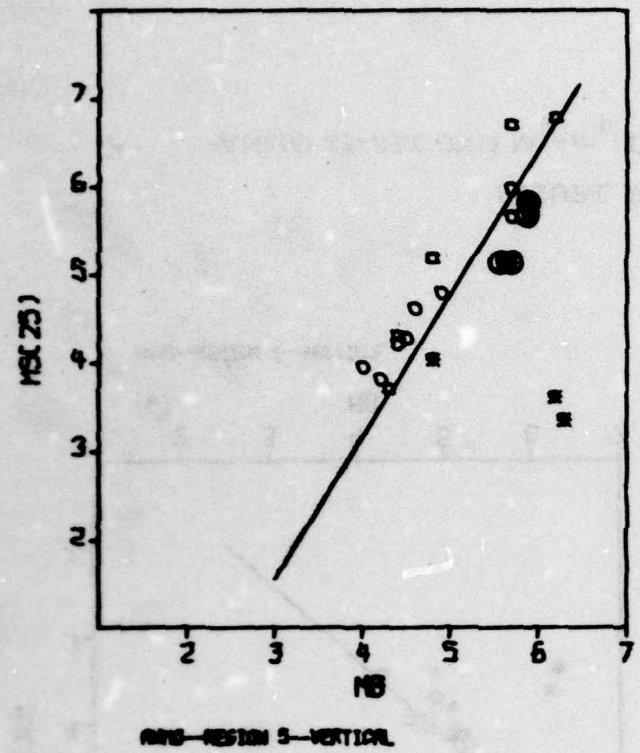

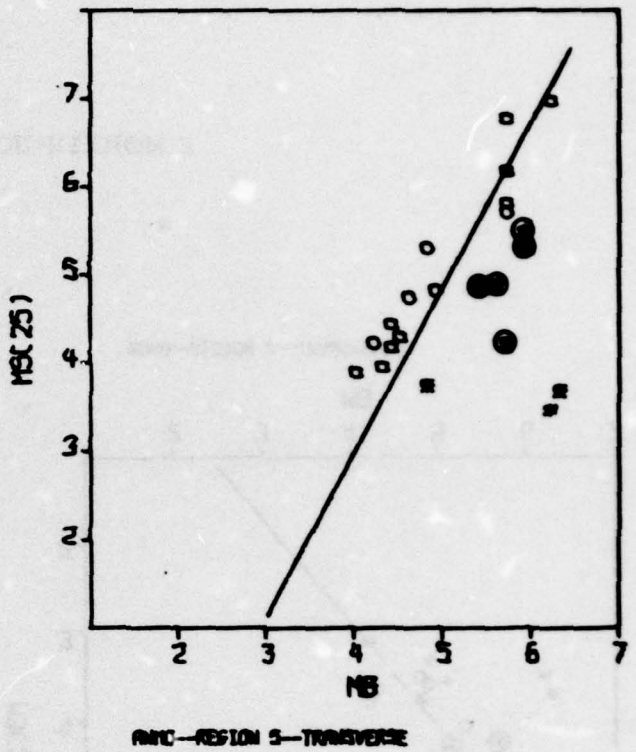

FIGURE VI-5

ANMO 25-SECOND M_s-m_b DATA FOR REGION 5

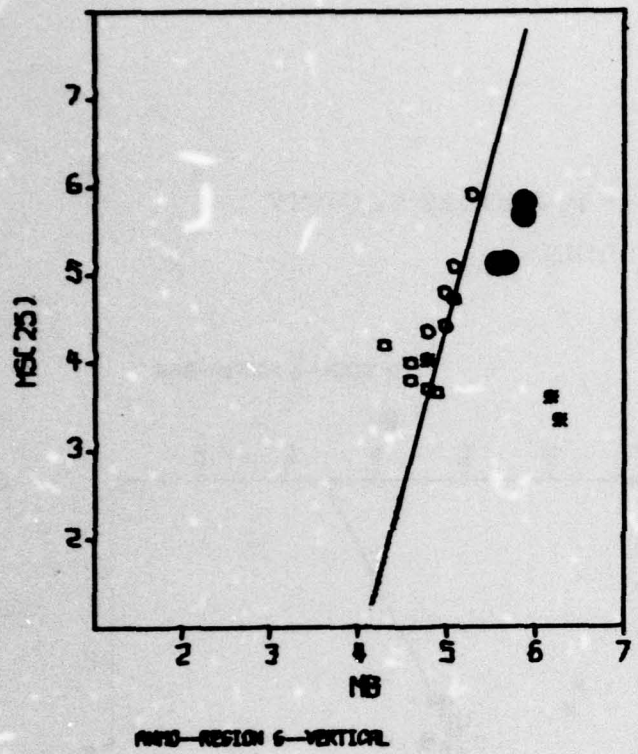

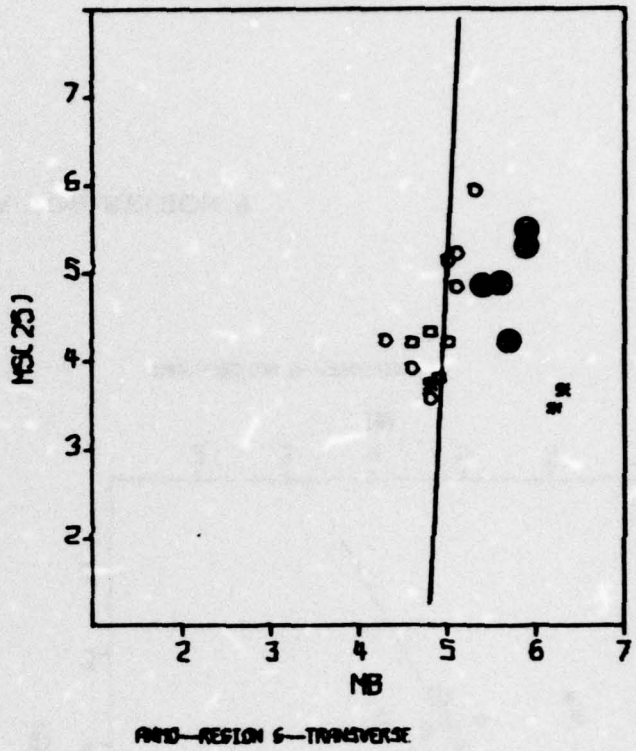

FIGURE VI-6

ANMO 25-SECOND M_s-m_b DATA FOR REGION 6

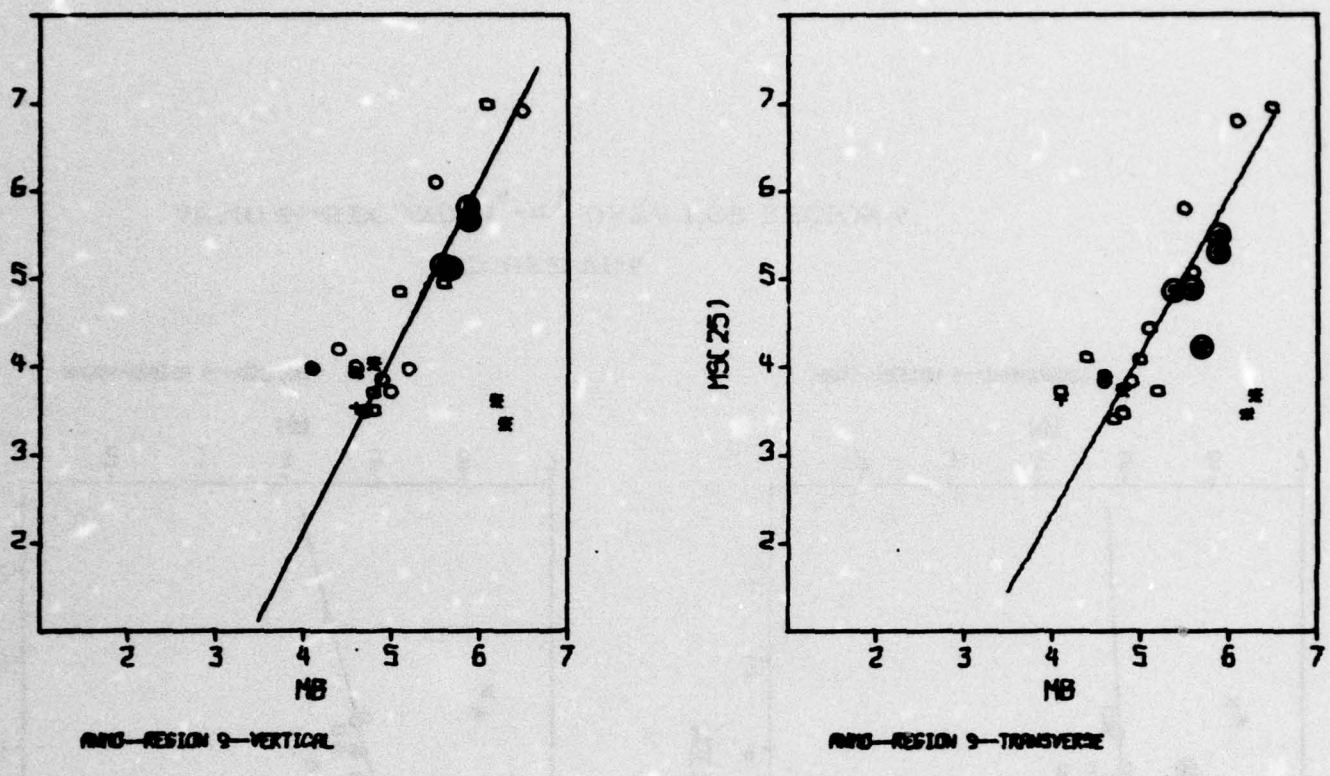

FIGURE VI-7

ANMO 25-SECOND M_s-m_b DATA FOR REGION 9

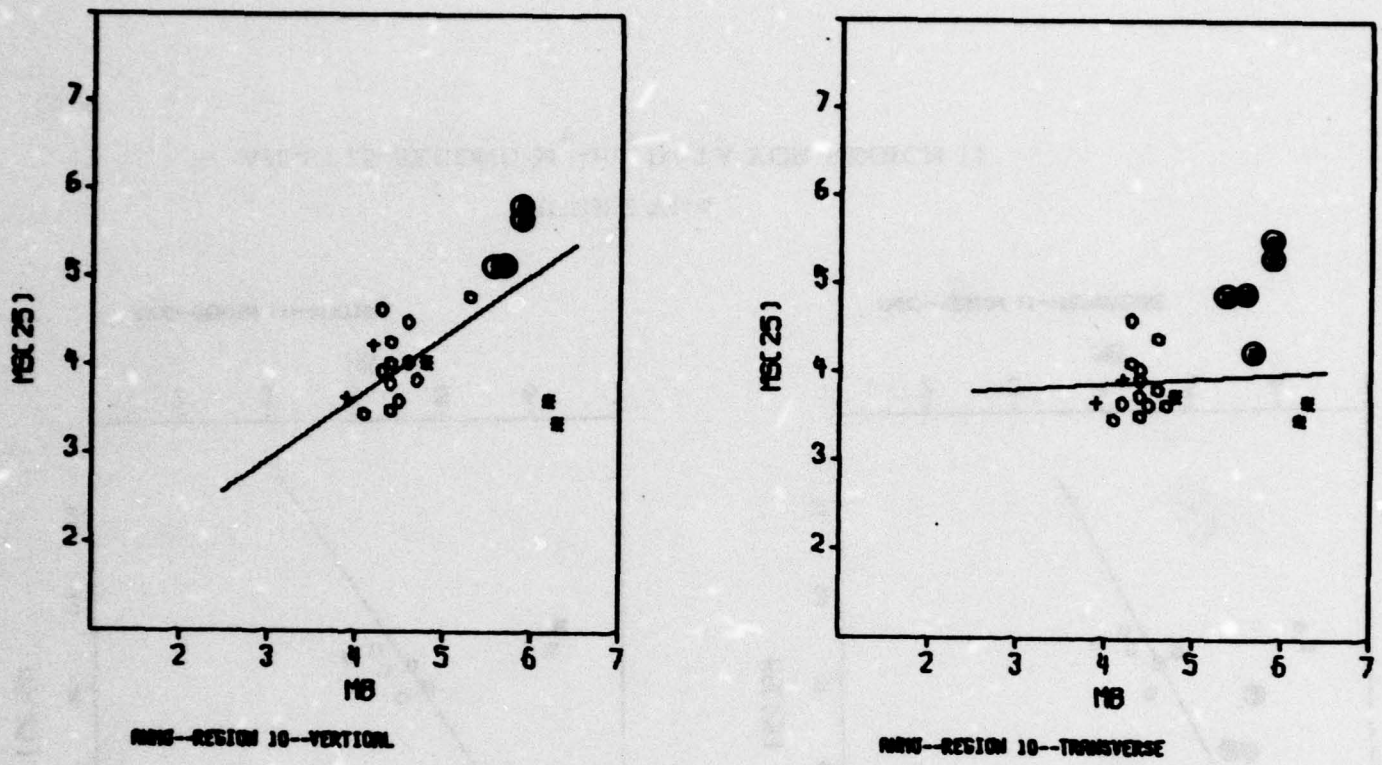

FIGURE VI- 8

ANMO 25-SECOND M_s-m_b DATA FOR REGION 10

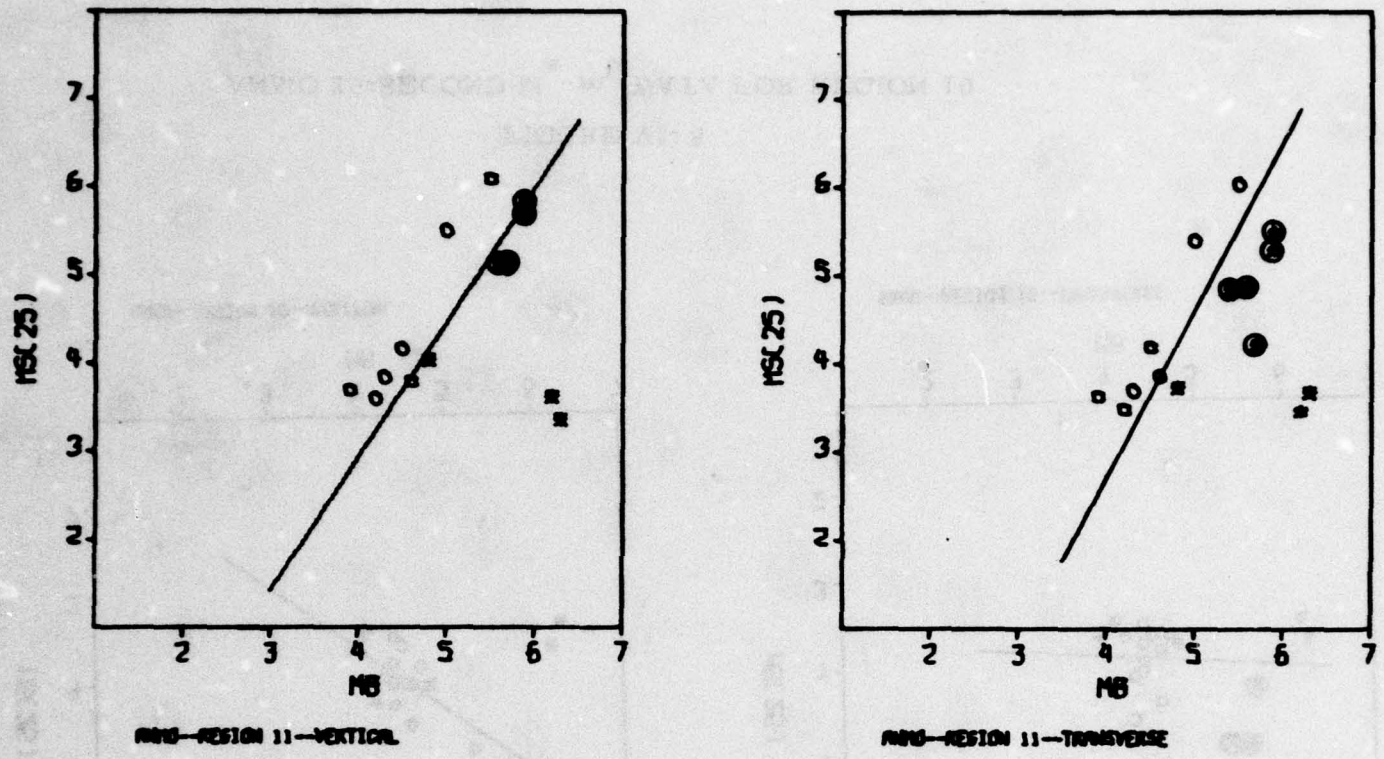

FIGURE VI-9

ANMO 25-SECOND M_s-m_b DATA FOR REGION 11

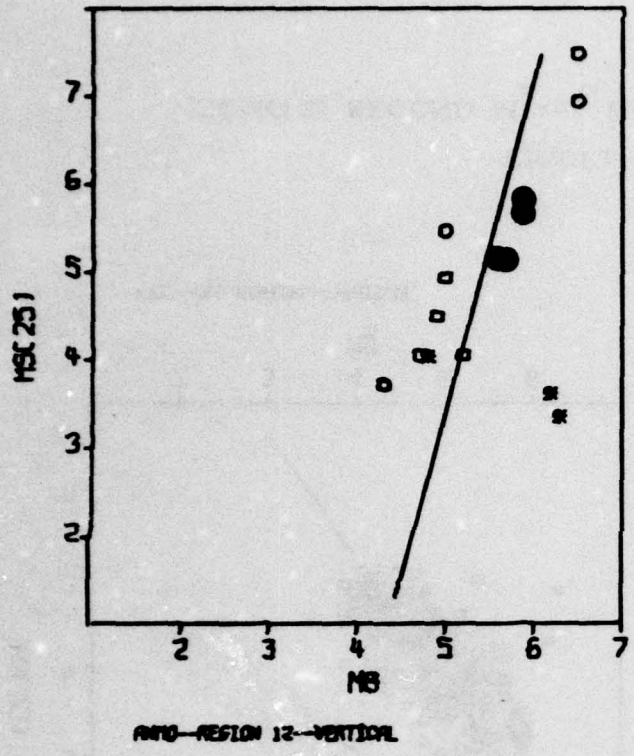

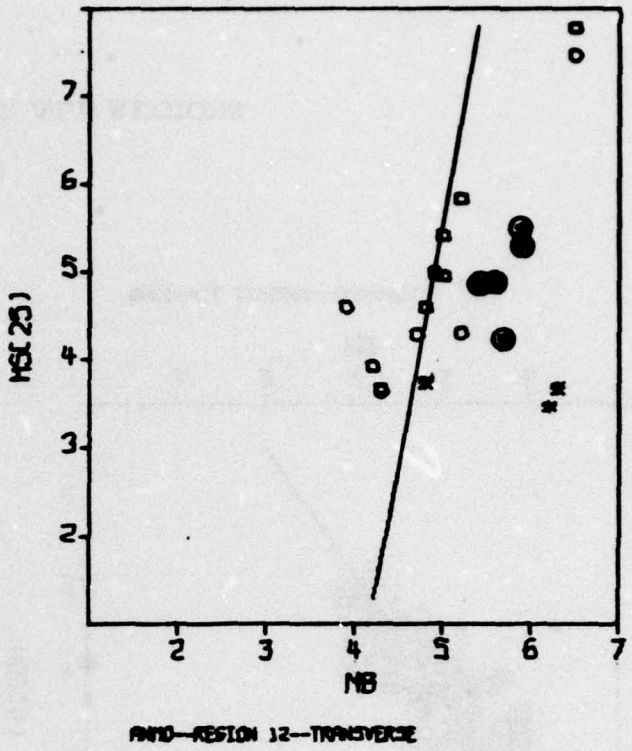

FIGURE VI-10

ANMO 25-SECOND M_s-m_b DATA FOR REGION 12

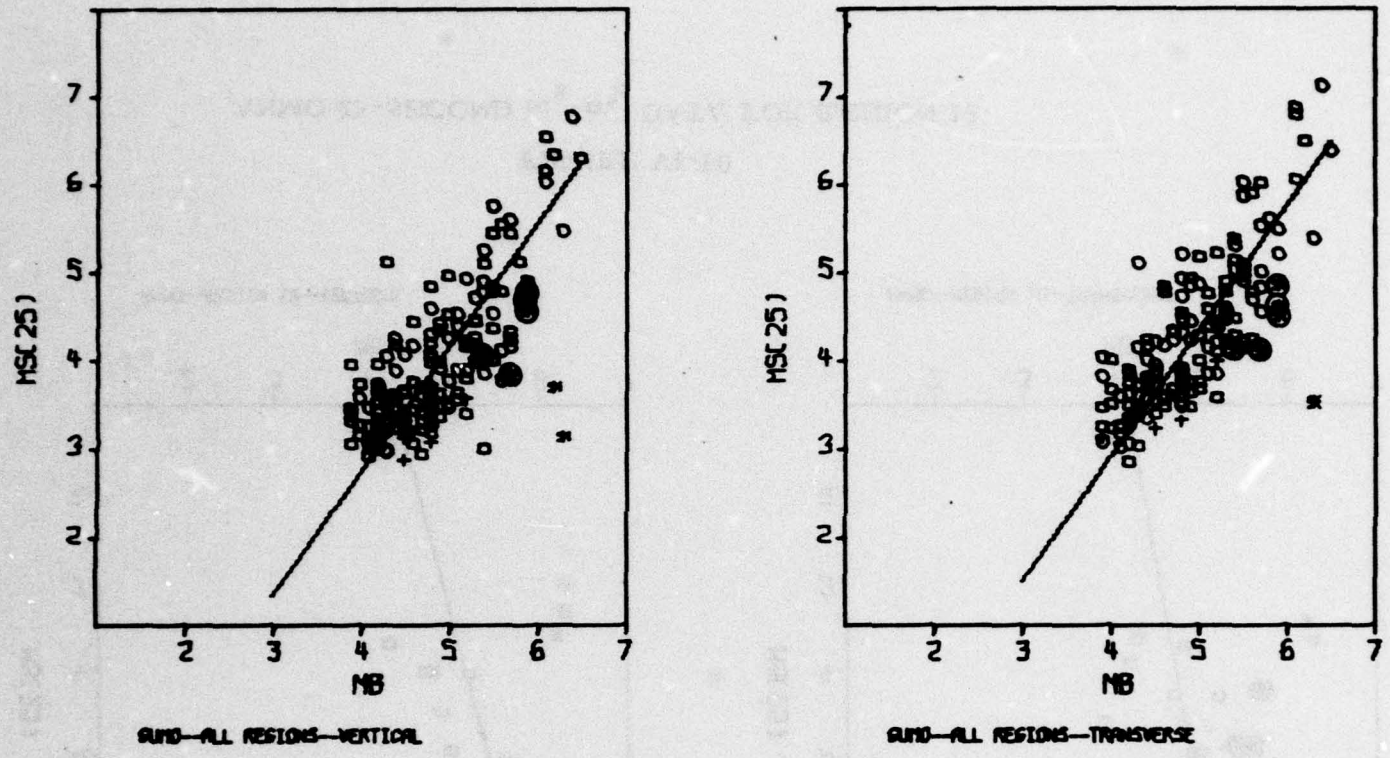

FIGURE VI-11

GUMO 25-SECOND M_s-m_b DATA FOR ALL REGIONS

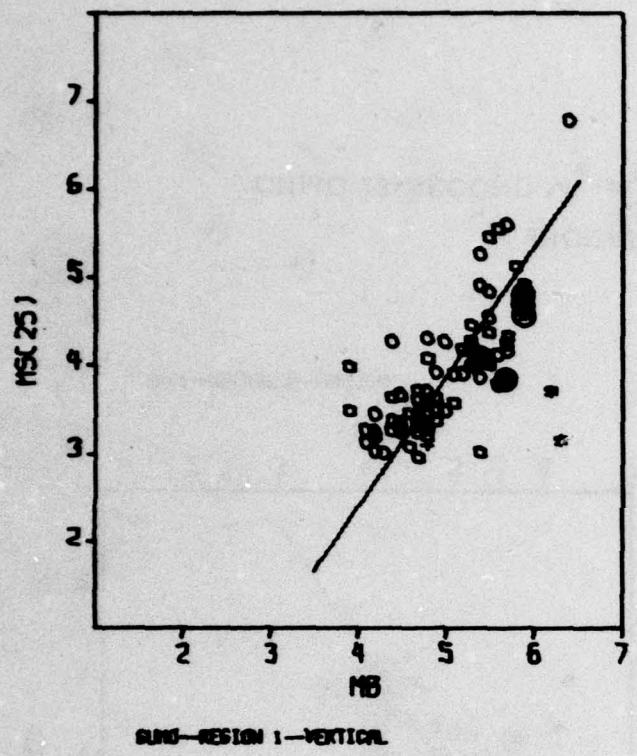

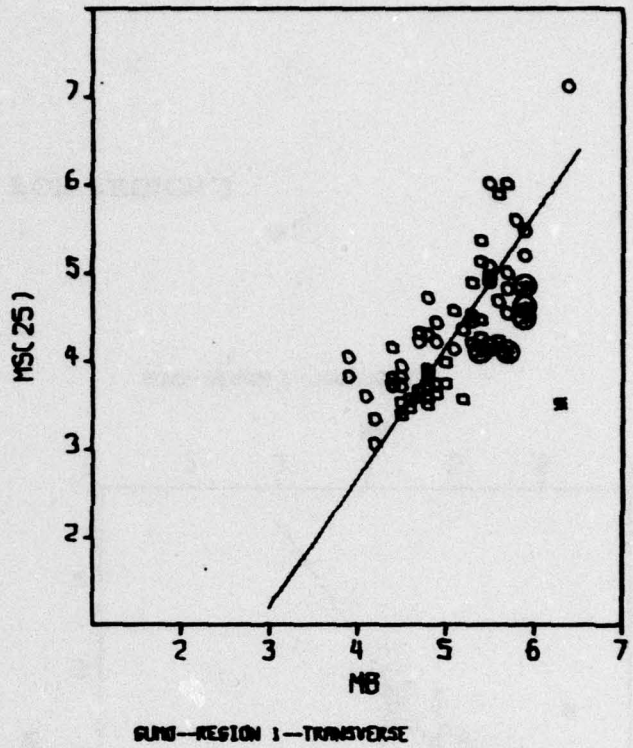

FIGURE VI-12

GUMO 25-SECOND M_s-m_b DATA FOR REGION 1

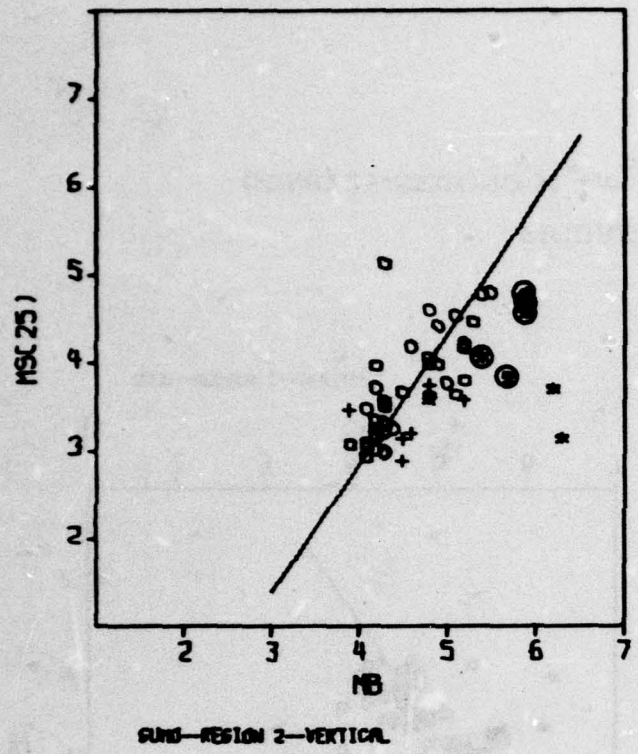

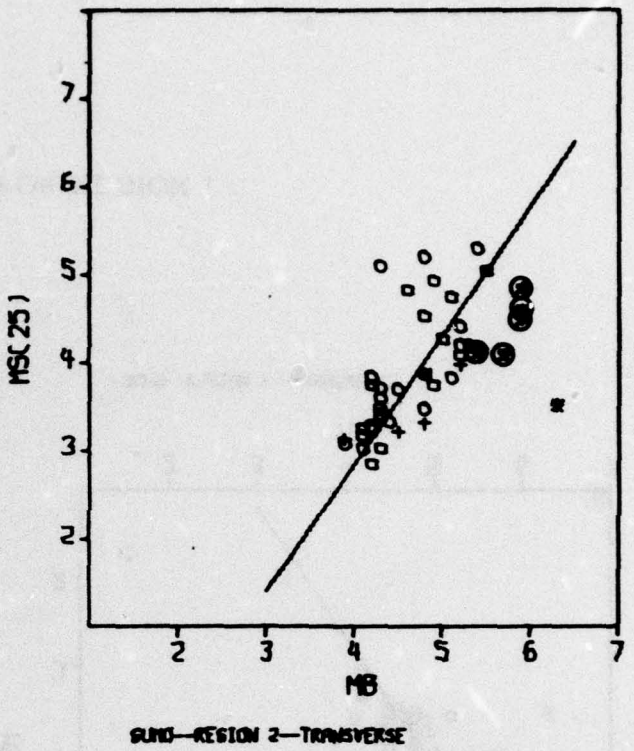

FIGURE VI-13

GUMO 25-SECOND M_s-m_b DATA FOR REGION 2

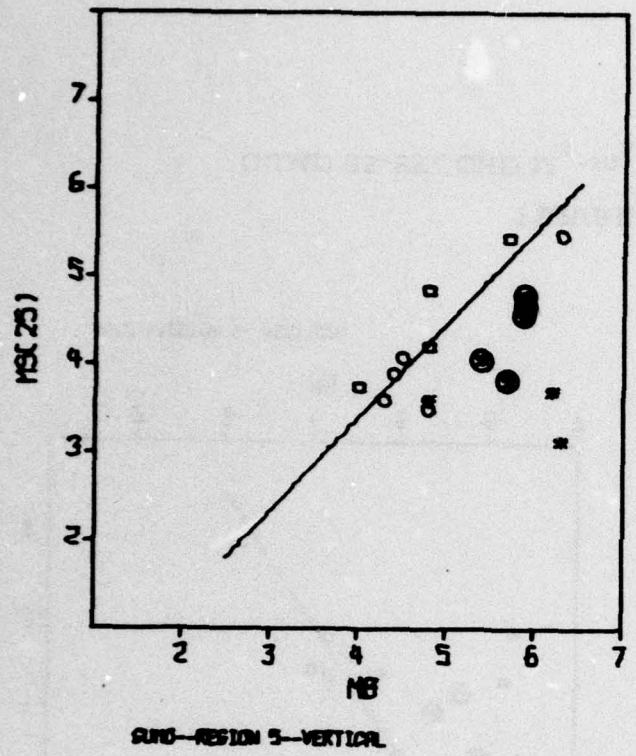

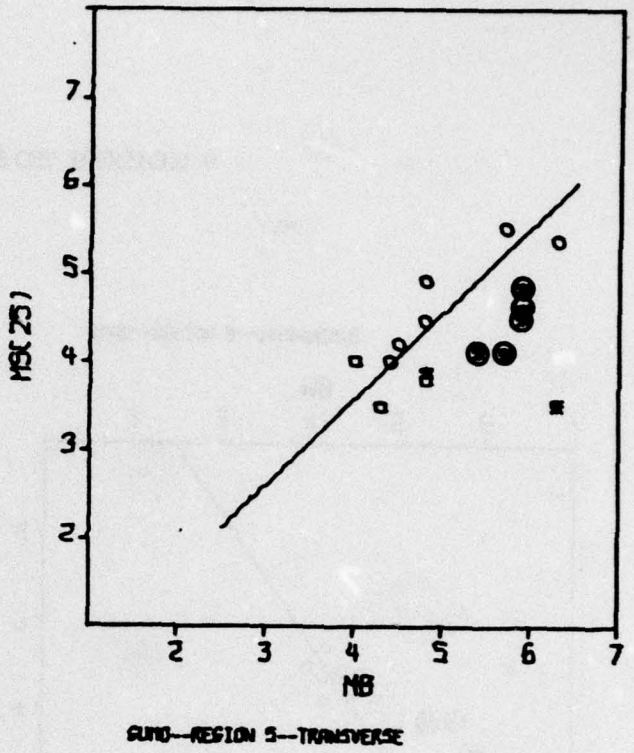

FIGURE VI-14

GUMO 25-SECOND M_s-m_b DATA FOR REGION 5

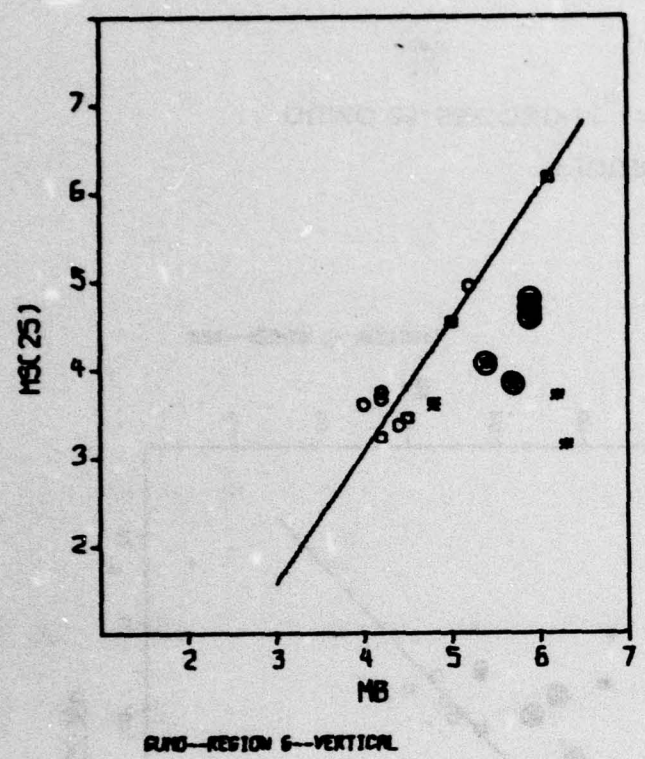

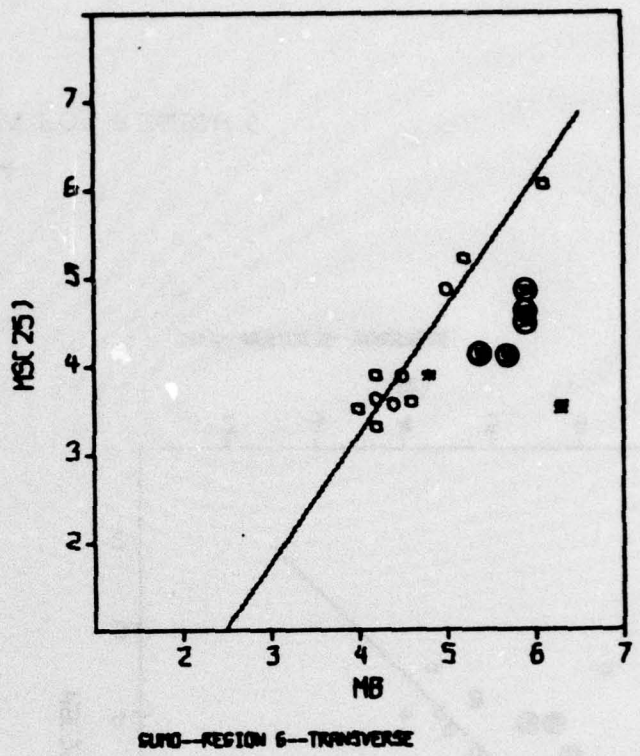

FIGURE VI-15

GUMO 25-SECOND M_s-m_b DATA FOR REGION 6

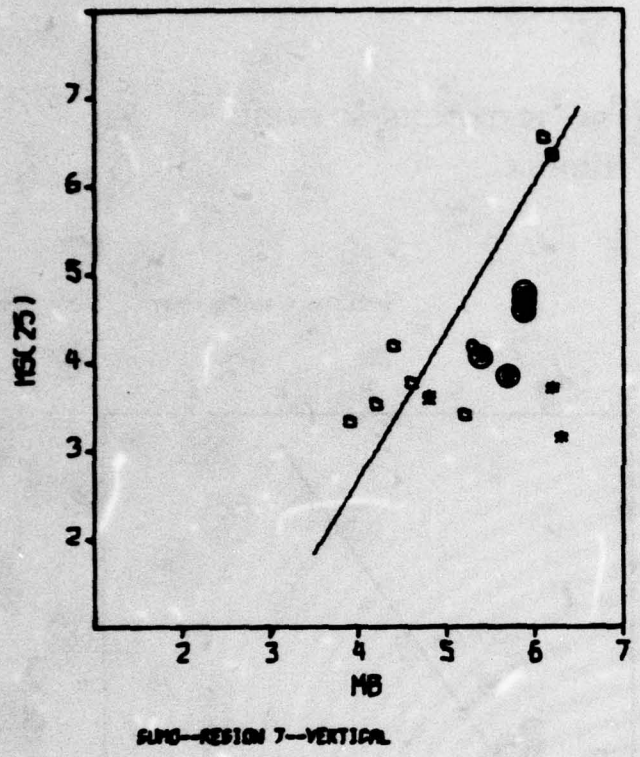

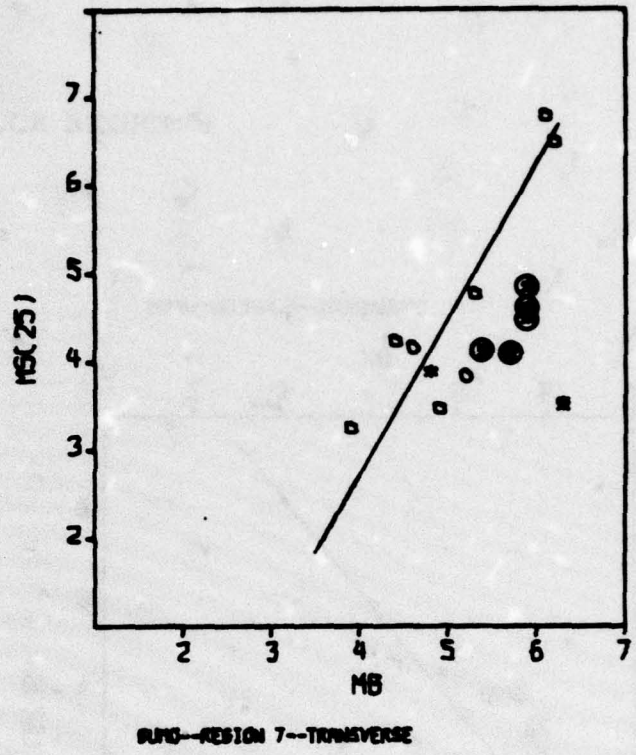

FIGURE VI-16

GUMO 25-SECOND M_s-m_b DATA FOR REGION 7

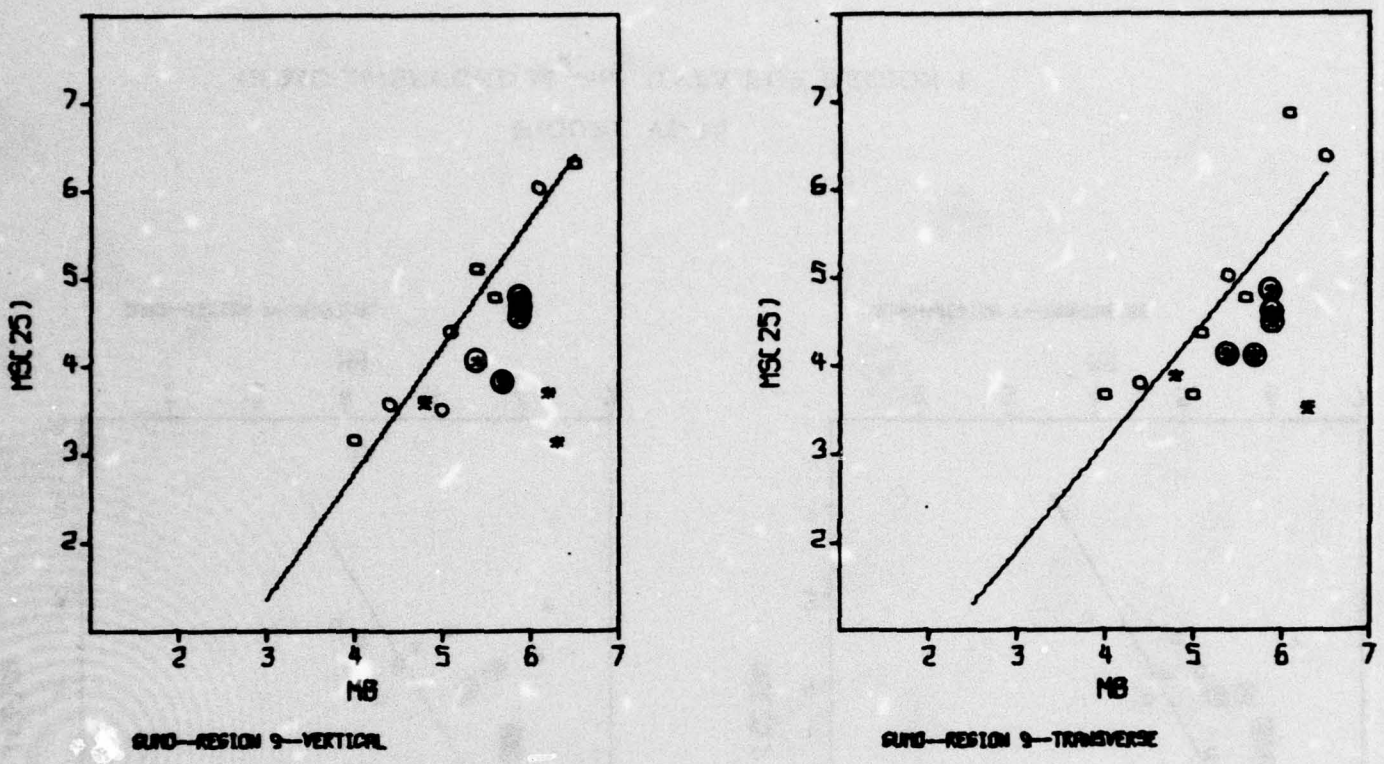

FIGURE VI-17

GUMO 25-SECOND M_s-m_b DATA FOR REGION 9

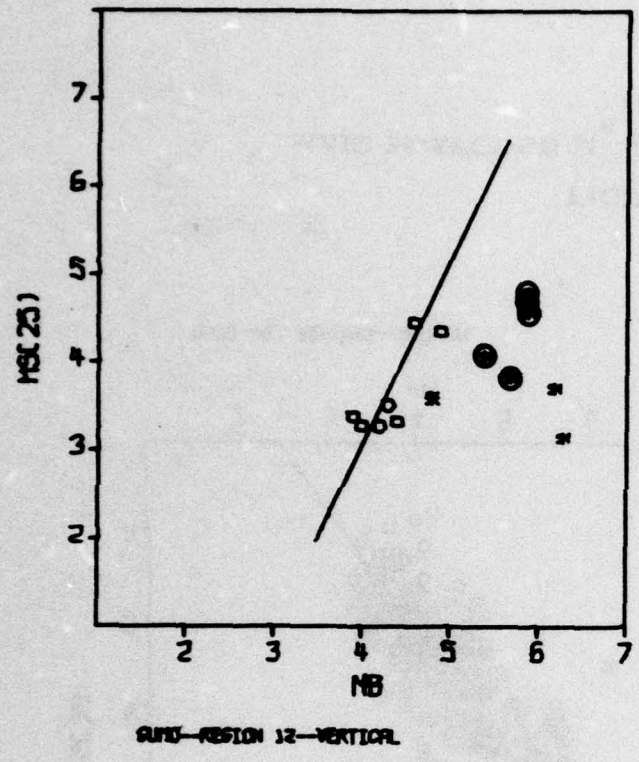

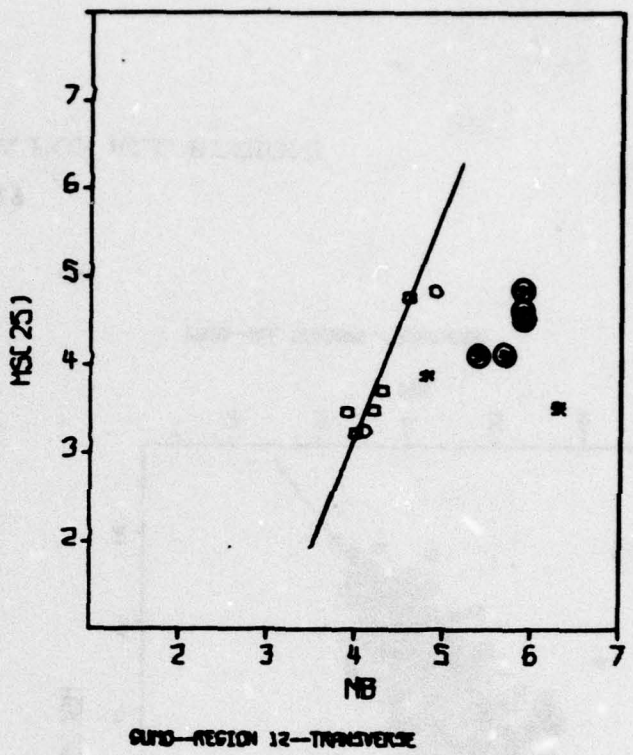

FIGURE VI-18

GUMO 25-SECOND M_s-m_b DATA FOR REGION 12

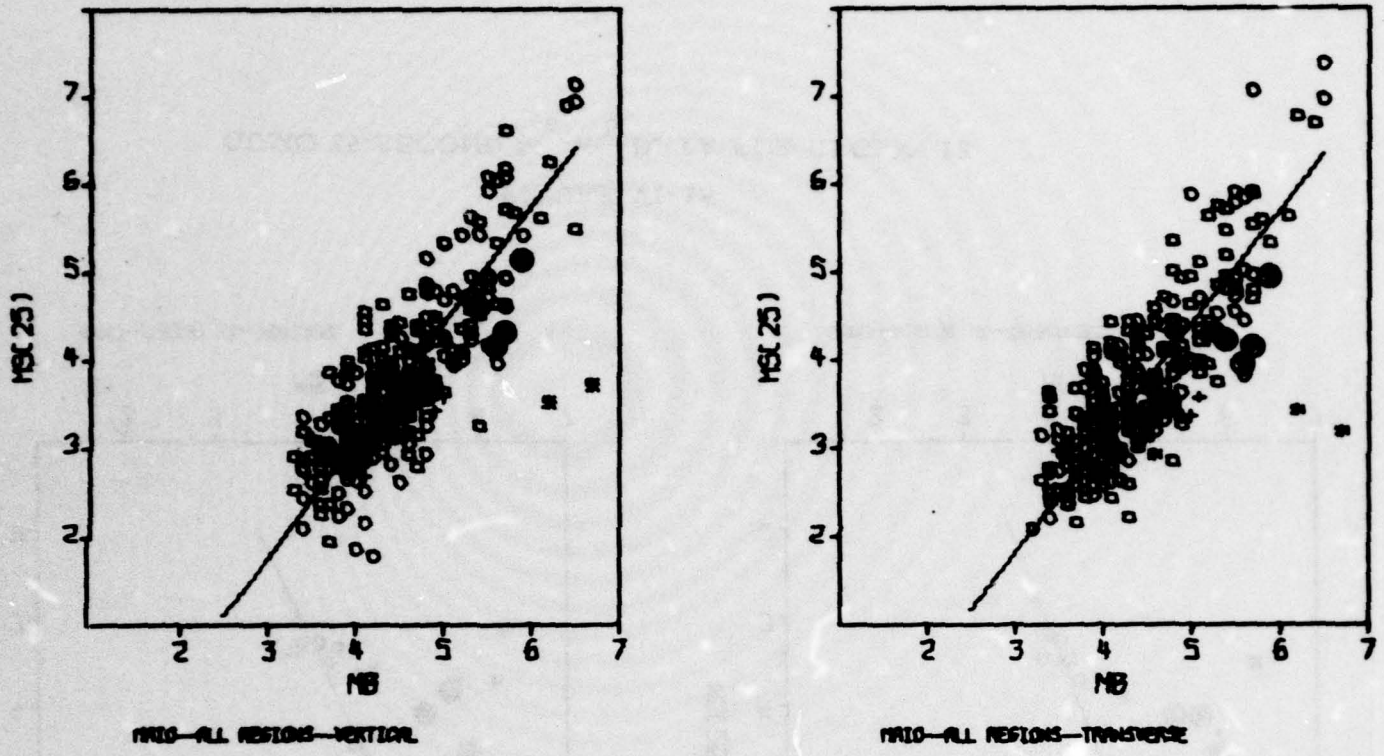

FIGURE VI-19

MAIO 25-SECOND M_s-m_b DATA FOR ALL REGIONS

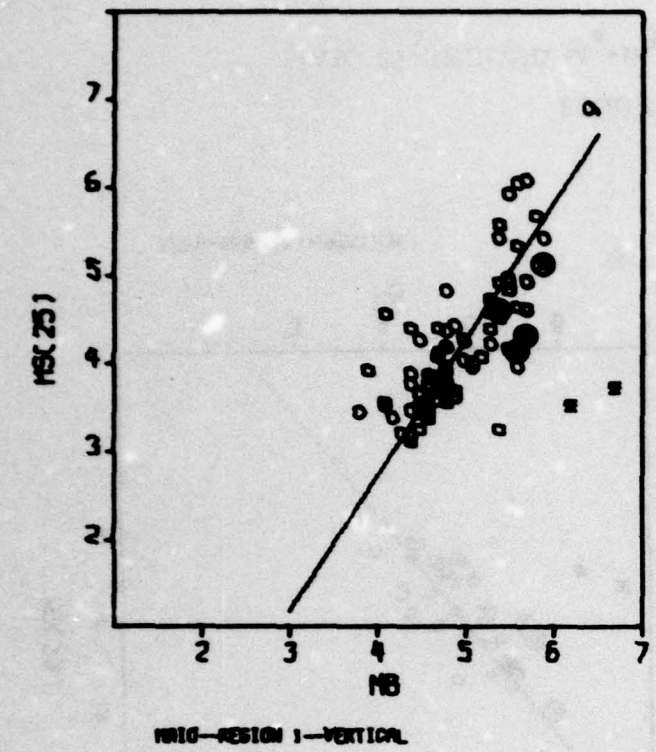

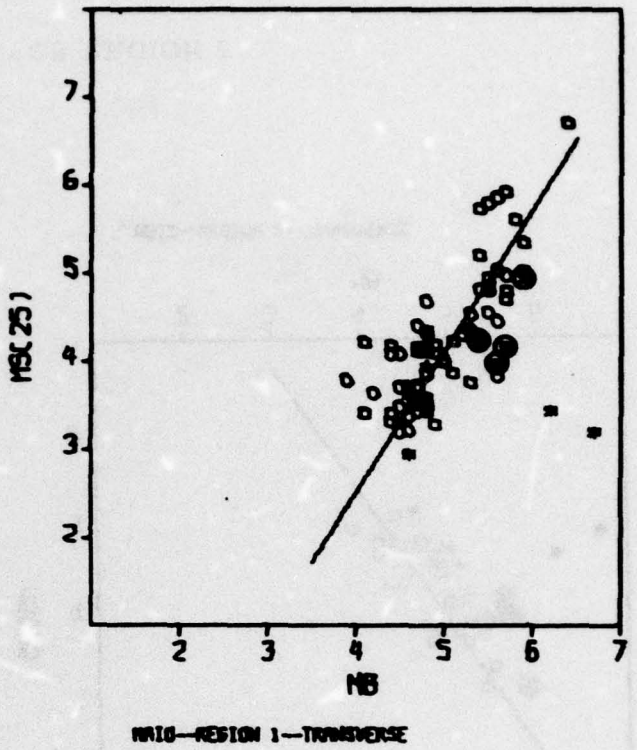

FIGURE VI-20

MAIO 25-SECOND M_s-m_b DATA FOR REGION 1

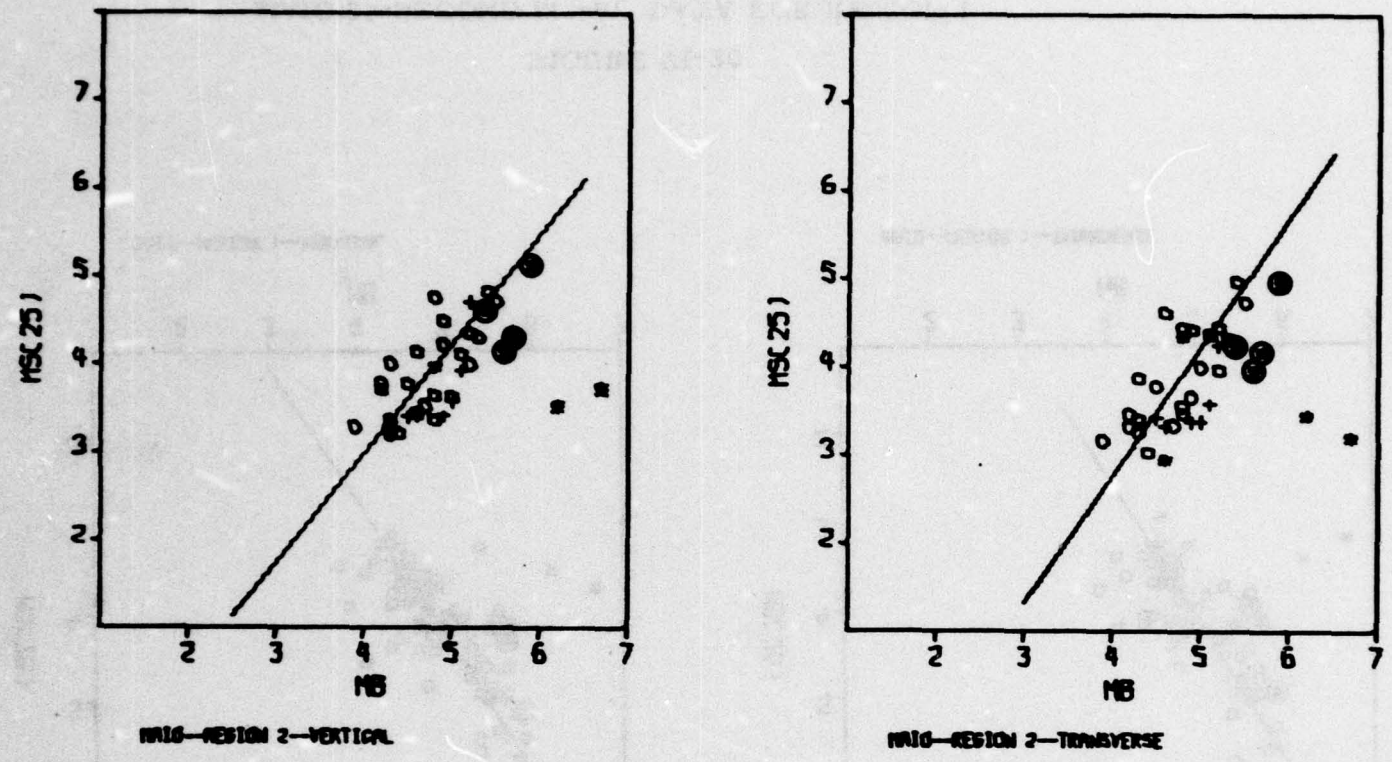

FIGURE VI-21

MAIO 25-SECOND M_s-m_b DATA FOR REGION 2

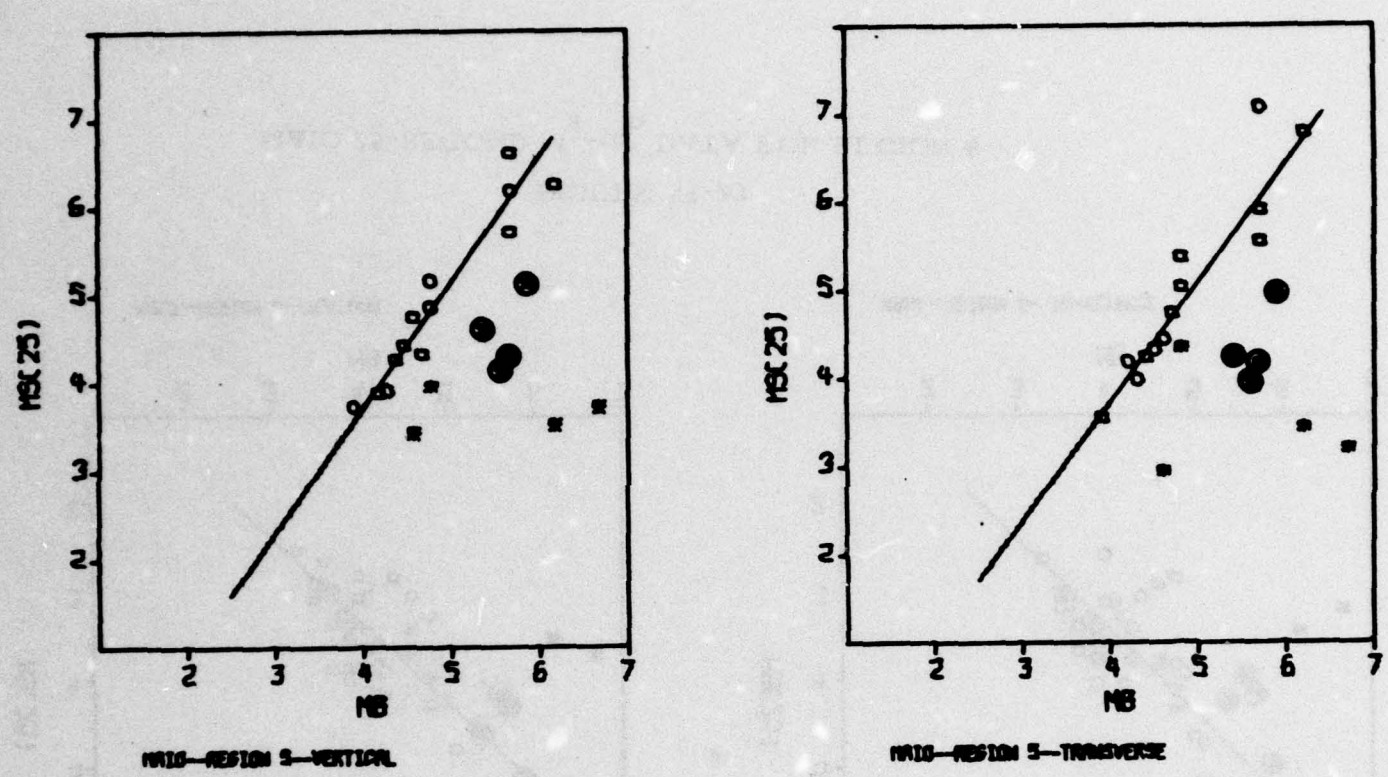

FIGURE VI- 22

MAIO 25-SECOND M_s-m_b DATA FOR REGION 5

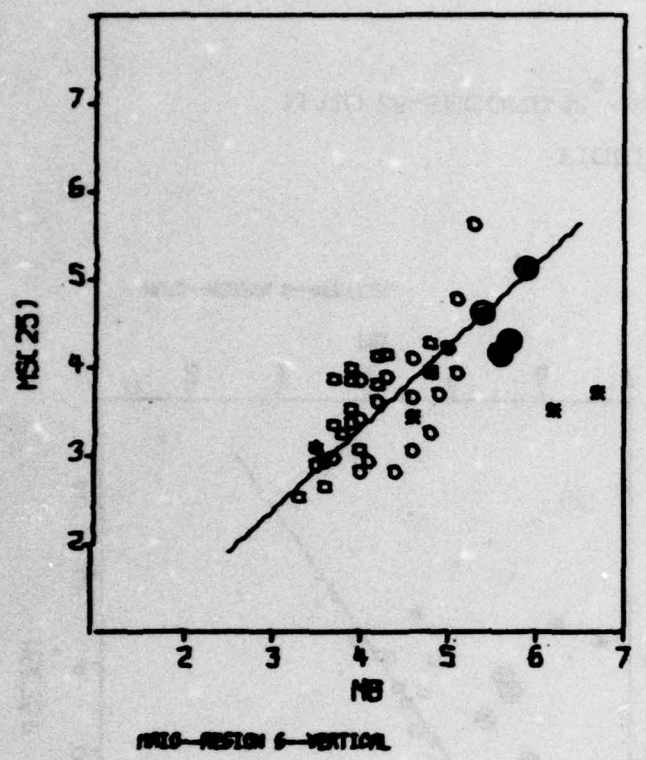

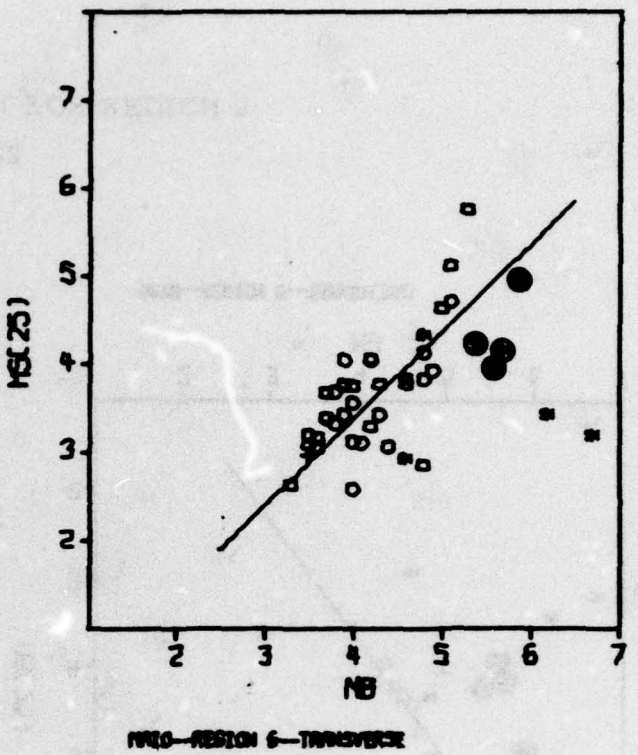

FIGURE VI-23

MAIO 25-SECOND M_s-m_b DATA FOR REGION 6

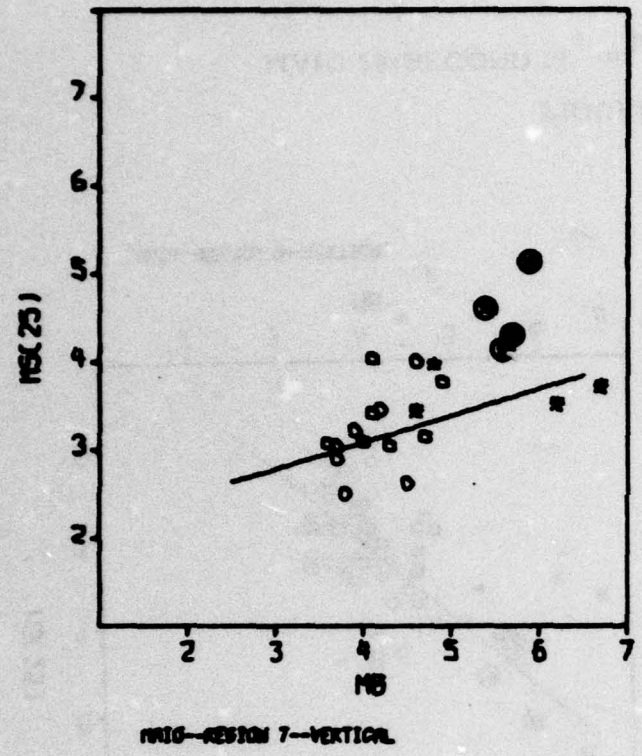

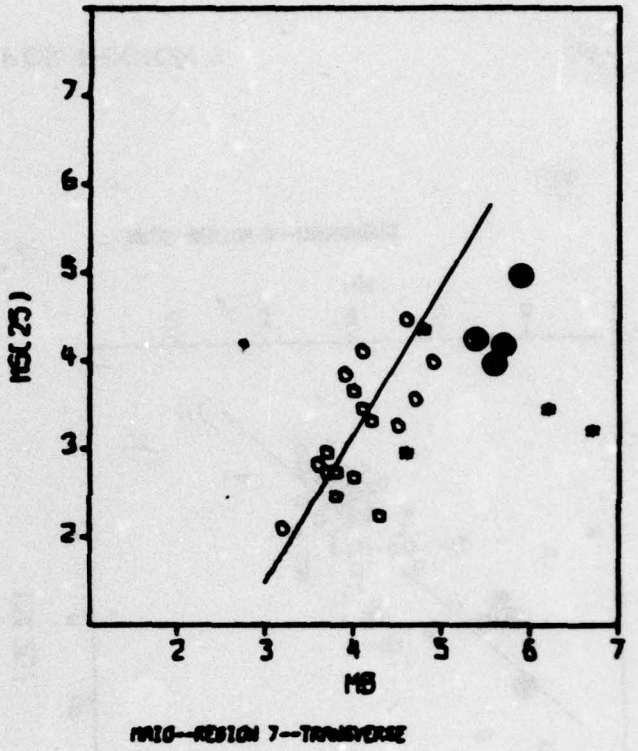

FIGURE VI-24

MAIO 25-SECOND M_s-m_b DATA FOR REGION 7

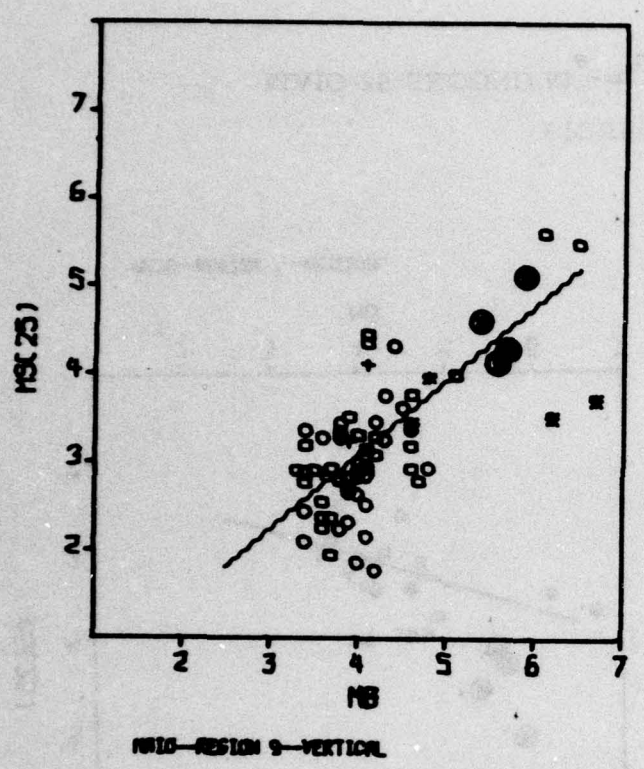

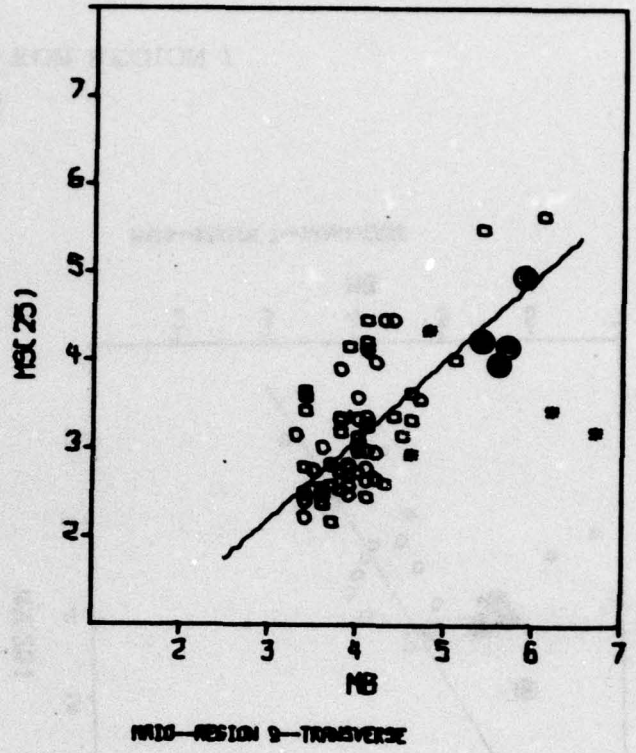

FIGURE VI-25

MAIO 25-SECOND M_s-m_b DATA FOR REGION 9

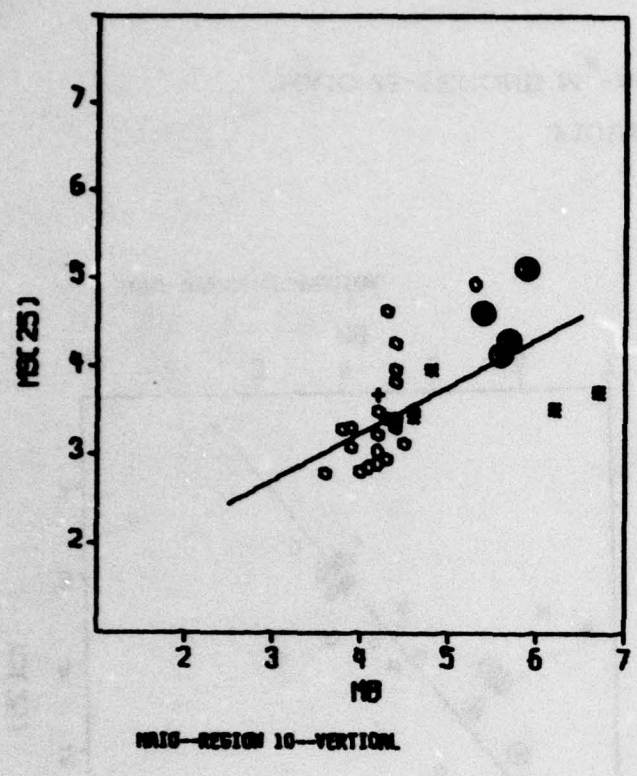

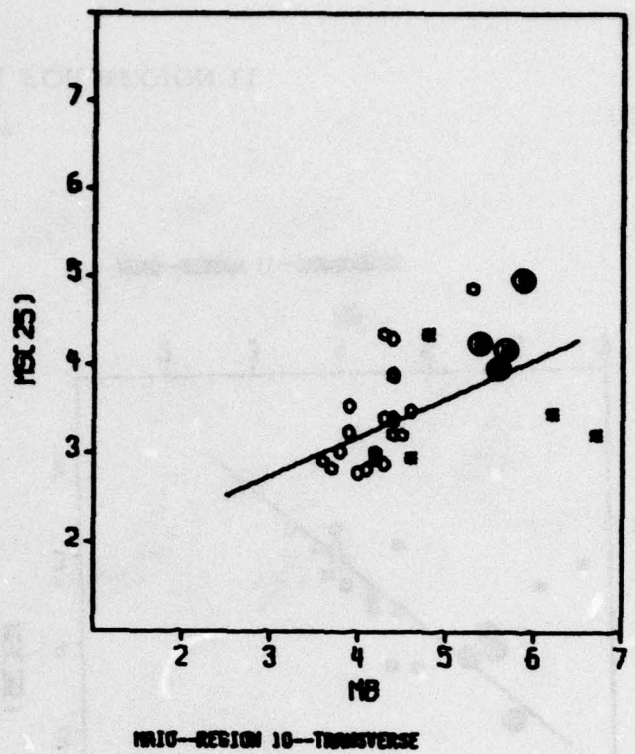

FIGURE VI-26

MAIC 25-SECOND M_s-m_b DATA FOR REGION 10

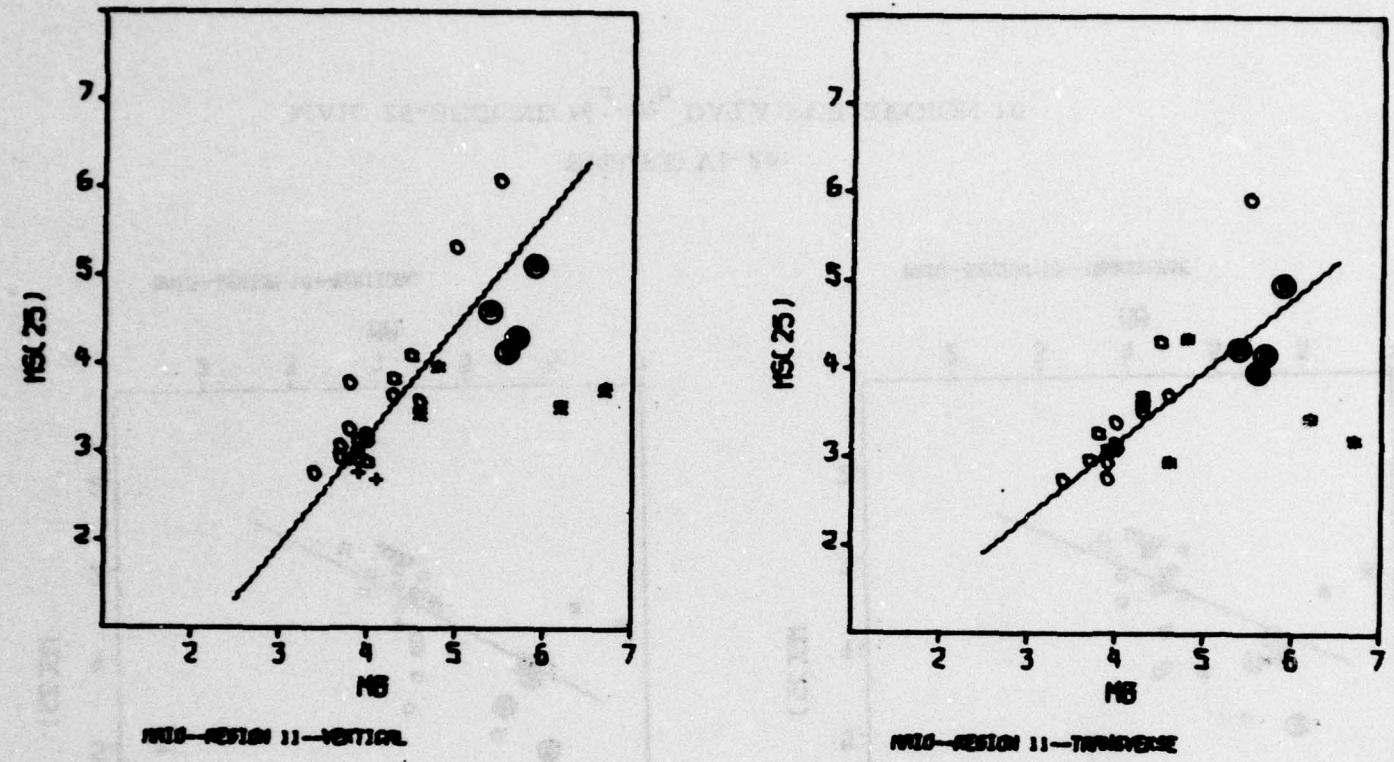

FIGURE VI-27

MAIO 25-SECOND M_s-m_b DATA FOR REGION 11

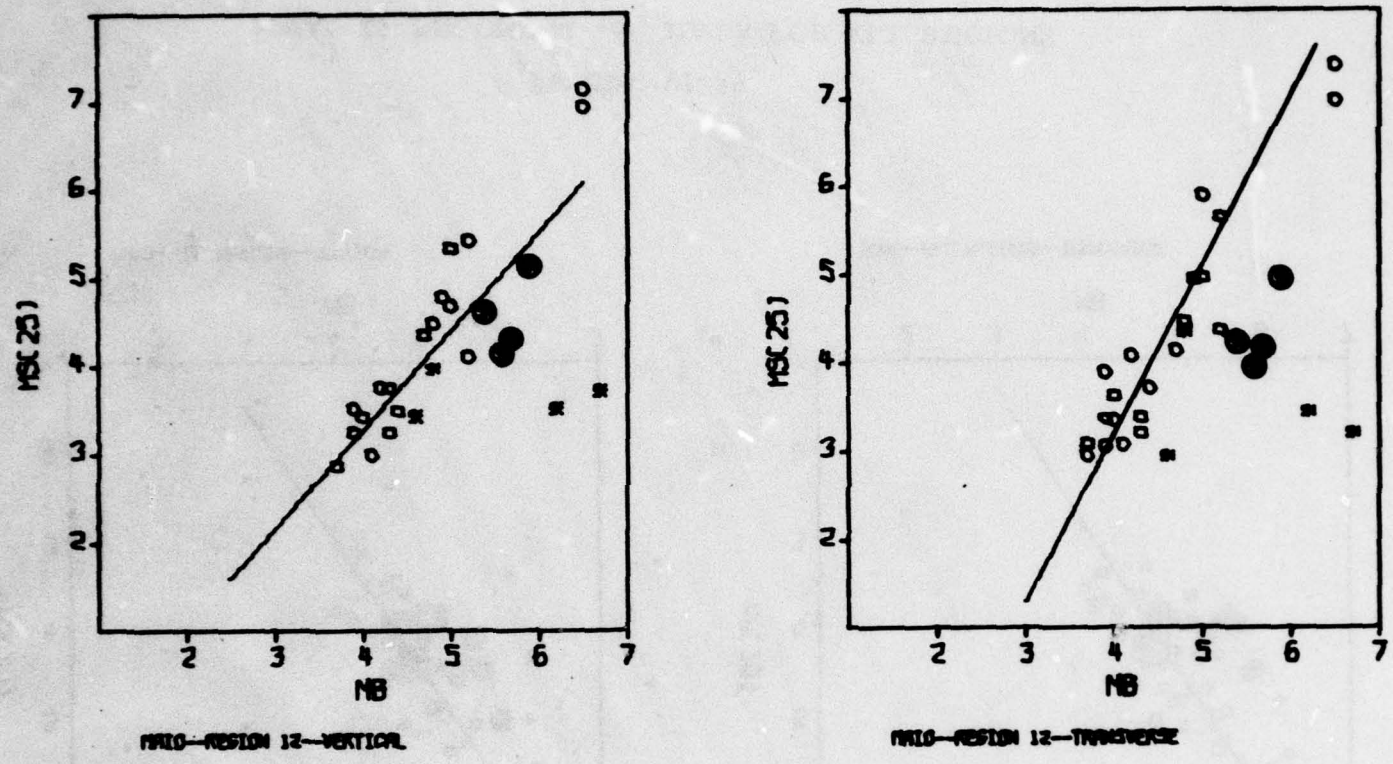

FIGURE VI-28

MAIO 25-SECOND M_s-m_b DATA FOR REGION 12

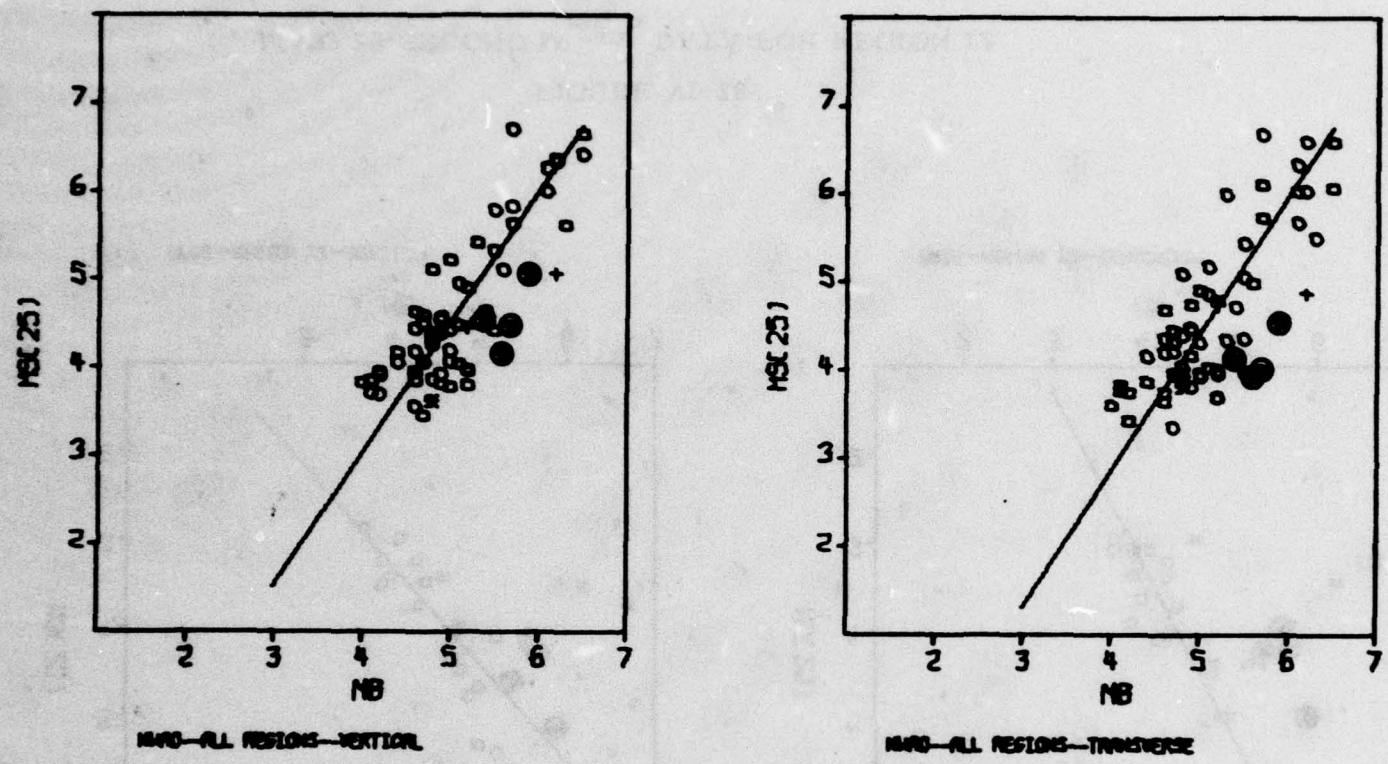

FIGURE VI-29

NWAO 25-SECOND M_s-m_b DATA FOR ALL REGIONS

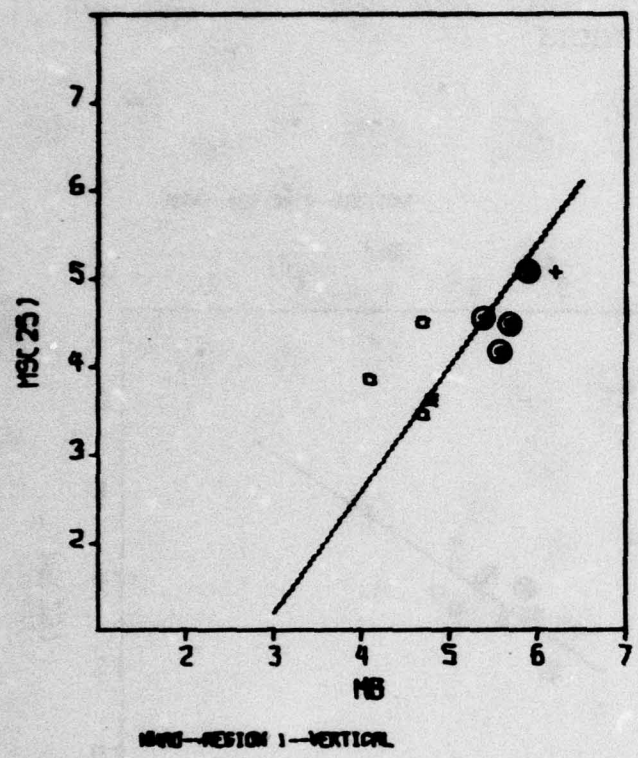

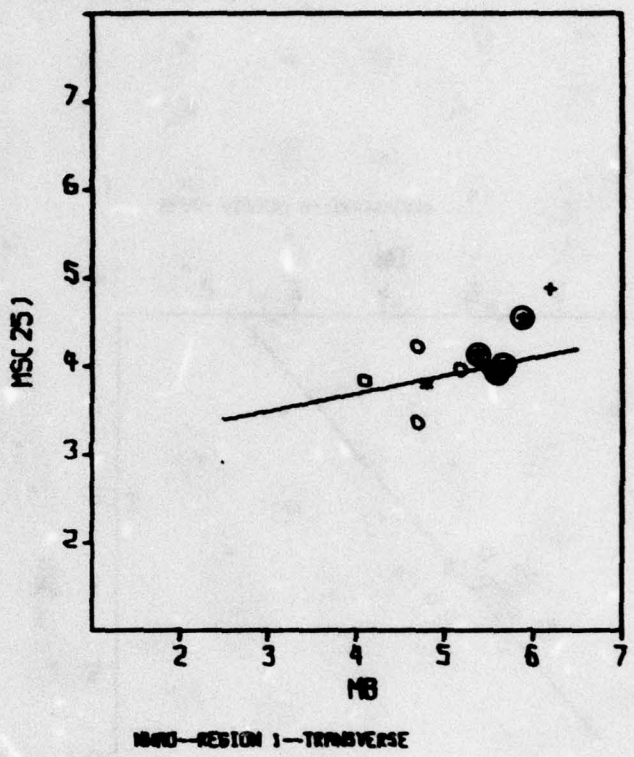

FIGURE VI-30

NWAO 25-SECOND M_s-m_b DATA FOR REGION 1

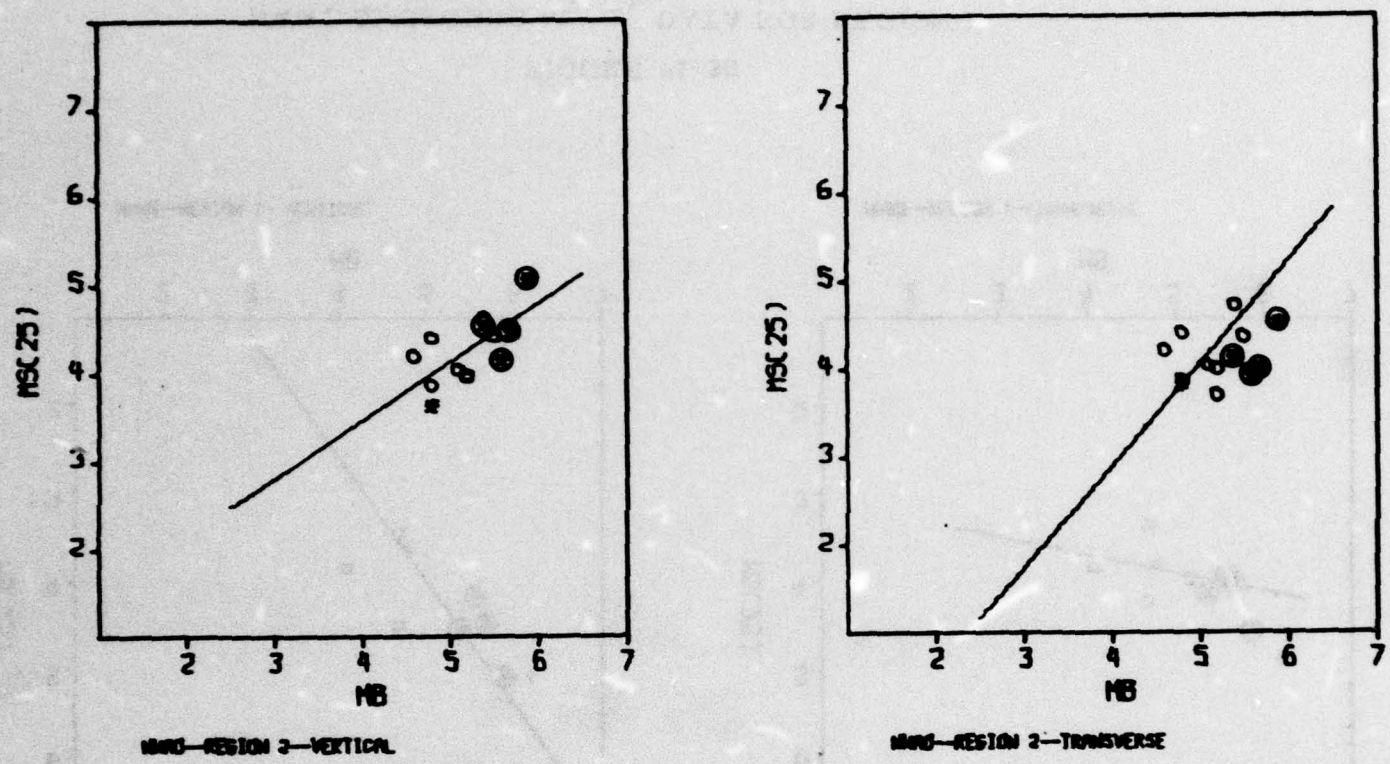

FIGURE VI-31

NWAO 25-SECOND M_s-m_b DATA FOR REGION 2

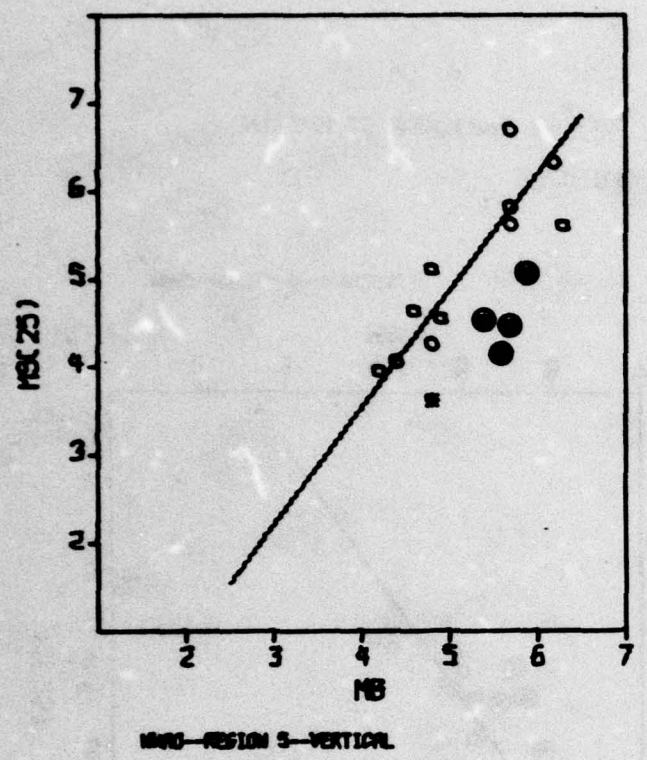

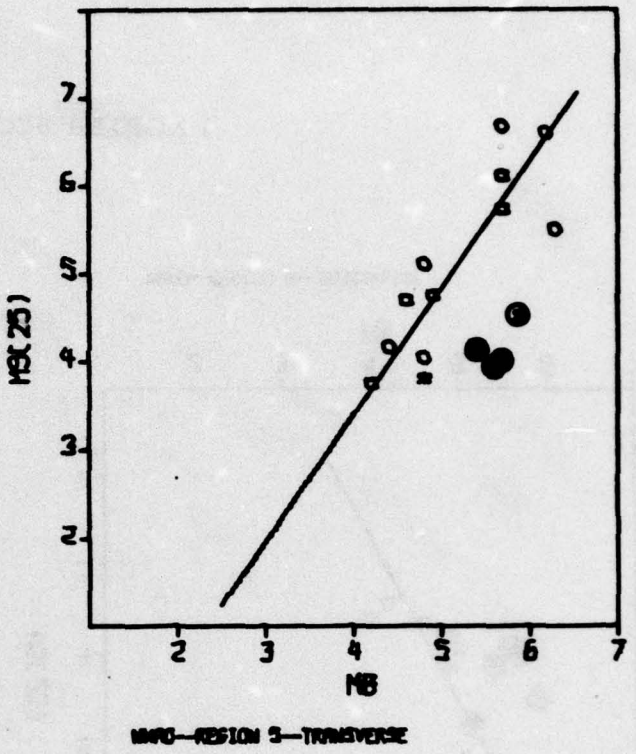

FIGURE VI-32

NWAO 25-SECOND M_s-m_b DATA FOR REGION 5

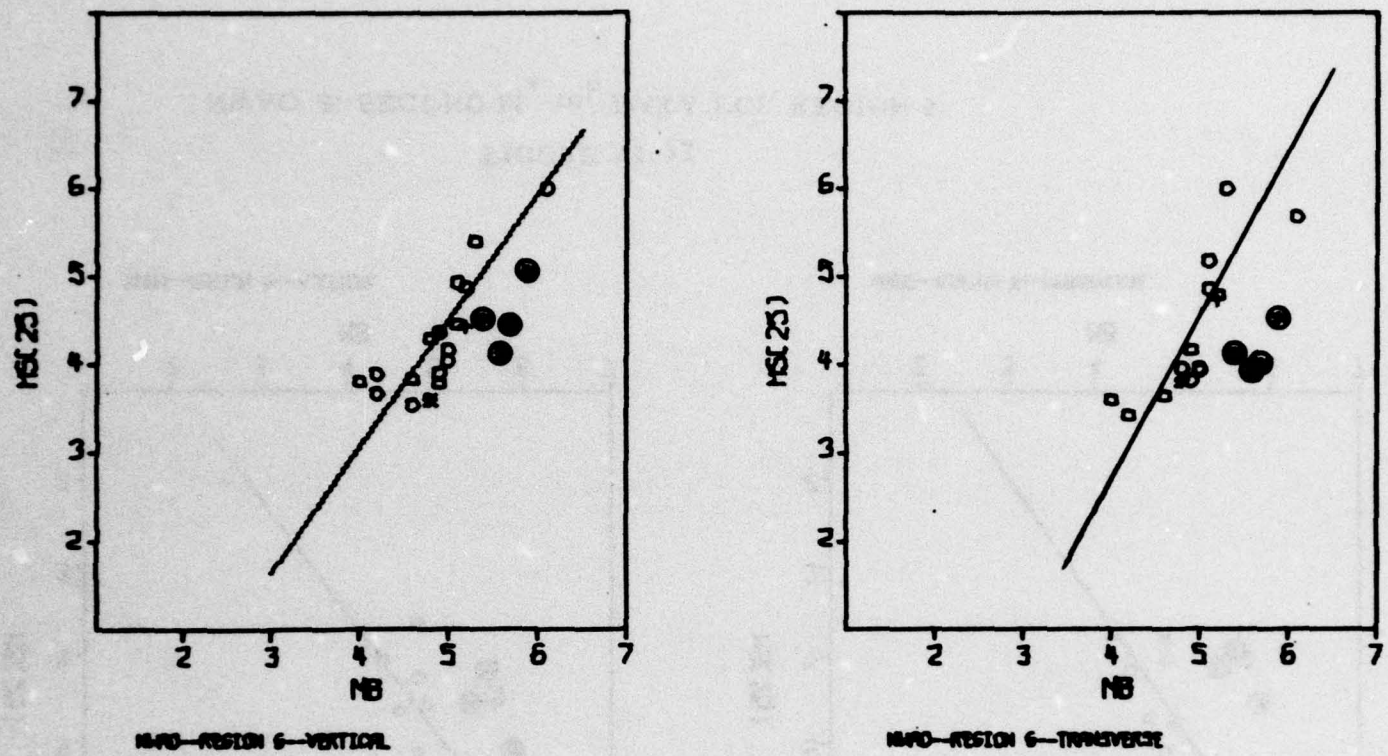

FIGURE VI-33

NWAO 25-SECOND M_s-m_b DATA FOR REGION 6

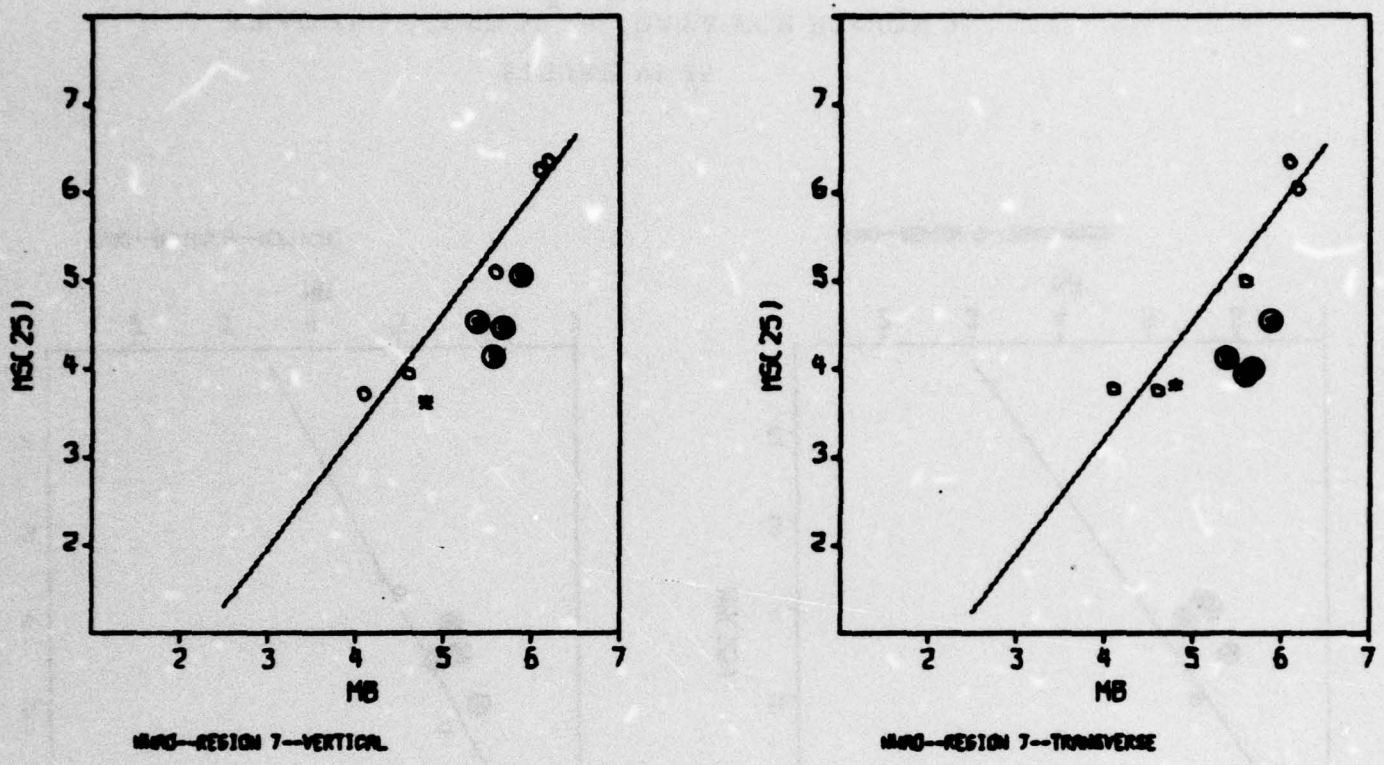

FIGURE VI-34

NWAO 25-SECOND M_s-m_b DATA FOR REGION 7

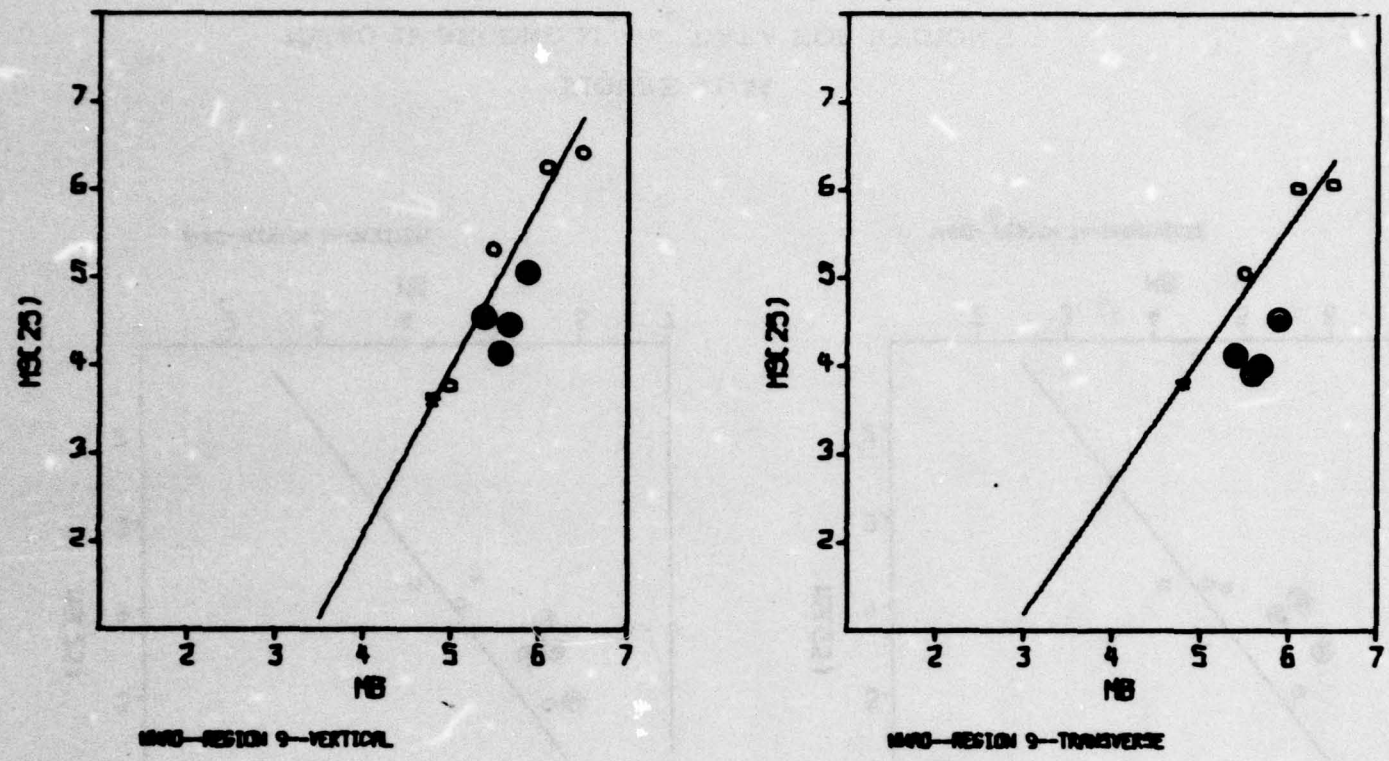

FIGURE VI-35

NWAO 25-SECOND M_s-m_b DATA FOR REGION 9

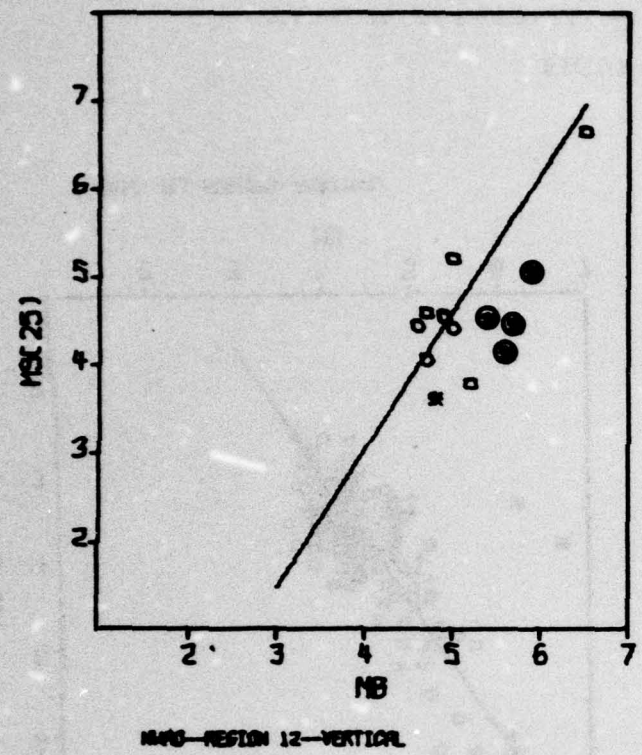

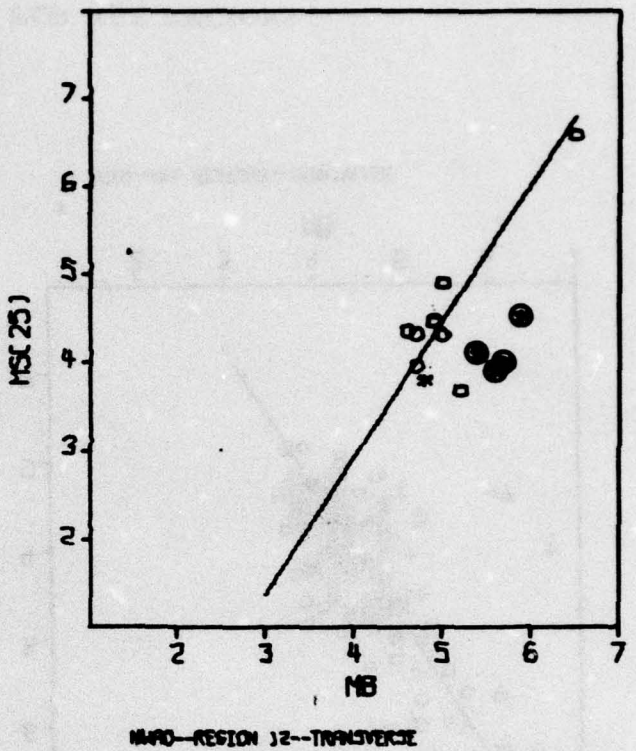

FIGURE VI-36

NWAO 25-SECOND M_s-m_b DATA FOR REGION 12

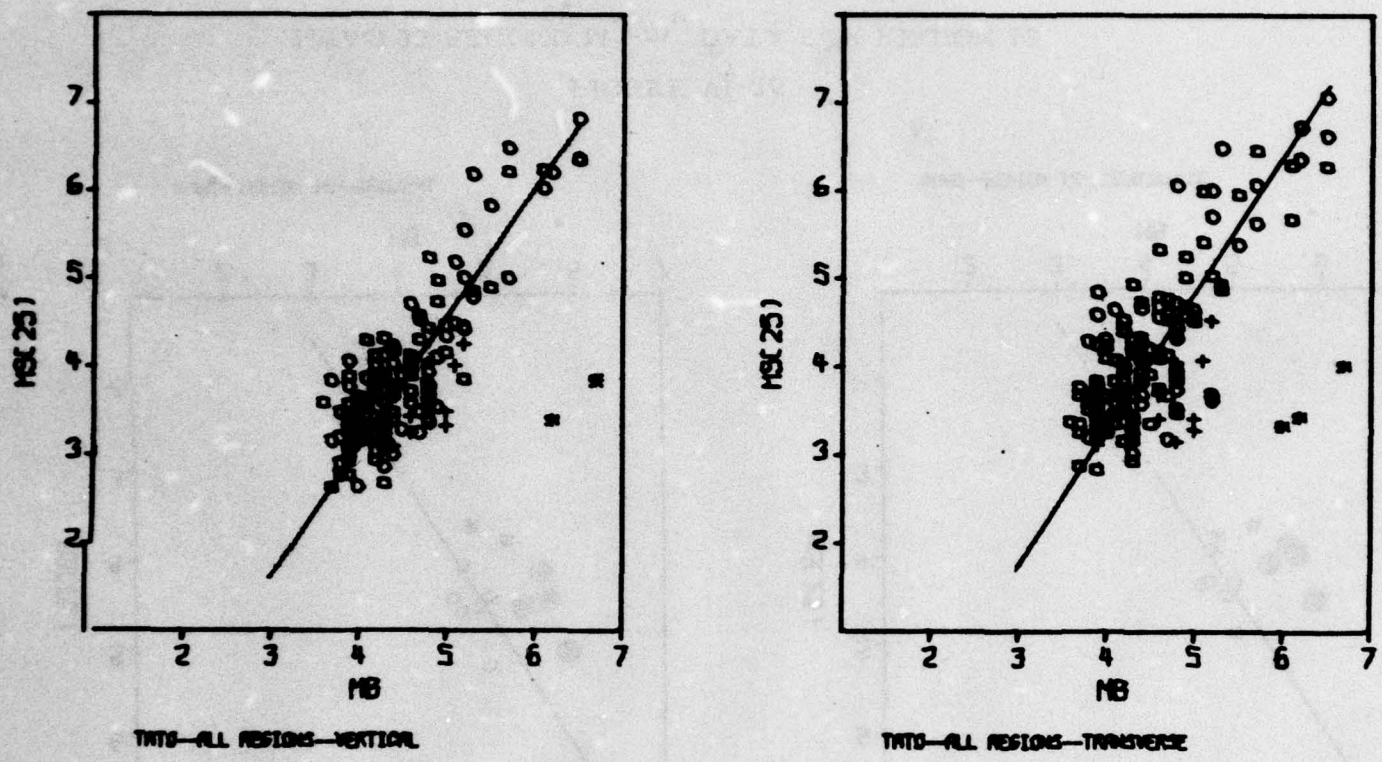

FIGURE VI-37

TATO 25-SECOND M_s-m_b DATA FOR ALL REGIONS

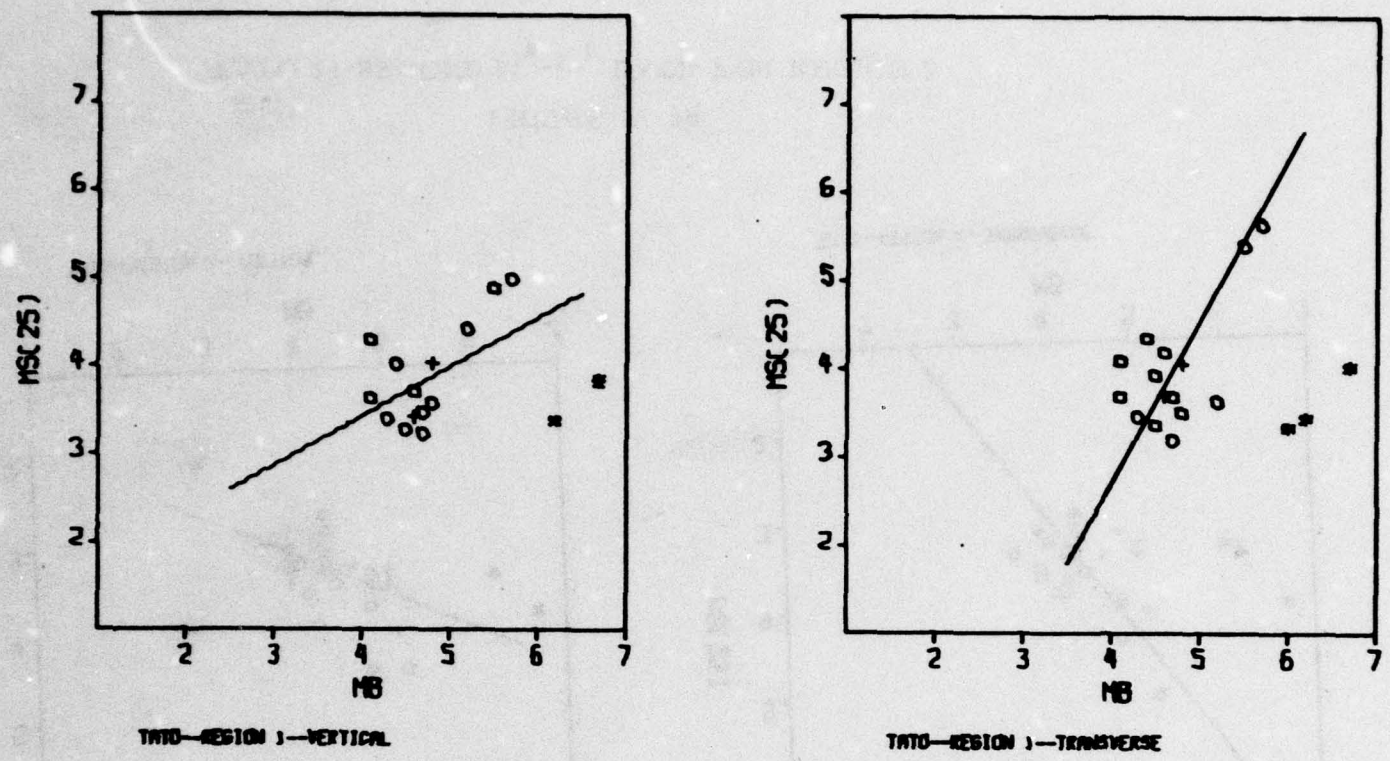

FIGURE VI-38

TATO 25-SECOND M_s-m_b DATA FOR REGION 1

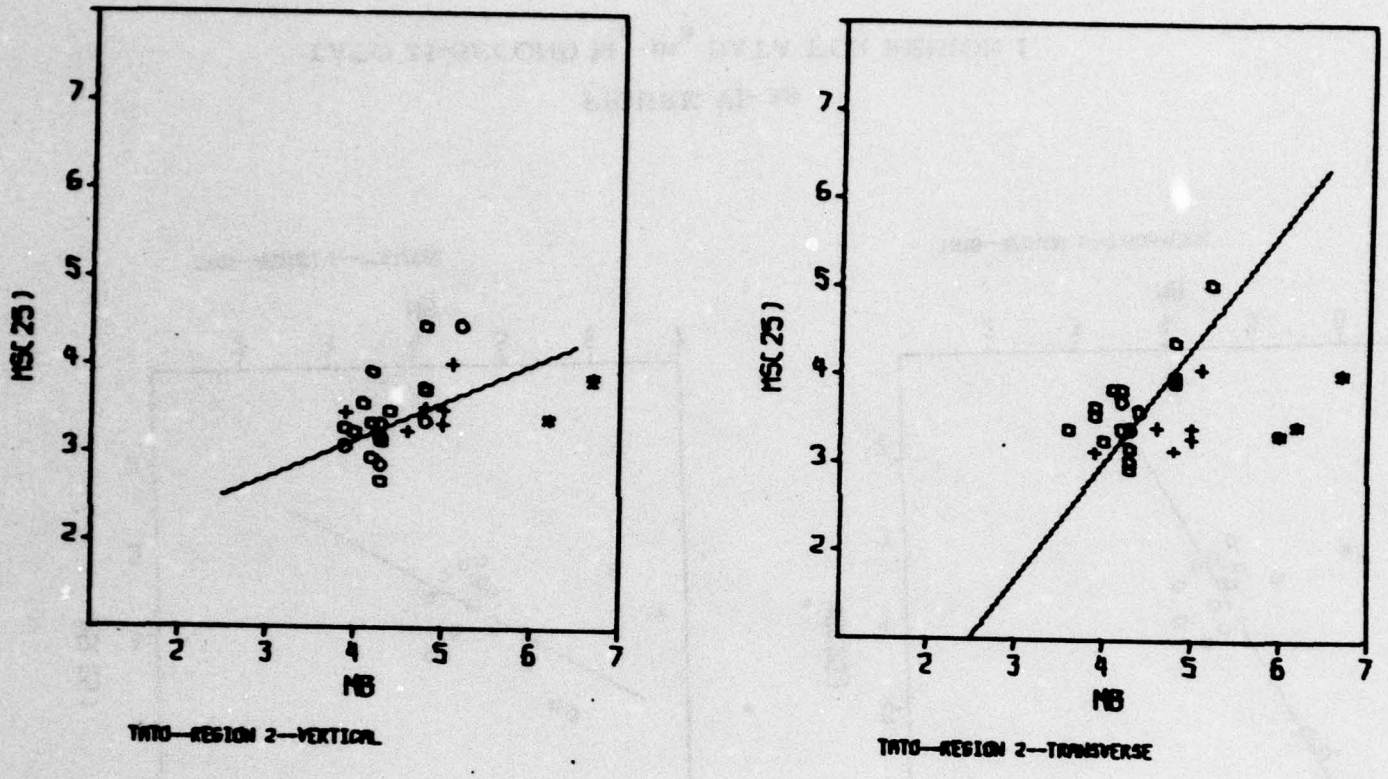

FIGURE VI-39

TATO 25-SECOND M_s-m_b DATA FOR REGION 2

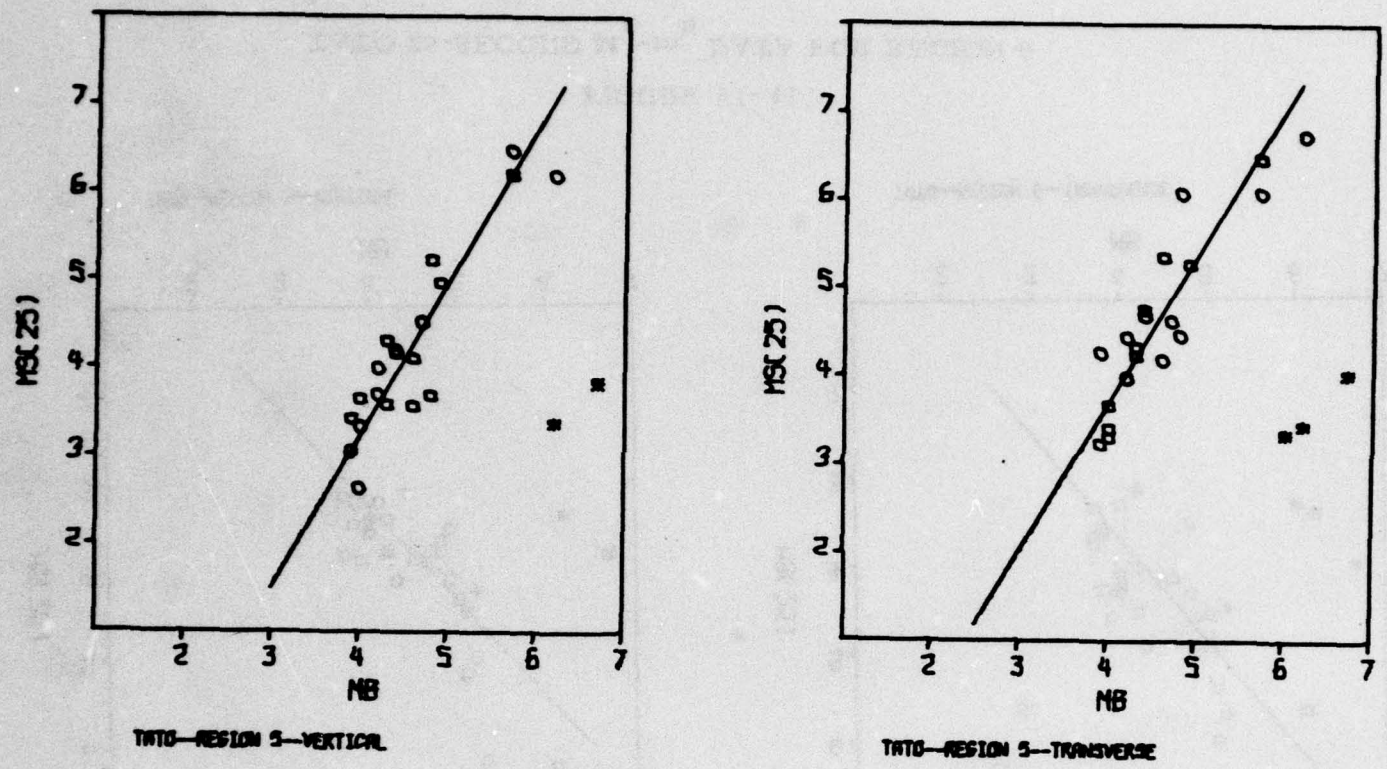

FIGURE VI-40

TATO 25-SECOND M_s-m_b DATA FOR REGION 5

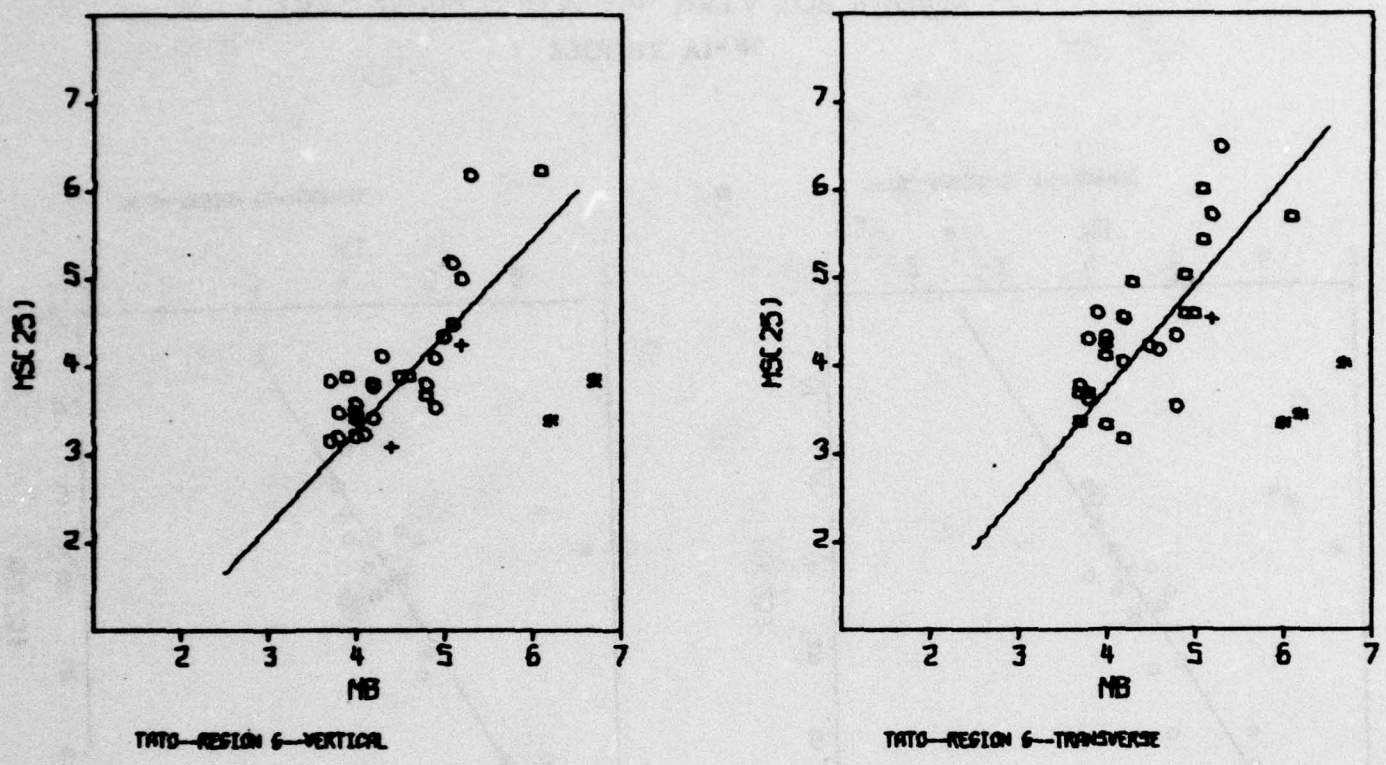

FIGURE VI-41

TATO 25-SECOND M_s-m_b DATA FOR REGION 6

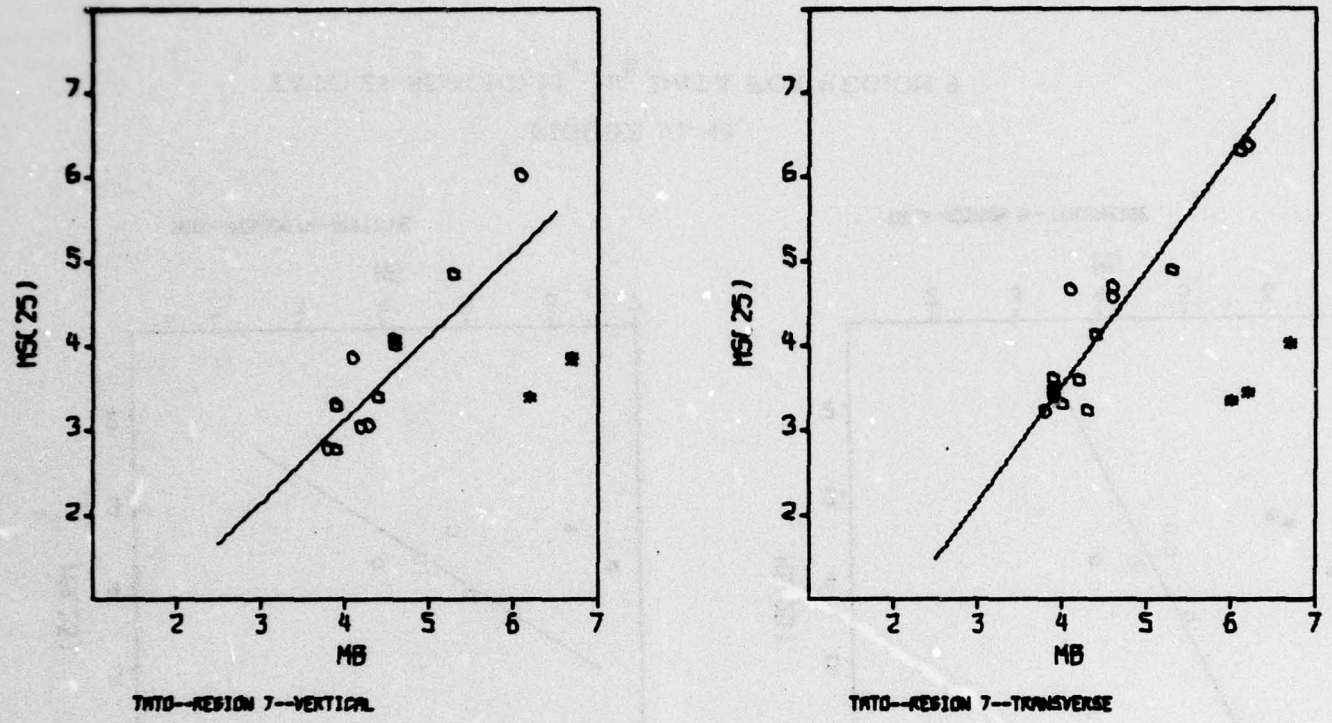

FIGURE VI-42

TATO 25-SECOND M_s-m_b DATA FOR REGION 7

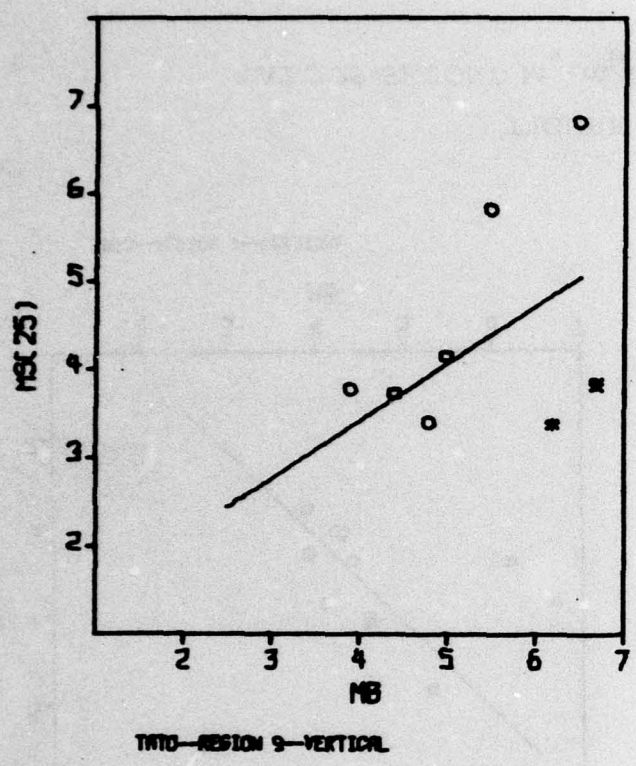

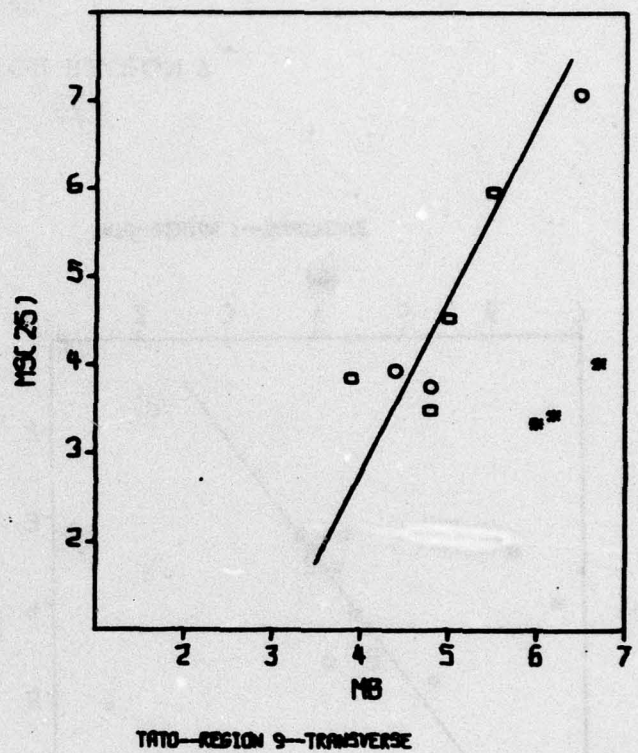

FIGURE VI-43

TATO 25-SECOND M_s-m_b DATA FOR REGION 9

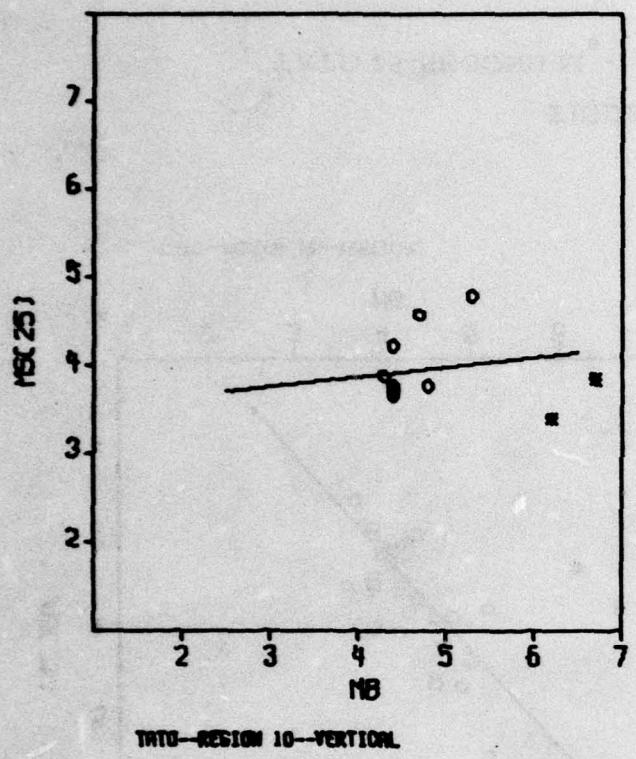

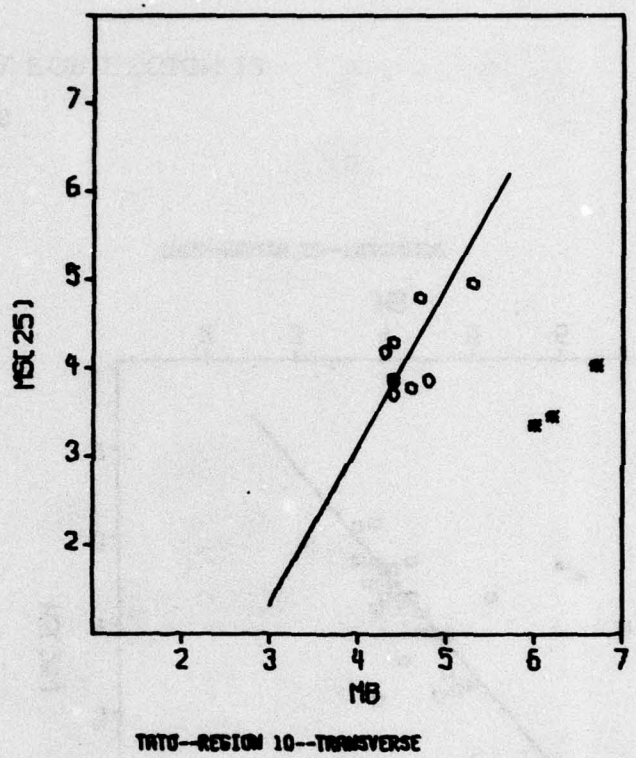

FIGURE VI-44

TATO 25-SECOND M_s-m_b DATA FOR REGION 10

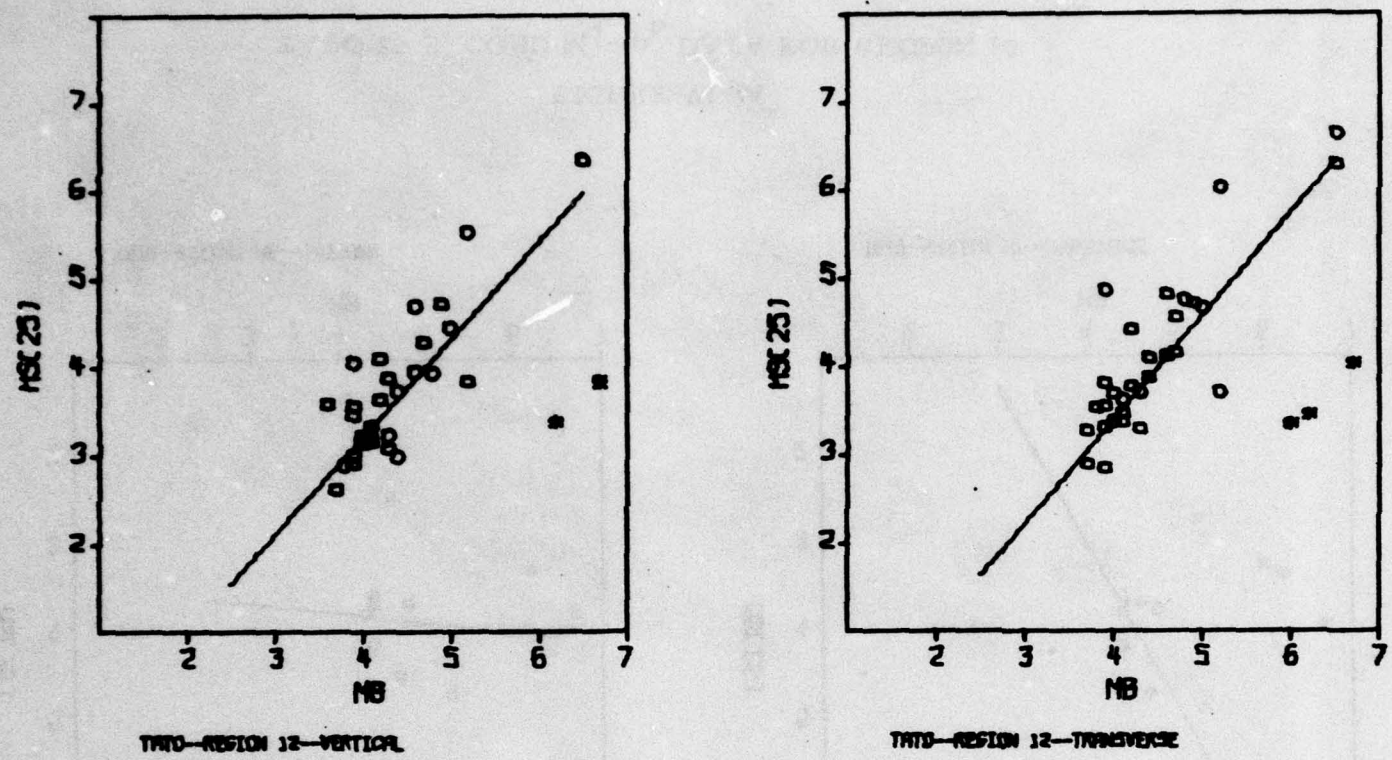

FIGURE VI-45

TATO 25-SECOND M_s-m_b DATA FOR REGION 12

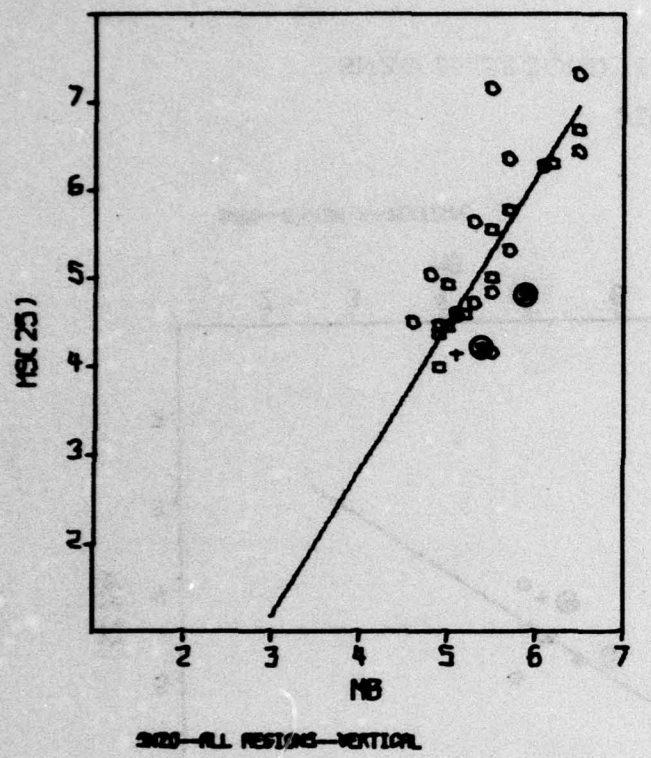

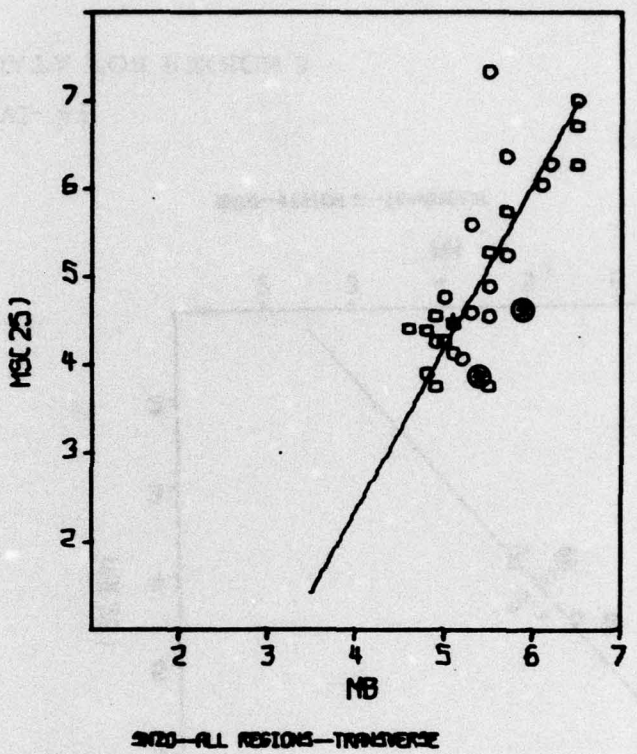

FIGURE VI-46

SNZO 25-SECOND M_s-m_b DATA FOR ALL REGIONS

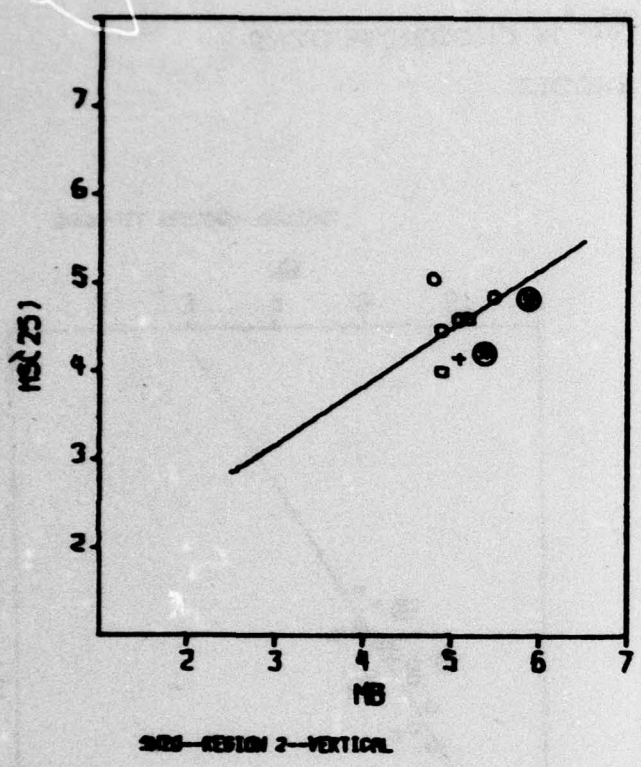

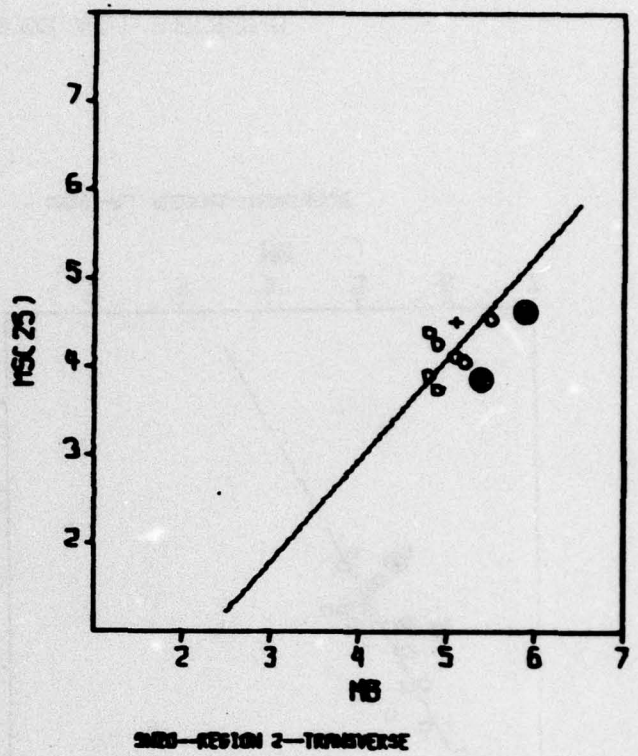

FIGURE VI- 47

SNZO 25-SECOND M_s-m_b DATA FOR REGION 2

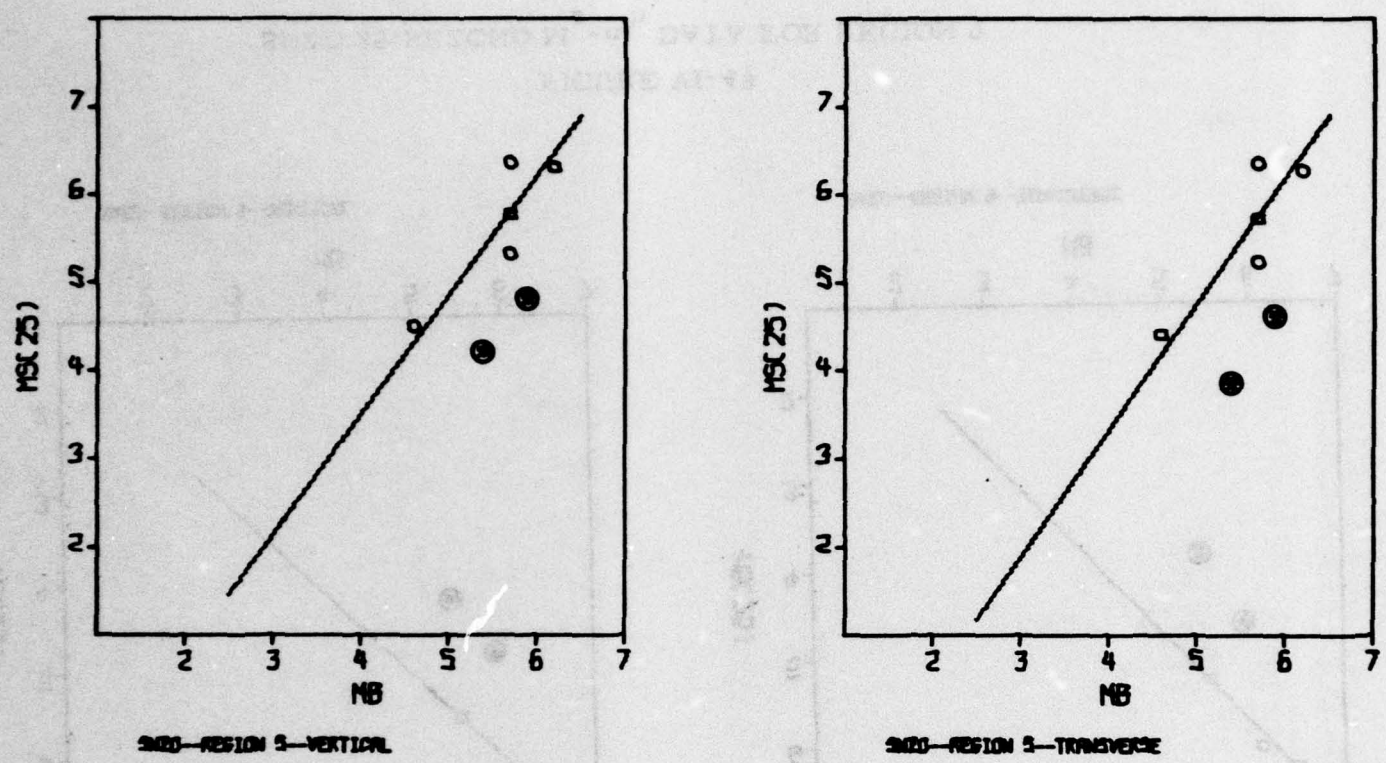

FIGURE VI-48

SNZO 25-SECOND M_s-m_b DATA FOR REGION 5

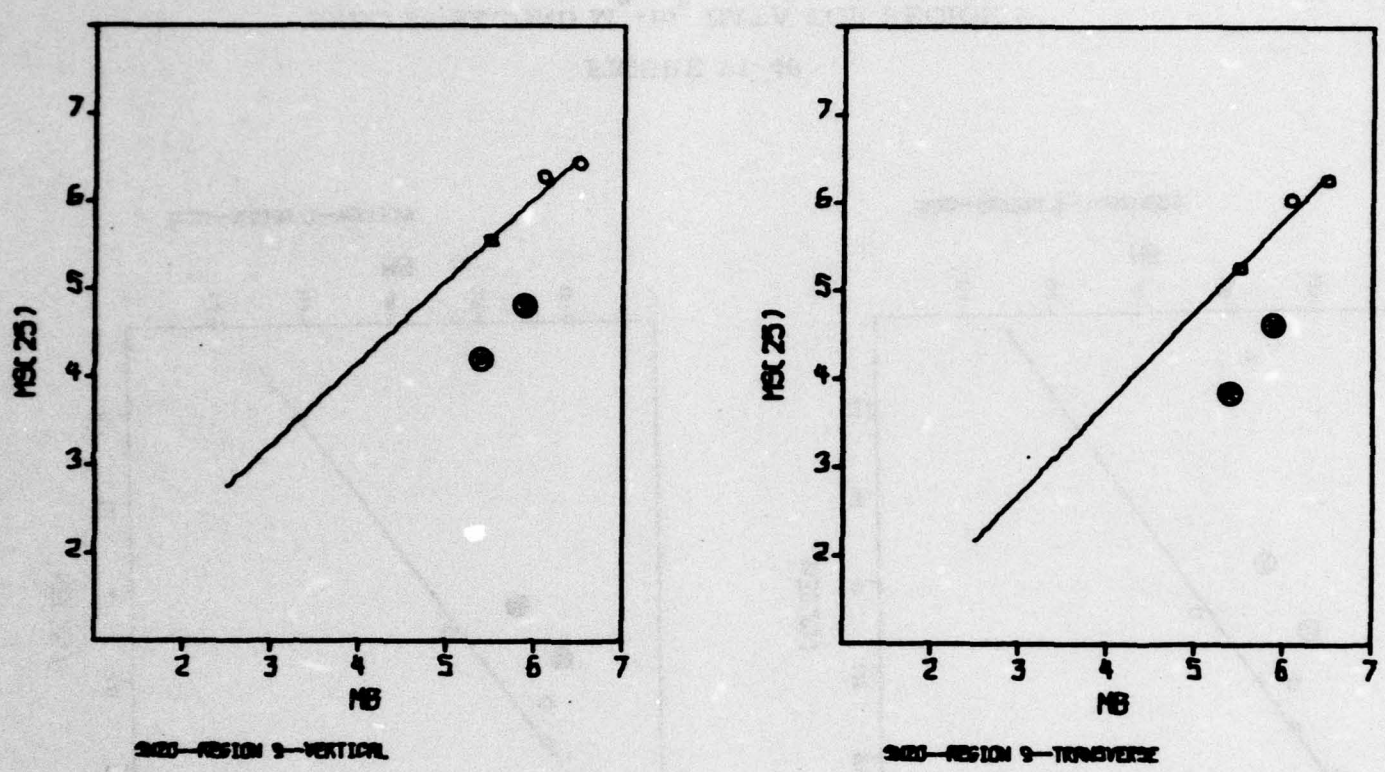

FIGURE VI-49

SNZO 25-SECOND M_s-m_b DATA FOR REGION 9

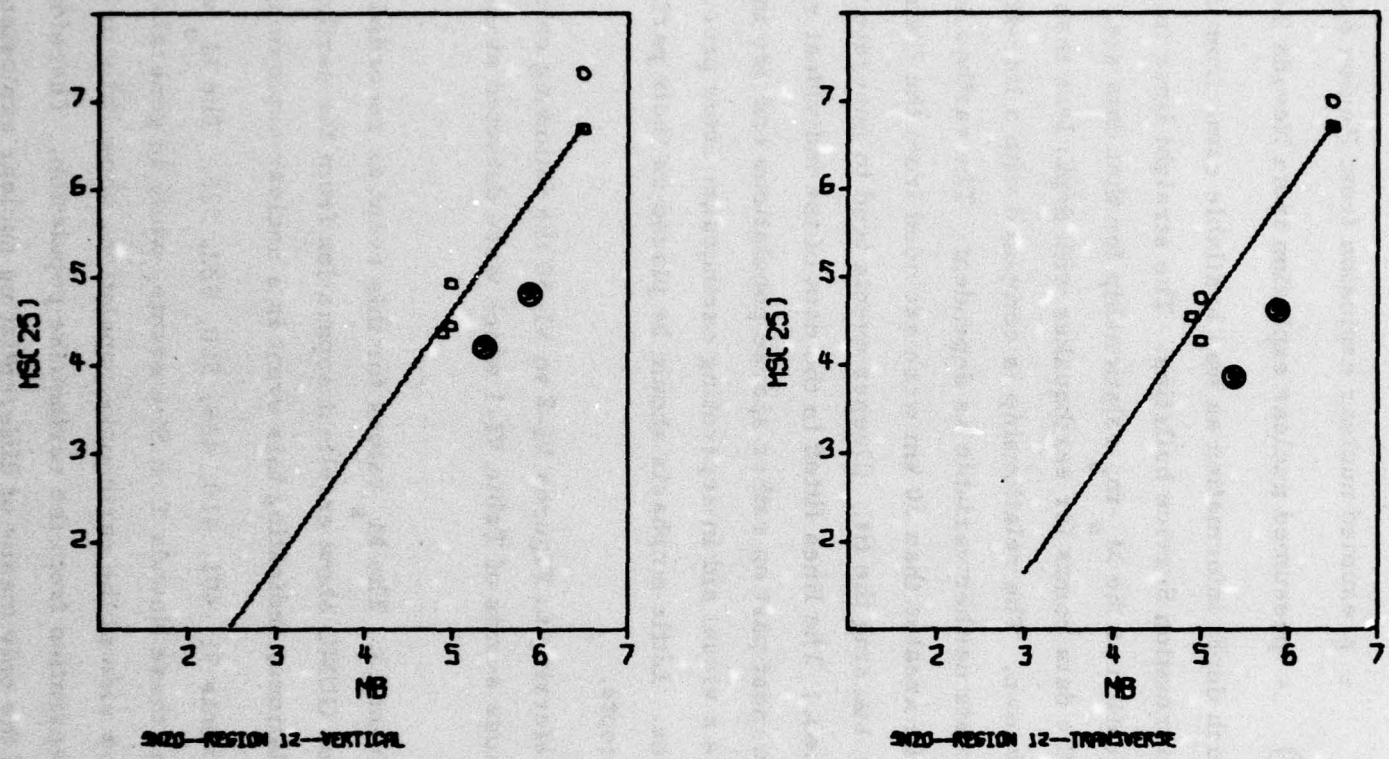

FIGURE VI-50

SNZO 25-SECOND M_s-m_b DATA FOR REGION 12

+ - earthquake with depth greater than 60 km

* - presumed nuclear explosion from Region 8 or 10

⊛ - presumed nuclear explosion from Nevada Test Site.

Such depth information as was available came from the National Earthquake Information Service bulletins. The straight lines in each plot represent the equation of the M_s-m_b relationship for that data set. This was computed using the data points for earthquakes with depth less than 60 km or with depth unknown. The relationship is computed with a line-fitting algorithm which treats neither variable as dependent. The earthquakes with depths known to be greater than 60 km were excluded from the fitting procedures to avoid biassing the fit. (Deeper events tend to generate relatively lower M_s values.) The lines fitted to the data of the individual regions are based for the most part on rather sparse populations and are intended to be used only as a visual aid in separating earthquakes from presumed nuclear explosions. Little emphasis should be placed on their particular slopes and intercepts.

Referring to Figures VI-2 to VI-50 the following comments can be made about those events of Table VI-1 which were detected at one or more stations:

- Event 13. The M_s values for this event as recorded at ANMO and GUMO show excellent separation from the earthquake populations, indicating this event is a nuclear explosion.
- Events 91, 401, 410, 485, 500, 522, 523. The M_s values for these Nevada Test Site events, while in general on the low side of the earthquake population, show little or no separation from the earthquake population. Therefore, if the only means of differentiating nuclear explosions from

earthquakes was the M_s-m_b discriminant, these events would be classified as earthquakes.

- Event 537. The M_s values for this event as recorded at ANMO, GUMO, MAIO, and NWAO all fall in the earthquake population, indicating this event is an earthquake.
- Event 839. The M_s values for this event as recorded at MAIO fall in the earthquake population, indicating this event is an earthquake.
- Event 1062. The M_s values for this event as recorded at ANMO, GUMO, MAIO, and TATO show excellent separation from the earthquake population, indicating this event is a nuclear explosion.
- Event 1200. The M_s values for this event as recorded at MAIO and TATO show excellent separation from the earthquake population, indicating this event is a nuclear explosion.
- Event 1368. The transverse component M_s value (the only component on which it was detected) for this event as recorded at TATO shows excellent separation from the earthquake population, indicating this event is a nuclear explosion.

In summary, the M_s-m_b discriminant appears to function quite well for Eurasian presumed nuclear explosions but not for Nevada Test Site presumed nuclear explosions. This discriminant indicates that two of the detected Eurasian events of Table VI-1 are earthquakes and the remainder are nuclear explosions. In corroboration of this, it is interesting to note that almost all known eastern Kazakh nuclear explosions have m_b values greater than 5.0.

D. M_s-m_b RELATIONSHIPS

Table VI-2 presents the results of fitting a straight line to the M_s-m_b points. The M_s-m_b relationships are presented only for the case of all data points measured at each station. The M_s-m_b relationships for the data points of the individual regions are not presented since in most cases the number of points is too low to yield trustworthy results.

The data of Table VI-2 shows that only at NWAO and SNZO is the M_s-m_b relationship for the vertical component significantly different from the M_s-m_b relationship for the transverse component. The difference is greater at SNZO, where fewer M_s-m_b points were available. Therefore, the M_s-m_b relationships at these two stations should be considered only approximate due to the relatively small number of M_s-m_b points available.

TABLE VI-2

SRO STATIONS M_s-m_b RELATIONSHIPS FOR 25-SECOND ENERGY

Station	Component	a	b	σ^2	Center of Mass		n	Refer to Figure #
					m_b	M_s		
ANMO	V	1.65	-3.83	0.14	4.92	4.27	119	VI-2
	T	1.66	-3.82	0.14	4.90	4.31	128	
GUMO	V	1.41	-2.88	0.12	4.87	3.97	156	VI-11
	T	1.42	-2.75	0.12	4.89	4.19	140	
MAIO	V	1.33	-2.21	0.12	4.53	3.80	270	VI-19
	T	1.29	-2.05	0.14	4.49	3.77	268	
NWAO	V	1.49	-2.93	0.09	5.11	4.66	60	VI-29
	T	1.56	-3.36	0.11	5.14	4.64	59	
TATO	V	1.47	-2.83	0.13	4.55	3.88	132	VI-37
	T	1.55	-2.91	0.18	4.54	4.15	141	
SNZO	V	1.65	-3.78	0.06	5.11	5.16	23	VI-46
	T	1.86	-5.08	0.07	5.39	4.92	24	

where: $M_s = am_b + b$

σ^2 = variance normal to the M_s-m_b estimate, and

n = number of M_s-m_b points used in computation.

SECTION VII

SRO NETWORK DETECTION CAPABILITY ESTIMATES

A. DISCUSSION

Up to this point, the Seismic Research Observatory stations have been evaluated on an individual station basis. This section investigates the detection capability of a network composed of the six stations under evaluation. Two approaches are used - the first utilizes the detection statistics collected for the individual stations and the second utilizes the noise level statistics collected for the individual stations. The first approach is used to compute detection capability estimates for the short-period network, the long-period network, and the combined short-period, long-period network. The second approach is used to compute detection capability estimates only for the long-period network, since the technique used does not have the capability of taking into account the effects on detection capability of an automatic detector.

B. NETWORK DETECTION CAPABILITY FROM DETECTION STATISTICS OF INDIVIDUAL STATIONS

In this direct estimate of network detection capability, an event was declared a detection if it was detected at one or more stations of the network using the detection criteria of Section V. The grouping 'ALL REGIONS A' and 'ALL REGIONS B' have the same meaning as in Section V. The events used in this study were events 36 to 1384 of the data base. These events were selected because data from at least three stations had been processed for each. Just as in Section V, the 50 percent detection threshold is used as the detection capability estimate.

The detection capability estimates for three networks are presented in Figures VII-1 to VII-9. First, Figures VII-1 to VII-3 present the detection capability estimates for the short-period network. Next, Figures VII-4 to VII-6 present the detection capability estimates for the long-period network. Finally, Figures VII-7 to VII-9 present the detection capability estimates for the combined short-period, long-period network, where an event is considered to be detected if it is detected on either the short-period or long-period network. Each of the 'sub-figures' in Figures VII-1 to VII-9 represents one network detection capability estimate. The upper portion of each sub-figure is a histogram giving the detection statistics as a function of bodywave magnitude for that particular case. The lower portion shows the percentage of events detected at each bodywave magnitude (represented by asterisks), the fitted maximum likelihood curve (represented by a solid line), and the 90 percent confidence limits for this curve (represented by dashed lines). The values for 'MB50' and 'MB90' shown on the figures are the 50 and 90 percent detection thresholds as picked from the maximum likelihood curve. The titles for each sub-figure define the type of network and the region of the events from which the detection statistics were derived.

Note that in Figures VII-1 to VII-9 the terms 'ALL REGIONS A' and 'ALL REGIONS B' differ only in that mixed events were counted as non-detections for the detection statistics of 'ALL REGIONS A' and were rejected from the detection statistics of 'ALL REGIONS B'. (For the events used, there were no cases in which no data were recorded or malfunctions obscured the data at all operational stations simultaneously.) Thus 'ALL REGIONS A' again represents the absolute detection capability estimate and 'ALL REGIONS B' again represents the conditional detection capability estimate as defined in Section V. For short-period data, events for which the automatic detector did not declare a detection are counted as non-detections. All individual region detection capability estimates are conditional detection capability estimates.

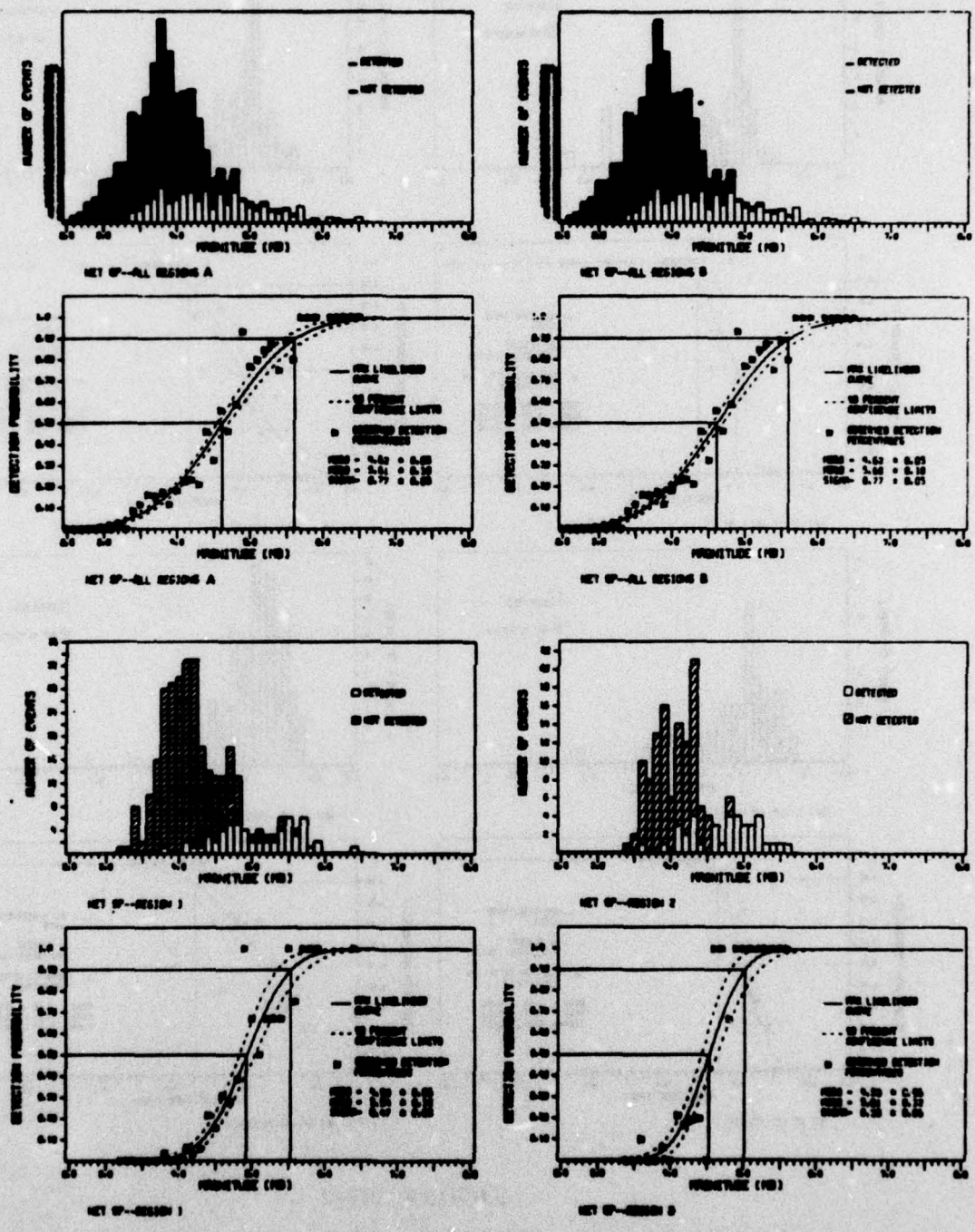

FIGURE VII-1

SHORT-PERIOD NETWORK DETECTION STATISTICS
ALL REGIONS A AND B--REGIONS 1 AND 2

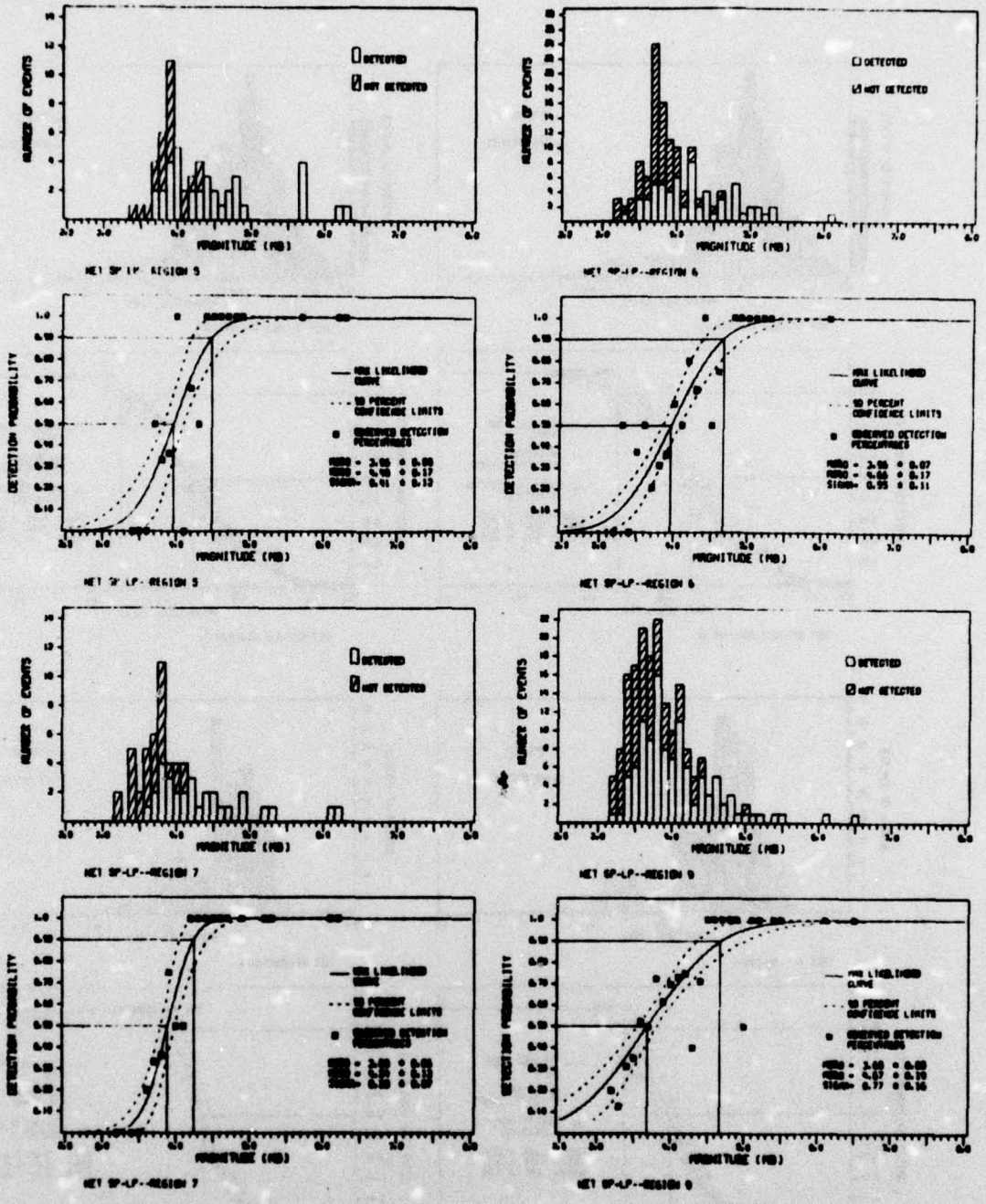

FIGURE VII-2

SHORT-PERIOD NETWORK DETECTION STATISTICS
REGIONS 5, 6, 7, AND 9

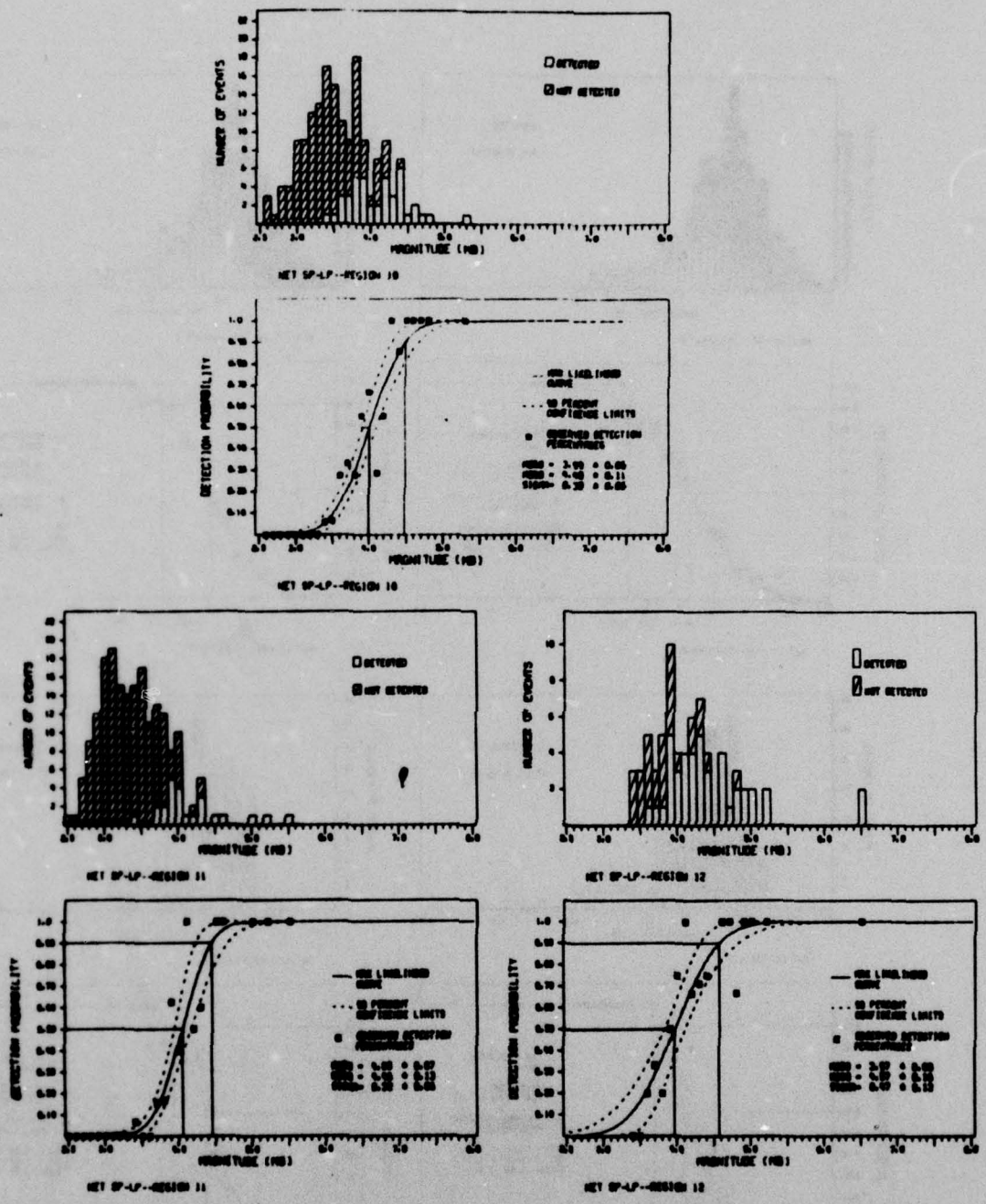

FIGURE VII-3

SHORT-PERIOD NETWORK DETECTION STATISTICS
REGIONS 10, 11, AND 12

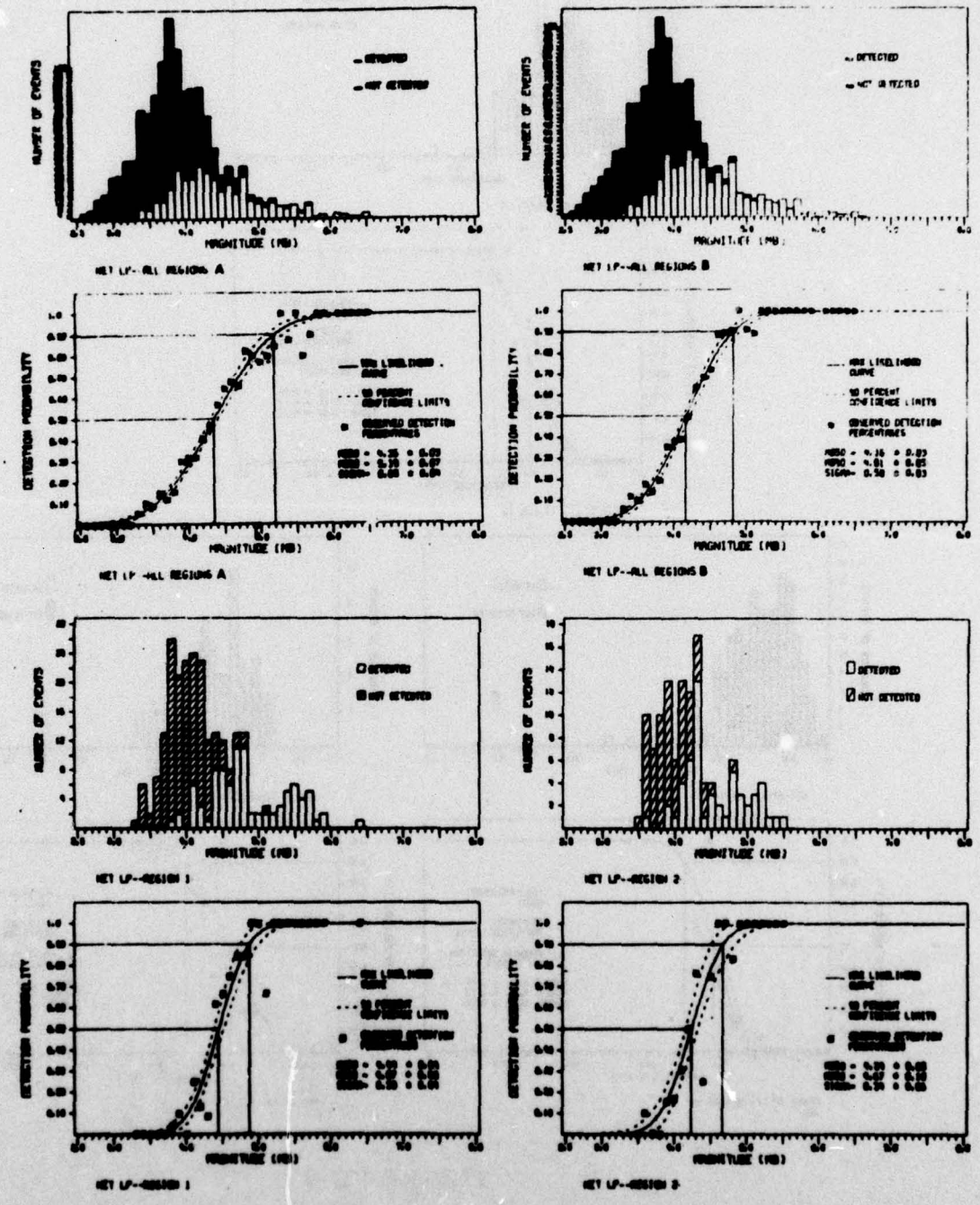

FIGURE VII-4

LONG-PERIOD NETWORK DETECTION STATISTICS
ALL REGIONS A AND B--REGIONS 1 AND 2

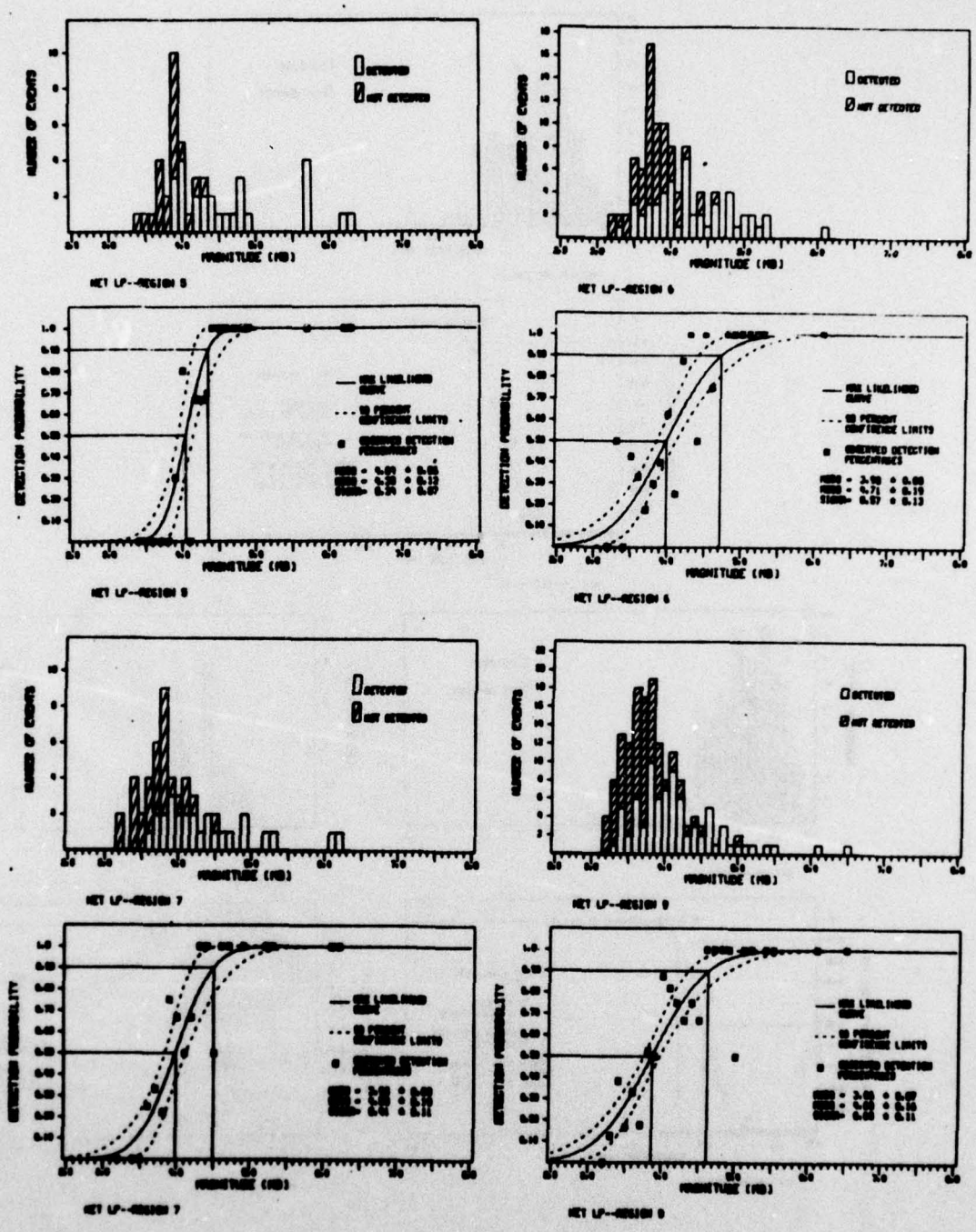

FIGURE VII-5

LONG-PERIOD NETWORK DETECTION STATISTICS
REGIONS 5, 6, 7, AND 9

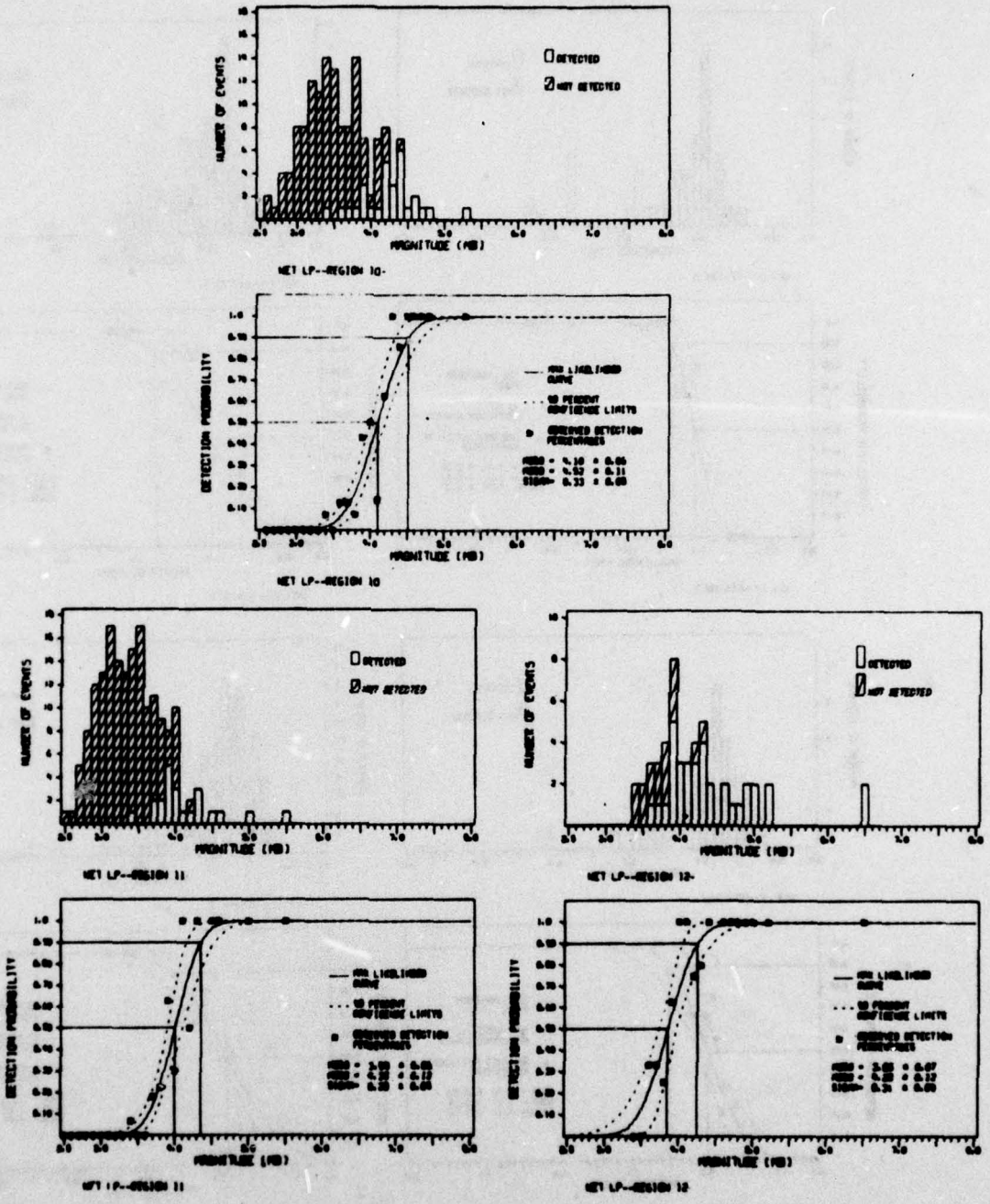

FIGURE VII-6

LONG-PERIOD NETWORK DETECTION STATISTICS
REGIONS 10, 11, AND 12

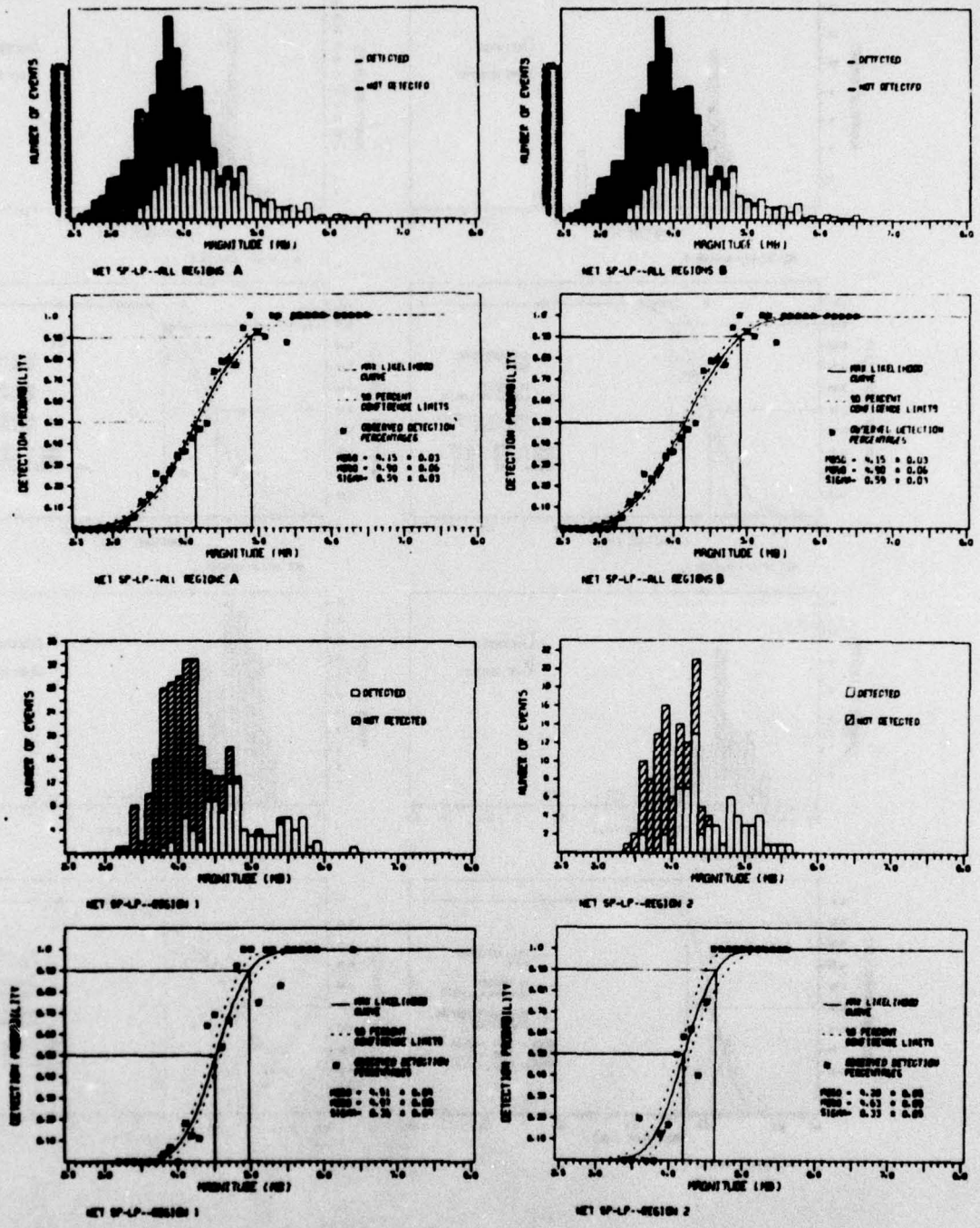

FIGURE VII-7

COMBINED NETWORK DETECTION STATISTICS
ALL REGIONS A AND B--REGIONS 1 AND 2

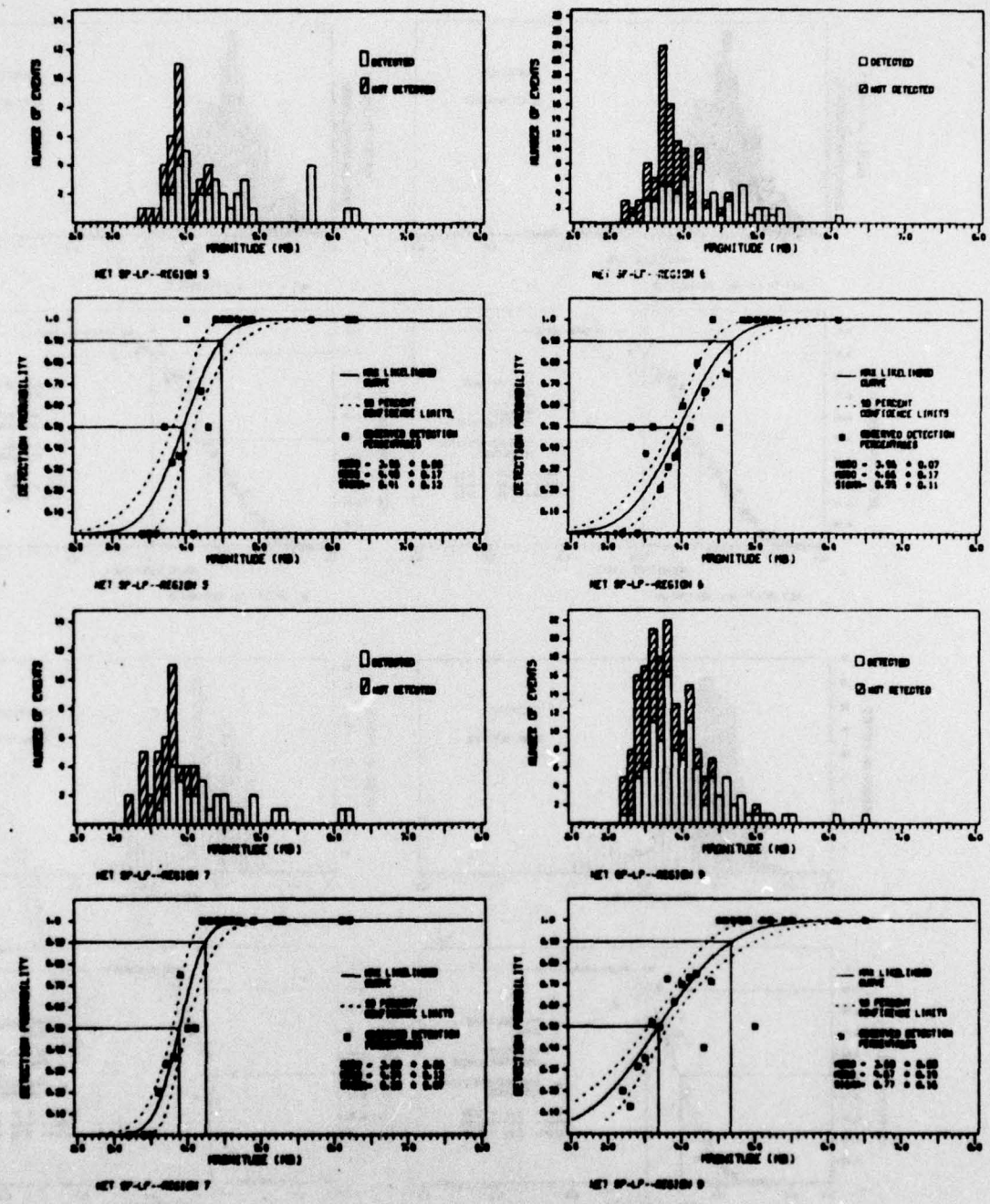

FIGURE VII-8

COMBINED NETWORK DETECTION STATISTICS
REGIONS 5, 6, 7, AND 9

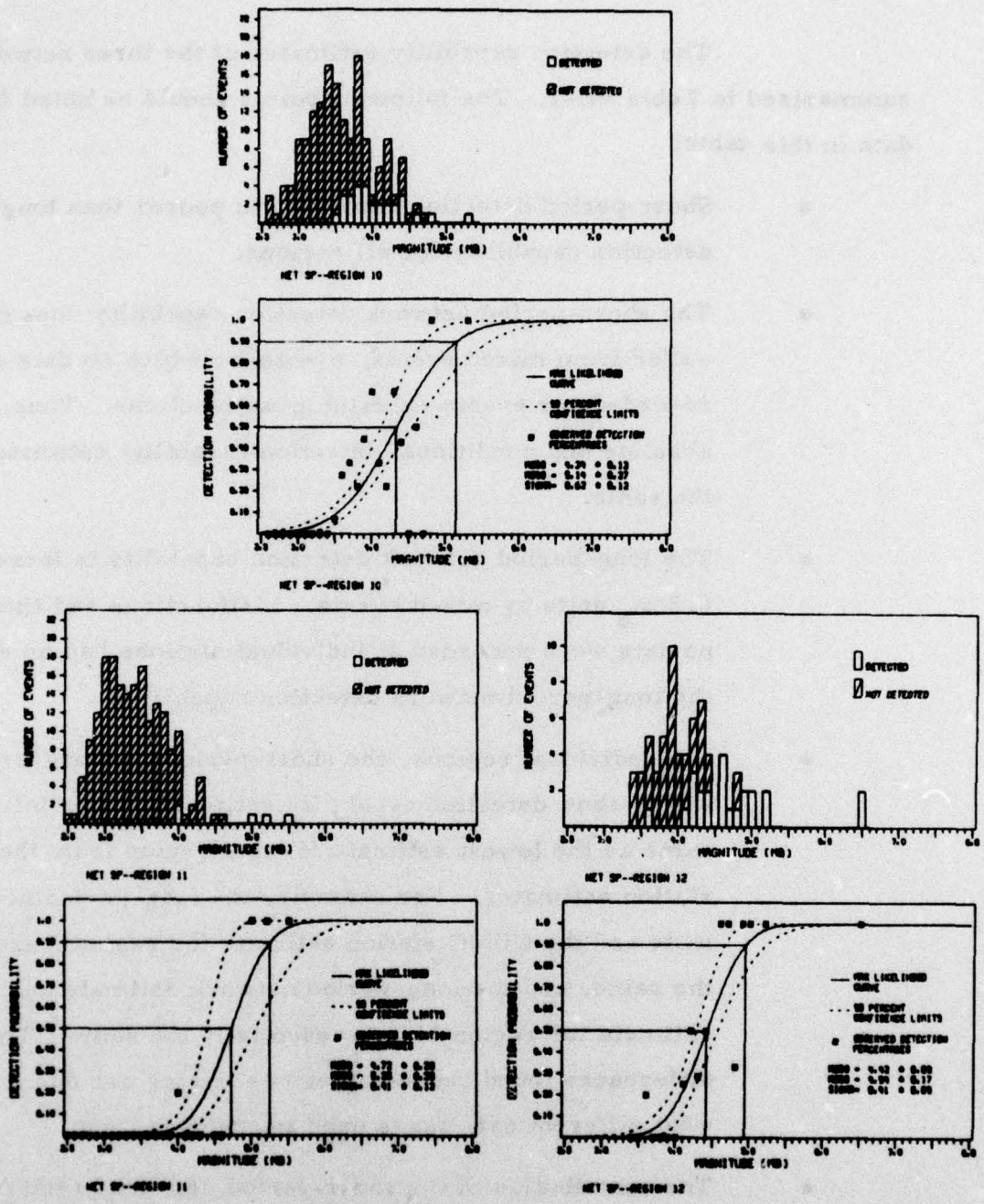

FIGURE VII-9

COMBINED NETWORK DETECTION STATISTICS
REGIONS 10, 11, AND 12

The detection capability estimates of the three networks are summarized in Table VII-1. The following points should be noted from the data in this table:

- Short-period detection capability is poorer than long-period detection capability for all regions.
- The short-period network detection capability does not suffer from mixed events, events for which no data were recorded, or events containing malfunctions. Thus, the absolute and conditional detection capability estimates are the same.
- The long-period network detection capability is increased 0.2 m_b units by mixed events. Malfunctions and times when no data were recorded at individual stations had no effect on the long-period network detection capability.
- For individual regions, the short-period and long-period networks show detection capability estimates essentially the same as the lowest estimate for that region from the individual station estimates. For example, the long-period network estimate and the GUMO station estimate for region 2 are essentially the same, and the long-period network estimate and the MAIO estimate for region 11 are essentially the same. The small differences found between these estimates are due to the somewhat different data bases used to generate them.
- The contribution of the short-period network to the combined network is to replace the mixed event statistics of the long-period data with detected and non-detected event statistics of the short-period data. This results in the elimination of

TABLE VII-1

SRO NETWORK DETECTION CAPABILITY ESTIMATES

	50 Percent Detection Threshold		
	Short-Period Net	Long-Period Net	Combined Short-Period and Long-Period Net
All Regions A	4.62	4.36	4.15
All Regions B	4.62	4.16	4.15
1	4.93	4.44	4.51
2	4.53	4.24	4.20
5	(4.2)	4.04	3.96
6	4.31	3.98	3.96
7	(4.4)	3.98	3.89
9	4.06	3.86	3.68
10	(4.3)	4.10	4.00
11	(4.7)	4.00	4.05
12	(4.4)	3.85	3.97

All Regions A	Mixed events were counted as non-detections.
All Regions B and individual regions	Mixed events were rejected from the detection statistics.
SP Data	Events for which the automatic detector did not declare a detection were counted as non-detections.

the difference between the absolute and conditional detection capability estimates observed for the long-period network.

- For individual regions, the combined network shows little difference from the long-period network. The differences observed are due to the addition to the detection statistics of events which were mixed on the long-period data.

C. LONG-PERIOD NETWORK DETECTION CAPABILITY FROM NOISE STATISTICS OF INDIVIDUAL STATIONS

This approach uses a modified version of the network capability estimation technique reported by Snell (Snell, 1976). This technique is based on the equations presented in Table VII-2. The signal amplitudes at all network stations are calculated for an assumed event at epicenter j with magnitude m_{bj} (equation VII-1). Signal and noise are assumed to be lognormally distributed; hence, the probability that the signal-to-noise ratio exceeds the station detection threshold is given by the normal cumulative probability function (equations VII-2 and VII-3). Signal and noise are measured zero-to-peak for use in this technique. The noise mean is input as the geometric mean of the noise amplitudes. The individual station detection probabilities are then combined into the network probability of at least station detections, $\hat{P}_j(\geq \alpha)$, using a recursive relation involving the individual station detection probabilities (equation VII-4). A detailed description of the operation of this technique is reported by Snell (Snell, 1976).

This technique was modified so that instead of computing detection threshold magnitudes (as defined by Snell) for the network, a measure of the probability of detecting an event of given magnitude is plotted. This measure of the probability of detecting is $\text{Log}_{10}\left[P_D/1\text{-}P_D\right]$, where P_D is the probability of detecting the event. This value was chosen as the measure

TABLE VII-2

EVALUATION OF NETWORK DETECTION CAPABILITY

$$\log_{10} A_{ij} = m_j + b_\Delta + c_\Delta \log_{10} \Delta_{ij} + E_{ij} \qquad \text{(VII-1)}$$

$$p_{ij} = \phi \left[\frac{\log_{10} A_{ij} - (\mu_N + \log_{10} SDT)}{\sigma_n^2 + \sigma_s^2}^{1/2} \right] \qquad \text{(VII-2)}$$

$$\phi(x) = \frac{1}{\sqrt{2\pi}} \int_{\infty}^{x} e^{-y^2/2} \, dy \qquad \text{(VII-3)}$$

$$\hat{p}_j(\geq \alpha) = \sum_{k=\alpha}^{N} \hat{p}_j(k) \qquad \text{(VII-4)}$$

Symbols above are defined as follows:

- A_{ij} - signal amplitude at station i for event j (0-p)
- m_j - magnitude of event j (m_b)
- b_Δ, c_Δ - standard table entries
- E_{ij} - station-epicenter bias corrections
- μ_N - mean $\log_{10}$ noise amplitude (0-p)
- σ_n^2 - variance of $\log_{10}$ noise
- σ_n^2 - variance of $\log_{10}$ signal
- $\phi(x)$ - normal cumulative probability function
- N - number of stations in the network
- $\hat{p}_j(k)$ - probability that k stations will detect event j
- $\hat{p}_j(\geq \alpha)$ - probability that α or more stations will detect event j
- SDT - station detection threshold, i.e., signal-to-noise ratio required for detection at station.

of probability of detecting rather than P_D itself, since P_D will round off to one for high probabilities of detection (for example P_D = 0.999968 would be rounded off to 1.0).

The mean and variance of the $\log_{10}$ noise amplitudes used to produce the estimates of network detection capability are the peak 25-second period noise amplitudes described in Section IV. Station reliability estimates were derived from the station reliability estimates and probability of mixed events estimates of Section II. The signal-to-noise ratio required for detection at a station was set at 6 dB.

Four cases of long-period network detection were prepared for this report. Figure VII-10 shows the probability of one station detecting an m_b=4.5 event. Figure VII-11 shows the probability of two stations detecting an m_b=4.5 event. Figure VII-12 shows the probability of one station detecting an m_b=5.5 event. Figure VII-13 shows the probability of two stations detecting an m_b=5.5 event. Table VII-3 translates the $LOG_{10}\left[P_D/1\text{-}P_D\right]$ contours into probability of detection.

It is difficult to make comparisons between these network detection capability estimates and the detection capability estimates presented in Table VII-1. The estimates for individual regions in Table VII-1 do not take into account the effects of mixed events while the estimates presented in Figures VII-10 to VII-13 do. However, some qualitative comparisons can be made by assuming that the detection thresholds of the individual regions will be raised by mixed events the same amount as were the combined regions. This would, for example, make the long-period network detection capability estimate (50 percent probability of detection) for region 5 equal to 4.2 m_b from Table VII-1 and the 90 percent detection threshold (from Figure VII-5) equal to 4.5 m_b. Figure VII-10 shows that the probability of detecting a Region 5 event with m_b=4.5 at one or more stations is approximately 0.9.

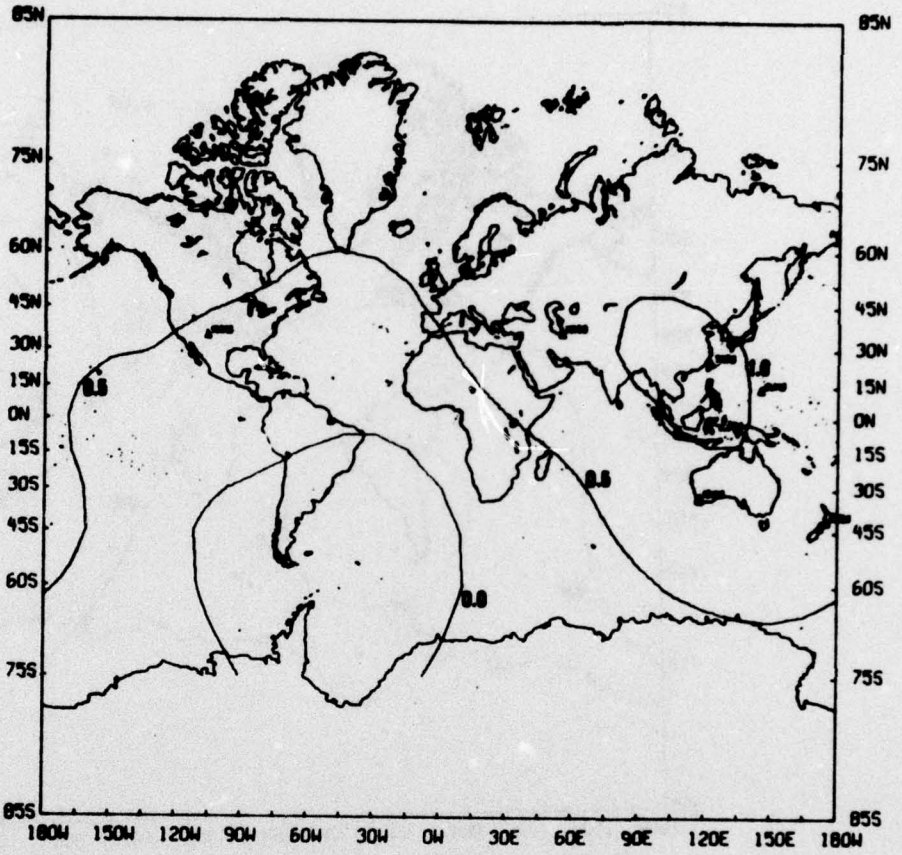

m_b = 4.5

1 Station Detecting

FIGURE VII-10

PROBABILITY OF ONE STATION OF THE NETWORK DETECTING AN m_b =4.5 EARTHQUAKE (LONG-PERIOD)

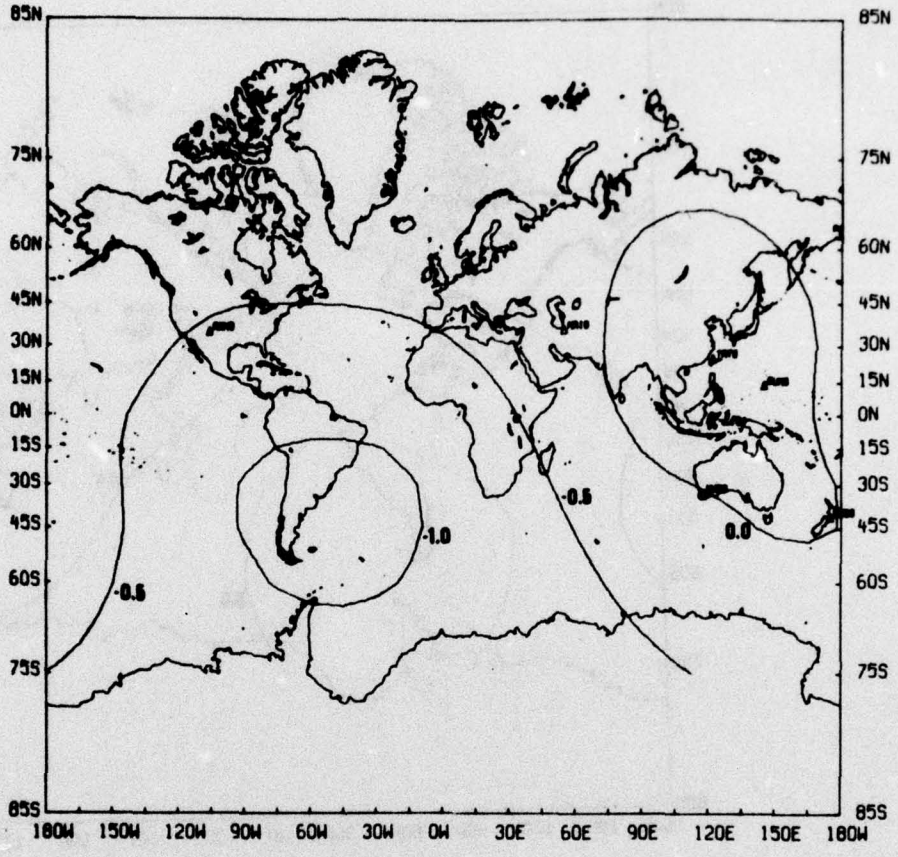

$m_b = 4.5$

2 Station Detecting

FIGURE VII-11

PROBABILITY OF TWO STATIONS OF THE NETWORK DETECTING AN m_b =4.5 EARTHQUAKE (LONG-PERIOD)

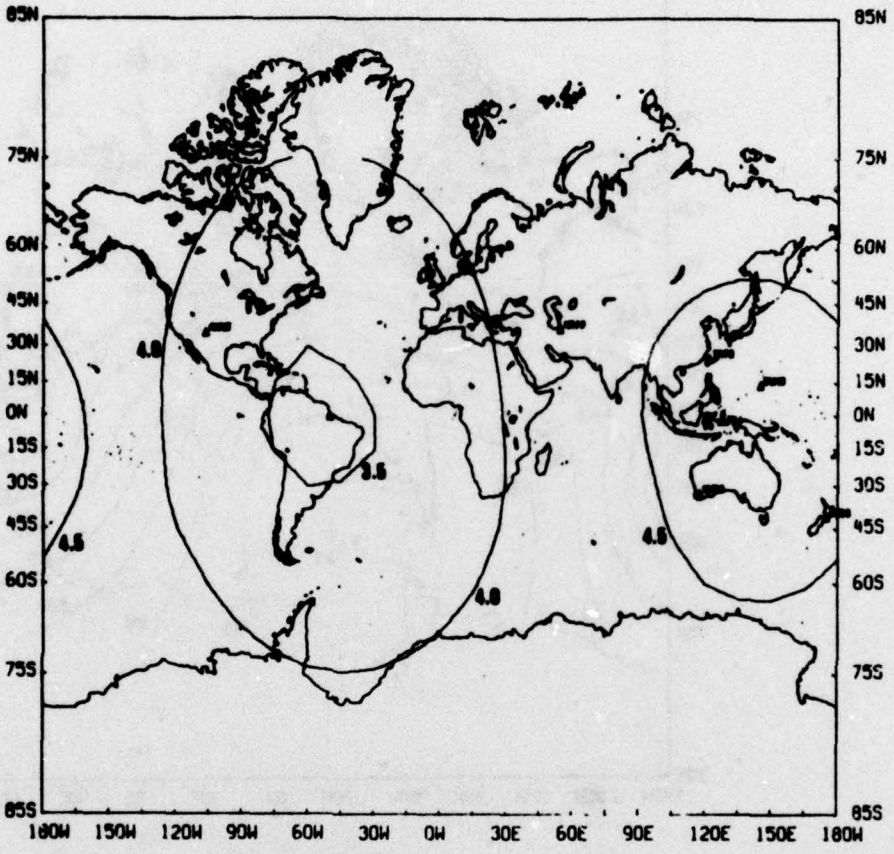

$m_b = 5.5$

1 Station Detecting

FIGURE VII-12

PROBABILITY OF ONE STATION OF THE NETWORK DETECTING AN m_b=5.5 EARTHQUAKE

(LONG-PERIOD)

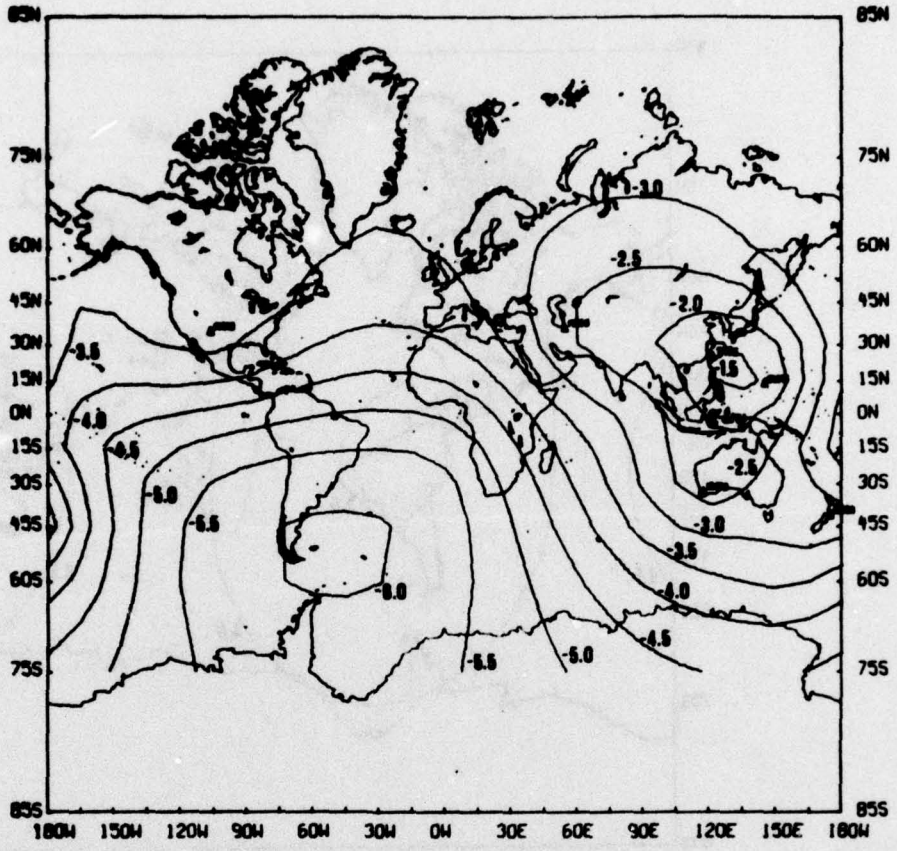

$m_b = 5.5$

2 Station Detecting

FIGURE VII-13

PROBABILITY OF TWO STATIONS OF THE NETWORK DETECTING AN m_b =5.5 EARTHQUAKE (LONG-PERIOD)

TABLE VII-3

CORRELATION OF LOG_{10} $P_D/(1-P_D)$ CONTOURS WITH PROBABILITY OF DETECTION

Contour	Probability of Detection
-1.0	0.09091
-0.5	0.31613
0.0	0.50000
0.5	0.75975
1.0	0.90909
1.5	0.96935
2.0	0.99010
2.5	0.99685
3.0	0.99900
3.5	0.99968
4.0	0.9990
4.5	0.99997

Thus, there appears to be fairly good agreement between the two methods of estimating network detection capability.

Note that in some other regions the indicated standard deviation of the event population is very large in contrast to the assumption of signal standard deviation used in network capability evaluation from noise. These may be due to large variations of B-Factor, source radiation pattern and other effects. It is difficult to explain large variations in observed event population standard deviations.

SECTION VIII
CONCLUSIONS

This section summarizes the results of this continued evaluation of the Seismic Research Observatory stations. The major results are:

A. DATA QUALITY

- In general, the data quality was good. At all stations except MAIO, short-period data were degraded by malfunctions one percent of the time or less. MAIO short-period data was degraded by a 1.7 Hz waveform of unknown origin approximately seven percent of the time. Long-period data were degraded by malfunctions three to eight percent of the time.
- Estimates of station reliability were based on the frequency of occurrence of malfunctions and on estimates of station down-time. GUMO had the lowest reliability (0.7) due to a relatively large amount of station down-time. The other stations had reliability factors of 0.8 or above.
- The probability of an event being mixed was estimated at approximately 0.3, with little variation from station to station, in a range of m_b values from 3.1 to 5.0.

B. SHORT-PERIOD AUTOMATIC DETECTOR

- The passband filter limits placed at the front-end of the short-period automatic detector should be changed from

0.5-2.0 Hz to 0.5-1.5 Hz, or some means such as a notch filter should be used to eliminate the 1.7 Hz waveform.

- The number of contiguous points for which the short-term average must exceed the scaled long-term average in order for a detection to be declared should be increased from 20 points to at least 30 points to reduce detection declarations caused by glitches.

- The automatic detector appears to be unstable in terms of turning off after a detected event dies back into the noise.

C. NOISE ANALYSIS

- In order of increasing magnitude, the mean short-period RMS noise values in the 0.5-4.0 Hz passband (uncorrected for instrument response) are: 0.38mμ at ANMO, 0.57 mμ at MAIO, 7.69 mμ at NWAO, 20.61 mμ at TATO, 28.92 mμ at SNZO, and 40.25 mμ at GUMO. These values show a strong correlation with station-nearest coastline separation, indicating that a majority of short-period noise is derived from ocean wave energy injected at the coastline.

- Based on mean long-period RMS noise levels in the 0.023 -0.059 Hz passband, the stations can be divided into two groups--ANMO and MAIO form the group with lower RMS noise levels and GUMO, NWAO, and TATO form the group with higher RMS noise levels. Considering the locations of these stations, this suggests that there is at least some correlation between station-coastline separation and long-period noise level.

- The long-period RMS noise levels at SNZO seem too high to be entirely due to seismic noise. It would be advisable to check the instrumentation at this station to determine whether instrumentation malfunctions are adding to the apparent noise levels.
- Oceanic wave energy appears to play a large part in determining the noise level, spectral content, and day-to-day variability of the noise field.

D. DETECTION CAPABILITY

- No short-period events of the data base were detected at SNZO, while only two were detected at GUMO.
- Mixed events had very little effect on short-period detection capability estimates.
- Station down-time caused an increase of approximately 0.2 m_b units in the ANMO short-period detection capability estimates.
- Malfunctions caused an increase of approximately 0.1 m_b units in the MAIO short-period detection capability estimates.
- Mixed events caused an increase of approximately 0.3 m_b units in the NWAO long-period detection capability estimates.
- Mixed events, system failures, and malfunctions equally contributed to an increase of approximately 0.3 m_b units in the SNZO long-period detection capability estimates.
- Mixed events, and to a lesser degree system failures and malfunctions, caused an increase of approximately 0.4 m_b units in the long-period detection capability estimates of ANMO, MAIO, and TATO.

- System failures, and to a lesser degree mixed events, caused an increase of approximately 0.5 m_b units in the GUMO long-period detection capability estimates.

E. DISCRIMINATION

- Surface wave magnitudes of presumed nuclear explosions from the Nevada Test Site fall in the earthquake population of the M_s-m_b discriminant.
- Events 537 and 839 show surface wave magnitudes indicating that they are earthquakes.
- Events 13, 1062, 1200, and 1368 show surface wave magnitudes indicating that they are nuclear explosions.

F. NETWORK DETECTION CAPABILITY

- Using direct estimates of detection capability derived from the events of the data base, it was found that the combined short-period, long-period network shows little difference from the long-period network detection capability estimates. The primary contribution of the short-period network is to replace the mixed-event statistics of the long-period data with detected and non-detected event statistics of the short-period data.
- Short-period detection capability is poorer than long-period detection capability for all regions. This appears to be due to the effect of automatic detector on the short-period data.
- The short-period network detection capability estimates are not affected by mixed events, malfunctions, or system failures at individual stations.

- The long-period network detection capability estimates are increased 0.2 m_b units by mixed events. Malfunctions and system failures at individual stations did not affect these estimates.
- For individual regions, the short-period and long-period networks show detection capability estimates essentially the same as the lowest estimate for a given region from the individual station estimates.
- Based on such comparisons as are possible, the above-described long-period direct network detection capability estimates appear to agree quite well with the network detection capability estimates derived from noise statistics.

Future work on the evaluation of the Seismic Research Observatory stations should be directed toward the following points:

- Evaluate all stations as they become operational.
- Expand the short-period and long-period noise data bases so that at least one year of data is available at each station for the study of noise level trends.
- Obtain continuous short-period data and the automatic detector algorithm so that the effects of changes in the detector input parameters can be studied.
- Expand the signal data base so that detection and discrimination results can be determined for new stations and better defined for particular regions for stations already under evaluation. This would also be used to better define station reliability and mixed event probability estimates.
- Investigate the discrimination of earthquakes and presumed nuclear explosions using short-period data.

SECTION IX
REFERENCES

Eterno, J.S., D.S. Burns, L.J. Freier, and S.W. Buck, 1974, Special Event Detection for an Unattended Seismic Observatory; Report Number R-765, ARPA Contract Number F44620-73-C-0057, The Charles Stark Draper Laboratory, Incorporated, Cambridge, Massachusetts.

Flinn, E.A., and E.R. Engdahl, 1965, A Proposed Basis for Geographical and Seismic Regionalization; Reviews of Geophysics, Volume 3, Number 1, pp. 123-149.

Ringdal, F., 1974, VLPE Network Evaluation and Automatic Processing Research; Technical Report No. 2, Texas Instruments Report No. ALEX(01)-TR-74-02, AFTAC Contract Number F08606-74-C-0033, Texas Instruments Incorporated, Dallas, Texas.

Ringdal, F., J.S. Shaub, and D.G. Black, 1975, Documentation of the Interactive Seismic Processing System (ISPS); Software Documentation Report No. 1, Texas Instruments Report No. ALEX(01)-SD-75-01, AFTAC Contract Number F08606-75-C-0029, Texas Instruments Incorporated, Dallas, Texas.

Robinson, E.A., 1967, Statistical Communication and Detection with Special Reference to Digital Data Processing of Radar and Seismic Signals, Charles Griffin and Company Limited, London, England.

Schmidt, A.W., and K.S. Wilson, 1977, Seismic Data Preparation Procedures; Technical Report No. 10, Texas Instruments Report No. ALEX(01)-TR-77-10, AFTAC Contract Number F08606-77-C-0004, Texas Instruments Incorporated, Dallas, Texas.

Snell, N.S., 1976, Network Capability Estimation, Technical Report No. 4, Texas Instruments Report No. ALEX(01)-TR-76-04, AFTAC Contract N Number F08606-76-C-0011, Texas Instruments Incorporated, Dallas, Texas.

Strauss, A.C., 1976, Preliminary Evaluation of the Seismic Research Observatories; Technical Report No. 2, Texas Instruments Report No. ALEX(01)-TR-76-02, AFTAC Contract Number F08606-76-C-0011, Texas Instruments Incorporated, Dallas, Texas.

Swindell, W.H., and N.S. Snell, 1977, Station Processor Automatic Signal Detection System, Phase 1: Final Report; Texas Instruments Report No. ALEX(01)-FR-77-01, AFTAC Contract Number F08606-76-C-0025, Texas Instruments Incorporated, Dallas, Texas.

Sun, D., 1977, Determination of Seismic Source Parameters from Long-Period Surface Wave Data; Technical Report No. 11, Texas Instruments Report No. ALEX(01)-TR-77-11, AFTAC Contract Number F08606-77-C-0004, Texas Instruments Incorporated, Dallas, Texas.

APPENDIX A
THE DATA BASE

The data base used for this evaluation of the Seismic Research Observatory stations is presented on the following pages. Table A-1 lists the events from the data base used in the evaluation of short-period and long-period data recorded at each station.

In the data base list, the column headed 'EVNO' gives the identifying number assigned to each event. The columns headed 'DATE' and 'TIME' give the date and origin time of each event. The epicentral coordinates are listed under 'LAT.' and 'LONG' for latitude in degrees north and longitude in degrees east. The bodywave magnitude is listed under the heading 'MB'. The column headed 'Q' gives the NORSAR quality rating for the parameters of each event where

1 = good to excellent quality

2 = fair to good quality

3 = poor to fair quality.

The seismic source area is listed in the column headed 'LOCATION'. Finally, the seismic sub-region as defined by Flinn and Engdahl (Flinn and Engdahl, 1965) for each event is listed under the heading 'SUBREG'.

TABLE A-1

EVENTS USED IN EVALUATING EACH STATION

Station	Event Nos. of Processed Events	
	SP	LP
ANMO	1-1402	1-1219
GUMO	1-1213 1228-1380	1-1384
MAIO	36-1406	36-1219
NWAO	483-1220 1296-1380	483-1472
TATO	780-1433	780-1433
SNZO	453-1206	453-1219

TABLE A-2

DATA BASE
(PAGE 1 OF 37)

EVNO	DATE	TIME	LAT.	LONG.	MB	Q	LOCATION	SUBREG
1	12/23/75	23.55. 0	33.0	88.0	3.9	3	TIBET	306
2	12/24/75	8.39.29	32.0	59.0	3.6	3	IRAN	348
3	12/24/75	11.48.58	27.0	56.0	5.6	1	SOUTHERN IRAN	353
4	12/24/75	12. 2.35	27.0	56.0	3.8	2	SOUTHERN IRAN	353
5	12/24/75	17. 4.29	35.0	24.0	4.5	2	CRETE	370
6	12/24/75	18.48. 1	45.0	152.0	5.4	1	KURILE ISLANDS REG.	222
7	12/24/75	19.55.17	28.0	55.0	5.0	1	SOUTHERN IRAN	353
8	12/24/75	21. 4.20	28.0	55.0	4.5	1	SOUTHERN IRAN	353
9	12/24/75	22.34.38	45.0	152.0	4.0	2	KURILE ISLANDS REG.	222
10	12/25/75	0.51. 1	51.0	159.0	4.0	3	OEC KAMCHATKA	219
11	12/25/75	1.55. 2	46.0	152.0	4.3	2	KURILE ISLANDS	221
12	12/25/75	3. 4.52	27.0	56.0	4.1	3	SOUTHERN IRAN	353
13	12/25/75	5.17. 3	50.0	78.0	6.3	1	EASTERN KAZAKH SSR	329
14	12/25/75	15. 6.35	46.0	152.0	4.0	2	KURILE ISLANDS	221
15	12/25/75	15.36.29	45.0	152.0	5.3	1	KURILE ISLANDS REG.	222
16	12/25/75	16. 0.13	45.0	152.0	5.5	1	KURILE ISLANDS	222
17	12/25/75	17. 6.30	46.0	152.0	4.2	2	KURILE ISLANDS	221
18	12/25/75	18.50.49	37.0	139.0	3.9	3	HONSHU, JAPAN	227
19	12/25/75	21.38.17	43.0	147.0	5.1	1	OFF COAST HOKKAIDO	225
20	12/25/75	22.21. 5	43.0	149.0	3.6	3	KURILE ISLANDS REG.	222
21	12/25/75	23.46.22	28.0	55.0	3.9	2	SOUTHERN IRAN	353
22	12/26/75	5.46.50	28.0	55.0	4.4	1	SOUTHERN IRAN	353
23	12/26/75	7.17. 2	42.0	146.0	4.2	2	OFF COAST HOKKAIDO	225
24	12/26/75	22. 2.39	28.0	55.0	3.8	2	SOUTHERN IRAN	353
25	12/27/75	2.25.34	28.0	55.0	3.6	3	SOUTHERN IRAN	353
26	12/27/75	4.31.51	44.0	12.0	3.8	2	CENTRAL ITALY	381
27	12/27/75	5.25.30	43.0	147.0	4.9	2	OFF COAST HOKKAIDO	225
28	12/27/75	5.33.10	40.0	142.0	4.6	2	NEC HONSHU, JAPAN	228
29	12/27/75	12.50.51	44.0	147.0	4.6	2	KURILE ISLANDS	221
30	12/27/75	16.14.42	43.0	147.0	3.8	3	KURILE ISLANDS	221
31	12/27/75	17. 3.48	44.0	147.0	4.7	2	KURILE ISLANDS	221
32	12/27/75	20.43.27	43.0	147.0	4.5	1	OFF COAST HOKKAIDO	225
33	12/27/75	22.21.29	28.0	55.0	4.1	3	SOUTHERN IRAN	353
34	12/28/75	3. 9.43	43.0	147.0	3.9	3	OFF COAST HOKKAIDO	225
35	12/28/75	6.12.10	31.0	50.0	3.5	3	IRAN	348
36	12/28/75	9. 6. 3	33.0	62.0	3.8	3	NW AFGHANISTAN	349
37	12/28/75	13.49.28	34.0	85.0	4.6	1	TIBET	306
38	12/28/75	16.29.34	37.0	142.0	4.8	1	NEC HONSHU, JAPAN	228
39	12/29/75	0. 1.49	36.0	20.0	3.5	3	MEDITERRANEAN SEA	400
40	12/29/75	1.20. 3	27.0	97.0	4.5	2	BURMA	296

TABLE A-2

DATA BASE
(PAGE 2 OF 37)

EVNO	DATE	TIME	LAT.	LONG.	MB	Q	LOCATION	SUBREG
41	12/29/75	5. 8. 2	27.0	96.0	5.7	1	BURMA-INDIA BORDER	294
42	12/29/75	6.26.29	28.0	96.0	4.1	3	INDIA-CHINA BORDER	313
43	12/30/75	15.54.18	36.0	22.0	3.8	3	MEDITERRANEAN SEA	400
44	12/30/75	23.23. 6	54.0	161.0	4.2	3	NEC KAMCHATKA	218
45	12/31/75	6.34.33	41.0	21.0	3.8	2	GREECE-ALBANIA BOR.	392
46	12/31/75	9.46.16	41.0	21.0	5.0	2	GREECE-ALBANIA BOR.	392
47	12/31/75	10. 7.59	41.0	21.0	3.6	3	GREECE-ALBANIA BOR	392
48	12/31/75	10.16.44	41.0	21.0	3.7	3	GREECE-ALBANIA BOR	392
49	12/31/75	10.26.24	40.0	21.0	3.5	3	GREECE	364
50	12/31/75	11.26.46	40.0	22.0	3.5	3	GREECE	364
51	12/31/75	11.31.56	41.0	21.0	3.8	3	GREECE-ALBANIA BOR	392
52	12/31/75	12.14.11	41.0	21.0	3.5	2	GREECE-ALBANIA BOR	392
53	12/31/75	12.19.45	42.0	20.0	3.3	3	YUGOSLAVIA	383
54	12/31/75	13. 2.37	41.0	21.0	3.8	3	GREECE-ALBANIA BOR.	392
55	12/31/75	13.51.49	41.0	21.0	4.3	2	GREECE-ALBANIA BOR	392
56	12/31/75	13.57.52	41.0	21.0	3.4	2	GREECE-ALBANIA BOR	392
57	12/31/75	14.12.24	40.0	143.0	5.3	1	NEC HONSHU, JAPAN	228
58	12/31/75	14.54. 8	41.0	21.0	4.3	2	GREECE-ALBANIA BOR.	392
59	12/31/75	15.15. 7	41.0	21.0	4.0	2	GREECE-ALBANIA BOR R	392
60	12/31/75	15.20.25	41.0	21.0	3.4	3	ALBANIA	391
61	12/31/75	15.25.54	41.0	21.0	3.3	3	GREECE-ALBANIA BOR	392
62	12/31/75	17. 7.48	41.0	21.0	3.7	2	GREECE-ALBANIA BOR.	392
63	12/31/75	17.37.19	41.0	21.0	3.5	3	GREECE-ALBANIA BOR.	392
64	12/31/75	22.55.14	41.0	20.0	3.9	2	GREECE-ALBANIA BOR.	392
65	1/ 1/76	0. 4.35	41.0	21.0	4.6	2	GREECE-ALBANIA BOR.	392
66	1/ 1/76	2.19.48	41.0	21.0	3.7	2	GREECE-ALBANIA BOR.	392
67	1/ 1/76	7.56.32	41.0	21.0	3.4	3	GREECE-ALBANIA BOR.	392
68	1/ 1/76	13.34.16	40.0	29.0	3.2	3	TURKEY	366
69	1/ 1/76	20. 1.16	36.0	22.0	3.3	3	SOUTHERN GREECE	368
70	1/ 1/76	20. 6.14	40.0	21.0	3.2	3	GREECE	364
71	1/ 1/76	20. 9.54	40.0	20.0	3.5	3	GREECE-ALBANIA BOR.	392
72	1/ 1/76	22.22. 1	49.0	154.0	3.7	3	KURILE ISLANDS	221
73	1/ 2/76	2.46.36	46.0	153.0	4.8	1	KURILE ISLANDS REG.	222
74	1/ 2/76	2.48.19	41.0	21.0	3.3	3	GREECE-ALBANIA BOR.	392
75	1/ 2/76	4.30.56	31.0	47.0	4.1	2	IRAN-IRAQ BOR. REG.	346
76	1/ 2/76	6.47.58	43.0	147.0	5.6	1	OFF COAST HOKKAIDO	225
77	1/ 2/76	11.11.18	41.0	21.0	3.1	3	GREECE-ALBAINI BOR	392
78	1/ 2/76	14.29.16	28.0	55.0	3.9	2	SOUTHERN IRAN	353
79	1/ 2/76	15. 8.59	28.0	55.0	4.1	2	SOUTHERN IRAN	353
80	1/ 2/76	21.36.44	52.0	160.0	4.7	1	OEC KAMCHATKA	219

TABLE A-2

DATA BASE
(PAGE 3 OF 37)

EVNO	DATE	TIME	LAT.	LONG.	MB	Q	LOCATION	SUBREG
81	1/ 2/76	22.45.13	41.0	21.0	4.2	2	GREECE-ALBANIA BOR.	392
82	1/ 3/76	4.30.53	41.0	21.0	3.3	3	ALBANIA	391
83	1/ 3/76	5.54.55	40.0	22.0	3.7	3	GREECE	364
84	1/ 3/76	13.16.58	41.0	21.0	4.3	2	GREECE-ALBANIA BOR.	392
85	1/ 3/76	13.50.40	41.0	21.0	3.8	2	GREECE-ALBANIA BOR R	392
86	1/ 3/76	14.36. 8	41.0	20.0	3.0	3	ALBANIA	391
87	1/ 3/76	14.46.21	41.0	21.0	3.8	3	GREECE-ALBANIA BOR R	392
88	1/ 3/76	15. 4.12	40.0	22.0	4.2	2	GREECE	364
89	1/ 3/76	15.44.39	41.0	21.0	3.7	3	GREECE-ALBANIA BOR	392
90	1/ 3/76	17. 0. 1	40.0	22.0	3.5	3	GREECE	364
91	1/ 3/76	19.15. 5	38.0	-116.0	5.9	1	NEVADA	37
92	1/ 3/76	20.26. 8	35.0	81.0	3.7	3	TIBET	306
93	1/ 3/76	22.45.52	41.0	21.0	3.5	3	GREECE-ALBANIA BOR.	392
94	1/ 4/76	16.40. 7	45.0	147.0	4.1	2	KURILE ISLANDS	221
95	1/ 4/76	21.14.57	42.0	18.0	3.1	3	ADRIATIC SEA	382
96	1/ 5/76	0. 3.20	52.0	162.0	4.6	2	OEC KAMCHATKA	219
97	1/ 5/76	2. 5.18	54.0	159.0	4.3	3	KAMCHATKA	217
98	1/ 5/76	7. 0. 0	52.0	162.0	4.1	2	OEC KAMCHATKA	219
99	1/ 5/76	23.33.23	39.0	74.0	3.8	2	S. SINKIANG PROV.	321
100	1/ 6/76	10.45.37	43.0	150.0	3.7	3	OFF COAST HOKKAIDO	225
101	1/ 6/76	16.40.40	41.0	20.0	3.0	3	ALBANIA	391
102	1/ 6/76	19.28.49	56.0	162.0	4.8	1	NEC KAMCHATKA	218
103	1/ 6/76	19.50.58	53.0	163.0	3.9	2	OFF E COAST KAMCHAT	219
104	1/ 6/76	19.51.50	54.0	163.0	4.9	2	OEC KAMCHATKA	219
105	1/ 6/76	20.11.52	40.0	20.0	3.4	3	GREECE-ALBANIA BOR.	392
106	1/ 6/76	20.57.12	51.0	159.0	5.2	1	NEC KAMCHATKA	218
107	1/ 6/76	21. 8.28	53.0	158.0	5.5	1	NEC KAMCHATKA	218
108	1/ 6/76	21.14.47	48.0	152.0	4.3	2	KURILE ISLANDS	221
109	1/ 6/76	21.23.56	53.0	157.0	4.9	1	KAMCHATKA	217
110	1/ 6/76	21.32.16	52.0	158.0	4.1	3	NEC KAMCHATKA	218
111	1/ 6/76	21.35.33	53.0	157.0	4.6	2	KAMCHATKA	217
112	1/ 6/76	21.42.19	53.0	157.0	3.9	2	KAMCHATKA	217
113	1/ 6/76	21.45.33	53.0	158.0	5.7	1	NEC KAMCHATKA	218
114	1/ 6/76	22.10. 5	53.0	157.0	4.1	2	KAMCHATKA	217
115	1/ 6/76	22.17.59	53.0	157.0	5.9	1	KAMCHATKA	217
116	1/ 6/76	22.24.25	53.0	157.0	4.7	1	KAMCHATKA	217
117	1/ 6/76	23.35. 7	33.0	96.0	4.4	2	TSINGHAI PROV CHINA	325
118	1/ 7/76	0.24.51	32.0	76.0	5.3	1	KASHMIR-INDIA BORDER	303
119	1/ 7/76	1.30.59	53.0	158.0	4.1	2	NEC KAMCHATKA	218
120	1/ 7/76	1.57. 8	53.0	158.0	5.5	1	NEC KAMCHATKA	218

TABLE A-2

DATA BASE
(PAGE 4 OF 37)

EVNO	DATE	TIME	LAT.	LONG.	MB	Q	LOCATION	SUBREG
121	1/ 7/76	2. 8.33	52.0	158.0	4.1	3	NEAR E COAST KAMCHAT	218
122	1/ 7/76	2.18.29	29.0	58.0	3.7	3	SOUTHERN IRAN	353
123	1/ 7/76	8.33. 4	53.0	158.0	5.3	1	NEC KAMCHATKA	218
124	1/ 7/76	5.10.41	48.0	120.0	3.5	3	NORTHEASTERN CHINA	658
125	1/ 7/76	7.10.33	32.0	58.0	4.3	3	IRAN	348
126	1/ 7/76	7.25.53	53.0	159.0	3.8	3	NEAR E COAST KAMCHAT	218
127	1/ 7/76	7.50.43	40.0	142.0	5.1	1	NEC HONSHU, JAPAN	228
128	1/ 7/76	7.58.59	51.0	159.0	4.8	1	OFF EAST COAST KAM	219
129	1/ 7/76	8. 3.43	51.0	161.0	4.6	1	OFF EAST COAST KAMCH	219
130	1/ 7/76	8.53. 2	35.0	140.0	4.5	2	NEC HONSHU, JAPAN	228
131	1/ 7/76	10. 6.43	38.0	140.0	4.4	2	HONSHU, JAPAN	227
132	1/ 7/76	10.15.40	32.0	93.0	3.9	3	TIBET	306
133	1/ 7/76	10.46.29	52.0	160.0	4.9	1	OEC KAMCHATKA	219
134	1/ 7/76	10.50.19	53.0	157.0	4.3	2	KAMCHATKA	217
135	1/ 7/76	11.38.31	51.0	159.0	4.4	2	OEC KAMCHATKA	219
136	1/ 7/76	11.51.12	39.0	142.0	4.2	2	NEC HONSHU, JAPAN	228
137	1/ 7/76	12.58.26	53.0	157.0	4.4	2	KAMCHATKA	217
138	1/ 7/76	13.58.53	38.0	41.0	4.0	3	TURKEY	366
139	1/ 7/76	21.27.42	36.0	139.0	4.2	3	HONSHU, JAPAN	227
140	1/ 7/76	23.34.32	53.0	158.0	5.8	1	NEC KAMCHATKA	218
141	1/ 7/76	23.54.49	51.0	161.0	3.9	3	OFF E COAST KAMCHAT	219
142	1/ 8/76	1.17. 4	54.0	161.0	4.2	3	NEC KAMCHATKA	218
143	1/ 8/76	3.34.28	51.0	159.0	4.5	2	OEC KAMCHATKA	219
144	1/ 8/76	6.55.15	52.0	158.0	4.0	3	NEAR E COAST KAMCHAT	218
145	1/ 8/76	8.40.25	41.0	21.0	3.6	3	GREECE-ALBANIA BOR.	392
146	1/ 8/76	9. 3.23	53.0	157.0	4.0	3	KAMCHATKA	217
147	1/ 8/76	10.30.41	51.0	160.0	5.9	1	OEC KAMCHATKA	219
148	1/ 8/76	13.25.31	53.0	158.0	4.2	3	KAMCHATKA	217
149	1/ 8/76	14.19.54	51.0	159.0	4.5	2	OEC KAMCHATKA	219
150	1/ 8/76	15.50.22	53.0	158.0	5.3	1	NEC KAMCHATKA	218
151	1/ 8/76	17.54.39	52.0	159.0	3.8	3	NEC KAMCHATKA	218
152	1/ 8/76	19.32.49	53.0	158.0	4.2	3	NEC KAMCHATKA	218
153	1/ 8/76	22.34.27	33.0	76.0	4.8	1	KASHMIR-INDIA BORDER	303
154	1/ 8/76	23.48.23	33.0	76.0	3.6	3	KASHMIR-INDIA BORDER	302
155	1/ 9/76	1.20.21	53.0	158.0	4.4	2	NEC KAMCHATKA	218
156	1/ 9/76	1.36.50	37.0	146.0	4.3	3	OFF E COAST HONSHU	229
157	1/ 9/76	2.19.28	35.0	24.0	3.6	3	CRETE	370
158	1/ 9/76	10.39.16	46.0	43.0	3.3	3	SW RUSSIA	357
159	1/10/76	3.37.23	51.0	159.0	5.0	1	OEC KAMCHATKA	219
160	1/10/76	5.42. 1	25.0	96.0	3.9	3	BURMA	296

TABLE A-2

DATA BASE

(PAGE 5 OF 37)

EVNO	DATE	TIME	LAT.	LONG.	MB	Q	LOCATION	SUBREG
161	1/10/76	7.11.43	40.0	29.0	3.8	2	TURKEY	366
162	1/10/76	11.58.30	45.0	149.0	3.6	3	KURILE ISLANDS	221
163	1/10/76	13.25.22	47.0	44.0	3.3	3	SW RUSSIA	357
164	1/10/76	14.54.20	41.0	83.0	3.9	2	SOUTHERN SINKIANG PR	321
165	1/10/76	21.40. 6	41.0	21.0	3.4	2	GREECE-ALBANIA BOR.	392
166	1/11/76	3.59. 9	38.0	21.0	3.7	3	IONIAN SEA	399
167	1/11/76	4.55.32	38.0	21.0	3.6	3	IONIAN SEA	399
168	1/11/76	10.48. 7	53.0	158.0	4.8	1	NEC KAMCHATKA	218
169	1/14/76	18.15. 3	40.0	29.0	3.9	3	TURKEY	366
170	1/14/76	21.44.34	42.0	142.0	4.3	2	HOKKAIDO JAP REG	224
171	1/15/76	4.46.47	49.0	80.0	5.0	1	EASTERN KAZAKH SSR	329
172	1/16/76	5.36.31	32.0	51.0	4.5	1	IRAN	348
173	1/16/76	8.24.31	28.0	95.0	4.0	3	INDIA-CHINA BOR REG	313
174	1/16/76	8.32.19	50.0	158.0	5.1	1	KURILE ISLANDS	221
175	1/16/76	8.51.59	46.0	43.0	2.9	3	SW RUSSIA	357
176	1/16/76	12.40.27	45.0	151.0	4.2	2	KURILE IS REG	222
177	1/16/76	15.35.34	44.0	150.0	4.4	2	KURILE IS	221
178	1/16/76	15.50.17	36.0	140.0	4.3	2	NEAR E COAST HONSHU	228
179	1/16/76	16.48.24	43.0	144.0	4.1	2	HOKKAIDO JAPAN REG	224
180	1/20/76	0. 3.25	41.0	21.0	3.5	3	GREECE-ALBANIA BOR.	392
181	1/20/76	1.25.26	41.0	22.0	3.2	3	GREECE	364
182	1/20/76	6.42.34	53.0	158.0	4.5	2	NEC KAMCHATKA	218
183	1/20/76	7.57. 6	33.0	80.0	3.9	3	TIBET	306
184	1/20/76	12.44.46	41.0	21.0	3.5	2	GREECE-ALBANIA BOR R	392
185	1/20/76	13.31.31	40.0	19.0	3.2	3	ALBANIA	391
186	1/20/76	14. 0.46	31.0	95.0	4.2	2	TIBET	306
187	1/20/76	23.18. 0	34.0	142.0	4.1	2	OEC HONSHU, JAPAN	229
188	1/21/76	0.25.30	29.0	85.0	4.1	3	TIBET	306
189	1/21/76	0.29.15	47.0	151.0	4.3	2	KURILE IS	221
190	1/21/76	10. 5.14	43.0	149.0	6.4	1	KURILE ISLANDS	222
191	1/21/76	10.30.58	45.0	149.0	4.7	2	KURILE IS	221
192	1/21/76	10.34.28	43.0	149.0	4.9	1	KURILE IS REG	222
193	1/21/76	10.39.37	44.0	150.0	3.9	3	KURILE KS REG	222
194	1/21/76	10.51.14	45.0	149.0	5.6	1	KURILE IS	221
195	1/21/76	11.21.50	43.0	149.0	4.2	2	KURILE IS REG	222
196	1/21/76	11.51. 7	44.0	149.0	4.2	2	KURILE IS REG	222
197	1/21/76	12.20.19	45.0	149.0	4.7	1	KURILE IS	221
198	1/21/76	12.26.27	45.0	149.0	3.9	2	KURILE IS	221
199	1/21/76	13.14.11	43.0	150.0	5.5	1	KURILE IS REG	222
200	1/21/76	13.20.14	44.0	148.0	4.5	2	KURILE IS REG	222

TABLE A-2

DATA BASE

(PAGE 6 OF 37)

EVNO	DATE	TIME	LAT.	LONG.	MB	Q	LOCATION	SUBREG
201	1/21/76	13.31.19	39.0	30.0	3.8	2	TURKEY	366
202	1/21/76	13.54. 8	45.0	149.0	4.6	2	KURILE IS	221
203	1/21/76	14.47.20	43.0	152.0	4.0	3	KURILE IS REG	222
204	1/21/76	15.44.43	44.0	149.0	4.6	1	KURILE IS	221
205	1/21/76	15.46.59	44.0	150.0	4.0	3	KURILE IS REG	222
206	1/21/76	16.30.15	44.0	150.0	4.2	2	KURILE IS	221
207	1/21/76	18. 1.54	57.0	163.0	5.4	1	NEC KAMCHATKA	218
208	1/21/76	18.15.21	40.0	29.0	3.4	3	TURKEY	366
209	1/21/76	18.26.19	60.0	164.0	4.0	3	KAMCHATKA	217
210	1/21/76	18.28.25	43.0	149.0	4.1	2	KURILE IS REG	222
211	1/21/76	18.29.19	45.0	149.0	4.2	2	KURILE IS	221
212	1/21/76	19.10.45	43.0	149.0	4.3	2	KURILE IS REG	222
213	1/21/76	20.56. 0	43.0	149.0	5.0	1	KURILE IS REG	222
214	1/21/76	21. 0.44	44.0	149.0	5.5	1	KURILE IS	221
215	1/21/76	21.18. 4	44.0	152.0	4.3	2	KURILE IS REG	222
216	1/21/76	21.22.26	46.0	150.0	4.2	2	KURILE IS	221
217	1/21/76	22.10.15	44.0	151.0	3.9	2	KURILE IS REG	222
218	1/21/76	22.18.35	41.0	21.0	4.0	2	GREECE-ALBANIA BOR R	392
219	1/21/76	23.49.29	44.0	149.0	4.3	2	KURILE IS	221
220	1/22/76	0.14.43	45.0	149.0	4.6	1	KURILE IS	221
221	1/22/76	0.17.12	44.0	150.0	4.3	2	KURILE IS REG	222
222	1/22/76	2. 9.38	43.0	149.0	4.4	1	KURILE ISLANDS REG.	222
223	1/22/76	2.22.23	43.0	149.0	4.8	1	KURILE IS REG	222
224	1/22/76	2.24. 8	42.0	84.0	3.4	3	SOUTHERN SINKIANG PR	321
225	1/22/76	4.27.15	44.0	149.0	4.0	2	KURILE IS	221
226	1/22/76	5.17.12	43.0	149.0	4.2	2	KURILE IS REG	222
227	1/22/76	5.40.50	44.0	149.0	4.3	2	KURILE IS	221
228	1/22/76	6.12.37	43.0	149.0	5.2	1	KURILE IS REG	222
229	1/22/76	8.15.35	44.0	150.0	5.4	1	KURILE IS	221
230	1/22/76	8.19. 8	43.0	149.0	5.1	1	KURILE IS REG	222
231	1/22/76	8.20.17	45.0	148.0	4.7	2	KURILE IS	221
232	1/22/76	8.46. 0	29.0	82.0	3.8	3	NEPAL	310
233	1/22/76	9. 0.58	45.0	149.0	5.4	2	KURILE IS	221
234	1/22/76	9.15.37	45.0	151.0	4.0	3	KURILE IS	221
235	1/22/76	9.39. 7	43.0	149.0	4.6	1	KURILE ISLANDS REG.	222
236	1/22/76	9.46.44	44.0	150.0	4.0	3	KURILE IS	221
237	1/22/76	10.50.36	53.0	158.0	4.8	1	NEC KAMCHATKA	218
238	1/22/76	11.42. 4	44.0	149.0	5.6	1	KURILE IS	221
239	1/22/76	12.15.41	44.0	150.0	4.5	2	KURILE IS	221
240	1/22/76	13.57.12	46.0	150.0	4.1	2	KURILE IS	221

TABLE A-2

DATA BASE

(PAGE 7 OF 37)

EVNO	DATE	TIME	LAT.	LONG.	MB	Q	LOCATION	SUBREG
241	1/22/76	14.51.10	40.0	29.0	3.3	3	TURKEY	366
242	1/22/76	15.13.18	44.0	149.0	4.4	2	KURILE IS	221
243	1/22/76	15.28.57	43.0	149.0	3.9	3	KURILE IS REG	222
244	1/22/76	16.21.17	45.0	149.0	5.3	1	KURILE IS	221
245	1/22/76	17. 4. 9	45.0	149.0	3.9	3	KURILE IS	221
246	1/22/76	17.46.22	43.0	149.0	4.1	3	KURILE IS REG	222
247	1/22/76	17.49. 3	44.0	149.0	5.7	1	KURILE IS	221
248	1/22/76	18. 1.45	45.0	149.0	4.1	2	KURILE IS	221
249	1/22/76	18.35.53	44.0	149.0	4.7	1	KURILE IS	221
250	1/22/76	18.53.22	44.0	149.0	4.1	2	KURILE IS	221
251	1/22/76	20.32. 1	57.0	163.0	3.9	2	NEAR E COAST KAMCHAT	218
252	1/22/76	20.42.35	45.0	149.0	3.8	3	KURILE IS	221
253	1/22/76	21.43.13	44.0	149.0	4.1	3	KURILE IS	221
254	1/22/76	21.45.41	23.0	101.0	3.9	3	YUNNAN PROV., CHINA	318
255	1/22/76	22.19.40	43.0	142.0	4.0	3	HOKKAIDO JAPAN REG	224
256	1/23/76	0.10.29	43.0	149.0	5.0	1	KURILE IS REG	222
257	1/23/76	0.41. 2	46.0	153.0	4.4	2	KURILE ISLANDS REG.	222
258	1/23/76	0.51.34	45.0	149.0	4.8	1	KURILE IS	221
259	1/23/76	2.45. 8	45.0	149.0	4.7	2	KURILE IS REG	222
260	1/23/76	6.11.15	45.0	149.0	3.9	2	KURILE IS	221
261	1/23/76	8. 4. 5	44.0	153.0	4.1	2	KURILE ISLANDS REG.	222
262	1/23/76	9.16.33	44.0	46.0	3.5	3	EASTERN CAUCASUS	337
263	1/23/76	12.14.42	44.0	151.0	3.3	3	KURILE IS REG	222
264	1/23/76	16. 9. 2	44.0	30.0	3.3	2	BLACK SEA	360
265	1/23/76	23.49.13	44.0	149.0	4.0	2	KURILE IS	221
266	1/24/76	0.54.55	45.0	151.0	4.2	2	KURILE IS REG	222
267	1/24/76	1.55. 9	43.0	147.0	4.2	2	OFF COAST HOKKAIDO J	225
268	1/24/76	2. 0.19	44.0	147.0	5.4	1	KURILE IS	221
269	1/24/76	9.44.12	45.0	148.0	4.7	1	KURILE IS	221
270	1/24/76	10.37.48	43.0	149.0	3.7	3	KURILE IS REG	222
271	1/24/76	10.41.32	45.0	149.0	4.7	1	KURILE IS	221
272	1/24/76	11.13.58	43.0	149.0	4.0	3	KURILE IS REG	222
273	1/24/76	13.13.51	44.0	146.0	3.9	3	HOKKAIDO JAPAN REG	224
274	1/24/76	13.21.53	43.0	149.0	4.7	1	KURILE IS REG	222
275	1/24/76	13.39.54	43.0	149.0	4.5	1	KURILE IS REG	222
276	1/24/76	14.47. 5	44.0	150.0	4.1	2	KURILE IS REG	222
277	1/24/76	16.50.16	45.0	149.0	3.7	3	KURILE IS	221
278	1/24/76	17.16.38	40.0	40.0	3.6	3	TURKEY	366
279	1/24/76	17.20.31	44.0	150.0	4.8	1	KURILE IS	221
280	1/24/76	18.26. 2	45.0	149.0	3.8	3	KURILE IS	221

TABLE A-2

DATA BASE

(PAGE 8 OF 37)

EVNO	DATE	TIME	LAT.	LONG.	MB	Q	LOCATION	SUBREG
281	1/24/76	19. 1.30	44.0	148.0	4.0	2	KURILE IS REG	222
282	1/24/76	19.39.29	43.0	152.0	4.0	3	KURILE IS REG	222
283	1/24/76	20.30.36	43.0	147.0	4.3	2	OFF COAST HOKKAIDO	225
284	1/24/76	21. 0.14	44.0	149.0	4.9	1	KURILE IS	221
285	1/24/76	22.10.25	43.0	149.0	4.0	3	KURILE IS REG	222
286	1/24/76	23.47.51	43.0	149.0	4.7	2	KURILE IS REG	222
287	1/25/76	5.21.16	47.0	151.0	3.9	3	KURILE IS	221
288	1/25/76	12.23.50	44.0	148.0	5.7	1	KURILE IS REG	222
289	1/25/76	12.34.11	45.0	151.0	4.1	3	KURILE IS REG	222
290	1/25/76	14.23.28	45.0	149.0	4.2	2	KURILE IS	221
291	1/25/76	14.36. 8	45.0	151.0	3.6	3	KURILE IS REG	222
292	1/25/76	17.59.38	43.0	149.0	4.2	2	KURILE IS REG	222
293	1/25/76	19.12.18	30.0	94.0	4.3	3	INDIA-CHINA BOR REG	313
294	1/25/76	19.49.17	43.0	149.0	4.7	1	KURILE IS REG	222
295	1/25/76	20.33. 5	45.0	151.0	4.1	2	KURILE IS REG	222
296	1/25/76	22. 4.48	45.0	149.0	4.4	1	KURILE IS	221
297	1/25/76	23.50.15	43.0	150.0	3.9	2	KURILE IS REG	222
298	1/26/76	0.21. 4	42.0	143.0	3.7	3	HOKKAIDO JAPAN REG	224
299	1/26/76	1.57.43	45.0	149.0	3.9	2	KURILE IS	221
300	1/26/76	10.59.33	43.0	144.0	4.1	2	HOKKAIDO JAPAN REG	224
301	1/26/76	11.57. 8	45.0	149.0	3.8	3	KURILE IS	221
302	1/26/76	17.10.42	44.0	148.0	4.8	1	KURILE IS REG	222
303	1/26/76	17.35.23	45.0	151.0	4.2	2	KURILE IS	221
304	1/26/76	19.49.15	45.0	149.0	3.8	3	KURILE IS	221
305	1/26/76	20.44. 4	45.0	149.0	4.7	1	KURILE IS	221
306	1/26/76	22.26.49	27.0	103.0	3.5	3	YUNAN PROV CHINA	318
307	1/26/76	22.45.18	38.0	30.0	4.2	2	TURKEY	366
308	1/26/76	22.55.41	33.0	49.0	3.2	3	WESTERN IRAN	347
309	1/26/76	23. 8.42	43.0	152.0	3.6	3	KURILE IS REG	222
310	1/26/76	23.23.18	44.0	150.0	3.9	3	KURILE IS	221
311	1/27/76	0.24.30	33.0	96.0	3.8	2	TSINGHAI, CHINA	325
312	1/27/76	8. 0. 0	31.0	51.0	3.6	2	IRAN	348
313	1/27/76	10.50.30	45.0	151.0	4.0	2	KURILE IS	221
314	1/27/76	12. 0.49	44.0	148.0	4.3	2	KURILE IS REG	222
315	1/27/76	19.23.18	32.0	76.0	4.4	2	KASHMIR-INDIA BOR.	303
316	1/27/76	21.34.42	36.0	75.0	3.6	3	EASTERN KASHMIR	302
317	1/27/76	23.19. 9	44.0	150.0	4.3	2	KURILE IS	221
318	1/27/76	23.22. 5	41.0	21.0	3.5	2	GREECE-ALBANIA BOR	392
319	1/28/76	11. 4. 7	45.0	45.0	3.2	3	SOUTHWESTERN RUSSIA	357
320	1/28/76	13.41.42	32.0	49.0	3.6	3	WESTERN IRAN	347

TABLE A-2

DATA BASE
(PAGE 9 OF 37)

EVNO	DATE	TIME	LAT.	LONG.	MB	Q	LOCATION	SUBREG
321	1/28/76	19.35.44	43.0	149.0	5.7	1	KURILE IS REG	222
322	1/29/76	4.19.49	40.0	46.0	4.0	2	IRAN-USSR BORDER	344
323	1/29/76	13.39.30	41.0	21.0	3.3	2	GREECE-ALBANIA BOR.	392
324	1/29/76	14.16.56	44.0	149.0	5.4	1	KURILE IS	221
325	1/29/76	16.53.57	41.0	21.0	3.4	2	GREECE-ALBANIA BOR	392
326	1/29/76	20. 3. 9	32.0	49.0	3.6	3	WESTERN IRAN	347
327	1/29/76	23.30. 2	43.0	152.0	4.0	3	KURILE IS REG	222
328	1/30/76	11.53.44	45.0	149.0	4.2	2	KURILE IS	221
329	1/30/76	12. 6. 5	43.0	149.0	4.1	2	KURILE IS REG	222
330	1/30/76	17.48.44	41.0	21.0	3.1	2	GREECE-ALBANIA BOR	392
331	1/31/76	0.25.40	45.0	148.0	5.7	1	KURILE IS	221
332	1/31/76	7.51.16	30.0	57.0	4.2	3	SOUTHERN IRAN	353
333	1/31/76	7.58. 0	53.0	157.0	4.1	2	KAMCHATKA	217
334	1/31/76	8.21.35	43.0	149.0	3.8	3	OFF COAST HOKKAIDO	225
335	1/31/76	23.43. 9	50.0	159.0	3.8	3	KURILE IS REG	222
336	2/ 1/76	11.27. 2	45.0	152.0	3.6	3	HOKKAIDO JAPAN REG	224
337	2/ 1/76	13.21.45	38.0	21.0	4.0	2	IONIAN SEA	399
338	2/ 1/76	14.37.14	45.0	149.0	3.7	2	KURILE IS	221
339	2/ 1/76	14.46.23	38.0	21.0	3.8	2	IONIAN SEA	399
340	2/ 1/76	15.38.44	25.0	93.0	3.9	2	BURMA-INDIA BOR REG	294
341	2/ 1/76	16. 4.41	44.0	151.0	3.5	2	KURILE IS REG	222
342	2/ 1/76	16. 5.23	45.0	149.0	3.8	3	KURILE IS	221
343	2/ 1/76	20.28.15	33.0	80.0	3.7	2	KASHMIR-TIBET BORDER	304
344	2/ 1/76	21.39.35	41.0	21.0	3.2	2	GREECE--ALBANIA BOR	392
345	2/ 1/76	21.41.44	41.0	21.0	2.9	2	GREECE-ALBANIA BOR	392
346	2/ 1/76	21.57.44	44.0	150.0	4.1	2	KURILE IS	221
347	2/ 1/76	23.33.53	41.0	21.0	3.8	2	GREECE-ALBANIA BOR	392
348	2/ 2/76	3. 0.16	51.0	159.0	5.6	1	OEC KAMCHATKA	219
349	2/ 2/76	6. 2.22	46.0	149.0	4.3	2	KURILE IS	221
350	2/ 2/76	6. 2.58	44.0	151.0	3.9	3	KURILE IS REG	222
351	2/ 2/76	7. 2.24	53.0	157.0	4.6	1	KAMCHATKA	217
352	2/ 2/76	12.13.41	43.0	17.0	4.0	2	ADRIATIC SEA	382
353	2/ 2/76	13.38. 9	42.0	26.0	3.8	2	GREECE-BULGARIA BOR	363
354	2/ 3/76	12.32.36	34.0	76.0	3.3	3	EASTERN KASHMIR	302
355	2/ 3/76	13.29.16	45.0	23.0	3.7	2	RUMANIA	358
356	2/ 3/76	14.25.15	44.0	150.0	3.4	3	KURILE IS REG	222
357	2/ 3/76	16.39.47	34.0	51.0	5.1	1	IRAN	348
358	2/ 3/76	18.37.21	45.0	149.0	4.4	2	KURILE IS	221
359	2/ 3/76	18.54.20	38.0	21.0	2.9	3	IONIAN SEA	399
360	2/ 4/76	2.34. 3	37.0	29.0	3.8	3	DODECANESE IS	369

TABLE A-2

DATA BASE
(PAGE 10 OF 37)

EVNO	DATE	TIME	LAT.	LONG.	MB	Q	LOCATION	SUBREG
361	2/ 4/76	10.57. 5	38.0	21.0	3.0	3	IONIAN SEA	399
362	2/ 4/76	21.25.14	44.0	150.0	3.8	2	KURILE IS	221
363	2/ 5/76	7.17.16	52.0	162.0	3.8	2	OFF EAST COAST KAMCH	219
364	2/ 5/76	12. 4.36	31.0	76.0	4.8	2	NORTHERN INDIA	308
365	2/ 5/76	18.23.27	43.0	145.0	3.8	3	KOKKAIDO JAPAN REG	224
366	2/ 5/76	19.38.29	40.0	29.0	3.4	3	TURKEY	366
367	2/ 6/76	13. 4.32	36.0	51.0	3.2	3	IRAN	348
368	2/ 6/76	17.41.55	43.0	149.0	4.2	2	KURILE IS REG	222
369	2/ 6/76	18. 9.38	40.0	22.0	3.0	3	GREECE	364
370	2/ 6/76	18.38.32	37.0	138.0	4.3	2	HONSHU JAPAN	227
371	2/ 6/76	19.37.22	31.0	97.0	3.9	3	TIBET	306
372	2/ 7/76	3.37.31	36.0	53.0	4.6	1	IRAN	348
373	2/ 7/76	8.41.24	41.0	75.0	4.0	2	KIRGIZ-SINKIANG BOR.	320
374	2/ 7/76	14. 4.40	35.0	27.0	3.8	3	CRETE	370
375	2/ 7/76	15. 8. 4	46.0	152.0	4.1	2	KURILE IS	221
376	2/ 7/76	15.54.15	33.0	89.0	4.1	2	TIBET	306
377	2/ 7/76	18. 7.16	38.0	21.0	3.1	3	IONIAN SEA	399
378	2/ 7/76	19.24.48	38.0	21.0	3.2	3	IONIAN SEA	399
379	2/ 7/76	23.21.55	38.0	21.0	3.8	3	IONIAN SEA	399
380	2/ 8/76	8.38.14	38.0	21.0	3.0	3	IONIAN SEA	399
381	2/ 8/76	11.29.27	46.0	153.0	4.5	2	KURILE IS REG	222
382	2/ 8/76	15.17.52	38.0	21.0	2.9	3	IONIAN SEA	399
383	2/ 8/76	18.26.44	35.0	27.0	3.5	3	CRETE	370
384	2/ 8/76	20. 6.53	39.0	24.0	3.4	3	AEGEAN SEA	365
385	2/ 8/76	21.11.41	41.0	21.0	3.0	3	GREECE-ALBANIA BOR	392
386	2/ 9/76	5.46.22	36.0	140.0	4.3	2	HONSHU JAPAN	227
387	2/ 9/76	6.30.20	31.0	49.0	3.4	3	WESTERN IRAN	347
388	2/ 9/76	6.45.16	44.0	150.0	4.1	2	KURILE IS	221
389	2/ 9/76	13. 9.51	38.0	21.0	2.9	3	IONIAN SEA	399
390	2/ 9/76	18.59. 5	55.0	162.0	4.5	2	NEC KAMCHATKA	218
391	2/10/76	1.15. 7	42.0	150.0	4.0	2	OFF COAST HOKKAIDO	225
392	2/10/76	4. 2.39	25.0	94.0	4.1	3	BURMA-INDIA BOR REG	294
393	2/10/76	7.51.24	43.0	149.0	4.2	2	KURILE IS REG	222
394	2/10/76	17.53.12	45.0	151.0	4.1	2	KURILE ISLANDS	221
395	2/11/76	1.21.30	38.0	21.0	3.2	3	IONIAN SEA	399
396	2/11/76	1.36.25	34.0	59.0	4.2	3	IRAN	348
397	2/11/76	4. 4.21	43.0	149.0	3.8	3	KURILE IS REG	222
398	2/11/76	7.36.39	51.0	159.0	4.6	1	OEC KAMCHATKA	219
399	2/11/76	11.58.44	45.0	34.0	2.9	3	CRIMEA REG	361
400	2/12/76	1.44.35	47.0	154.0	4.4	1	KURILE ISLANDS	221

TABLE A-2

DATA BASE
(PAGE 11 OF 37)

EVNO	DATE	TIME	LAT.	LONG.	MB	Q	LOCATION	SUBREG
401	2/12/76	14.45. 6	38.0	-116.0	5.9	1	NEVADA	37
402	2/12/76	17.50. 5	25.0	93.0	3.9	2	BURMA-INDIA BOR REG	294
403	2/12/76	20.59.56	41.0	21.0	3.6	2	GREECE-ALBANIA BOR R	392
404	2/12/76	22.45.47	46.0	151.0	4.0	2	KURILE IS	221
405	2/13/76	5.39.43	53.0	159.0	3.4	2	NEC KAMCHATKA	218
406	2/13/76	7.27.48	39.0	24.0	3.2	2	AEGEAN SEA	365
407	2/13/76	9.14.57	47.0	40.0	3.4	3	SOUTHWESTERN RUSSIA	357
408	2/13/76	18.35. 8	44.0	150.0	3.7	3	KURILE IS	221
409	2/14/76	9. 5.31	34.0	142.0	4.2	2	OFF E COAST HONSHU	229
410	2/14/76	11.30. 4	38.0	-115.0	5.6	1	SOUTHERN NEVADA	41
411	2/14/76	16.18.18	38.0	21.0	3.2	3	IONIAN SEA	399
412	2/14/76	18.19.54	34.0	83.0	4.2	2	TIBET	306
413	2/14/76	19.39.18	36.0	74.0	4.0	2	NW KASHMIR	720
414	2/14/76	20.25.36	30.0	103.0	4.2	2	SZECHWAN PROV CHINA	307
415	2/15/76	5.47.36	33.0	48.0	3.9	2	WESTERN IRAN	347
416	2/15/76	21. 0.56	31.0	49.0	3.4	3	WESTERN IRAN	347
417	2/16/76	14. 0. 8	56.0	162.0	4.0	2	NEAR E COAST KAMCHAT	218
418	2/16/76	14.45.46	23.0	101.0	5.0	2	YUNNAN PROV., CHINA	318
419	2/16/76	23.41.40	52.0	160.0	4.2	2	OEC KAMCHATKA	219
420	2/17/76	7.51. 0	21.0	96.0	4.0	3	BURMA	296
421	2/17/76	21.43. 2	35.0	140.0	4.3	1	NEAR E COAST HONSHU	228
422	2/18/76	11.24.54	39.0	21.0	3.4	3	GREECE	364
423	2/18/76	11.42.13	42.0	22.0	3.8	3	BULGARIA	359
424	2/18/76	13.17.30	47.0	44.0	3.2	3	SOUTHWESTERN RUSSIA	357
425	2/18/76	17.29.58	38.0	21.0	3.1	3	IONIAN SEA	399
426	2/18/76	20.59.25	43.0	149.0	3.9	2	KURILE IS REG	222
427	2/18/76	23. 7.50	45.0	30.0	3.9	3	BLACK SEA	360
428	2/19/76	7. 1.44	38.0	21.0	2.9	3	IONIAN SEA	399
429	2/19/76	9.38.40	23.0	100.0	4.8	2	BURMA-CHINA BORDER	297
430	2/19/76	11.45.34	23.0	101.0	3.7	3	YUNNAN PROV., CHINA	318
431	2/19/76	12.46.44	35.0	139.0	3.8	3	NEAR S COAST HONSHU	230
432	2/19/76	20.35.19	37.0	29.0	3.5	3	DODECANESE IS	369
433	2/20/76	0.32.36	53.0	157.0	3.8	2	KAMCHATKA	217
434	2/20/76	2.13.33	45.0	152.0	4.2	2	KURILE IS	221
435	2/20/76	12.13.58	43.0	149.0	3.8	2	KURILE IS REG	222
436	2/20/76	12.24.23	49.0	152.0	4.1	2	KURILE IS	221
437	2/20/76	13.37.52	31.0	51.0	4.2	1	IRAN	348
438	2/20/76	16.43.38	40.0	29.0	3.1	3	TURKEY	366
439	2/20/76	19.28.36	43.0	146.0	4.4	1	HOKKAIDO JAPAN REG	224
440	2/21/76	17.38.38	38.0	75.0	3.5	3	SOUTHERN SINKIANG	321

TABLE A-2

DATA BASE
(PAGE 12 OF 37)

EVNO	DATE	TIME	LAT.	LONG.	MB	Q	LOCATION	SUBREG
441	2/22/76	1.12. 1	34.0	142.0	5.2	1	OFF E COAST HONSHU	229
442	2/22/76	12. 2.53	39.0	21.0	4.3	2	GREECE	364
443	2/22/76	16.15. 5	43.0	17.0	4.2	2	ADRIATIC SEA	382
444	2/22/76	22. 1.47	39.0	21.0	4.4	2	GREECE	364
445	2/22/76	22.42. 0	33.0	91.0	4.1	2	TSINGHAI PROV CHINA	325
446	2/22/76	22.45. 5	41.0	21.0	3.2	3	GREECE-ALBANIA BOR	392
447	2/22/76	22.54.34	39.0	21.0	4.2	2	GREECE	364
448	2/22/76	22.56.30	39.0	21.0	4.0	2	GREECE	364
449	2/23/76	10.13.37	40.0	29.0	3.9	3	TURKEY	366
450	2/23/76	16.18.54	40.0	22.0	4.6	2	GREECE	364
451	2/24/76	21.57.59	35.0	81.0	4.2	2	TIBET	306
452	2/25/76	16.57.16	27.0	59.0	3.8	3	SOUTHERN IRAN	353
453	2/26/76	3.23.46	36.0	75.0	4.0	3	EASTERN KASHMIR	302
454	2/26/76	15. 6.43	35.0	143.0	4.9	2	OFF E COAST HONSHU	229
455	2/28/76	18. 2. 5	27.0	105.0	3.8	3	YUNNAN PROV., CHINA	318
456	2/29/76	3.45.29	31.0	50.0	3.6	3	IRAN	348
457	2/29/76	7.23.42	38.0	21.0	2.9	3	IONIAN SEA	399
458	2/29/76	9.27.13	36.0	140.0	4.9	1	HONSHU, JAPAN	227
459	2/29/76	12.49.38	46.0	150.0	3.8	3	KURILE ISLANDS	221
460	2/29/76	20.23.18	44.0	142.0	3.9	2	HOKKAIDO, JAPAN	224
461	2/29/76	20.34.13	36.0	22.0	3.9	3	MEDITERRANEAN SEA	400
462	2/29/76	21.58.15	46.0	151.0	3.8	2	KURILE IS	221
463	3/ 2/76	2.49.38	31.0	142.0	4.2	2	S OF HONSHU	221
464	3/ 2/76	5.52.17	41.0	14.0	3.3	2	SOUTHERN ITALY	390
465	3/ 3/76	2.50.15	34.0	142.0	4.2	2	OEC HONSHU, JAPAN	229
466	3/ 3/76	13.30.12	51.0	158.0	3.8	2	KURILE ISLANDS	221
467	3/ 4/76	6.12.48	43.0	149.0	4.0	2	KURILE ISLANDS REG.	222
468	3/ 4/76	9.42.14	44.0	148.0	3.8	2	KURILE ISLANDS	221
469	3/ 4/76	17.57.16	55.0	161.0	4.1	2	NEAR E COAST KAMCHAT	218
470	3/ 4/76	18.45.39	33.0	76.0	3.7	3	EASTERN KASHMIR	302
471	3/ 4/76	22.23. 0	38.0	21.0	3.5	3	IONIAN SEA	399
472	3/ 4/76	23.57.49	49.0	156.0	3.7	2	KURILE ISLANDS	221
473	3/ 5/76	11.50.41	44.0	148.0	3.8	2	KURILE ISLANDS	221
474	3/ 5/76	20.49. 3	41.0	21.0	3.5	2	GREECE-ALBANIA BOR.	392
475	3/ 6/76	1.52.23	46.0	154.0	3.8	2	KURILE ISLANDS REG.	222
476	3/ 6/76	13.35.42	33.0	48.0	4.1	2	IRAN-IRAQ BORDER	346
477	3/ 6/76	16.35.43	35.0	27.0	3.7	3	CRETE	370
478	3/ 7/76	0.42.22	27.0	59.0	4.0	2	SOUTHERN IRAN	353
479	3/ 7/76	12.18.26	35.0	24.0	3.7	3	CRETE	370
480	3/ 7/76	21.53.52	40.0	19.0	3.4	3	ALBANIA	391

TABLE A-2

DATA BASE
(PAGE 13 OF 37)

EVNO	DATE	TIME	LAT.	LONG.	MB	Q	LOCATION	SUBREG
481	3/ 8/76	0.48.47	41.0	16.0	3.4	2	SOUTHERN ITALY	390
482	3/ 8/76	17. 3. 7	46.0	152.0	3.4	3	KURILE ISLANDS	221
483	3/ 9/76	5.26.47	38.0	21.0	2.9	3	IONIAN SEA	399
484	3/ 9/76	6.33.28	43.0	146.0	3.9	3	HOKKAIDO, JAPAN	224
485	3/ 9/76	14. 0.11	38.0	-116.0	5.4	1	NEVADA	37
486	3/ 9/76	17.36.26	33.0	47.0	3.7	2	IRAN-IRAQ BORDER REG	346
487	3/10/76	3.49.25	35.0	24.0	4.1	3	CRETE	370
488	3/10/76	4.39.12	28.0	58.0	4.1	2	SOUTHERN IRAN	353
489	3/10/76	7.51.49	38.0	21.0	3.3	3	IONIAN SEA	399
490	3/10/76	12.43. 3	44.0	150.0	4.4	2	KURILE ISLANDS	221
491	3/10/76	21. 6.56	45.0	151.0	3.9	2	KURILE ISLANDS REG.	222
492	3/10/76	22.30.49	55.0	161.0	3.6	2	NEC KAMCHATKA	218
493	3/11/76	0.32.51	28.0	91.0	4.6	1	TIBET	306
494	3/11/76	22.31.38	40.0	40.0	3.8	2	TURKEY	366
495	3/13/76	4.46. 7	37.0	21.0	3.5	2	SOUTHERN GREECE	368
496	3/13/76	9.31.40	39.0	48.0	3.9	2	NORTHWESTERN IRAN	345
497	3/13/76	11.27.20	35.0	27.0	3.7	3	CRETE	370
498	3/13/76	13.52.38	49.0	152.0	3.9	2	KURILE ISLANDS	221
499	3/14/76	7.57. 1	43.0	145.0	4.2	2	HOKKAIDO, JAPAN REG.	224
500	3/14/76	12.30. 6	38.0	-116.0	5.9	1	NEVADA	37
501	3/14/76	20.22.47	44.0	149.0	4.8	1	KURILE ISLANDS	221
502	3/14/76	21.53.25	28.0	58.0	3.5	3	SOUTHERN IRAN	353
503	3/14/76	23.54.10	51.0	158.0	3.4	3	KURILE ISLANDS	221
504	3/15/76	1.11.28	45.0	144.0	3.9	2	HOKKAIDO, JAPAN REG.	224
505	3/15/76	2.36.36	40.0	143.0	4.3	2	NEC HONSHU, JAPAN	228
506	3/15/76	3.57.23	42.0	142.0	4.3	2	HOKKAIDO, JAPAN REG.	224
507	3/15/76	7. 2.44	36.0	138.0	3.9	3	HONSHU, JAPAN	227
508	3/15/76	13.48.29	41.0	142.0	4.5	1	NEC HONSHU, JAPAN	228
509	3/15/76	20. 1.54	38.0	21.0	3.1	3	IONIAN SEA	399
510	3/16/76	4.55.54	25.0	93.0	3.8	3	BURMA-INDIA BOR. REG	294
511	3/16/76	5.18. 6	45.0	151.0	3.7	2	KURILE ISLANDS	221
512	3/16/76	6.19. 9	41.0	77.0	5.2	1	KIRGIZ-SINKIANG BOR.	320
513	3/16/76	8.42.50	41.0	77.0	3.6	3	KIRGIZ-SINKIANG BOR.	320
514	3/16/76	11.54.28	34.0	47.0	4.1	2	IRAN-IRAQ BOR REG	346
515	3/16/76	12.46.34	35.0	27.0	3.6	3	CRETE	370
516	3/16/76	14.15.58	38.0	21.0	3.0	3	IONIAN SEA	399
517	3/16/76	16.35. 8	28.0	55.0	4.1	2	SOUTHERN IRAN	353
518	3/16/76	17. 0.18	43.0	142.0	3.7	3	HOKKAIDO JAPAN REG	224
519	3/16/76	17.28.36	27.0	55.0	3.6	2	SOUTHERN IRAN	353
520	3/17/76	4.32.49	27.0	56.0	3.6	2	SOUTHERN IRAN	353

TABLE A-2

DATA BASE
(PAGE 14 OF 37)

EVNO	DATE	TIME	LAT.	LONG.	MB	Q	LOCATION	SUBREG
521	3/17/76	13.58.47	27.0	55.0	3.7	2	SOUTHERN IRAN	353
522	3/17/76	14.15. 4	38.0	-115.0	5.7	1	SOUTHERN NEVADA	41
523	3/17/76	14.45. 6	38.0	-116.0	5.6	1	NEVADA	37
524	3/18/76	4.27.18	39.0	23.0	3.1	3	AEGEAN SEA	365
525	3/18/76	5.56. 9	28.0	55.0	4.2	2	SOUTHERN IRAN	353
526	3/18/76	7.26.17	24.0	94.0	3.6	3	BURMA-INDIA BOR. REG	294
527	3/18/76	17.51.43	28.0	55.0	4.2	1	SOUTHERN IRAN	353
528	3/19/76	3.24. 2	28.0	54.0	3.5	3	SOUTHERN IRAN	353
529	3/19/76	3.31.26	37.0	87.0	4.1	1	S. SINKIANG PROV.	321
530	3/19/76	9. 3.57	37.0	83.0	3.7	3	SOUTHERN SINKIANG PR	321
531	3/19/76	11.49. 5	46.0	43.0	3.0	3	SOUTHWEST RUSSIA	357
532	3/19/76	13.48.25	27.0	55.0	3.6	2	SOUTHERN IRAN	353
533	3/19/76	17.12. 2	40.0	143.0	3.6	2	NEC HONSHU, JAPAN	228
534	3/19/76	17.42.50	39.0	74.0	3.2	3	S. SINKIANG PROV.	321
535	3/20/76	3.19.35	43.0	21.0	3.5	3	YUGOSLAVIA	383
536	3/20/76	3.31.10	39.0	15.0	2.8	3	SICILY	398
537	3/20/76	4. 3.33	49.0	79.0	4.8	2	EASTERN KAZAKH SSR	329
538	3/20/76	4.33.53	41.0	91.0	4.9	1	S. SINKIANG PROV.	321
539	3/20/76	4.53.26	20.0	95.0	4.2	2	BURMA	296
540	3/20/76	9.24. 3	28.0	55.0	4.6	1	SOUTHERN IRAN	353
541	3/21/76	10.32.20	42.0	146.0	4.7	1	OC HOKKAIDO, JAPAN	225
542	3/21/76	19.59.28	43.0	144.0	4.1	2	HOKKAIDO, JAPAN REG.	224
543	3/22/76	2.42.52	28.0	55.0	3.8	2	SOUTHERN IRAN	353
544	3/22/76	6.24. 5	28.0	55.0	3.9	2	SOUTHERN IRAN	353
545	3/22/76	8.13.35	28.0	55.0	3.7	3	SOUTHERN IRAN	353
546	3/22/76	9. 4.43	38.0	21.0	3.0	3	IONIAN SEA	399
547	3/22/76	11.50. 7	51.0	156.0	4.2	2	KURILE ISLANDS	221
548	3/22/76	19.50.23	47.0	154.0	4.5	1	KURILE ISLANDS	221
549	3/22/76	21.58.40	42.0	145.0	3.6	3	HOKKAIDO, JAPAN REG.	224
550	3/23/76	10. 8.12	38.0	143.0	4.1	2	NEC HONSHU, JAPAN	228
551	3/23/76	23.47. 4	44.0	150.0	4.1	2	KURILE ISLANDS	221
552	3/24/76	14.53. 8	51.0	160.0	4.5	2	OEC KAMCHATKA	219
553	3/24/76	21.14.59	30.0	53.0	3.8	2	SOUTHERN IRAN	353
554	3/25/76	1.48. 7	46.0	152.0	4.3	2	KURILE ISLANDS	221
555	3/25/76	11.54.27	34.0	48.0	4.4	3	WESTERN IRAN	347
556	3/25/76	22.29.48	35.0	27.0	3.7	3	CRETE	370
557	3/25/76	22.59. 6	43.0	141.0	3.8	3	HOKKAIDO JAPAN REG	224
558	3/27/76	0. 9.41	48.0	151.0	3.8	3	KURILE IS	221
559	3/28/76	4.20.47	41.0	21.0	3.1	3	GREECE-ALBANIA BOR	392
560	3/28/76	6.19. 9	38.0	139.0	4.1	3	HONSHU, JAPAN	227

TABLE A-2

DATA BASE
(PAGE 15 OF 37)

EVNO	DATE	TIME	LAT.	LONG.	MB	Q	LOCATION	SUBREG
561	3/28/76	8.48.51	41.0	81.0	4.7	2	SOUTHERN SINKIANG	321
562	3/28/76	16.49.40	39.0	140.0	4.2	2	HONSHU, JAPAN	227
563	3/28/76	22.20. 7	42.0	142.0	5.2	1	HOKKAIDO, JAPAN	224
564	3/29/76	6.59.50	46.0	48.0	4.5	2	SOUTHWESTERN RUSSIA	357
565	3/29/76	14.58.40	28.0	55.0	4.0	2	SOUTHERN IRAN	353
566	3/29/76	19.48.24	46.0	151.0	5.5	1	KURILE ISLANDS	221
567	3/29/76	21.59.25	34.0	49.0	3.8	3	WESTERN IRAN	347
568	3/30/76	3.32.44	41.0	143.0	4.3	2	NEC HONSHU, JAPAN	228
569	3/30/76	5.53.16	40.0	142.0	5.5	1	NEC HONSHU, JAPAN	228
570	3/30/76	5.56.16	40.0	142.0	4.9	2	NEAR E COAST HONSHU	228
571	3/30/76	6. 4.18	40.0	142.0	5.6	1	NEC HONSHU, JAPAN	228
572	3/30/76	6.48.27	24.0	94.0	4.3	2	BURMA-INDIA BOR. REG	294
573	3/30/76	7. 1.41	41.0	87.0	3.5	3	S SINKIANG PROV	321
574	3/30/76	7. 5.26	37.0	142.0	3.9	3	OFF E COAST HONSHU	229
575	3/30/76	9. 9.25	40.0	141.0	5.1	1	HONSHU, JAPAN	227
576	3/30/76	9.24.51	37.0	142.0	5.2	1	OEC HONSHU JAPAN	229
577	3/30/76	9.50.47	39.0	143.0	4.0	3	NEAR E COAST HONSHU	228
578	3/30/76	11.23.18	35.0	140.0	4.2	3	NEC HONSHU JAPAN	228
579	3/30/76	23.53. 2	39.0	142.0	4.3	3	NEC HONSHU, JAPAN	228
580	3/31/76	2.34.33	30.0	56.0	4.4	2	SOUTHERN IRAN	353
581	3/31/76	10.35.44	54.0	161.0	4.0	3	NEC KAMCHATKA	218
582	3/31/76	12.20.24	39.0	146.0	3.9	3	OFF E COAST HONSHU	229
583	3/31/76	13. 7.20	25.0	57.0	3.3	3	SOUTHERN IRAN	353
584	3/31/76	15.37.45	39.0	74.0	3.8	2	SOUTHERN SINKIANG PR	321
585	3/31/76	23.38.38	32.0	58.0	4.5	1	IRAN	348
586	4/ 2/76	1.42.22	31.0	51.0	3.8	2	IRAN	348
587	4/ 2/76	12.31.33	35.0	24.0	3.8	3	CRETE	370
588	4/ 2/76	16.25.52	43.0	149.0	3.8	2	KURILE IS	222
589	4/ 2/76	16.57.46	38.0	45.0	4.3	2	NW IRAN	345
590	4/ 2/76	17.52.55	44.0	41.0	4.1	2	WESTERN CAUCASUS	362
591	4/ 3/76	4.37. 8	39.0	15.0	3.4	3	SICILY	398
592	4/ 3/76	6.28.57	44.0	149.0	3.6	3	KURILE IS	221
593	4/ 3/76	9.50.55	43.0	37.0	3.0	3	BLACK SEA	360
594	4/ 4/76	7.25. 4	45.0	149.0	3.7	3	KURILE IS	221
595	4/ 4/76	7.31.26	42.0	146.0	3.9	2	FF COAST HOKKAIDO	225
596	4/ 4/76	21.15.39	40.0	142.0	4.7	1	NEAR E COAST HONSHU	228
597	4/ 5/76	16.54.31	39.0	114.0	5.0	2	NE CHINA	658
598	4/ 5/76	17.23.52	44.0	149.0	4.0	3	KURILE IS	221
599	4/ 5/76	20.25.22	32.0	48.0	3.5	3	WESTERN IRAN	347
600	4/ 6/76	9. 8.55	39.0	16.0	4.1	3	SOUTHERN ITALY	390

TABLE A-2

DATA BASE
(PAGE 16 OF 37)

EVNO	DATE	TIME	LAT.	LONG.	MB	Q	LOCATION	SUBREG
601	4/ 7/76	10.12.11	38.0	21.0	3.1	3	IONIAN SEA	399
602	4/ 7/76	19.41.54	43.0	149.0	3.8	3	KURILE IS REG	222
603	4/ 7/76	21.43.59	33.0	91.0	3.6	2	TSINGHAI PROV CHINA	325
604	4/ 7/76	22.58.19	25.0	95.0	3.9	2	BURMA-INDIA BOR REG	294
605	4/ 8/76	2.58.59	39.0	64.0	6.0	1	UZBEK SSR	339
606	4/ 8/76	3.23.55	41.0	63.0	3.8	2	UZBEK SSR	339
607	4/ 8/76	3.51.41	39.0	64.0	3.5	2	TURKMEN SSR	340
608	4/ 8/76	4.27.48	40.0	63.0	3.6	3	UZBEK SSR	339
609	4/ 8/76	4.59. 6	41.0	63.0	4.4	2	UZBEK SSR	339
610	4/ 8/76	7.47.45	40.0	140.0	3.9	3	HONSHU JAPAN	227
611	4/ 8/76	7.48.46	39.0	64.0	3.6	2	UZBEK SSR	339
612	4/ 8/76	12. 3.59	42.0	62.0	5.2	1	UZBEK SSR	339
613	4/ 8/76	14.41.23	40.0	64.0	3.7	3	UZBEK SSR	339
614	4/ 8/76	18.15.53	36.0	139.0	3.8	3	HONSHU JAPAN	227
615	4/ 8/76	22.54.11	39.0	64.0	4.0	2	UZBEK SSR	339
616	4/ 9/76	7.49.35	38.0	21.0	3.2	3	IONIAN SEA	399
617	4/ 9/76	11.21.39	31.0	50.0	3.7	3	IRAN	348
618	4/ 9/76	12. 1. 7	41.0	62.0	3.8	3	UZBEK SSR	339
619	4/ 9/76	12.42.20	36.0	141.0	4.1	3	NEAR E COAST HONSHU	228
620	4/ 9/76	16.34.29	38.0	21.0	3.3	3	IONIAN SEA	399
621	4/ 9/76	18.33.29	40.0	29.0	3.0	3	TURKEY	366
622	4/10/76	0.41.12	40.0	142.0	4.6	2	NEC HONSHU JAPAN	228
623	4/10/76	0.54.26	38.0	21.0	3.0	3	IONIAN SEA	399
624	4/10/76	1.33.26	40.0	146.0	4.1	3	OFF E C HONSHU JAPAN	229
625	4/10/76	1.41.46	40.0	143.0	5.0	2	NEAR E COAST HONSHU	228
626	4/10/76	7. 9.23	34.0	77.0	4.0	2	KASHMIR-INDIA BOR RE	303
627	4/10/76	7.25.36	39.0	144.0	4.8	2	OFF E COAST HONSHU	229
628	4/10/76	18. 2.51	31.0	75.0	3.7	3	NORTHERN INDIA	308
629	4/10/76	23.28.19	28.0	55.0	3.9	3	SOUTHERN IRAN	353
630	4/11/76	2.52.50	43.0	147.0	5.4	1	OFF COAST HOKKAIDO	225
631	4/11/76	16.20.48	40.0	29.0	3.3	3	TURKEY	366
632	4/11/76	18.49.17	31.0	50.0	4.0	3	WESTERN IRAN	347
633	4/11/76	18.59.48	39.0	65.0	3.6	3	TURKMEN SSR	340
634	4/11/76	20.57.30	36.0	74.0	4.1	2	NW KASHMIR	720
635	4/12/76	1. 5.21	40.0	29.0	3.2	3	TURKEY	366
636	4/12/76	3. 8.14	38.0	21.0	3.1	3	IONIAN SEA	399
637	4/12/76	6. 3.55	29.0	76.0	3.7	3	NORTHERN INDIA	308
638	4/12/76	14. 0.44	39.0	21.0	3.3	3	IONIAN SEA	399
639	4/12/76	16.12.51	39.0	64.0	3.9	2	UZBEK SSR	339
640	4/12/76	22.10.34	39.0	21.0	3.1	3	GREECE-ALBANIA BOR	392

TABLE A-2

DATA BASE
(PAGE 17 OF 37)

EVNO	DATE	TIME	LAT.	LONG.	MB	Q	LOCATION	SUBREG
641	4/12/76	23.16.44	31.0	76.0	3.5	2	NORTHERN INDIA	308
642	4/13/76	1.54.43	40.0	145.0	3.8	3	OFF E COAST HONSHU	229
643	4/13/76	3.21. 1	32.0	76.0	3.7	3	NORTHERN INDIA	308
644	4/13/76	7.26.12	47.0	154.0	5.1	1	KURILE IS	221
645	4/13/76	12.19.15	38.0	21.0	3.0	3	IONIAN SEA	399
646	4/13/76	22. 0.55	32.0	50.0	3.7	3	WESTERN IRAN	347
647	4/14/76	19.26.59	40.0	63.0	3.5	2	UZBEK SSR	339
648	4/15/76	6.15.13	39.0	64.0	4.1	2	UZBEK SSR	339
649	4/15/76	8.10. 2	39.0	63.0	3.4	3	TURKMEN SSR	340
650	4/15/76	12.19.49	35.0	24.0	3.5	2	CRETE	370
651	4/15/76	12.41.22	53.0	158.0	4.5	2	NEAR E C KAMCHATKA	218
652	4/15/76	18.51. 7	41.0	34.0	3.5	3	TURKEY	366
653	4/15/76	19.35.52	35.0	24.0	3.7	3	CRETE	370
654	4/15/76	22. 1. 7	38.0	21.0	2.9	3	IONIAN SEA	399
655	4/16/76	0.39. 4	36.0	51.0	3.2	3	IRAN	348
656	4/16/76	2.36.37	39.0	64.0	3.8	2	TURKMEN SSR	340
657	4/16/76	8.15. 6	44.0	38.0	3.0	3	BLACK SEA	360
658	4/16/76	15.17.13	35.0	27.0	3.8	3	CRETE	370
659	4/16/76	17. 7. 1	40.0	144.0	4.6	2	OFF E COAST HONSHU	229
660	4/16/76	20.15.20	34.0	75.0	3.5	3	EASTERN KASHMIR	302
661	4/16/76	21.20.40	55.0	163.0	4.3	2	OFF E COAST KAMCHATK	219
662	4/16/76	23.22.30	33.0	57.0	3.8	2	IRAN	348
663	4/17/76	3.28. 8	43.0	149.0	4.2	2	KURILE IS REG	222
664	4/17/76	5. 5.45	45.0	149.0	4.0	3	KURILE IS REG	221
665	4/17/76	12.11. 0	39.0	65.0	4.0	2	TURKMEN SSR	340
666	4/17/76	13.47.49	39.0	64.0	3.9	3	UZBEK SSR	339
667	4/18/76	5.13. 8	46.0	151.0	4.2	3	KURILE IS	221
668	4/18/76	14.20.29	44.0	148.0	3.9	3	KURILE IS	221
669	4/19/76	8.12.52	43.0	149.0	4.1	2	KURILE IS REG	222
670	4/19/76	10.50.58	40.0	143.0	5.4	1	NEAR E COAST HONSHU	228
671	4/19/76	13.58.24	40.0	142.0	4.2	1	NEAR E COAST HONSHU	228
672	4/19/76	15.32. 5	32.0	49.0	3.8	3	WESTERN IRAN	347
673	4/20/76	9.27.51	48.0	154.0	5.1	1	KURILE IS	221
674	4/20/76	20.23.45	44.0	148.0	4.2	2	KURILE IS	221
675	4/21/76	4.57.48	49.0	80.0	4.9	1	EASTERN KAZAKH SSR	329
676	4/21/76	5. 2.49	49.0	80.0	5.4	1	EASTERN KAZAKH SSR	329
677	4/21/76	14.41.49	41.0	62.0	4.9	1	UZBEK SSR	339
678	4/21/76	17.16.49	39.0	21.0	3.6	3	IONIAN SEA	399
679	4/21/76	20. 0.28	45.0	22.0	3.8	3	YUGOSLAVIA	383
680	4/21/76	21.57.35	38.0	45.0	4.1	3	TURKEY-IRAN BOR REG	343

TABLE A-2

DATA BASE
(PAGE 18 OF 37)

EVNO	DATE	TIME	LAT.	LONG.	MB	Q	LOCATION	SUBREG
681	4/21/76	22. 8.36	30.0	86.0	3.9	3	TIBET	306
682	4/21/76	23.18.27	39.0	64.0	4.0	2	UZBEK SSR	339
683	4/22/76	0. 7.38	21.0	94.0	3.7	3	BURMA	296
684	4/22/76	0.58. 3	38.0	21.0	3.4	3	IONIAN SEA	399
685	4/22/76	14.43. 7	39.0	52.0	3.3	3	CASPIAN SEA	338
686	4/22/76	16.22.39	52.0	162.0	3.9	3	OFF E COAST KAMCHATK	219
687	4/22/76	19. 0.14	38.0	101.0	3.6	3	TSINGHAI PROVINCE CH	325
688	4/23/76	3.14.22	32.0	49.0	4.1	2	WESTERN IRAN	347
689	4/23/76	4.23.29	35.0	27.0	3.1	3	CRETE	370
690	4/23/76	5.59.36	40.0	29.0	2.8	3	TURKEY	366
691	4/23/76	9.35.45	43.0	146.0	4.3	2	HOKKAIDO JAPAN REG	224
692	4/23/76	20.55.45	41.0	62.0	4.4	1	UZBEK SSR	339
693	4/23/76	23.45.17	25.0	93.0	3.7	2	BURMA-INDIA BOR REG	294
694	4/24/76	1.23.49	38.0	21.0	3.0	3	IONIAN SEA	399
695	4/24/76	1.25.14	34.0	142.0	4.8	2	OFF E COAST HONSHU	229
696	4/24/76	5.30.57	31.0	51.0	3.8	3	IRAN	348
697	4/24/76	10.19.48	28.0	56.0	4.2	2	SOUTHERN IRAN	353
698	4/24/76	10.48.27	41.0	53.0	3.5	3	UZBEK SSR	339
699	4/24/76	18.15. 7	42.0	123.0	3.9	2	NE CHINA	658
700	4/25/76	12.31.45	32.0	48.0	3.3	3	WESTERN IRAN	347
701	4/26/76	4.57.41	30.0	51.0	5.0	2	IRAN	348
702	4/26/76	7.13.39	27.0	93.0	3.9	2	EASTERN INDIA	317
703	4/26/76	22.42.24	39.0	24.0	3.5	3	AEGEAN SEA	365
704	4/27/76	16.35.52	43.0	146.0	4.4	2	HOKKAIDO JAP REG	224
705	4/27/76	16.40.19	38.0	21.0	2.7	3	IONIAN SEA	399
706	4/28/76	23.22.20	39.0	65.0	3.6	3	TURKMEN SSR	340
707	4/29/76	14.41.36	41.0	79.0	3.7	2	KIRGIZ-SINKIANG BOR	320
708	4/29/76	18. 3.58	39.0	142.0	4.1	3	NEAR E COAST HONSHU	228
709	4/29/76	18.21.56	36.0	141.0	4.1	3	NEAR E COAST HONSHU	228
710	4/29/76	22.44.18	46.0	34.0	3.0	2	CRIMEA REG	361
711	4/29/76	23.59.30	36.0	74.0	3.7	3	NW KASHMIR	720
712	4/30/76	6.11. 9	53.0	159.0	3.7	3	NEAR E COAST KAMCHAT	218
713	4/30/76	12.49.33	45.0	149.0	4.0	2	KURILE IS	221
714	4/30/76	16. 9.11	35.0	27.0	4.1	3	CRETE	370
715	5/ 1/76	8.28.59	34.0	80.0	3.7	3	TIBET	306
716	5/ 1/76	11.35.33	38.0	89.0	4.1	2	S. SINKIANG PROV.	321
717	5/ 1/76	15.30.10	32.0	62.0	3.8	3	SW AFGHANISTAN	350
718	5/ 1/76	19.34.12	41.0	142.0	4.9	1	NEC HONSHU, JAPAN	228
719	5/ 2/76	0.25.29	35.0	27.0	3.5	3	CRETE	370
720	5/ 2/76	15.20.25	50.0	155.0	4.1	2	KURILE ISLANDS	221

TABLE A-2

DATA BASE

(PAGE 19 CF 37)

EVNO	DATE	TIME	LAT.	LONG.	MB	Q	LOCATION	SUBREG
721	5/ 2/76	15.41.30	39.0	64.0	3.6	3	UZBEK SSR	339
722	5/ 2/76	16.37.30	53.0	158.0	3.7	3	NEC KAMCHATKA	218
723	5/ 2/76	16.57.26	30.0	51.0	4.1	2	IRAN	348
724	5/ 3/76	11. 3.29	40.0	76.0	3.7	2	KIRGIZ-SINKIANG BOR.	320
725	5/ 4/76	3.39.39	47.0	154.0	4.2	1	KURILE ISLANDS	221
726	5/ 4/76	5.23. 9	32.0	50.0	3.5	2	WESTERN IRAN	347
727	5/ 4/76	6. 1.51	29.0	98.0	4.3	2	TIBET	306
728	5/ 4/76	7. 5.11	27.0	81.0	3.5	2	NORTHERN INDIA	308
729	5/ 5/76	10. 2.36	42.0	141.0	3.8	3	HOKKAIDO, JAPAN REG.	224
730	5/ 5/76	13.26.18	45.0	149.0	4.6	1	KURILE ISLANDS	221
731	5/ 5/76	16.13.22	44.0	146.0	3.5	3	HOKKAIDO, JAPAN REG.	224
732	5/ 6/76	8.21.35	31.0	77.0	4.2	2	NORTHERN INDIA	308
733	5/ 6/76	11.13. 2	44.0	149.0	4.0	2	KURILE ISLANDS	221
734	5/ 6/76	16.53.20	43.0	80.0	4.2	2	KIRGIZ-SINKIANG BOR.	320
735	5/ 6/76	17.42.43	44.0	147.0	4.7	1	KURILE ISLANDS	221
736	5/ 6/76	17.59. 4	35.0	24.0	4.7	2	CRETE	370
737	5/ 6/76	20.36. 7	39.0	64.0	3.8	2	UZBEK SSR	339
738	5/ 7/76	0.10.42	39.0	64.0	4.5	1	UZBEK SSR	339
739	5/ 7/76	2. 9.54	43.0	140.0	4.0	2	HOKKAIDO, JAPAN REG.	224
740	5/ 7/76	4.34.20	48.0	154.0	3.9	2	KURILE ISLANDS	221
741	5/ 7/76	18. 2.53	32.0	78.0	3.8	3	KASHMIR-TIBET BOR.	304
742	5/ 7/76	23. 5.23	40.0	29.0	3.6	3	TURKEY	366
743	5/ 9/76	2.55.58	40.0	30.0	3.8	3	TURKEY	366
744	5/ 9/76	5.53.45	36.0	22.0	3.6	3	MEDITERRANEAN SEA	400
745	5/ 9/76	7.51.25	41.0	63.0	5.0	2	UZBEK SSR	339
746	5/ 9/76	8.13. 4	45.0	149.0	3.5	3	KURILE ISLANDS	221
747	5/ 9/76	11.19.47	40.0	30.0	4.0	3	TURKEY	366
748	5/ 9/76	13.14.27	35.0	140.0	4.2	2	NEC HONSHU, JAPAN	228
749	5/ 9/76	15. 1.25	40.0	30.0	4.1	2	TURKEY	366
750	5/ 9/76	15.30.25	46.0	150.0	3.6	2	KURILE ISLANDS	221
751	5/ 9/76	20.11. 8	40.0	30.0	3.3	3	TURKEY	366
752	5/ 9/76	22. 5.17	46.0	35.0	2.6	3	CRIMEA REGION	361
753	5/10/76	4.34.31	39.0	19.0	3.5	3	GREECE-ALBANIA BOR.	392
754	5/10/76	8.14.56	39.0	15.0	3.3	2	SICILY	398
755	5/10/76	12. 1.38	40.0	29.0	4.2	3	TURKEY	366
756	5/10/76	15.20.49	39.0	30.0	4.2	2	TURKEY	366
757	5/10/76	18.37.24	29.0	82.0	4.0	3	NEPAL	310
758	5/10/76	18.43.40	28.0	83.0	5.0	2	NEPAL-INDIA BOR.	309
759	5/10/76	23.34.15	46.0	36.0	2.8	3	SOUTHWESTERN RUSSIA	357
760	5/10/76	23.54.14	40.0	30.0	4.3	2	TURKEY	366

TABLE A-2

DATA BASE
(PAGE 20 OF 37)

EVNO	DATE	TIME	LAT.	LONG.	MB	Q	LOCATION	SUBREG
761	5/11/76	3. 2. 3	30.0	81.0	3.4	3	NEPAL	310
762	5/11/76	3.32. 8	40.0	30.0	4.2	3	TURKEY	366
763	5/11/76	4. 4.16	36.0	141.0	4.1	2	NEC HONSHU, JAPAN	228
764	5/11/76	7.14.13	33.0	53.0	3.9	3	IRAN	348
765	5/11/76	13.26.51	45.0	149.0	4.2	2	KURILE ISLANDS	221
766	5/11/76	17. 0.23	41.0	21.0	5.5	2	GREECE-ALBANIA BOR.	392
767	5/11/76	17. 9.55	36.0	22.0	5.2	2	MEDITERRANEAN SEA	400
768	5/11/76	19.25. 0	32.0	49.0	3.4	3	WESTERN IRAN	347
769	5/11/76	21.11.51	36.0	22.0	4.0	3	MEDITERRANEAN SEA	400
770	5/12/76	5.11.49	40.0	30.0	4.1	2	TURKEY	366
771	5/12/76	5.26.16	38.0	21.0	3.2	3	IONIAN SEA	399
772	5/12/76	16.45.40	52.0	160.0	4.1	2	OBC KAMCHATKA	219
773	5/12/76	18. 5.20	38.0	21.0	2.9	3	IONIAN SEA	399
774	5/12/76	18.40.15	42.0	146.0	4.4	2	OC HOKKAIDO, JAPAN	225
775	5/13/76	0.44.48	43.0	20.0	4.0	2	YUGOSLAVIA	383
776	5/13/76	9.50.10	44.0	149.0	3.9	2	KURILE ISLANDS	221
777	5/13/76	11. 0. 8	36.0	140.0	3.8	3	HONSHU, JAPAN	227
778	5/13/76	13.18.29	40.0	30.0	3.5	3	TURKEY	366
779	5/13/76	14.47.34	36.0	22.0	3.5	3	MEDITERRANEAN SEA	400
780	5/13/76	19.23. 1	38.0	21.0	2.8	3	IONIAN SEA	399
781	5/13/76	20.28.46	35.0	140.0	4.5	2	NEC HONSHU, JAPAN	228
782	5/13/76	20.44.32	35.0	24.0	4.2	2	CRETE	370
783	5/13/76	21.13. 5	38.0	21.0	3.1	3	IONIAN SEA	399
784	5/13/76	22.17.48	36.0	22.0	4.0	2	MEDITERRANEAN SEA	400
785	5/13/76	23.17.21	40.0	143.0	3.8	2	NEC HONSHU, JAPAN	228
786	5/14/76	1.23.17	38.0	32.0	3.5	3	TURKEY	366
787	5/14/76	11. 6.17	39.0	30.0	3.9	3	TURKEY	366
788	5/14/76	16. 1.30	43.0	149.0	4.2	2	KURILE ISLANDS REG.	222
789	5/14/76	20.24.53	39.0	142.0	3.9	3	NEC HONSHU, JAPAN	228
790	5/14/76	20.40.13	41.0	144.0	5.2	1	HOKKAIDO, JAPAN	224
791	5/14/76	22.27.54	40.0	143.0	3.9	2	NEC HONSHU, JAPAN	228
792	5/15/76	3. 3.25	35.0	24.0	4.2	2	CRETE	370
793	5/15/76	4.24. 3	35.0	27.0	3.5	3	CRETE	370
794	5/15/76	6.55.54	24.0	94.0	3.5	3	BURMA-INDIA BOR.	294
795	5/15/76	8.11.59	19.0	95.0	4.8	1	BURMA	296
796	5/15/76	11. 6. 6	40.0	30.0	3.4	2	TURKEY	366
797	5/15/76	19.12.28	38.0	21.0	2.8	3	IONIAN SEA	399
798	5/15/76	22.23.29	42.0	141.0	3.7	3	HOKKAIDO, JAPAN REG.	224
799	5/15/76	23. 6.23	38.0	144.0	3.8	3	OEC HONSHU, JAPAN	229
800	5/16/76	8. 1.16	36.0	51.0	3.7	2	IRAN	348

TABLE A-2

DATA BASE
(PAGE 21 OF 37)

EVNO	DATE	TIME	LAT.	LONG.	MB	Q	LOCATION	SUBREG
801	5/16/76	15.40.36	36.0	74.0	3.5	3	NORTHWESTERN KASHMIR	720
802	5/16/76	20.25.16	48.0	154.0	4.2	2	KURILE ISLANDS	221
803	5/17/76	2.58.35	39.0	64.0	6.5	1	UZBEK SSR	339
804	5/17/76	3.21.30	39.0	64.0	4.3	2	UZBEK SSR	339
805	5/17/76	3.29.14	39.0	64.0	4.1	2	UZBEK SSR	339
806	5/17/76	3.57.25	41.0	62.0	4.1	2	TURKMEN SSR	340
807	5/17/76	4.14.26	42.0	62.0	4.4	2	UZBEK SSR	339
808	5/17/76	4.34.33	39.0	65.0	3.5	2	TURKMEN SSR	340
809	5/17/76	4.54.15	42.0	61.0	4.7	2	TURKMEN SSR	340
810	5/17/76	5.53.10	39.0	64.0	4.0	2	UZBEK SSR	339
811	5/17/76	6. 6.32	39.0	64.0	3.2	3	TURKMEN SSR	340
812	5/17/76	6.37. 8	41.0	61.0	3.8	2	UZBEK SSR	339
813	5/17/76	6.58.11	39.0	64.0	3.9	2	UZBEK SSR	339
814	5/17/76	7.20. 3	41.0	63.0	3.6	3	UZBEK SSR	339
815	5/17/76	8.10.26	39.0	64.0	3.8	2	TURKMEN SSR	340
816	5/17/76	10.44.12	41.0	63.0	3.4	2	UZBEK SSR	339
817	5/17/76	11. 1.36	41.0	62.0	4.0	2	UZBEK SSR	339
818	5/17/76	15.39.16	40.0	30.0	3.7	3	TURKEY	366
819	5/17/76	16.11.36	38.0	21.0	3.7	3	IONIAN SEA	399
820	5/17/76	16.38.10	41.0	63.0	3.2	3	UZBEK SSR	339
821	5/17/76	17.46.18	40.0	64.0	4.7	2	UZBEK SSR	339
822	5/17/76	20.18.24	42.0	62.0	3.5	3	UZBEK SSR	339
823	5/17/76	21.52.28	41.0	62.0	3.7	2	UZBEK SSR	339
824	5/17/76	22.18.25	56.0	162.0	4.8	1	NEC KAMCHATKA	218
825	5/18/76	5.35.37	43.0	61.0	3.4	3	UZBEK SSR	339
826	5/18/76	7.59.41	35.0	27.0	3.3	3	CRETE	370
827	5/18/76	8.30.14	35.0	27.0	4.2	3	CRETE	370
828	5/18/76	8.57.37	41.0	63.0	4.6	1	UZBEK SSR	339
829	5/18/76	13.54.33	41.0	62.0	4.8	1	TURKMEN SSR	340
830	5/18/76	16.15.50	38.0	21.0	3.5	3	IONIAN SEA	399
831	5/18/76	17. 7.51	38.0	21.0	2.8	3	IONIAN SEA	399
832	5/18/76	20.11.39	39.0	64.0	3.7	2	TURKMEN SSR	340
833	5/18/76	20.22. 2	39.0	64.0	3.6	2	UZBEK SSR	339
834	5/18/76	20.24.29	39.0	145.0	3.6	3	OEC HONSHU, JAPAN	229
835	5/18/76	22.48.47	39.0	64.0	3.4	2	TURKMEN SSR	340
836	5/18/76	23. 9.47	36.0	22.0	3.5	3	MEDITERRANEAN SEA	400
837	5/19/76	1.11.12	39.0	64.0	4.2	1	UZBEK SSR	339
838	5/19/76	2.26. 9	41.0	63.0	3.5	3	UZBEK SSR	339
839	5/19/76	2.56.48	49.0	80.0	4.6	1	EASTERN KAZAKH SSR	329
840	5/19/76	7.30.16	39.0	65.0	3.6	3	TURKMEN SSR	340

TABLE A-2

DATA BASE
(PAGE 22 OF 37)

EVNO	DATE	TIME	LAT.	LONG.	MB	Q	LOCATION	SUBREG
841	5/19/76	15.54.54	41.0	62.0	4.8	1	TURKMEN SSR	340
842	5/19/76	16.44. 9	38.0	21.0	3.0	3	IONIAN SEA	399
843	5/20/76	6.43.33	33.0	55.0	3.9	2	IRAN	348
844	5/20/76	11.37.15	39.0	64.0	3.9	2	UZBEK SSR	339
845	5/20/76	19.42.40	46.0	152.0	4.3	2	KURILE ISLANDS	221
846	5/20/76	22. 4.24	45.0	149.0	3.9	2	KURILE ISLANDS	221
847	5/21/76	0.50.41	51.0	155.0	3.7	3	KURILE ISLANDS	221
848	5/21/76	4.33.38	41.0	63.0	3.4	3	UZBEK SSR	339
849	5/21/76	13. 0.18	37.0	140.0	3.6	3	HONSHU, JAPAN	227
850	5/21/76	16. 5.21	39.0	64.0	4.2	1	UZBEK SSR	339
851	5/21/76	18.28.50	39.0	64.0	3.9	2	UZBEK SSR	339
852	5/22/76	18. 2. 8	40.0	29.0	3.9	3	TURKEY	366
853	5/22/76	18.32.36	31.0	76.0	3.8	2	NORTHERN INDIA	308
854	5/22/76	18.51.11	46.0	148.0	3.8	2	KURILE ISLANDS	221
855	5/23/76	3.53.50	39.0	30.0	3.6	3	TURKEY	366
856	5/23/76	9.20.52	38.0	21.0	2.8	3	IONIAN SEA	399
857	5/23/76	9.49.10	39.0	64.0	4.0	2	UZBEK SSR	339
858	5/23/76	10.58.33	40.0	143.0	4.1	2	NEC HONSHU, JAPAN	228
859	5/23/76	13.26.48	39.0	64.0	3.4	2	UZBEK SSR	339
860	5/24/76	6.10.46	39.0	64.0	3.8	2	UZBEK SSR	339
861	5/24/76	6.49.44	47.0	152.0	3.8	3	KURILE ISLANDS	221
862	5/24/76	14.56.25	41.0	62.0	4.3	2	UZBEK SSR	339
863	5/24/76	17.52. 7	44.0	12.0	3.7	3	CENTRAL ITALY	381
864	5/25/76	4.48.49	27.0	94.0	4.6	1	EASTERN INDIA	317
865	5/25/76	7.29.11	44.0	148.0	3.6	3	KURILE ISLANDS	221
866	5/25/76	8. 9.17	53.0	158.0	5.5	1	NEC KAMCHATKA	218
867	5/25/76	8.16.53	53.0	158.0	5.7	1	NEC KAMCHATKA	218
868	5/25/76	10.53.16	53.0	158.0	4.0	2	NEC KAMCHATKA	218
869	5/25/76	11. 9.42	50.0	158.0	4.6	2	KURILE ISLANDS	221
870	5/25/76	11.17. 3	52.0	160.0	3.9	2	OEC KAMCHATKA	219
871	5/25/76	12.12.42	32.0	50.0	3.4	3	WESTERN IRAN	347
872	5/25/76	15.34.20	51.0	158.0	4.1	2	KURILE ISLANDS	221
873	5/25/76	18.43.25	39.0	30.0	4.6	2	TURKEY	366
874	5/27/76	2.19.49	31.0	83.0	3.6	3	TIBET	306
875	5/27/76	6.44.14	40.0	64.0	3.7	2	UZBEK SSR	339
876	5/28/76	3.36.43	36.0	139.0	3.9	2	HONSHU, JAPAN	227
877	5/28/76	14. 5.30	39.0	64.0	4.8	1	UZBEK SSR	339
878	5/28/76	23. 2.19	39.0	30.0	4.4	2	TURKEY	366
879	5/28/76	23. 9.54	43.0	36.0	3.2	3	BLACK SEA	360
880	5/29/76	1.59. 9	35.0	140.0	3.7	3	NEC HONSHU, JAPAN	228

TABLE A-2

DATA BASE
(PAGE 23 OF 37)

EVNO	DATE	TIME	LAT.	LONG.	MB	Q	LOCATION	SUBREG
881	5/29/76	3.45.33	39.0	30.0	3.9	2	TURKEY	366
882	5/29/76	8.38.22	39.0	114.0	3.7	3	NORTHEASTERN CHINA	658
883	5/29/76	10.21.13	38.0	21.0	2.8	3	IONIAN SEA	399
884	5/29/76	11.42.47	56.0	162.0	3.7	3	NEC KAMCHATKA	218
885	5/29/76	11.58.39	27.0	97.0	4.7	1	BURMA	296
886	5/29/76	12.23.13	24.0	100.0	5.7	1	BURMA-CHINA BORDER	297
887	5/29/76	12.35.36	28.0	96.0	4.2	2	INDIA-CHINA BORDER	313
888	5/29/76	12.59. 5	25.0	97.0	3.8	3	BURMA-CHINA BORDER	297
889	5/29/76	13.55.51	28.0	96.0	4.0	3	INDIA-CHINA BORDER	313
890	5/29/76	14. 0.16	24.0	99.0	6.2	1	BURMA-CHINA BORDER	297
891	5/29/76	14.11.14	28.0	96.0	3.8	3	INDIA-CHINA BORDER	313
892	5/29/76	14.28.32	28.0	96.0	3.7	3	INDIA-CHINA BORDER	313
893	5/29/76	14.32. 7	27.0	97.0	4.7	2	BURMA	296
894	5/29/76	14.53.10	26.0	98.0	4.4	2	BURMA-CHINA BORDER	297
895	5/29/76	15. 3. 9	28.0	95.0	3.7	3	INDIA-CHINA BORDER	313
896	5/29/76	15.26.15	40.0	30.0	3.4	3	TURKEY	366
897	5/29/76	16. 5.44	24.0	98.0	3.8	3	BURMA-CHINA BORDER	297
898	5/29/76	17. 9.15	27.0	97.0	3.8	3	BURMA	296
899	5/29/76	18.25.53	31.0	77.0	3.2	3	NORTHERN INDIA	308
900	5/29/76	19.37.25	28.0	96.0	5.1	2	INDIA-CHINA BORDER	313
901	5/29/76	21.57.13	41.0	20.0	3.2	3	GREECE-ALBANIA BOR.	392
902	5/29/76	22. 5.19	35.0	24.0	3.5	2	CRETE	370
903	5/29/76	23.12.11	37.0	140.0	4.3	2	HONSHU, JAPAN	227
904	5/29/76	23.31.29	25.0	99.0	3.8	3	YUNNAN PROV. CHINA	318
905	5/30/76	0.40.12	28.0	99.0	3.9	3	BURMA-CHINA BORDER	297
906	5/30/76	3.15.19	39.0	64.0	3.4	3	UZBEK SSR	339
907	5/30/76	4.19. 4	27.0	97.0	4.9	2	BURMA	296
908	5/30/76	4.53.52	43.0	17.0	3.1	3	ADRIATIC SEA	382
909	5/30/76	5.32.34	34.0	47.0	3.7	2	WESTERN IRAN	347
910	5/30/76	8. 1.48	52.0	160.0	4.0	1	OEC KAMCHATKA	219
911	5/30/76	13.11.47	53.0	157.0	4.3	1	KAMCHATKA	217
912	5/30/76	13.46.11	41.0	21.0	3.3	2	GREECE-ALBANIA BOR.	392
913	5/30/76	16.27.21	41.0	21.0	3.2	2	GREECE-ALBANIA BOR.	392
914	5/30/76	17.31.18	34.0	48.0	3.3	3	WESTERN IRAN	347
915	5/30/76	19.43.39	25.0	97.0	3.7	3	BURMA-CHINA BORDER	297
916	5/30/76	21.12.43	43.0	13.0	3.2	3	CENTRAL ITALY	381
917	5/30/76	22.16.20	41.0	77.0	3.8	3	KIRGIZ-SINKIANG BOR.	320
918	5/30/76	22.31.31	24.0	98.0	4.4	1	BURMA-CHINA BORDER	297
919	5/31/76	4.57.10	36.0	51.0	3.9	3	IRAN	348
920	5/31/76	5. 8.35	25.0	99.0	5.3	1	YUNNAN PROV. CHINA	318

TABLE A-2

DATA BASE
(PAGE 24 OF 37)

EVNO	DATE	TIME	LAT.	LONG.	MB	Q	LOCATION	SUBREG
921	5/31/76	8. 6. 7	32.0	61.0	4.6	2	IRAN	348
922	5/31/76	13.17.19	47.0	154.0	4.6	1	KURILE ISLANDS	221
923	5/31/76	18.35.35	28.0	96.0	5.1	2	INDIA-CHINA BORDER	313
924	5/31/76	20.31.48	38.0	21.0	3.1	3	IONIAN SEA	399
925	5/31/76	20.51.38	43.0	150.0	3.6	3	KURILE ISLANDS REG.	222
926	6/ 1/76	1.37.41	40.0	29.0	2.8	3	TURKEY	366
927	6/ 1/76	1.59. 2	27.0	97.0	3.9	3	BURMA	296
928	6/ 1/76	10.59.16	28.0	94.0	4.9	1	INDIA-CHINA BORDER	313
929	6/ 1/76	20.39.35	27.0	97.0	4.0	3	BURMA	296
930	6/ 2/76	5.49.27	41.0	142.0	5.1	1	NEC HONSHU JAPAN	228
931	6/ 2/76	16.28.29	38.0	21.0	2.9	3	IONIAN SEA	399
932	6/ 2/76	18. 5. 3	30.0	51.0	4.1	1	IRAN	348
933	6/ 2/76	21.58.49	48.0	24.0	3.1	3	RUMANIA	358
934	6/ 3/76	18. 5.14	24.0	98.0	4.5	3	BURMA-CHINA BORDER	297
935	6/ 3/76	21.36.54	40.0	30.0	3.8	3	TURKEY	366
936	6/ 4/76	5. 7.48	35.0	48.0	3.5	3	WESTERN IRAN	347
937	6/ 4/76	5.26.59	39.0	142.0	3.9	2	NEC HONSHU JAPAN	228
938	6/ 4/76	5.44.52	38.0	21.0	3.0	3	IONIAN SEA	399
939	6/ 4/76	6.28.50	41.0	21.0	3.6	2	GREECE-ALBANIA BORDE	392
940	6/ 4/76	9.23.45	47.0	43.0	3.0	3	SW RUSSIA	357
941	6/ 4/76	11.13.26	41.0	143.0	4.3	2	NEC HONSHU JAPAN	228
942	6/ 5/76	10.46.24	28.0	95.0	3.9	2	INDIA-CHINA BORDER	313
943	6/ 5/76	14.21.29	41.0	21.0	3.6	2	GREECE-ALBANIA BOR	392
944	6/ 5/76	20.30.38	41.0	21.0	3.7	2	GREECE-ALBANIA BOR	392
945	6/ 5/76	22.22.27	41.0	21.0	3.9	2	GREECE-ALBANIA BOR	392
946	6/ 6/76	13.51.44	47.0	154.0	4.1	2	KURILE IS	221
947	6/ 6/76	14. 1.13	35.0	140.0	5.0	1	NSC HONSHU JAPAN	230
948	6/ 6/76	14. 6.59	38.0	21.0	3.1	3	IONIAN SEA	399
949	6/ 6/76	14.43.53	38.0	21.0	3.9	2	IONIAN SEA	399
950	6/ 7/76	4.31.41	39.0	74.0	3.7	3	S SINKIANG PROV	321
951	6/ 7/76	10.45.49	38.0	21.0	2.7	3	IONIAN SEA	399
952	6/ 7/76	11.59.30	39.0	64.0	3.7	2	TURKMEN SSR	340
953	6/ 8/76	7.37.22	27.0	94.0	3.7	3	EASTERN INDIA	317
954	6/ 8/76	18.33.43	38.0	21.0	3.6	2	IONIAN SEA	399
955	6/ 8/76	22.31.31	33.0	88.0	4.0	3	TIBET	306
956	6/ 8/76	23.15. 6	28.0	96.0	4.3	2	INDIA-CHINA BORDER	313
957	6/ 9/76	0.20.56	27.0	97.0	5.7	1	BURMA	296
958	6/ 9/76	3. 2.48	50.0	81.0	5.3	1	EASTERN KAZAKH SSR	329
959	6/ 9/76	10. 2.42	40.0	29.0	4.4	2	TURKEY	366
960	6/ 9/76	17.41.14	31.0	96.0	4.2	3	TIBET	306

TABLE A-2

DATA BASE
(PAGE 25 OF 37)

EVNO	DATE	TIME	LAT.	LONG.	MB	Q	LOCATION	SUBREG
961	6/ 9/76	18.47.49	43.0	13.0	3.7	3	CENTRAL ITALY	381
962	6/ 9/76	20.58.54	40.0	64.0	3.6	2	UZBEK SSR	339
963	6/ 9/76	23.41.27	38.0	21.0	2.8	3	IONIAN SEA	399
964	6/10/76	0.38.30	27.0	94.0	3.6	3	EASTERN INDIA	317
965	6/10/76	5.55.12	35.0	24.0	3.9	2	CRETE	370
966	6/11/76	0.52.44	40.0	30.0	3.7	2	TURKEY	366
967	6/11/76	5. 8.50	40.0	76.0	4.6	1	KIRGIZ-SINKIANG BOR	320
968	6/11/76	9. 7.54	47.0	42.0	3.1	3	SW RUSSIA	357
969	6/11/76	9.55.19	39.0	30.0	3.8	3	TURKEY	366
970	6/11/76	10. 5.31	39.0	30.0	3.4	3	TURKEY	366
971	6/11/76	10.25.56	38.0	21.0	2.7	3	IONIAN SEA	399
972	6/11/76	18.27. 0	43.0	17.0	3.9	2	ADRIATIC SEA	382
973	6/12/76	0.11.49	37.0	21.0	2.8	3	MEDITERRANEAN SEA	400
974	6/12/76	0.59.28	38.0	22.0	5.3	2	GREECE	364
975	6/12/76	2.41.16	35.0	24.0	3.8	2	CRETE	370
976	6/12/76	3.41.37	37.0	22.0	3.8	3	SOUTHERN GREECE	368
977	6/12/76	4.55.26	41.0	21.0	4.0	2	GREECE-ALBANIA BOR	392
978	6/12/76	10.25.33	41.0	20.0	3.5	2	ALBANIA	391
979	6/13/76	0.20.24	40.0	19.0	3.9	2	GREECE-ALBANIA BOR	392
980	6/13/76	1.42.41	41.0	63.0	3.6	3	UZBEK SSR	339
981	6/13/76	8.25. 7	29.0	86.0	3.8	3	TIBET	306
982	6/13/76	11.47. 2	32.0	85.0	3.8	3	TIBET	306
983	6/13/76	16.34. 0	35.0	139.0	3.8	2	HONSHU JAPAN	227
984	6/13/76	16.54.17	27.0	57.0	3.6	3	SOUTHERN IRAN	353
985	6/13/76	17.20.39	38.0	21.0	3.1	3	IONIAN SEA	399
986	6/14/76	0.16.39	33.0	94.0	3.8	3	TSINGHIA PROV CHINA	325
987	6/14/76	6.52.43	40.0	29.0	4.4	2	TURKEY	366
988	6/14/76	11.10.19	33.0	86.0	4.1	2	TIBET	306
989	6/14/76	20.14.34	53.0	157.0	4.8	1	KAMCHATKA	217
990	6/15/76	0. 9.11	41.0	21.0	3.4	3	ALBANIA	391
991	6/15/76	0. 9.55	40.0	27.0	3.6	2	TURKEY	366
992	6/15/76	6.38. 4	31.0	96.0	3.7	3	TIBET	306
993	6/15/76	12.21.57	27.0	95.0	3.9	3	BURMA-INDIA BOR	294
994	6/15/76	12.46.25	35.0	24.0	4.4	2	CRETE	370
995	6/15/76	16.22.33	46.0	151.0	3.9	2	KURILE IS	221
996	6/15/76	18. 1.19	40.0	29.0	3.4	3	TURKEY	366
997	6/15/76	20.33.59	35.0	140.0	4.8	1	NEC HONSHU JAPAN	230
998	6/16/76	0. 5.23	37.0	139.0	4.3	2	HONSHU JAPAN	227
999	6/16/76	4.20.13	36.0	77.0	3.7	2	EASTERN KASHMIR	302
1000	6/16/76	13.33.59	48.0	47.0	3.2	3	SW RUSSIA	357

TABLE A-2

DATA BASE
(PAGE 26 OF 37)

EVNO	DATE	TIME	LAT.	LONG.	MB	Q	LOCATION	SUBREG
1001	6/16/76	13.50.47	27.0	89.0	3.8	2	SIKKIM	311
1002	6/17/76	18.39.56	33.0	143.0	4.0	2	OFF E C HONSHU	229
1003	6/18/76	22.19.15	36.0	139.0	4.3	2	HONSHU JAPAN	227
1004	6/19/76	8.52.28	36.0	22.0	3.6	3	MEDITERRANEAN SEA	400
1005	6/19/76	14.25.33	40.0	29.0	3.4	3	TURKEY	366
1006	6/19/76	16.12.16	41.0	39.0	3.6	3	TURKEY	366
1007	6/19/76	16.17.23	39.0	64.0	3.5	3	TURKMEN SSR	340
1008	6/20/76	2.33.28	27.0	97.0	4.4	3	BURMA	296
1009	6/20/76	2.48. 7	39.0	21.0	3.4	3	GREECE	364
1010	6/20/76	4.51.41	41.0	21.0	4.3	2	GREECE/ALBANIA BOR	392
1011	6/20/76	15.28.32	28.0	96.0	4.0	3	INDIA/CHINA BOR	313
1012	6/20/76	15.30. 2	27.0	97.0	4.3	2	BURMA	296
1013	6/20/76	23.33.56	41.0	63.0	5.4	1	UZBEK SSR	339
1014	6/21/76	1.28.17	41.0	77.0	3.8	2	KIRGIZ-SINKIANG BOR	320
1015	6/21/76	9.11.27	39.0	48.0	3.7	2	NW IRAN/USSR BORDER	344
1016	6/21/76	10.59.40	37.0	23.0	3.8	2	SOUTHERN GREECE	368
1017	6/21/76	20. 4.53	39.0	141.0	4.3	2	HONSHU JAPAN	227
1018	6/22/76	18.48.53	32.0	56.0	3.4	3	IRAN	348
1019	6/23/76	9.49.24	39.0	64.0	4.6	1	UZBEK SSR	339
1020	6/23/76	13. 5.58	29.0	55.0	3.6	3	SOUTHERN IRAN	353
1021	6/23/76	15.38.50	23.0	88.0	4.8	1	INDIA-BANGLADESH BOR	315
1022	6/24/76	3.54.56	44.0	149.0	3.4	3	KURILE ISLANDS	221
1023	6/24/76	18.46.16	43.0	142.0	3.6	3	HOKKAIDO JAPAN REG	224
1024	6/25/76	7. 2. 9	41.0	21.0	4.5	3	GREECE-ALBANIA BOR	392
1025	6/25/76	12. 9.14	41.0	76.0	4.3	1	KIRGIZ-SINKIANG BOR	320
1026	6/26/76	1.22. 7	29.0	77.0	3.7	2	NORTHERN INDIA	308
1027	6/26/76	9.24.39	38.0	21.0	3.1	3	IONIAN SEA	399
1028	6/26/76	11.13. 0	42.0	13.0	3.8	2	CENTRAL ITALY	381
1029	6/27/76	9.27.57	32.0	49.0	3.9	2	WESTERN IRAN	347
1030	6/27/76	11.55.46	32.0	53.0	3.8	3	IRAN	348
1031	6/28/76	6.35.25	56.0	162.0	4.0	3	NEC KAMCHATKA	218
1032	6/28/76	7.53.56	38.0	145.0	4.1	2	OEC HONSHU JAPAN	229
1033	6/29/76	4.27. 0	32.0	51.0	3.4	3	IRAN	348
1034	6/29/76	9.48.21	35.0	24.0	3.5	3	CRETE	370
1035	6/29/76	13.47.58	44.0	144.0	4.6	2	HOKKAIDO JAPAN	224
1036	6/30/76	5.51.23	38.0	77.0	4.0	1	S SINKIANG PROV	321
1037	6/30/76	7. 6.33	37.0	29.0	3.2	3	TURKEY	366
1038	6/30/76	11.18.40	28.0	64.0	3.5	3	WESTERN PAKISTAN	354
1039	6/30/76	11.48.16	36.0	74.0	3.8	3	NW KASHMIR	720
1040	6/30/76	12.18.46	37.0	78.0	4.5	1	KASHMIR-SINKIANG BOR	324

TABLE A-2

DATA BASE
(PAGE 27 OF 37)

EVNO	DATE	TIME	LAT.	LONG.	MB	Q	LOCATION	SUBREG
1041	6/30/76	23.15.24	25.0	93.0	4.0	2	BURMA-INDIA BOR REG	294
1042	7/ 1/76	7.22.25	39.0	142.0	4.4	2	NEC HONSHU JAPAN	228
1043	7/ 1/76	15.37.27	45.0	44.0	3.4	3	SW RUSSIA	357
1044	7/ 1/76	17.47.38	41.0	21.0	3.3	3	GREECE-ALBANIA BOR	392
1045	7/ 2/76	0.52.25	47.0	154.0	4.7	1	KURILE ISLANDS	221
1046	7/ 2/76	2. 6. 7	31.0	50.0	3.3	3	WESTERN IRAN	347
1047	7/ 2/76	5.16. 0	35.0	24.0	4.4	3	CRETE	370
1048	7/ 2/76	6.30.23	30.0	85.0	3.8	2	TIBET	306
1049	7/ 2/76	8.50.24	40.0	40.0	4.1	3	TURKEY	366
1050	7/ 2/76	12.36.23	43.0	149.0	4.4	2	KURILE ISLANDS REG	222
1051	7/ 2/76	15.54.44	49.0	151.0	3.8	2	KURILE ISLANDS	221
1052	7/ 2/76	16.58.30	37.0	29.0	3.2	3	TURKEY	366
1053	7/ 2/76	20.51.27	40.0	40.0	3.6	3	TURKEY	366
1054	7/ 3/76	1. 1. 3	43.0	147.0	4.6	1	OC HOKKAIDO JAPAN	225
1055	7/ 3/76	4.51.49	42.0	142.0	3.6	3	HOKKAIDO JAPAN REG	224
1056	7/ 3/76	15.14.21	36.0	74.0	3.5	3	NW KASHMIR	720
1057	7/ 3/76	16.33.36	26.0	97.0	4.8	2	BURMA	296
1058	7/ 3/76	18.36.34	38.0	21.0	3.0	3	IONIAN SEA	399
1059	7/ 3/76	19. 1.53	35.0	24.0	3.8	2	CRETE	370
1060	7/ 4/76	1.28.57	41.0	80.0	3.4	3	S SINKIANG PROV.	321
1061	7/ 4/76	2.34.44	38.0	21.0	2.8	3	IONIAN SEA	399
1062	7/ 4/76	2.56.50	49.0	80.0	6.2	1	EASTERN KAZAKH SSR	329
1063	7/ 4/76	4. 0. 3	30.0	103.0	3.5	2	SZECHWAN PROV. CHINA	307
1064	7/ 4/76	13.58.11	31.0	104.0	3.7	3	SZECHWAN PROV. CHINA	307
1065	7/ 4/76	17.27.24	43.0	146.0	3.8	2	HOKKAIDO JAPAN REG	224
1066	7/ 5/76	10. 0.58	41.0	21.0	3.4	3	GREECE-ALBANIA REG	392
1067	7/ 5/76	19. 5.18	40.0	29.0	2.9	3	TURKEY	366
1068	7/ 6/76	2.20. 9	40.0	61.0	3.3	3	TURKMEN SSR	340
1069	7/ 6/76	2.56. 1	34.0	78.0	4.8	1	EASTERN KASHMIR	302
1070	7/ 6/76	10.25. 9	25.0	98.0	3.9	3	BURMA-CHINA REG	297
1071	7/ 6/76	17.51.21	39.0	64.0	3.9	2	UZBEK SSR	339
1072	7/ 7/76	6.24.33	38.0	21.0	3.0	3	IONIAN SEA	399
1073	7/ 7/76	11.22.40	29.0	52.0	3.4	3	SOUTHERN IRAN	353
1074	7/ 7/76	12. 5.41	23.0	97.0	3.4	3	BURMA	296
1075	7/ 8/76	10.41.39	45.0	36.0	2.7	3	CRIMEA REGION	361
1076	7/ 8/76	11. 2.34	35.0	24.0	3.4	3	CRETE	370
1077	7/ 8/76	15.20. 9	35.0	24.0	4.5	2	CRETE	370
1078	7/ 8/76	18.[illegible].53	31.0	51.0	3.4	3	IRAN	348
1079	7/ 9/76	9.33. 9	41.0	39.0	3.9	3	TURKEY	366
1080	7/ 9/76	12.27. 3	43.0	142.0	3.7	3	HOKKAIDO JAPAN REG	224

TABLE A-2

DATA BASE
(PAGE 28 OF 37)

EVNO	DATE	TIME	LAT.	LONG.	MB	Q	LOCATION	SUBREG
1081	7/10/76	4.10.37	42.0	13.0	3.7	2	CENTRAL ITALY	381
1082	7/10/76	9.24.53	28.0	96.0	3.7	2	INDIA-CHINA BORD REG	313
1083	7/10/76	10.24. 6	34.0	142.0	4.3	2	OEC HONSHU JAPAN	229
1084	7/11/76	0.29.33	38.0	21.0	2.9	3	IONIAN SEA	399
1085	7/11/76	5.42.26	40.0	141.0	3.7	3	NEC HONSHU JAPAN	228
1086	7/11/76	10.22.36	48.0	152.0	4.5	1	KURILE ISLANDS	221
1087	7/11/76	14.28. 8	38.0	21.0	3.7	3	IONIAN SEA	399
1088	7/11/76	14.39.14	36.0	22.0	4.0	2	MEDITERRANEAN SEA	400
1089	7/11/76	14.49.33	36.0	22.0	3.7	2	MEDITERRANEAN SEA	400
1090	7/11/76	18. 1.51	35.0	21.0	3.8	2	MEDITERRANEAN SEA	400
1091	7/12/76	3.12.46	34.0	86.0	4.6	2	TIBET	306
1092	7/12/76	18.26.41	30.0	103.0	3.7	2	SZECHWAN PROV CHINA	307
1093	7/12/76	19.26.17	27.0	96.0	3.8	2	BURMA-INDIA BORD REG	294
1094	7/13/76	7.29. 5	28.0	96.0	4.2	2	INDIA-CHINA BORD REG	313
1095	7/13/76	7.37.33	35.0	80.0	4.0	2	KASHMIR-TIBET BORDER	304
1096	7/13/76	8. 0.46	35.0	80.0	3.5	3	KASHMIR-TIBET BORDER	304
1097	7/13/76	8.42.37	35.0	79.0	3.5	2	KASHMIR-TIBET BORDER	304
1098	7/13/76	12.10.23	44.0	16.0	3.6	3	YUGOSLAVIA	383
1099	7/13/76	18.40.23	35.0	79.0	3.5	3	KASHMIR-TIBET BORDER	304
1100	7/13/76	18.49.40	35.0	79.0	4.0	2	KASHMIR-TIBET BORDER	304
1101	7/13/76	21.41. 9	35.0	24.0	3.4	2	CRETE	370
1102	7/13/76	21.48.19	35.0	24.0	3.3	3	CRETE	370
1103	7/14/76	0.57. 6	38.0	21.0	3.2	3	IONIAN SEA	399
1104	7/14/76	5. 2.23	39.0	79.0	3.8	3	S SINKIANG PROV.	321
1105	7/14/76	5.38.44	42.0	14.0	3.9	3	CENTRAL ITALY	381
1106	7/14/76	6. 4.35	38.0	21.0	2.5	3	IONIAN SEA	399
1107	7/14/76	12.24.52	36.0	22.0	4.0	2	MEDITERRANEAN SEA	400
1108	7/14/76	13.54.49	43.0	148.0	3.9	2	KURILE ISLANDS	221
1109	7/14/76	15.19.25	34.0	80.0	3.6	3	KASHMIR-TIBET BORDER	304
1110	7/14/76	16.16.55	42.0	143.0	4.1	2	HOKKAIDO JAPAN REG	224
1111	7/14/76	21.19.19	34.0	80.0	3.9	2	KASHMIR-TIBET BORDER	304
1112	7/14/76	21.38.14	36.0	22.0	3.5	2	MEDITERRANEAN SEA	400
1113	7/15/76	0. 6. 4	34.0	80.0	4.2	2	KASHMIR-TIBET BORDER	304
1114	7/15/76	2.10.37	46.0	153.0	4.0	2	KURILE ISLANDS REG	222
1115	7/15/76	19.41.47	42.0	21.0	3.4	3	YUGOSLAVIA	383
1116	7/15/76	20.24.29	40.0	35.0	4.3	3	TURKEY	366
1117	7/15/76	22.14.21	35.0	98.0	3.9	3	TSINGHAI PROV. CHINA	325
1118	7/16/76	6.56.21	37.0	140.0	3.8	3	HONSHU JAPAN	227
1119	7/16/76	15. 3.58	36.0	79.0	4.1	2	KASHMIR-SINKIANG BOR	324
1120	7/16/76	18.53.14	41.0	21.0	2.9	3	GREECE-ALBANIA BORD	392

TABLE A-2

DATA BASE
(PAGE 29 OF 37)

EVNO	DATE	TIME	LAT.	LONG.	MB	Q	LOCATION	SUBREG
1121	7/16/76	18.59.20	41.0	21.0	3.4	2	GREECE-ALBANIA BORD	392
1122	7/17/76	2. 2.29	34.0	83.0	3.8	3	TIBET	306
1123	7/17/76	4.35.12	55.0	163.0	3.6	3	OEC KAMCHATKA	219
1124	7/17/76	7.27.36	16.0	95.0	3.9	2	SOUTH BURMA	298
1125	7/17/76	8.37. 4	30.0	51.0	4.1	2	IRAN	348
1126	7/17/76	14.14. 9	38.0	76.0	4.5	2	SOUTH SINKIANG PROV.	321
1127	7/17/76	19.57.17	35.0	140.0	3.8	2	NEC HONSHU JAPAN	228
1128	7/18/76	2.17.30	39.0	24.0	3.3	3	AEGEAN SEA	365
1129	7/18/76	5.11.14	55.0	162.0	4.2	2	NEC KAMCHATKA	218
1130	7/18/76	8. 7.17	35.0	140.0	4.3	2	NEC HONSHU JAPAN	228
1131	7/18/76	13.31.14	41.0	21.0	3.7	2	GREECE-ALBANIA BORD	392
1132	7/18/76	21.22.53	42.0	143.0	3.6	3	HOKKAIDO JAPAN REG	224
1133	7/18/76	22. 9.45	41.0	21.0	3.2	3	GREECE-ALBANIA BORD	392
1134	7/19/76	9.39.25	47.0	152.0	4.7	1	KURILE ISLANDS	221
1135	7/20/76	17.27.28	36.0	139.0	3.9	3	HONSHU JAPAN	227
1136	7/21/76	3.23.18	35.0	27.0	3.3	3	CRETE	370
1137	7/21/76	4.28.22	38.0	21.0	3.1	3	IONIAN SEA	399
1138	7/21/76	15.11. 5	27.0	98.0	5.7	1	BURMA	296
1139	7/21/76	15.30.51	27.0	97.0	4.3	2	BURMA	296
1140	7/21/76	16.59.47	40.0	141.0	4.3	2	NEC HONSHU JAPAN	228
1141	7/22/76	4.26.39	27.0	97.0	4.2	2	BURMA	296
1142	7/22/76	6.57.13	46.0	152.0	4.8	1	KURILE ISLANDS	221
1143	7/22/76	13.53.38	42.0	142.0	4.0	3	HOKKAIDO JAPAN REG	224
1144	7/22/76	14.42.30	33.0	77.0	3.9	2	KASHMIR-INDIA BORDER	303
1145	7/22/76	16. 9. 2	53.0	162.0	3.8	2	OEC KAMCHATKA	219
1146	7/22/76	16.48.18	40.0	144.0	4.2	2	/EC HONSHU JAPAN	229
1147	7/22/76	17.20. 0	54.0	164.0	3.7	3	OEC KAMCHATKA	219
1148	7/22/76	18.53.32	39.0	64.0	3.7	3	UZBEK SSR	339
1149	7/22/76	21.32.56	29.0	53.0	3.6	3	SOUTHERN IRAN	353
1150	7/23/76	1.43.55	24.0	98.0	4.6	1	BURMA-CHINA BORDER	297
1151	7/23/76	1.56.15	33.0	83.0	4.8	1	TIBET	306
1152	7/23/76	2.32.53	49.0	80.0	4.9	1	EASTERN KAZAKH SSR	329
1153	7/23/76	15.49.46	28.0	96.0	3.9	2	INDIA-CHINA BORDER	313
1154	7/23/76	20.51.34	41.0	21.0	3.9	2	GREECE-ALBANIA BORD	392
1155	7/23/76	22.17.44	44.0	152.0	4.1	2	KURILE ISLANDS REG	222
1156	7/24/76	3.31.38	30.0	95.0	3.6	3	TIBET	306
1157	7/24/76	6.55.55	49.0	40.0	3.1	3	SOUTHWESTERN RUSSIA	357
1158	7/24/76	8.30.39	49.0	156.0	4.0	2	KURILE ISLANDS	221
1159	7/24/76	15.56.38	38.0	143.0	3.9	3	OEC HONSHU JAPAN	229
1160	7/26/76	6.27.14	41.0	21.0	3.0	3	GREECE-ALBANIA BORD	392

TABLE A-2

DATA BASE

(PAGE 30 OF 37)

EVNO	DATE	TIME	LAT.	LONG.	MB	Q	LOCATION	SUBREG
1161	7/26/76	11.46.48	43.0	43.0	4.4	2	WESTERN CAUCASUS	362
1162	7/27/76	13.43.31	38.0	21.0	3.3	3	IONIAN SEA	399
1163	7/27/76	18.38.57	36.0	50.0	4.4	1	IRAN	348
1164	7/27/76	19.42.53	40.0	120.0	6.5	1	NORTHEASTERN CHINA	658
1165	7/27/76	19.56.26	39.0	121.0	4.2	2	NORTHEASTERN CHINA	658
1166	7/27/76	20. 3.21	53.0	121.0	3.7	3	NORTHEASTERN CHINA	658
1167	7/27/76	20. 7.17	40.0	119.0	4.6	1	NORTHEASTERN CHINA	658
1168	7/27/76	20. 9.57	40.0	120.0	4.4	3	NORTHEASTERN CHINA	658
1169	7/27/76	20.13. 3	40.0	120.0	4.8	2	NORTHEASTERN CHINA	658
1170	7/27/76	20.35. 2	42.0	119.0	3.9	3	NORTHEASTERN CHINA	658
1171	7/27/76	21. 4.22	38.0	120.0	4.6	2	NORTHEASTERN CHINA	658
1172	7/27/76	21.10.52	38.0	120.0	4.1	2	NORTHEASTERN CHINA	658
1173	7/27/76	22.31.27	38.0	120.0	3.6	3	NORTHEASTERN CHINA	658
1174	7/27/76	23. 3.17	40.0	121.0	4.3	2	NORTHEASTERN CHINA	658
1175	7/27/76	23.17.30	40.0	120.0	5.2	1	NORTHEASTERN CHINA	658
1176	7/27/76	23.36.18	40.0	117.0	3.5	3	NORTHEASTERN CHINA	658
1177	7/28/76	0. 4. 9	39.0	119.0	3.6	3	NORTHEASTERN CHINA	658
1178	7/28/76	0.56. 8	40.0	119.0	3.9	2	NORTHEASTERN CHINA	658
1179	7/28/76	0.57.15	43.0	147.0	3.9	2	OC HOKKAIDO JAPAN	225
1180	7/28/76	0.58.25	37.0	122.0	4.8	2	NORTHEASTERN CHINA	658
1181	7/28/76	1.13.47	40.0	121.0	4.2	3	NORTHEASTERN CHINA	658
1182	7/28/76	1.21.35	39.0	119.0	4.6	2	NORTHEASTERN CHINA	658
1183	7/28/76	1.45.25	38.0	120.0	4.9	2	NORTHEASTERN CHINA	658
1184	7/28/76	5. 8.33	40.0	119.0	4.0	3	NORTHEASTERN CHINA	658
1185	7/28/76	7.15.10	42.0	119.0	4.2	2	NORTHEASTERN CHINA	658
1186	7/28/76	9.27.58	38.0	120.0	3.9	3	NORTHEASTERN CHINA	658
1187	7/28/76	9.42.20	40.0	120.0	4.7	2	NORTHEASTERN CHINA	658
1188	7/28/76	10.23.12	38.0	120.0	4.0	3	NORTHEASTERN CHINA	658
1189	7/28/76	10.45.34	40.0	120.0	6.5	1	NORTHEASTERN CHINA	658
1190	7/28/76	10.58.23	39.0	121.0	4.8	1	NORTHEASTERN CHINA	658
1191	7/28/76	11.15.57	40.0	121.0	4.3	2	NORTHEASTERN CHINA	658
1192	7/28/76	11.46.26	37.0	122.0	4.4	3	NORTHEASTERN CHINA	658
1193	7/28/76	15.35.56	40.0	120.0	5.0	2	NORTHEASTERN CHINA	658
1194	7/28/76	16.23.48	38.0	120.0	3.8	3	NORTHEASTERN CHINA	658
1195	7/28/76	17.45.47	44.0	148.0	4.1	2	KURILE ISLANDS	221
1196	7/28/76	18.49.31	40.0	119.0	4.2	2	NORTHEASTERN CHINA	658
1197	7/28/76	20.16.45	37.0	49.0	5.5	2	NORTHWESTERN IRAN	345
1198	7/28/76	21. 4.27	40.0	46.0	4.1	2	NW IRAN-USSR BORDER	344
1199	7/28/76	23. 1. 6	40.0	46.0	4.3	2	NW IRAN-USSR BORDER	344
1200	7/29/76	5. 0. 0	48.0	47.0	6.7	1	SOUTHWESTERN RUSSIA	357

TABLE A-2

DATA BASE
(PAGE 31 OF 37)

EVNO	DATE	TIME	LAT.	LONG.	MB	Q	LOCATION	SUBREG
1201	7/29/76	11. 0.41	45.0	43.0	3.8	3	SOUTHWESTERN RUSSIA	357
1202	7/29/76	11. 5.34	38.0	120.0	4.3	2	NORTHEASTERN CHINA	658
1203	7/29/76	11.10. 1	41.0	122.0	4.3	3	NORTHEASTERN CHINA	658
1204	7/29/76	12.29.36	40.0	117.0	4.1	2	NORTHEASTERN CHINA	658
1205	7/29/76	13.59.54	42.0	122.0	3.9	3	NORTHEASTERN CHINA	658
1206	7/30/76	0.10.46	39.0	65.0	3.6	3	TURKMEN SSR	340
1207	7/30/76	5.29.40	39.0	118.0	3.7	3	NORTHEASTERN CHINA	658
1208	7/30/76	7.23.49	40.0	36.0	3.9	3	TURKEY	366
1209	7/30/76	7.31.48	40.0	63.0	3.4	3	UZBEK SSR	339
1210	7/30/76	12. 8.36	45.0	146.0	3.9	3	HOKKAIDO JAPAN REG	224
1211	7/30/76	21.22.52	37.0	122.0	5.2	1	NORTHEASTERN CHINA	658
1212	7/30/76	22.26.25	40.0	117.0	3.8	3	NORTHEASTERN CHINA	658
1213	7/30/76	23.53. 5	40.0	121.0	4.3	2	NORTHEASTERN CHINA	658
1214	7/31/76	7.23.40	40.0	121.0	4.4	2	NORTHEASTERN CHINA	658
1215	7/31/76	15.19.54	38.0	121.0	4.0	3	NORTHEASTERN CHINA	658
1216	7/31/76	15.33.10	34.0	51.0	3.7	2	IRAN	348
1217	7/31/76	15.46.46	35.0	80.0	3.7	3	KASHMIR-TIBET BORDER	304
1218	7/31/76	18. 1.23	40.0	117.0	4.3	2	NORTHEASTERN CHINA	658
1219	7/31/76	22.26.37	39.0	118.0	3.9	2	NORTHEASTERN CHINA	658
1220	8/ 1/76	2. 5.29	35.0	79.0	4.5	2	KASHMIR-TIBET BOR	304
1221	8/ 1/76	10.32.21	40.0	119.0	3.5	3	NE CHINA	658
1222	8/ 1/76	13.32.46	21.0	94.0	4.0	2	BURMA	296
1223	8/ 1/76	17.20.22	30.0	53.0	3.4	3	SOUTHERN IRAN	353
1224	8/ 1/76	18. 2.34	27.0	98.0	4.2	2	BURMA	296
1225	8/ 1/76	18.46.22	56.0	163.0	3.7	2	NEAR E COAST KAMCHAT	218
1226	8/ 1/76	18.53. 7	40.0	121.0	3.9	3	NE CHINA	658
1227	8/ 1/76	20.53.47	39.0	118.0	4.4	1	NE CHINA	658
1228	8/ 2/76	5. 8.57	44.0	144.0	4.4	2	HOKKAIDO JAP	224
1229	8/ 2/76	5.15.20	35.0	27.0	4.1	3	CRETE	370
1230	8/ 2/76	5.58.50	28.0	94.0	3.4	3	INDIA-CHINA BOR REG	313
1231	8/ 2/76	9.15.55	39.0	118.0	3.9	3	NE CHINA	658
1232	8/ 2/76	14.12.55	53.0	157.0	4.1	2	KAMCHATKA	217
1233	8/ 2/76	16.16.25	52.0	160.0	4.5	2	OFF E COAST KAMCHAT	219
1234	8/ 3/76	7.50.28	41.0	77.0	5.3	1	KIRGIZ-SINKIANG BOR	320
1235	8/ 3/76	8.20.33	26.0	95.0	3.8	2	BURMA-INDIA BOR REG	294
1236	8/ 3/76	9.44.39	16.0	95.0	4.3	3	SOUTH BURMA	298
1237	8/ 3/76	17.53. 3	38.0	76.0	3.7	3	SOUTHERN SINKIANG	321
1238	8/ 3/76	23.37.48	37.0	138.0	4.8	2	HONSHU JAPAN	227
1239	8/ 4/76	2.23.37	39.0	64.0	3.7	3	UZBEK SSR	339
1240	8/ 4/76	9.28.17	27.0	98.0	4.0	3	BURMA	296

TABLE A-2

DATA BASE
(PAGE 32 OF 37)

EVNO	DATE	TIME	LAT.	LONG.	MB	Q	LOCATION	SUBREG
1241	8/ 5/76	4.26.40	49.0	152.0	3.9	3	KURILE IS	221
1242	8/ 5/76	10.24.12	28.0	92.0	4.4	2	INDIA CHINA BOR REG	313
1243	8/ 5/76	18.26.23	45.0	148.0	4.0	2	KURILE IS	221
1244	8/ 6/76	20. 0. 1	39.0	143.0	3.6	3	NEAR E COAST HONSHU	228
1245	8/ 7/76	18.43. 1	46.0	153.0	3.7	3	KURILE IS	221
1246	8/ 8/76	1.56.59	48.0	154.0	4.2	2	KURILE IS	221
1247	8/ 8/76	22.41.33	40.0	119.0	4.6	2	NE CHINA	658
1248	8/ 8/76	23.12. 7	41.0	21.0	3.2	3	GREECE-ALBANIA BOR R	392
1249	8/ 8/76	23.36. 8	40.0	121.0	3.6	3	NE CHINA	658
1250	8/ 9/76	1.12.27	38.0	21.0	2.7	3	IONIAN SEA	399
1251	8/ 9/76	3.20.32	47.0	152.0	3.4	3	KURILE IS	221
1252	8/ 9/76	4.35.41	39.0	64.0	3.8	2	UZBEK SSR	339
1253	8/ 9/76	5.46. 4	33.0	146.0	3.4	3	OFF E COAST HONSHU	229
1254	8/ 9/76	8.50.46	33.0	97.0	3.8	3	TSINGHAI PROV	325
1255	8/ 9/76	10.29. 0	33.0	97.0	4.4	2	TSINGHAI PROV	325
1256	8/10/76	6.32.20	29.0	78.0	3.7	2	NORTHERN INDIA	308
1257	8/10/76	19.18.26	52.0	162.0	3.4	3	OFF E COAST KAMCHAT	219
1258	8/10/76	22.38.26	42.0	119.0	3.4	3	NE CHINA	658
1259	8/10/76	23.32.32	30.0	79.0	3.2	3	NORTHERN INDIA	308
1260	8/11/76	0.15. 9	38.0	21.0	2.6	3	IONIAN SEA	399
1261	8/11/76	6.57.31	34.0	91.0	3.8	3	TSINGHAI PROV	325
1262	8/11/76	9.10.45	46.0	153.0	3.6	2	KURILE IS REG	222
1263	8/12/76	6.17.58	38.0	13.0	3.1	2	SICILY	398
1264	8/12/76	14. 1.22	50.0	44.0	3.1	3	SW RUSSIA	357
1265	8/12/76	23.26.53	27.0	97.0	6.3	1	BURMA-INDIA BOR REG	294
1266	8/12/76	23.28.18	43.0	144.0	5.0	2	HOKKAIDO JAPAN REG	224
1267	8/13/76	0. 6.35	28.0	96.0	4.0	2	INDIA-CHINA BOR REG	313
1268	8/13/76	2.54.23	28.0	96.0	3.7	2	INDIA-CHINA BOR REG	313
1269	8/13/76	23.22.13	35.0	138.0	4.5	1	NEAR S COAST HONSHU	230
1270	8/13/76	23.55.33	28.0	96.0	3.7	2	INDIA CHINA BOR REG	313
1271	8/13/76	23.56.10	40.0	121.0	3.9	3	NE CHINA	658
1272	8/14/76	1.23.40	28.0	96.0	4.4	1	INDIA CHINA BOR REG	313
1273	8/14/76	4.30.34	35.0	27.0	3.2	3	CRETE	370
1274	8/14/76	7.10.49	40.0	121.0	3.6	3	NE CHINA	658
1275	8/14/76	8.22.54	32.0	62.0	3.7	2	SW AFGHANISTAN	350
1276	8/14/76	8.48.35	45.0	40.0	2.8	3	SW RUSSIA	357
1277	8/14/76	9.26.46	31.0	53.0	3.3	3	IRAN	348
1278	8/14/76	10.16.47	43.0	29.0	3.1	3	BLACK SEA	360
1279	8/14/76	16. 2.38	40.0	121.0	4.2	2	NE CHINA	658
1280	8/14/76	22.56.22	28.0	61.0	3.5	3	SOUTHERN IRAN	353

TABLE A-2

DATA BASE
(PAGE 33 OF 37)

EVNO	DATE	TIME	LAT.	LONG.	MB	Q	LOCATION	SUBREG
1281	8/15/76	3.40.48	42.0	141.0	4.0	2	HOKKAIDO JAPAN REG	224
1282	8/15/76	5.18.51	21.0	94.0	3.7	2	BURMA	296
1283	8/15/76	9.37. 6	36.0	74.0	3.6	2	NW KASHMIR	720
1284	8/15/76	10.21.17	40.0	119.0	4.0	3	NE CHINA	658
1285	8/15/76	10.28.32	38.0	117.0	3.8	3	NE CHINA	658
1286	8/15/76	10.53. 9	38.0	119.0	3.8	3	NE CHINA	658
1287	8/15/76	12.42.48	36.0	139.0	3.5	3	HONSHU JAPAN	227
1288	8/15/76	14.32.58	39.0	119.0	3.6	2	NE CHINA	658
1289	8/15/76	22.39.44	39.0	118.0	3.9	2	NE CHINA	658
1290	8/16/76	2. 6.21	48.0	152.0	3.2	3	KURILE IS	221
1291	8/16/76	4.11.52	39.0	48.0	3.5	3	NW IRAN	345
1292	8/16/76	7.25.32	36.0	79.0	3.7	2	KASHMIR-SINKIANG BOR	324
1293	8/16/76	8.42. 8	35.0	24.0	3.5	3	CRETE	370
1294	8/16/76	9.34.51	46.0	45.0	2.9	3	SW RUSSIA	357
1295	8/16/76	12.28.28	52.0	158.0	5.2	1	NEAR E COAST KAMCHAT	218
1296	8/16/76	14. 6.54	34.0	104.0	6.2	1	KANSU PROV CHIAA	322
1297	8/16/76	14.56.25	31.0	105.0	3.8	2	SZECHWAN CHINA	307
1298	8/16/76	14.57.40	35.0	103.0	3.8	0	TSINGHAI PROV CHINA	325
1299	8/16/76	15. 0.54	33.0	105.0	4.5	1	SZECHWAN PROV CHINA	307
1300	8/16/76	15.26.14	33.0	105.0	4.4	1	SZECHWAN PROV CHINA	307
1301	8/16/76	18.15.54	35.0	103.0	4.0	2	TSINGHAI PROV CHINA	325
1302	8/16/76	18.54.35	33.0	105.0	3.4	3	SZECHWAN PROV CHINA	307
1303	8/16/76	20.26.50	33.0	104.0	3.7	2	SZECHAN PROV CHINA	307
1304	8/16/76	21.20.17	40.0	117.0	3.4	3	NE CHINA	658
1305	8/16/76	21.23.34	26.0	81.0	3.2	3	NORTHERN INDIA	308
1306	8/16/76	21.30.32	31.0	105.0	3.8	2	SZECHWAN PROV CHINA	307
1307	8/16/76	22. 6.38	33.0	105.0	3.8	2	SZECHWAN PROV CHINA	307
1308	8/16/76	22.41.26	41.0	39.0	3.1	3	TURKEY	366
1309	8/17/76	2. 3. 5	43.0	149.0	4.4	1	KURILE ISLANDS	222
1310	8/17/76	2. 3.33	39.0	64.0	3.8	2	UZBEK SSR	339
1311	8/17/76	2.27.43	35.0	103.0	3.4	3	TSINGHAI PROV CHINA	325
1312	8/17/76	3.48.27	38.0	100.0	3.6	3	TSINGHAI PROV CHINA	325
1313	8/17/76	5.19.54	35.0	103.0	3.4	2	TSINGHAI PROV CHINA	325
1314	8/17/76	17.19. 9	35.0	138.0	4.8	1	HONSHU JAPAN	227
1315	8/17/76	22.17.31	34.0	104.0	3.9	2	KANSU PROV CHINA	322
1316	8/18/76	0.58.24	39.0	24.0	3.6	3	AEGEAN SEA	365
1317	8/18/76	2.25.37	38.0	21.0	2.7	3	IONIAN SEA	399
1318	8/18/76	2.30.53	30.0	94.0	3.7	2	INDIA CHINA BOR REG	313
1319	8/18/76	17. 6.11	35.0	27.0	3.8	3	CRETE	370
1320	8/19/76	7.52.29	53.0	158.0	3.9	2	NEAR E COAST KAMCHAT	218

TABLE A-2

DATA BASE
(PAGE 34 OF 37)

EVNO	DATE	TIME	LAT.	LONG.	MB	Q	LOCATION	SUBREG
1321	8/19/76	12.49.45	33.0	105.0	5.2	1	SZECHWAN PROV CHINA	307
1322	8/19/76	19. 2.16	41.0	21.0	3.4	3	GREECE	364
1323	8/20/76	1. 9.43	43.0	141.0	3.6	2	HOKKAIDO JAP REG	224
1324	8/20/76	15.41.44	40.0	29.0	3.0	3	TURKEY	366
1325	8/20/76	19. 5.25	36.0	74.0	3.4	2	NW KASHMIR	720
1326	8/20/76	21. 1.23	37.0	77.0	3.4	3	KASHMIR-SINKIANG BOR	324
1327	8/20/76	22.18. 2	39.0	82.0	3.2	3	S SINKIANG PROV	321
1328	8/20/76	23.43.36	43.0	148.0	4.2	2	OFF COAST HOKKAIDO	225
1329	8/21/76	8. 9.20	26.0	95.0	4.1	2	BURMA-INDIA BOR REG	294
1330	8/21/76	20. 2. 2	40.0	121.0	3.4	3	NE CHINA	658
1331	8/21/76	21.49.54	32.0	104.0	6.1	1	SZECHWAN PROV CHINA	307
1332	8/21/76	22.40.50	33.0	105.0	3.7	3	SZECHWAN PROV CHINA	307
1333	8/22/76	3. 5.15	41.0	39.0	3.6	2	TURKEY	366
1334	8/22/76	8.48.20	43.0	17.0	3.4	2	ADRIATIC SEA	332
1335	8/22/76	9.42. 8	40.0	23.0	2.6	3	GREECE	364
1336	8/22/76	13.19.55	33.0	105.0	4.2	2	SZECHWAN PROV CHINA	307
1337	8/22/76	13.28.56	40.0	29.0	4.8	2	TURKEY	366
1338	8/22/76	14.46.19	38.0	14.0	3.2	3	SICILY	398
1339	8/22/76	16. 6.17	41.0	21.0	3.0	2	GREECE-ALBANIA BOR	392
1340	8/22/76	21.55.15	45.0	34.0	2.6	3	CRIMEA REG	361
1341	8/23/76	1.52. 9	27.0	96.0	3.9	2	BURMA-INDIA BOR REG	294
1342	8/23/76	3.15.40	41.0	20.0	4.3	2	ALBANIA	391
1343	8/23/76	3.30.22	34.0	103.0	6.1	1	KANSU PROV CHINA	322
1344	8/23/76	4.31.11	33.0	105.0	3.9	2	SZECHWAN PROV CHINA	307
1345	8/23/76	4.34.11	35.0	27.0	3.0	3	CRETE	370
1346	8/23/76	6.43.30	33.0	105.0	3.8	2	SZECHWAN PROV CHINA	307
1347	8/23/76	8.58.37	35.0	103.0	4.0	2	KANSU PROVV CHINA	322
1348	8/23/76	10.17. 6	35.0	140.0	3.9	2	NEAR E COAST HONSHU	228
1349	8/23/76	12.12.17	46.0	152.0	3.4	3	KURILE IS	221
1350	8/23/76	17.15.37	38.0	119.0	4.1	2	NE CHINA	658
1351	8/23/76	20.35.11	36.0	75.0	3.4	3	NW KASHMIR	720
1352	8/23/76	21. 2.29	35.0	103.0	4.2	2	TSINGHAI PROV CHINA	325
1353	8/24/76	0.52.16	32.0	49.0	3.3	3	WESTERN IRAN	347
1354	8/24/76	4.31.47	29.0	102.0	3.8	2	SZECHWAN PROV CHINA	307
1355	8/24/76	5.52.45	37.0	142.0	4.3	2	NEAR COAST HONSHU	228
1356	8/24/76	7.26.46	36.0	22.0	3.3	3	MED SEA	400
1357	8/24/76	8. 0. 6	38.0	21.0	3.0	3	IONIAN SEA	399
1358	8/24/76	16.10.36	41.0	21.0	3.1	2	GREECE ALBANIA BOR	392
1359	8/24/76	23.26. 6	42.0	124.0	3.8	3	NE CHINA	658
1360	8/25/76	1.56.19	35.0	27.0	3.3	3	CRETE	370

TABLE A-2

DATA BASE
(PAGE 35 OF 37)

EVNO	DATE	TIME	LAT.	LONG.	MB	Q	LOCATION	SUBREG
1361	8/25/76	17.31.38	37.0	119.0	4.2	2	NE CHINA	658
1362	8/26/76	12. 6.31	42.0	142.0	4.2	2	HOKKAIDO JAPAN REG	224
1363	8/27/76	2.32.14	45.0	149.0	4.7	1	KURILE IS	221
1364	8/27/76	2.53.27	30.0	54.0	3.5	3	IRAN	348
1365	8/27/76	16. 1.31	38.0	78.0	3.6	3	SOUTHERN SINKIANG	321
1366	8/27/76	22.45.43	35.0	27.0	3.4	3	CRETE	370
1367	8/27/76	23.57.37	39.0	64.0	3.7	3	UZBEK SSR	339
1368	8/28/76	2.56.43	49.0	81.0	6.0	1	EASTERN KAZAKH SSR	329
1369	8/28/76	6.33.53	39.0	121.0	4.3	2	NE CHINA	658
1370	8/28/76	10.32.53	36.0	101.0	3.9	3	TSINGHAI PROV CHINA	325
1371	8/28/76	16.23.48	45.0	117.0	4.1	3	NE CHINA	658
1372	8/28/76	18.59.55	35.0	103.0	3.8	3	TSINGHAI PROV CHINA	325
1373	8/28/76	23. 1.12	38.0	78.0	4.2	1	S SINKIANG PROV	321
1374	8/29/76	0.14.56	26.0	91.0	3.3	3	EASTERN INDIA	317
1375	8/29/76	1.51.25	41.0	143.0	3.7	3	HOKKAIDO JAP REG	224
1376	8/29/76	16.49.52	36.0	140.0	3.7	3	NEAR S COAST HONSHU	230
1377	8/29/76	19.31. 7	43.0	20.0	3.0	2	YUGOSLAVIA	383
1378	8/29/76	20. 1.21	31.0	47.0	4.4	2	IRAN-IRAQ BOR REG	346
1379	8/29/76	23.39. 7	44.0	142.0	4.2	2	HOKKAIDO JAP REG	224
1380	8/30/76	0. 8.18	20.0	96.0	3.9	2	BURMA	296
1381	8/30/76	15.49.47	44.0	147.0	4.3	2	KURILE IS	221
1382	8/30/76	17.41.16	42.0	143.0	4.3	2	HOKKAIDO JAP	224
1383	8/31/76	3.25. 5	37.0	122.0	4.9	2	NE CHINA	658
1384	8/31/76	11.20.23	43.0	23.0	3.3	2	BULGARIA	359
1385	9/ 1/76	1. 7.14	35.0	103.0	4.6	2	TSINGHAI PROV. CHINA	325
1386	9/ 2/76	11.15.10	39.0	64.0	3.7	3	TURKMEN SSR	340
1387	9/ 2/76	19.54. 6	32.0	49.0	4.0	2	WESTERN IRAN	347
1388	9/ 2/76	21.37. 3	38.0	21.0	3.4	3	IONIAN SEA	399
1389	9/ 3/76	9.57.39	29.0	99.0	4.9	1	SZECHWAN PROV. CHINA	307
1390	9/ 5/76	0.14. 6	41.0	122.0	4.3	2	NORTHEASTERN CHINA	658
1391	9/ 5/76	9.54.32	36.0	80.0	3.6	3	KASHMIR-TIBET BORDER	304
1392	9/ 5/76	10.42.16	44.0	142.0	5.0	1	HOKKAIDO JAPAN REG	224
1393	9/ 5/76	16.43. 8	31.0	51.0	5.0	1	IRAN	348
1394	9/ 5/76	20.33.13	51.0	158.0	3.7	3	KURILE ISLANDS	221
1395	9/ 5/76	22. 7.58	41.0	40.0	4.7	2	TURKEY	366
1396	9/ 6/76	7. 7.39	36.0	64.0	3.3	3	TURKMEN-AFGHANISTAN	342
1397	9/ 6/76	11. 2.44	46.0	48.0	3.9	3	SOUTHWESTERN RUSSIA	357
1398	9/ 6/76	16. 4.41	31.0	51.0	4.5	1	IRAN	348
1399	9/ 6/76	17. 1.38	37.0	122.0	4.4	2	NORTHEASTERN CHINA	658
1400	9/ 7/76	3.27.57	45.0	130.0	4.1	2	NORTHEASTERN CHINA	658

TABLE A-2

DATA BASE
(PAGE 36 OF 37)

EVNO	DATE	TIME	LAT.	LONG.	MB	Q	LOCATION	SUBREG
1401	9/ 7/76	6. 3.21	39.0	143.0	4.8	2	OEC HONSHU JAPAN	229
1402	9/ 7/76	9.20.27	39.0	115.0	4.1	3	NORTHEASTERN CHINA	658
1403	9/ 7/76	17.37.51	43.0	23.0	3.7	2	BULGARIA	359
1404	9/ 7/76	19.27.18	49.0	156.0	3.5	3	KURILE ISLANDS REG	222
1405	9/ 8/76	17.59.47	38.0	78.0	3.5	3	SOUTHERN SINKIANG PR	321
1406	9/ 8/76	20.13. 4	32.0	79.0	5.0	1	TIBET-INDIA BORDER	305
1407	9/12/76	0.43. 1	41.0	21.0	3.2	3	GREECE-ALBANIA BORD	392
1408	9/12/76	7.29.33	41.0	103.0	3.5	3	NORTHERN CHINA	323
1409	9/13/76	4.16.47	35.0	27.0	3.1	2	CRETE	370
1410	9/13/76	5.45.38	40.0	120.0	3.9	3	NORTHEASTERN CHINA	658
1411	9/13/76	19.41.53	44.0	12.0	3.5	3	CENTRAL ITALY	381
1412	9/13/76	19.57. 8	33.0	105.0	3.7	2	SZECHWAN PROV. CHINA	307
1413	9/14/76	6.43.52	30.0	89.0	5.2	1	TIBET	306
1414	9/14/76	10.52.19	41.0	81.0	3.7	3	SOUTHERN SINKIANG	321
1415	9/14/76	15.38.31	37.0	96.0	4.3	2	TSINGHAI PROV. CHINA	325
1416	9/14/76	18.23.43	27.0	86.0	3.6	3	NEPAL	310
1417	9/14/76	23.41.35	29.0	53.0	4.4	1	SOUTHERN IRAN	353
1418	9/15/76	8.20.16	39.0	143.0	4.8	1	NEC HONSHU JAPAN	228
1419	9/15/76	9.57.34	43.0	17.0	3.2	3	ADRIATIC SEA	382
1420	9/15/76	18.52.58	31.0	105.0	3.7	2	SZECHWAN PROV. CHINA	307
1421	9/15/76	20.59.10	37.0	139.0	4.1	2	HONSHU JAPAN	227
1422	9/16/76	1.45. 7	32.0	49.0	3.6	3	WESTERN IRAN	347
1423	9/17/76	11.11.19	44.0	151.0	4.2	2	HOKKAIDO JAPAN REG	224
1424	9/17/76	23. 7.24	33.0	59.0	4.0	2	IRAN	348
1425	9/18/76	11.48. 7	42.0	51.0	3.5	3	CASPIAN SEA	338
1426	9/18/76	19.14.59	40.0	120.0	4.7	2	NORTHEASTERN CHINA	658
1427	9/19/76	0.48.11	20.0	93.0	3.9	2	BURMA	296
1428	9/19/76	2. 1. 7	43.0	146.0	4.1	2	HOKKAIDO JAPAN REG	224
1429	9/19/76	8.46.15	39.0	143.0	3.9	3	OEC HONSHU JAPAN	229
1430	9/19/76	9.13.11	40.0	143.0	4.2	2	NEC HONSHU JAPAN	228
1431	9/19/76	13.12. 0	40.0	142.0	4.1	2	NEC HONSHU JAPAN	228
1432	9/19/76	13.15.39	40.0	142.0	3.7	3	NEC HONSHU JAPAN	228
1433	9/19/76	14.51.53	43.0	12.0	3.9	2	CENTRAL ITALY	381
1434	9/20/76	5.11.53	31.0	96.0	4.0	3	TIBET	306
1435	9/20/76	18. 9.45	40.0	29.0	2.6	3	TURKEY	366
1436	9/20/76	22.45.27	33.0	105.0	4.9	1	SZECHWAN PROV. CHINA	307
1437	9/21/76	4.49.17	40.0	29.0	2.5	3	TURKEY	366
1438	9/21/76	15. 1.15	37.0	15.0	4.8	2	SICILY	398
1439	9/22/76	0.16. 6	45.0	149.0	6.2	1	KURILE ISLANDS	221
1440	9/22/76	0.27. 3	30.0	80.0	4.3	2	TIBET-INDIA BORDER	305

TABLE A-2

DATA BASE
(PAGE 37 OF 37)

EVNO	DATE	TIME	LAT.	LONG.	MB	Q	LOCATION	SUBREG
1441	9/22/76	20. 7.14	41.0	105.0	5.6	1	NORHTERN CHINA	323
1442	9/23/76	1.25. 4	39.0	107.0	3.9	2	NORTHERN CHINA	323
1443	9/23/76	19.39.54	38.0	120.0	4.1	2	NORTHEASTERN CHINA	658
1444	9/24/76	0. 9.32	23.0	96.0	4.7	1	BURMA	296
1445	9/24/76	3.11.50	44.0	147.0	3.9	2	KURILE ISLANDS	221
1446	9/24/76	5.12.22	39.0	75.0	3.7	3	S SINKIANG PROV.	321
1447	9/24/76	8.37.24	38.0	21.0	3.1	3	IONIAN SEA	399
1448	9/24/76	9.25.29	32.0	50.0	3.7	3	WESTERN IRAN	347
1449	9/24/76	15.56.47	38.0	21.0	3.1	3	IONIAN SEA	399
1450	9/24/76	20. 3.45	38.0	21.0	2.9	3	IONIAN SEA	399
1451	9/25/76	11.50. 2	37.0	122.0	4.2	2	NORTHEASTERN CHINA	658
1452	9/26/76	12.14.32	54.0	161.0	4.5	1	NEC KAMCHATKA	218
1453	9/26/76	14.51. 5	40.0	22.0	3.3	3	GREECE	364
1454	9/26/76	16. 5.36	28.0	103.0	3.4	3	SZECHWAN PROV. CHINA	307
1455	9/27/76	0.40.33	27.0	60.0	3.9	2	SOUTHERN IRAN	353
1456	9/27/76	17. 0.53	38.0	21.0	3.2	3	IONIAN SEA	399
1457	9/27/76	20. 2.44	38.0	43.0	3.2	3	TURKEY	366
1458	9/27/76	22.55. 2	47.0	15.0	3.6	3	YUGOSLAVIA	383
1459	9/28/76	19.51.18	46.0	36.0	2.8	3	SOUTHWESTERN RUSSIA	357
1460	9/28/76	22.30.50	30.0	85.0	3.9	2	TIBET	306
1461	9/28/76	23.12.43	38.0	121.0	4.5	2	NORTHEASTERN CHINA	658
1462	9/29/76	1.52. 7	39.0	64.0	3.7	3	UZBEK SSR	339
1463	9/29/76	2.51.24	29.0	82.0	4.9	1	NEPAL	310
1464	9/29/76	2.59.57	73.0	55.0	6.0	2	NOVAYA ZEMLYA	648
1465	9/29/76	4.49.49	44.0	147.0	4.3	2	KURILE ISLANDS	221
1466	9/29/76	6.53.26	34.0	81.0	3.5	3	TIBET	306
1467	9/29/76	7.47. 8	31.0	79.0	4.6	2	TIBET-INDIA BORDER	305
1468	9/29/76	14.34. 3	36.0	74.0	4.4	2	NORTHWESTERN KASHMIR	720
1469	9/29/76	15.25.10	20.0	93.0	3.8	3	BURMA	296
1470	9/29/76	20.42.51	36.0	138.0	4.3	2	HONSHU JAPAN	227
1471	9/30/76	0.34.16	44.0	17.0	5.0	2	YUGOSLAVIA	383
1472	9/30/76	6.37.13	38.0	21.0	3.2	3	IONIAN SEA	399

APPENDIX B

INSTRUMENT-RESPONSE CORRECTED NOISE CHARACTERISTICS

In the course of the evaluation of the Seismic Research Observatory stations, instrument-response corrected noise field characteristics were studied at each station under evaluation. In this appendix to the continuation of the Seismic Research Observatories evaluation, the extension to this study is presented.

To correct the data for the effects of the instrument response, the data were first Fourier transformed to the frequency domain. Noise amplitude spectra were then computed and smoothed to 64 frequencies. The smoothing was performed to simplify the task of making the instrument response corrections. In the course of this smoothing, the spectral values were scaled so that Parseval's formula would hold. This formula, which permits the computation of RMS noise from frequency domain data, is expressed as:

$$RMS_a^b = \left[\Delta f \sum_{i=a}^{b} |A(f_i)|^2 * C(f_i)^2 \right]^{1/2} \quad \text{(frequency-domain estimate)}$$

where

Δf = the elemental frequency interval,

$|A(f_i)|^2$ = the discrete Fourier transform spectral density estimate at frequency f_i,

$C(f_i)$ = the instrument response correction at frequency f_i,

a = the initial frequency index

b = the final frequency index.

During the course of studying the noise field this year, the RMS noise values produced by this method were checked against those produced by bandpass filtering the data and computing RMS noise from the equation

$$RMS = \left[\frac{\sum_{i=1}^{n} (X_i)^2}{n} \right]^{1/2} \qquad \text{(time-domain estimate)}$$

where

n = number of data points, and

X_i = the i^{th} data point.

Since this equation does not allow for making instrument response corrections, $C(f_i)$ in Parseval's formula above was set equal to one. The RMS values so computed with Parseval's formula were found to be approximately 10 percent higher than those computed with the second equation. Therefore, before proceeding further, it was necessary to investigate the causes of this difference between the frequency-domain and time-domain estimates of RMS noise.

The algorithm used to filter the data was the first point of inquiry. The design of this filter is such that if one specifies a passband of 0.023-0.059 Hz with 0.002 taper, the corners are not at 0.023 Hz and 0.059 Hz as might be expected but are 0.02466 Hz and 0.05737 Hz. (This is illustrated by Fibure B-1.) Thus, instead of passing all energy with periods between 16.9 and 43.5 seconds as intended, the filter passes all energy with periods between 17.4 and 40.6 seconds. The difference at the shorter-period end is insignificant. At the high end, however, this difference results in more energy being added to the RMS estimate than desired.

The next stage in investigating the difference between the frequency-domain and time-domain RMS estimates was to test the two methods

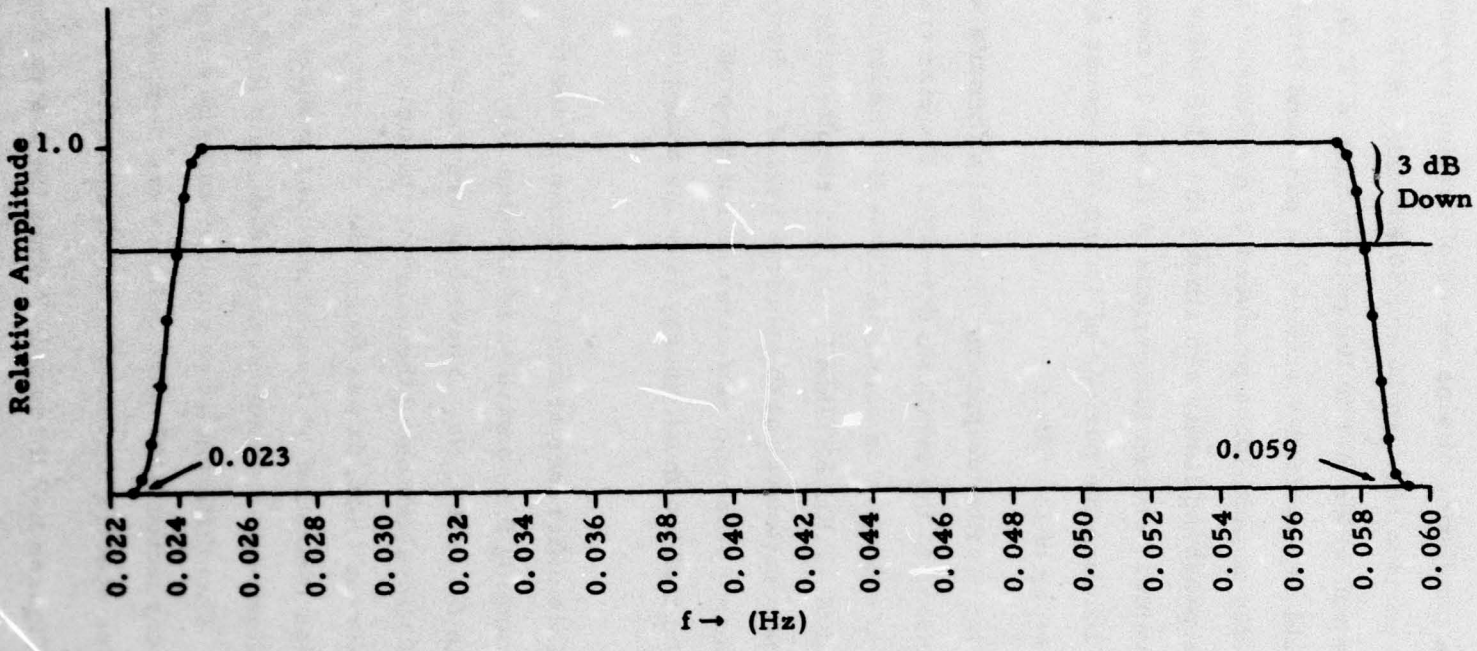

FIGURE B-1

SPECIFIED FILTER: 0.023 - 0.059 Hz with 0.002 Hz TAPER

on synthetic data consisting of sine waves of varying periods. This data was processed using periods between 10 and 50 seconds, with 1 second increments. The results shown in Table B-1 in the column headed 'T. D. ESTIMATES' are exactly what would be expected-- outside the passband limits, the small non-zero values are due to side-lobes produced by the Fourier transform. The values inside the passband limits are simply the RMS value of a sine wave. The increasing values between the periods of 16 and 18 seconds and the decreasing values between the periods of 40 and 44 seconds are due to the cosine-squared taper of the filter.

The results of applying Parseval's formula without instrument response corrections to the synthetic data after Fourier transforming and smoothing to 64 frequencies is shown in Table B-1 under the heading '64 FREQ SMOOTHING--F. D. ESTIMATE'. The results here are the same as the time-domain estimates at the shorter periods. However, at longer periods, the frequency-domain estimates do not drop off until 47 seconds period, indicating that too much energy is being added into the RMS noise estimate.

This difference at longer periods is due to the smoothing procedure. By smoothing the spectra to 64 frequencies, the energy is divided into bins of width 0.0039062 Hz. These bins are too wide to permit the frequency domain RMS values being the same as the time domain values. After some trial-and-error tests, it was found that if the spectra were smoothed to 128 frequencies instead of 64 frequencies, the frequency-domain RMS values would differ from the equivalent time-domain RMS values by less than 2 percent. This difference was considered to be acceptable, so instrument-response corrected RMS noise values were computed using Parseval's formula and noise spectra smoothed to 128 frequencies.

Figures B-2 through B-7 show the instrument-response corrected RMS noise values plotted against Julian day, while Figures B-8 through

TABLE B-1

RMS NOISE TEST
BP=0.023-0.059 WITH 0.002 TAPER
I/P=SINE WAVE WITH MAX AMP=1.0
NO INSTRUMENT RESPONSE

Period	T.D. Estimate	64 Frequency Smoothing F.D. Estimate	Period	T.D. Estimate	64 Frequency Smoothing F.D. Estimate
10	0.01	0.01	31	0.71	0.71
12	0.02	0.02	32	0.71	0.71
14	0.02	0.03	33	0.71	0.71
15	0.01	0.01	34	0.71	0.71
16	0.00	0.00	35	0.71	0.71
17	0.11	0.71	36	0.71	0.71
18	0.70	0.71	37	0.71	0.71
19	0.71	0.71	38	0.71	0.71
20	0.71	0.71	39	0.71	0.71
21	0.71	0.71	40	0.70	0.70
22	0.71	0.71	41	0.68	0.71
23	0.71	0.71	42	0.44	0.70
24	0.71	0.71	43	0.16	0.70
25	0.71	0.71	44	0.03	0.71
26	0.71	0.71	45	0.01	0.71
27	0.71	0.71	46	0.01	0.71
28	0.71	0.71	47	0.03	0.12
29	0.71	0.71	48	0.05	0.12
30	0.71	0.71	50	0.02	0.02

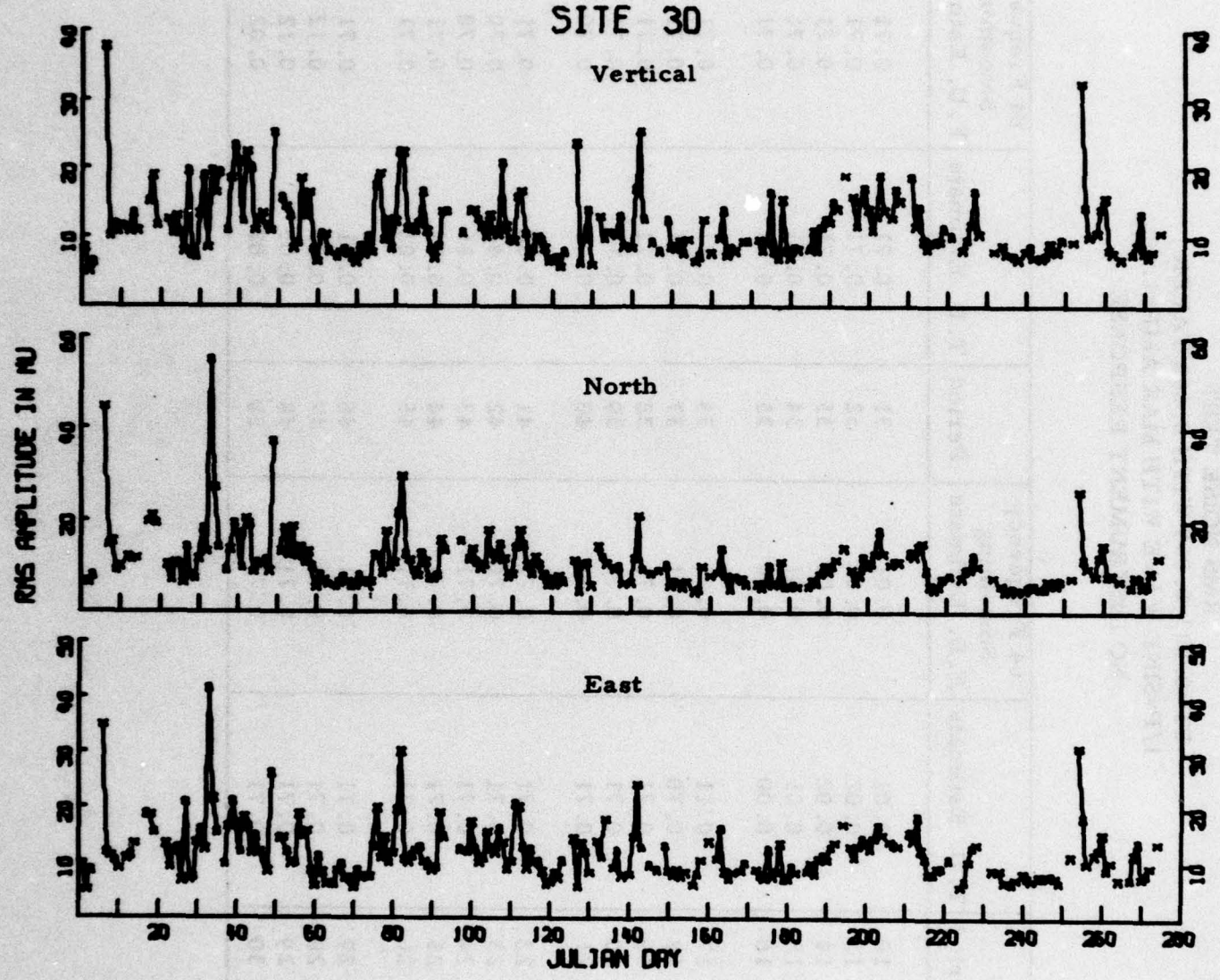

FIGURE B-2

INSTRUMENT-RESPONSE CORRECTED RMS NOISE VALUES
PLOTTED AGAINST JULIAN DAY FOR ANMO

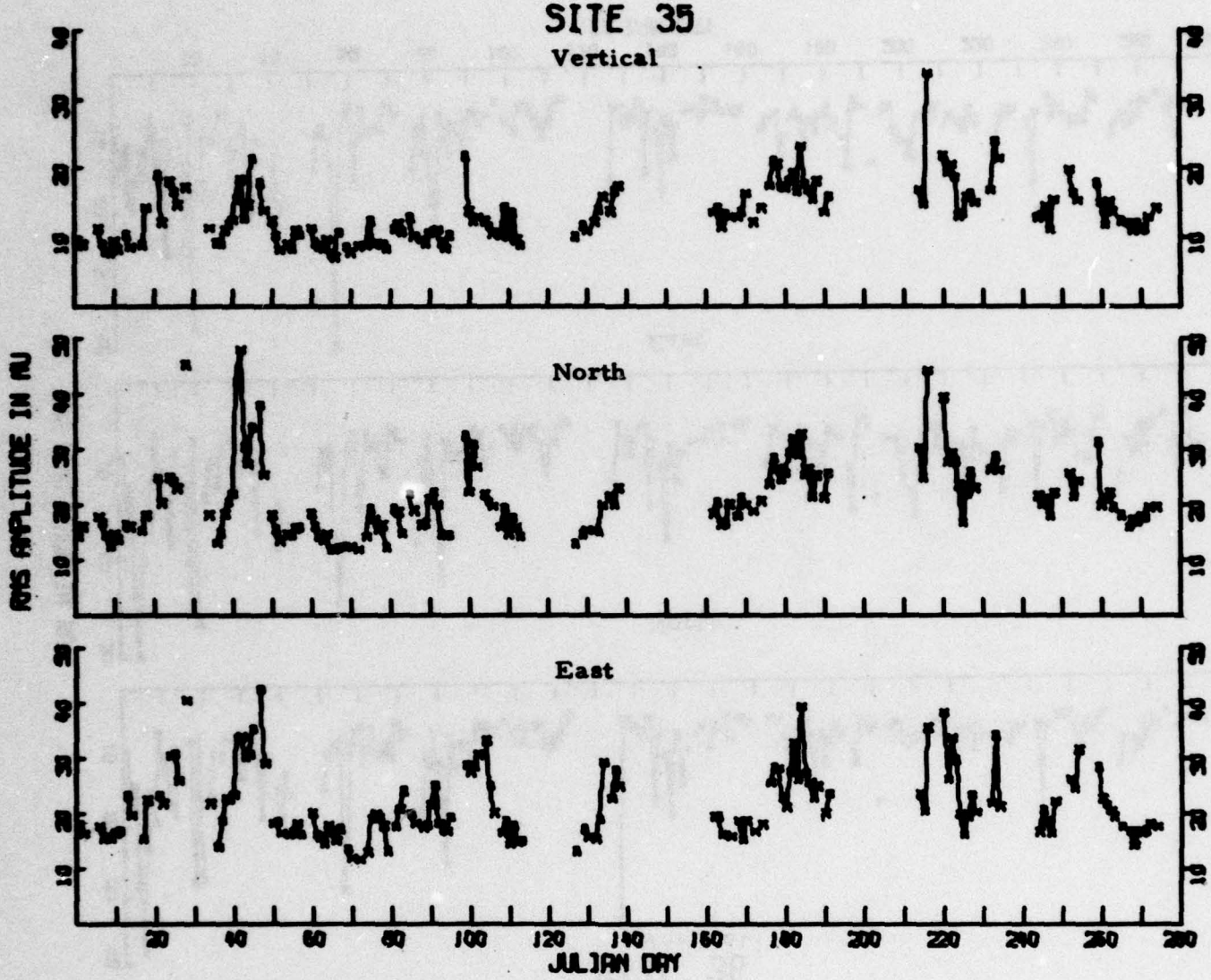

FIGURE B-3

INSTRUMENT-RESPONSE CORRECTED RMS NOISE VALUES
PLOTTED AGAINST JULIAN DAY FOR GUMO

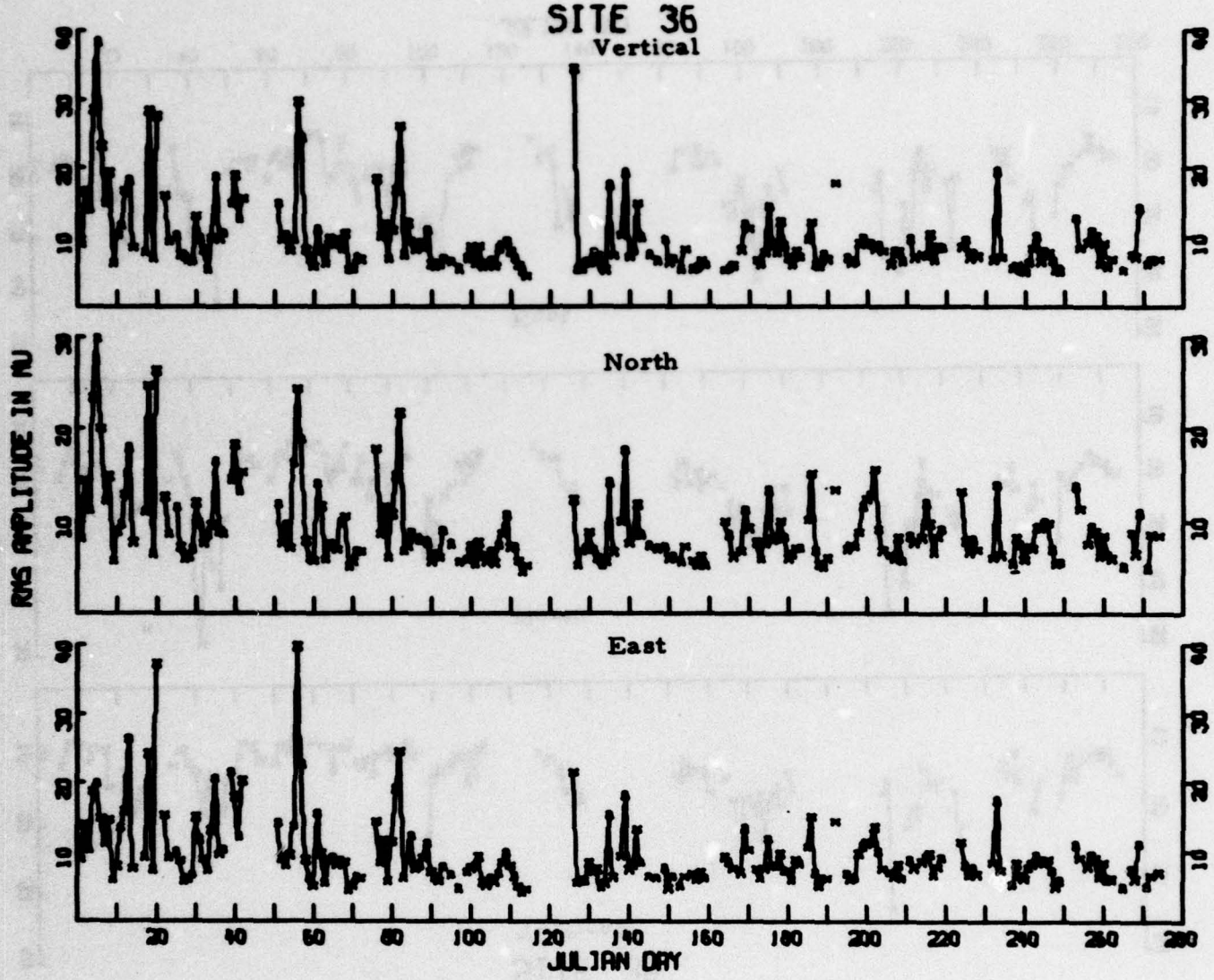

FIGURE B-4

INSTRUMENT-RESPONSE CORRECTED RMS NOISE VALUES
PLOTTED AGAINST JULIAN DAY FOR MAIO

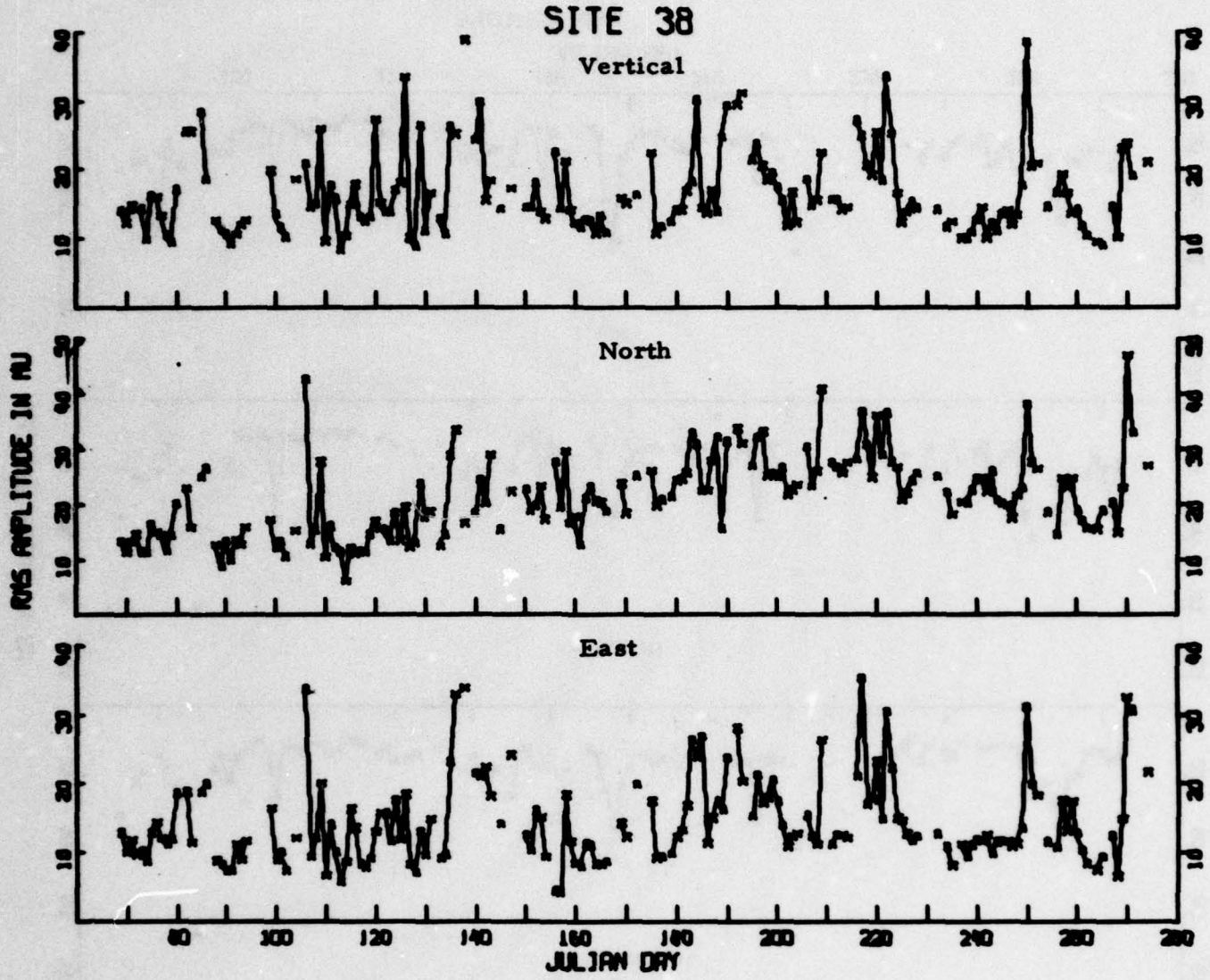

FIGURE B-5

INSTRUMENT-RESPONSE CORRECTED RMS NOISE VALUES
PLOTTED AGAINST JULIAN DAY FOR NWAO

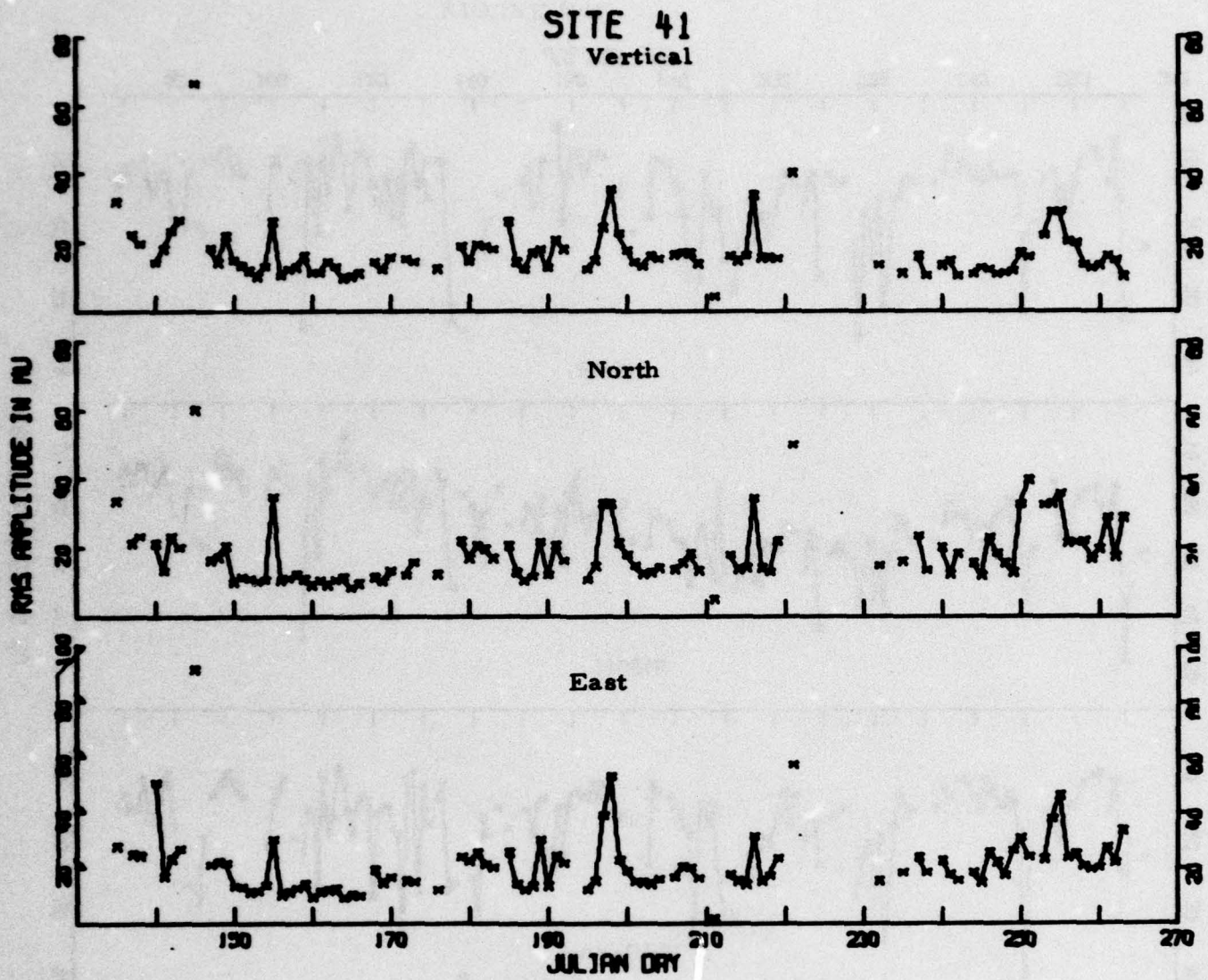

FIGURE B-6

INSTRUMENT-RESPONSE CORRECTED RMS NOISE VALUES
PLOTTED AGAINST JULIAN DAY FOR TATO

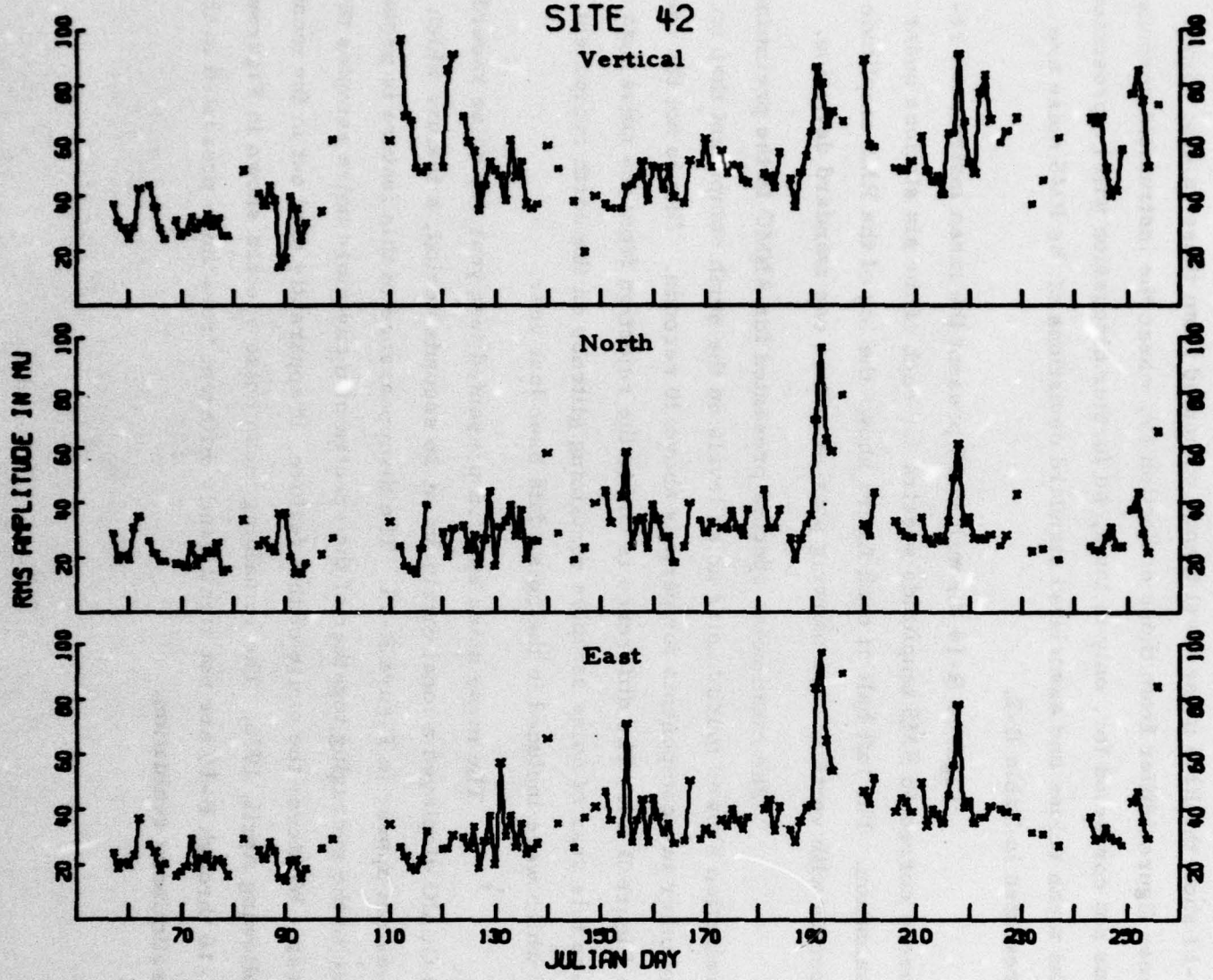

FIGURE B-7

INSTRUMENT-RESPONSE CORRECTED RMS NOISE VALUES
PLOTTED AGAINST JULIAN DAY FOR SNZO

B-13 show the RMS noise level trends computed from these values. Since these figures differ from those of Section IV, where the instrument response was not corrected for, only in level, no further discussion will be presented. The mean values and associated standard deviations of the RMS noise are presented in Table B-2.

Figures B-14 through B-19 present the mean instrument-response corrected RMS amplitude spectra for each of the six stations under evaluation. The left half of each figure shows the log of the RMS amplitude spectra with vertical bars showing plus-or-minus one standard deviation.

The mean noise spectra presented for ANMO in the preliminary evaluation showed much higher noise levels on the north component than on the other two components for periods above 30 seconds. This is not the case in Figure B-14. The difference is due to the rejection from the noise data base this year of noise samples containing glitches on the north component, some of which were included in the noise data base last year.

The mean noise spectra presented last year for noise recorded at GUMO displayed a local maximum at 26 seconds period, a feature which does not appear in Figure B-15. The disappearance of this feature is probably due to the averaging together of the spectra of many more noise samples this year. Whatever the cause of this feature, it apparently died out in the months following April, 1976. The remaining mean noise spectra shown in Figures B-16 through B-19 are not significantly different from those presented in the preliminary evaluation.

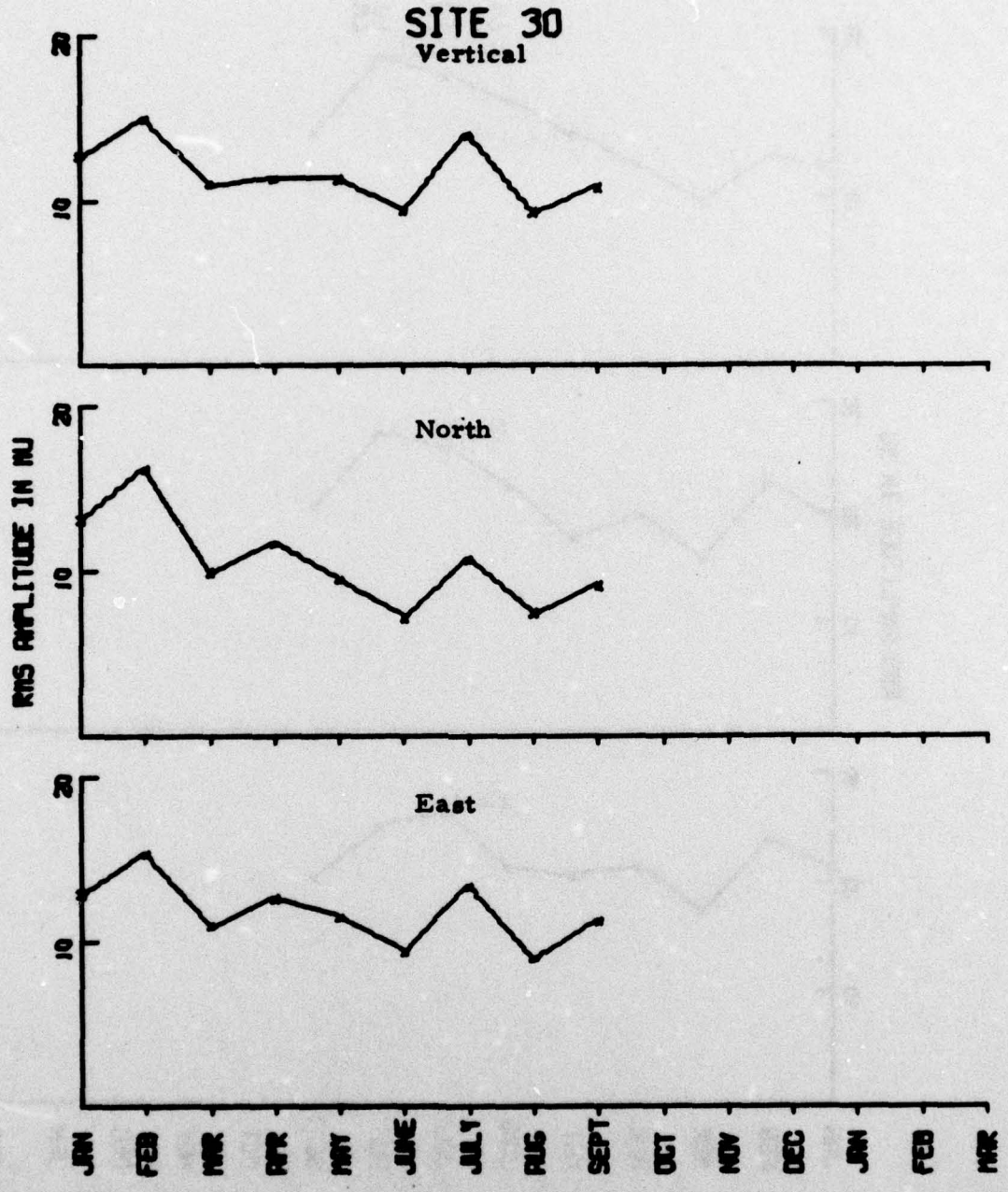

FIGURE B-8

RMS NOISE LEVEL TRENDS
PLOTTED AGAINST JULIAN DAY FOR ANMO

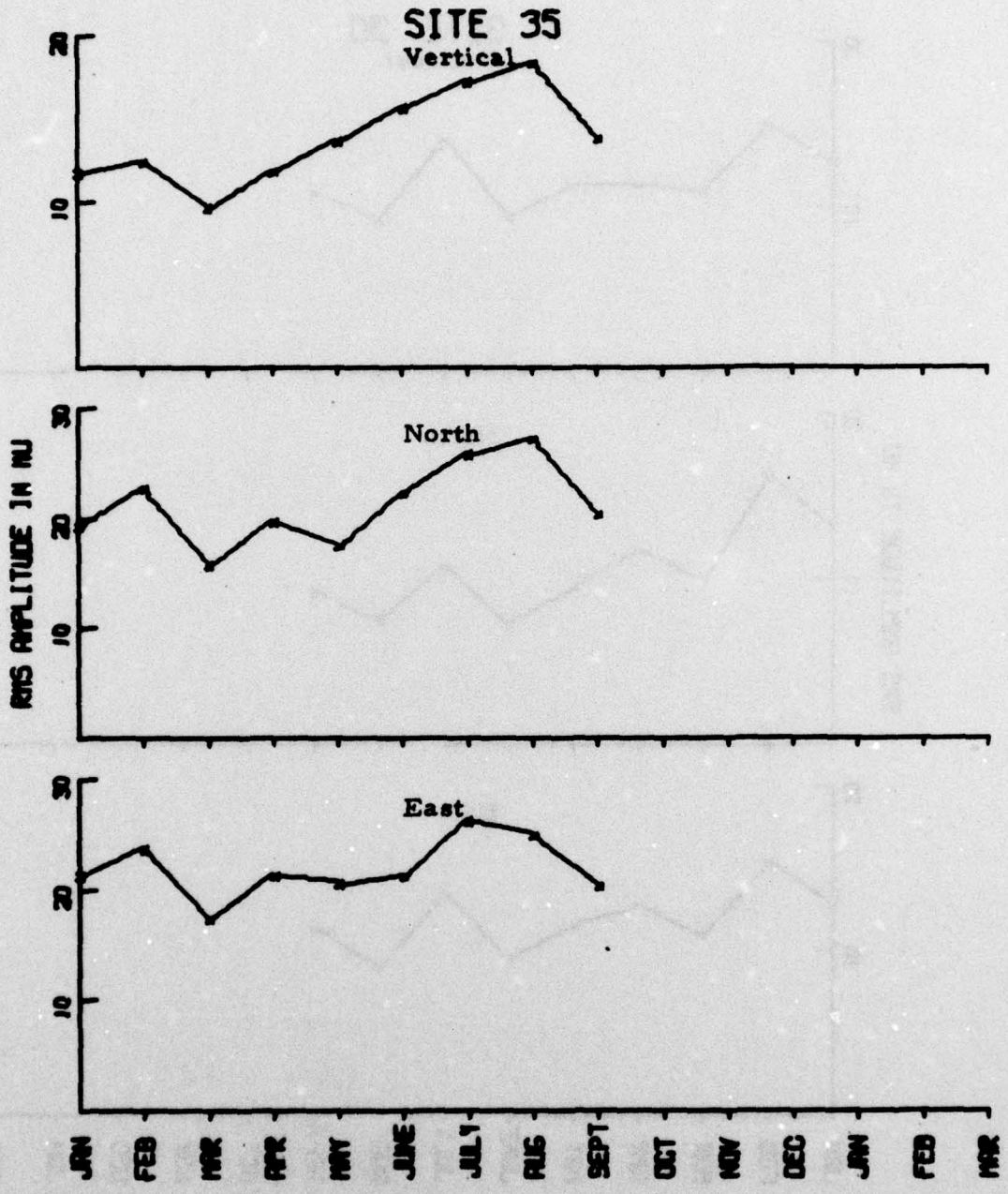

FIGURE B-9

RMS NOISE LEVEL TRENDS
PLOTTED AGAINST JULIAN DAY FOR GUMO

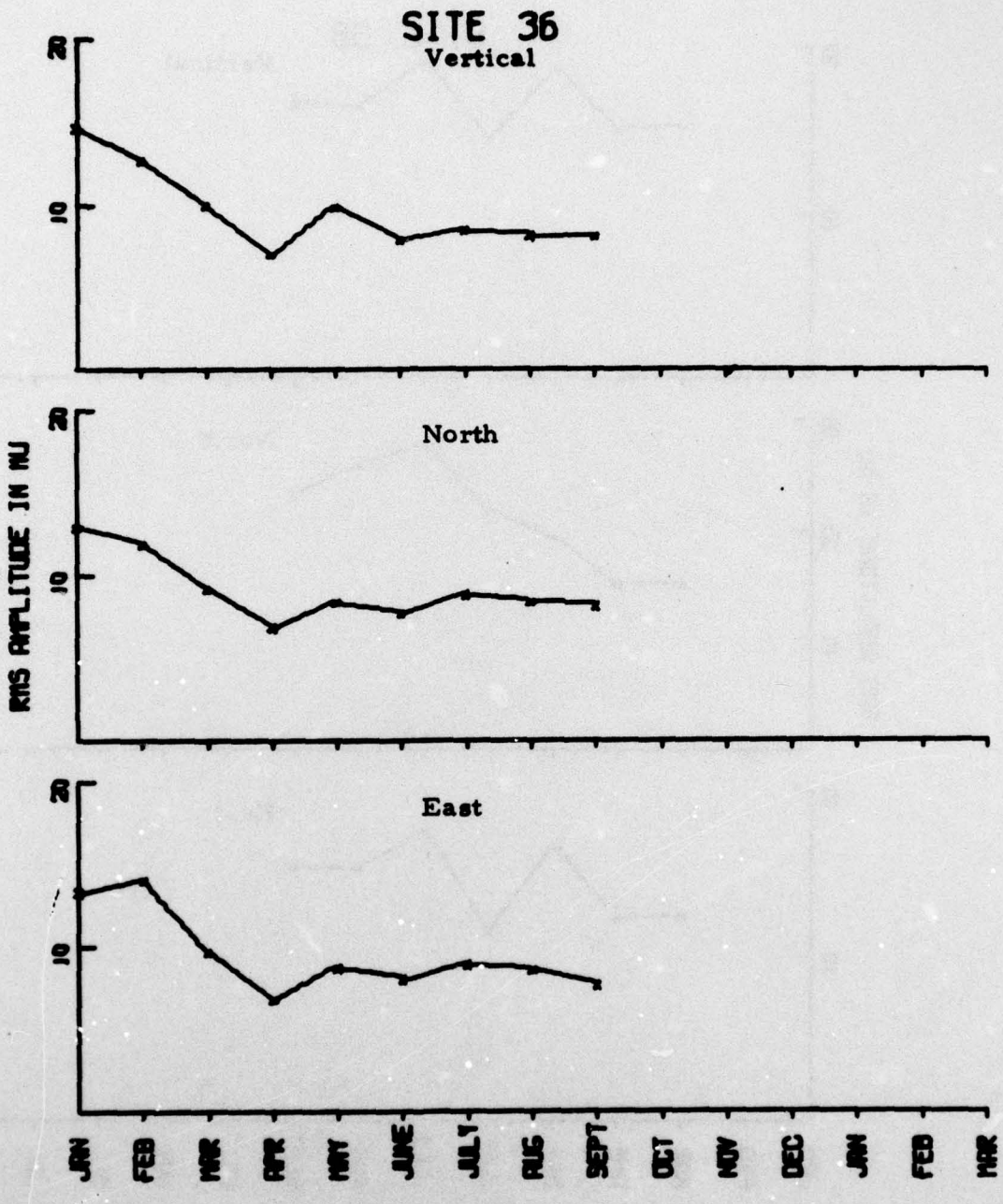

FIGURE B-10

RMS NOISE LEVEL TRENDS
PLOTTED AGAINST JULIAN DAY FOR MAIO

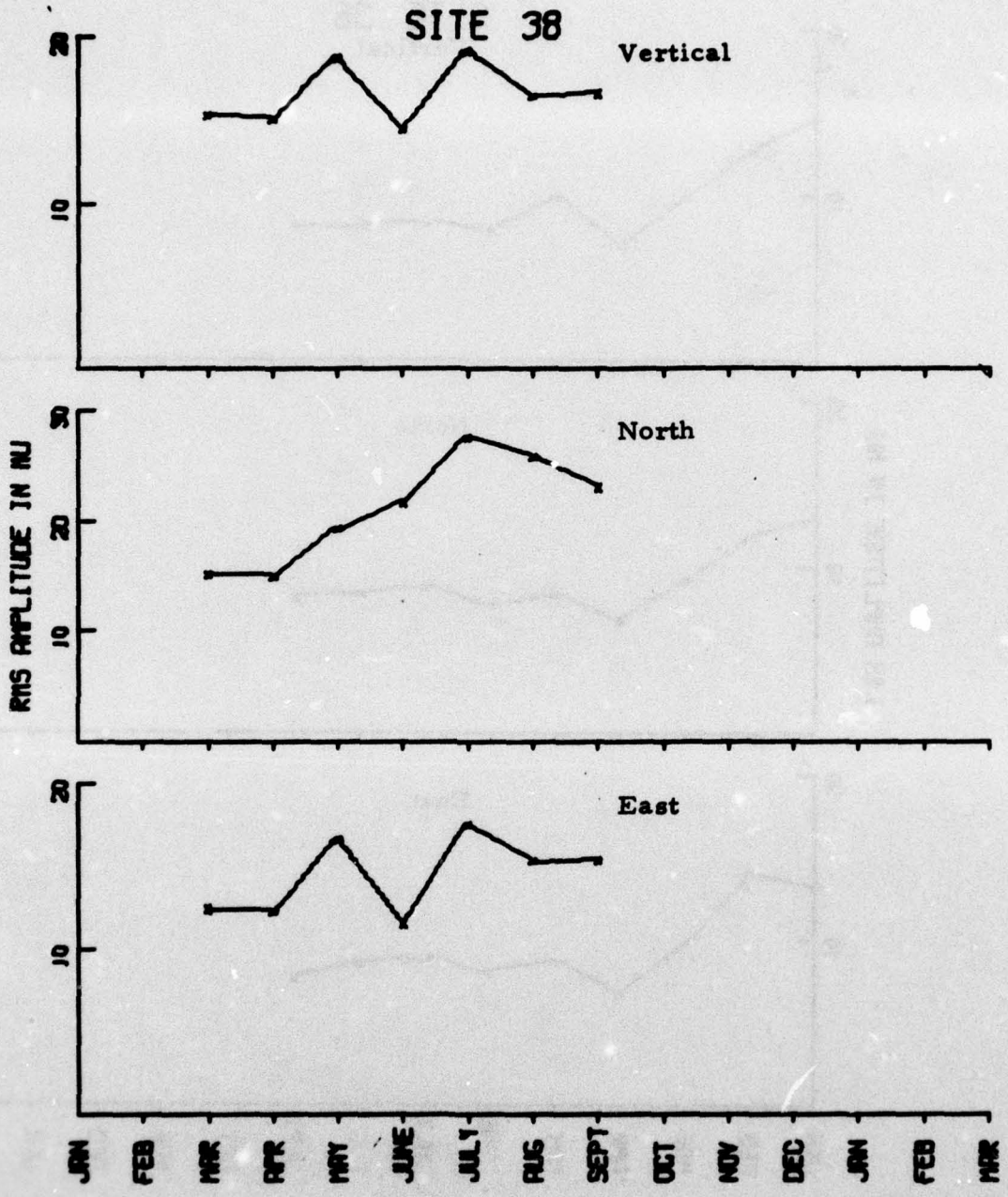

FIGURE B-11

RMS NOISE LEVEL TRENDS
PLOTTED AGAINST JULIAN DAY FOR NWAO

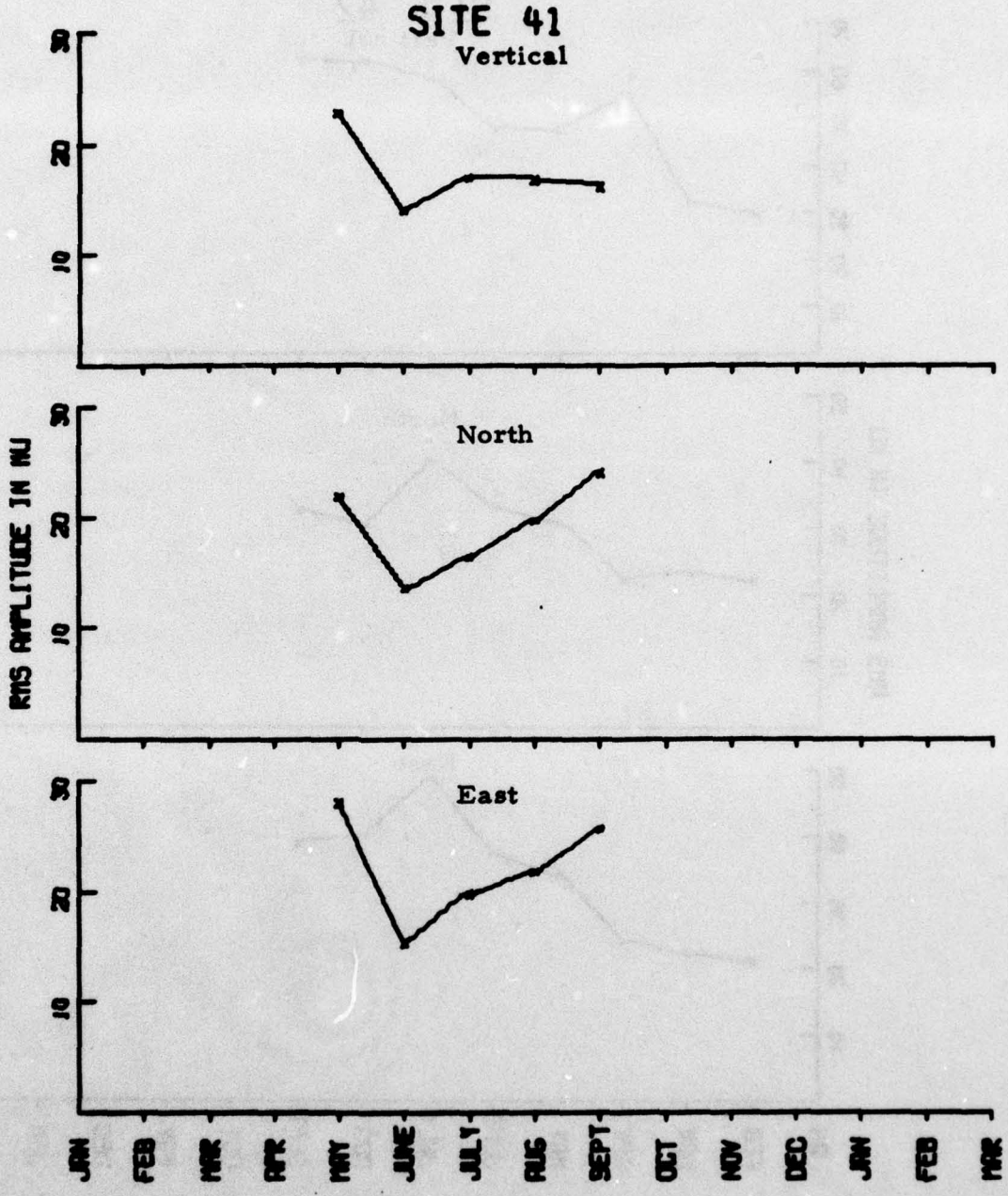

FIGURE B-12

RMS NOISE LEVEL TRENDS
PLOTTED AGAINST JULIAN DAY FOR TATO

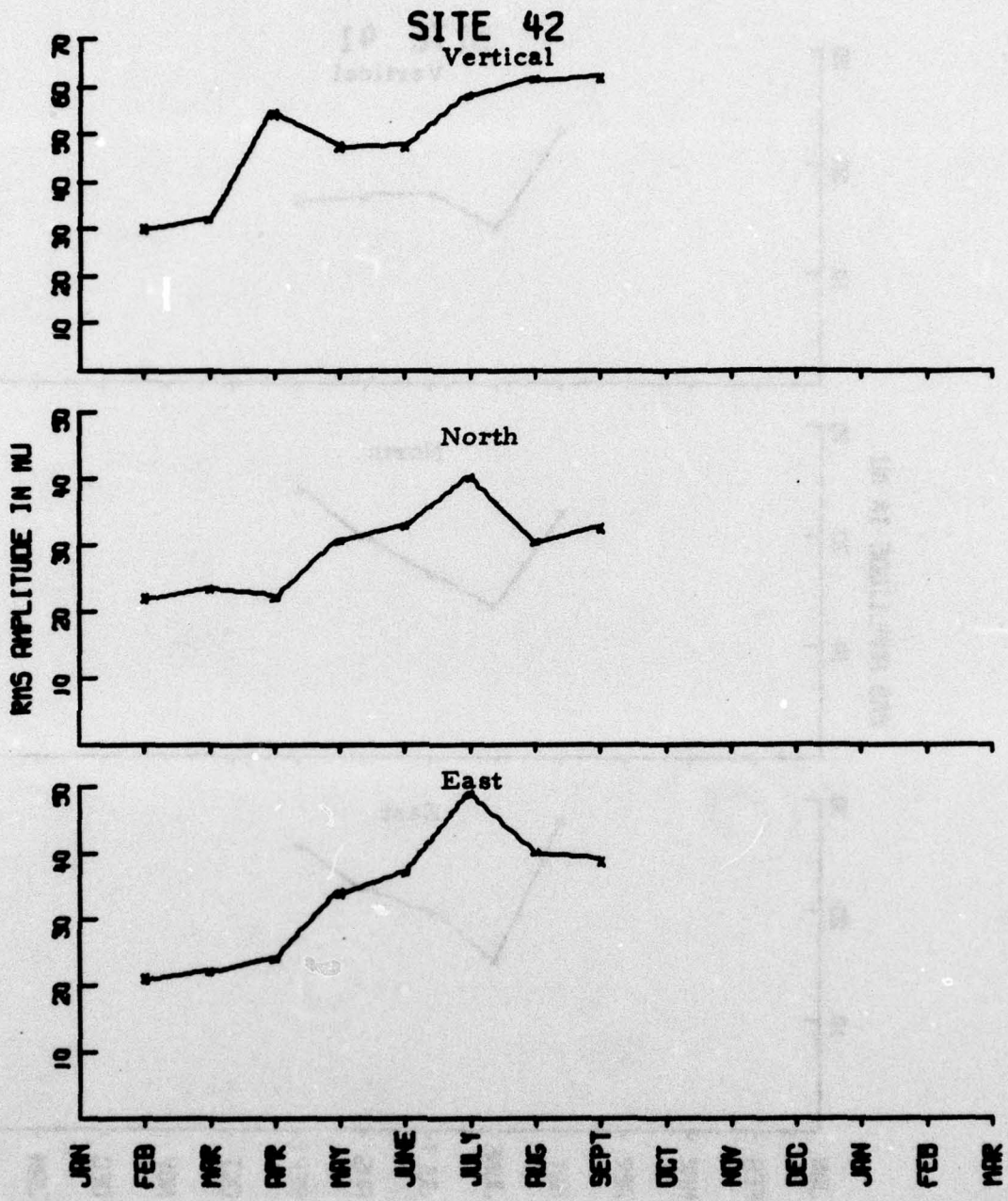

FIGURE B-13

RMS NOISE LEVEL TRENDS
PLOTTED AGAINST JULIAN DAY FOR SNZO

TABLE B-2

MEAN RMS INSTRUMENT-RESPONSE CORRECTED NOISE

Station	Mean	S.D.	Mean	S.D.	Mean	S.D.	No. Samples
ANMO	11.71	4.72	10.64	6.03	11.87	4.97	221
GUMO	13.27	4.13	20.78	6.84	21.44	6.32	151
MAIO	9.72	5.35	9.19	4.19	9.58	5.01	207
NWAO	16.63	6.00	21.31	7.28	14.56	6.25	167
TATO	16.93	7.89	18.44	9.13	21.32	11.84	95
SNZO	49.33	16.56	30.23	12.66	34.56	14.52	141

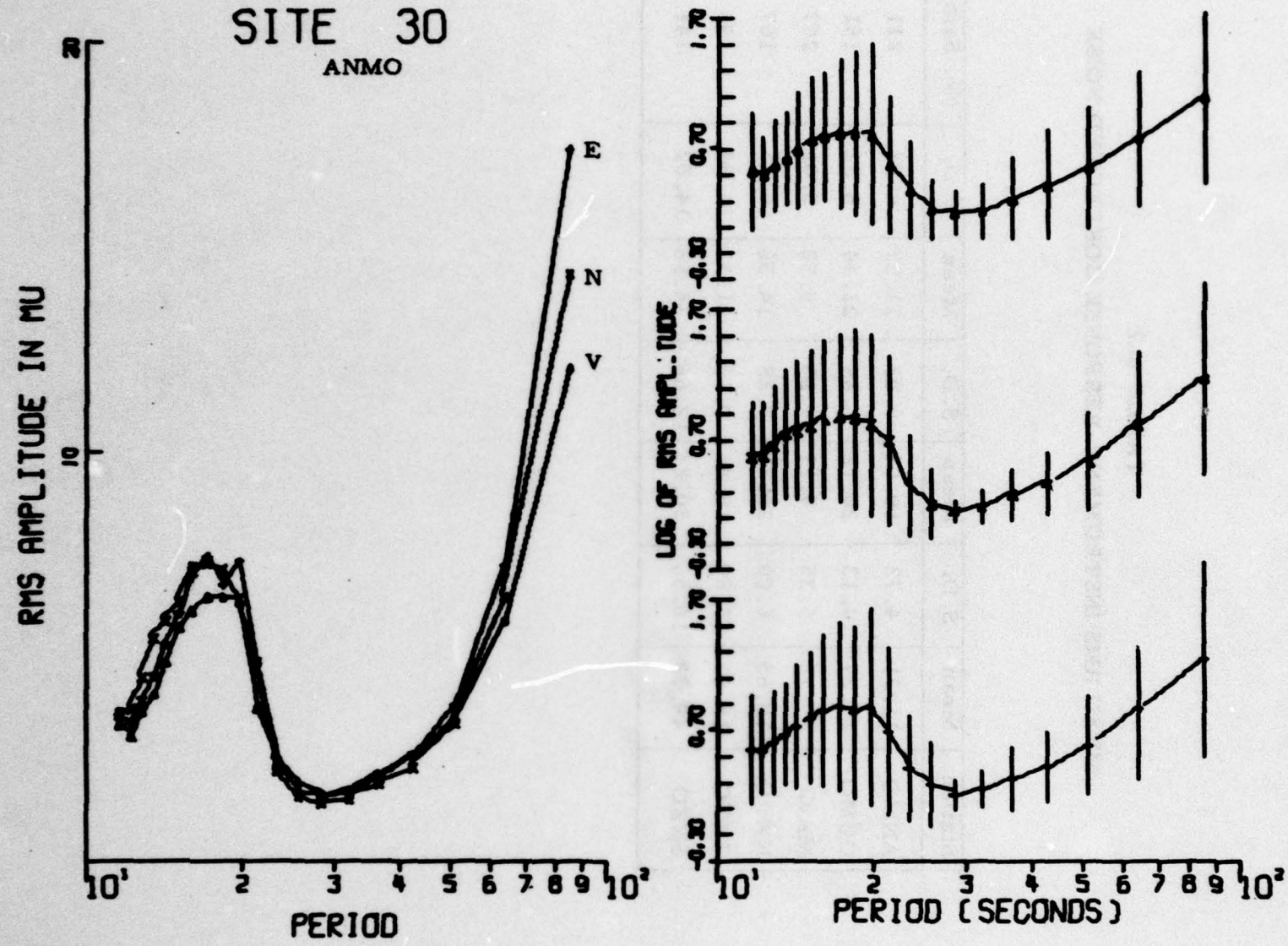

FIGURE B-14

AVERAGE RMS AMPLITUDE SPECTRA--ANMO LONG-PERIOD NOISE

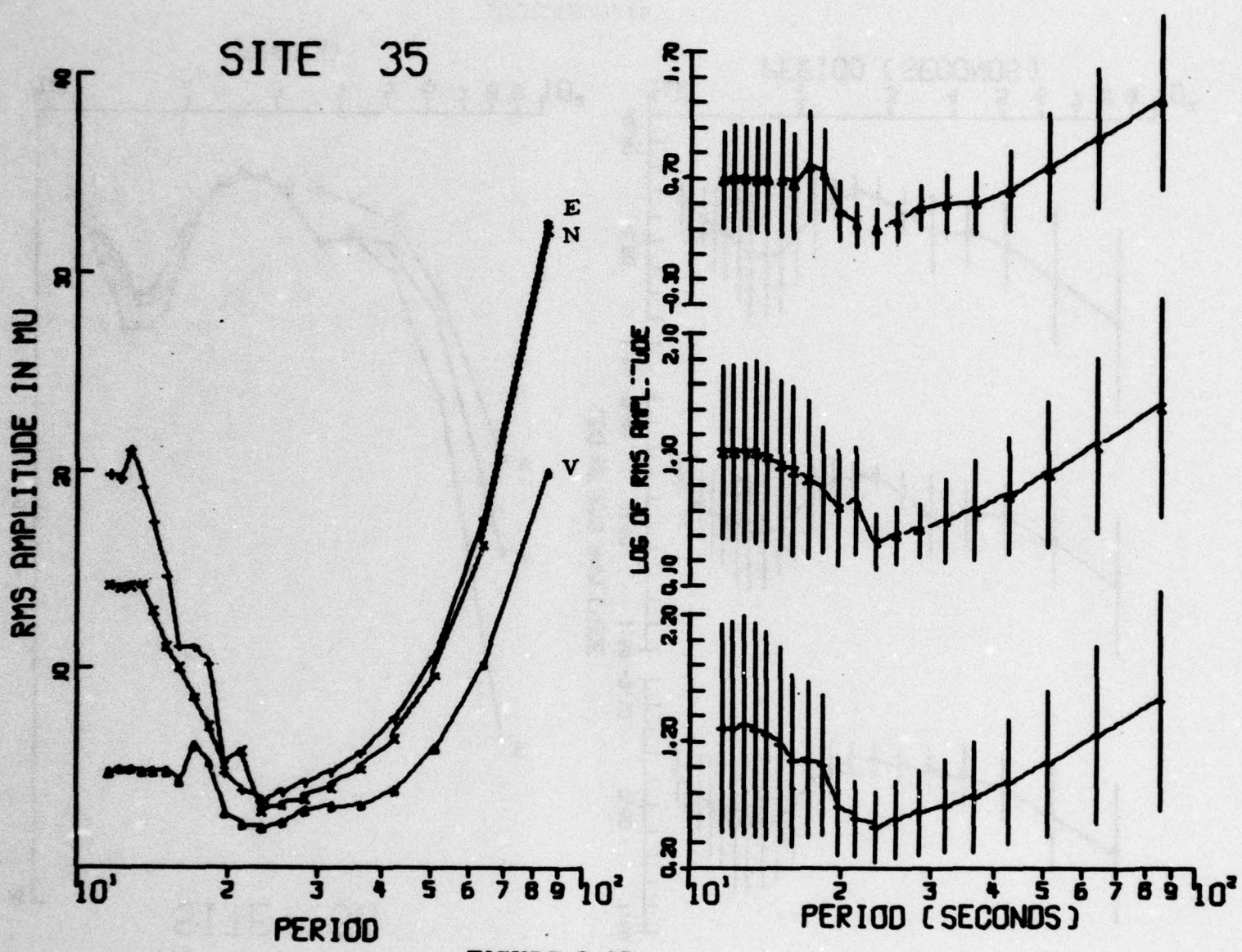

FIGURE E-15

AVERAGE RMS AMPLITUDE SPECTRA--GUMO LONG-PERIOD NOISE

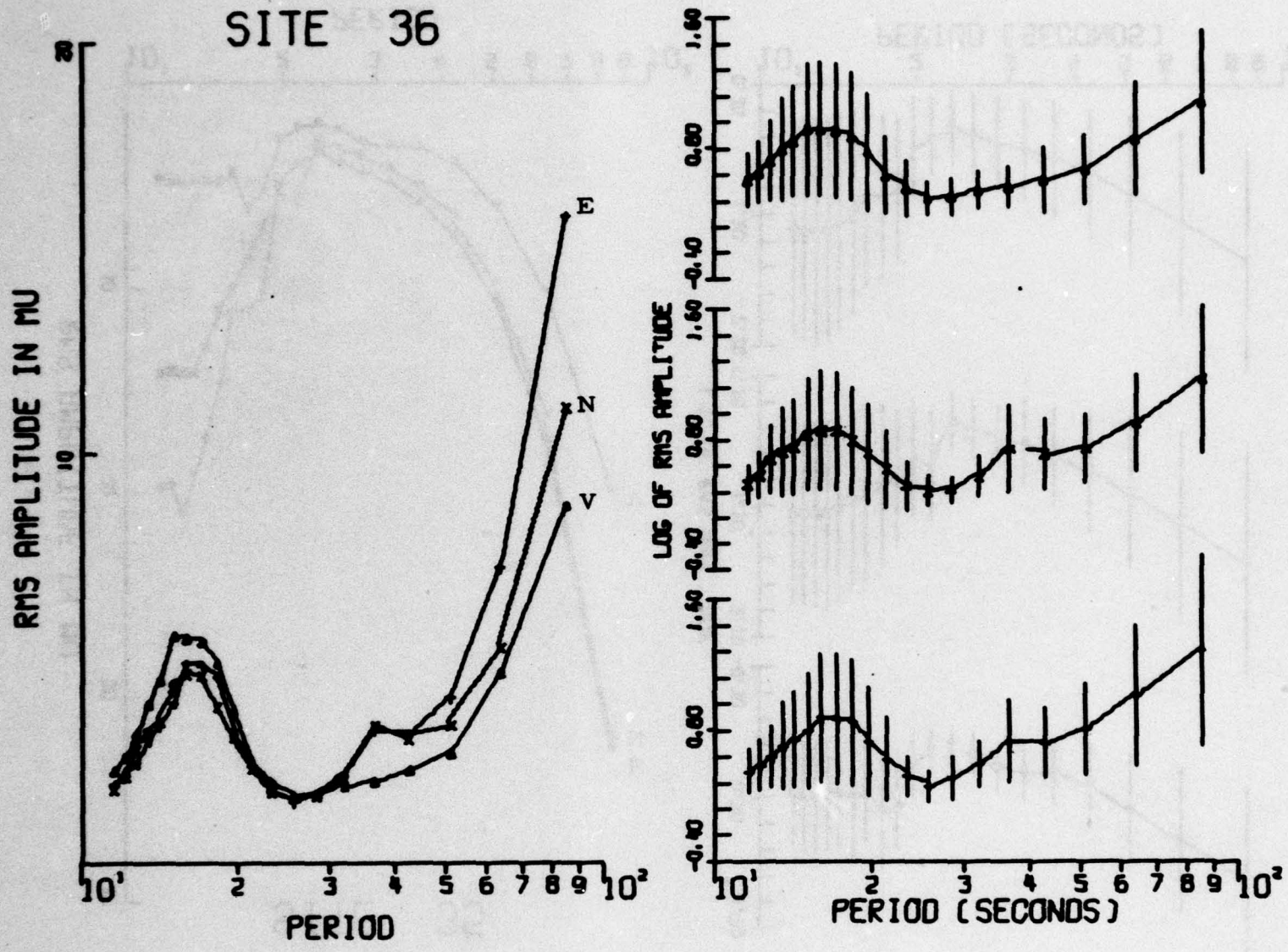

FIGURE B-16

AVERAGE RMS AMPLITUDE SPECTRA--MAIO LONG-PERIOD NOISE

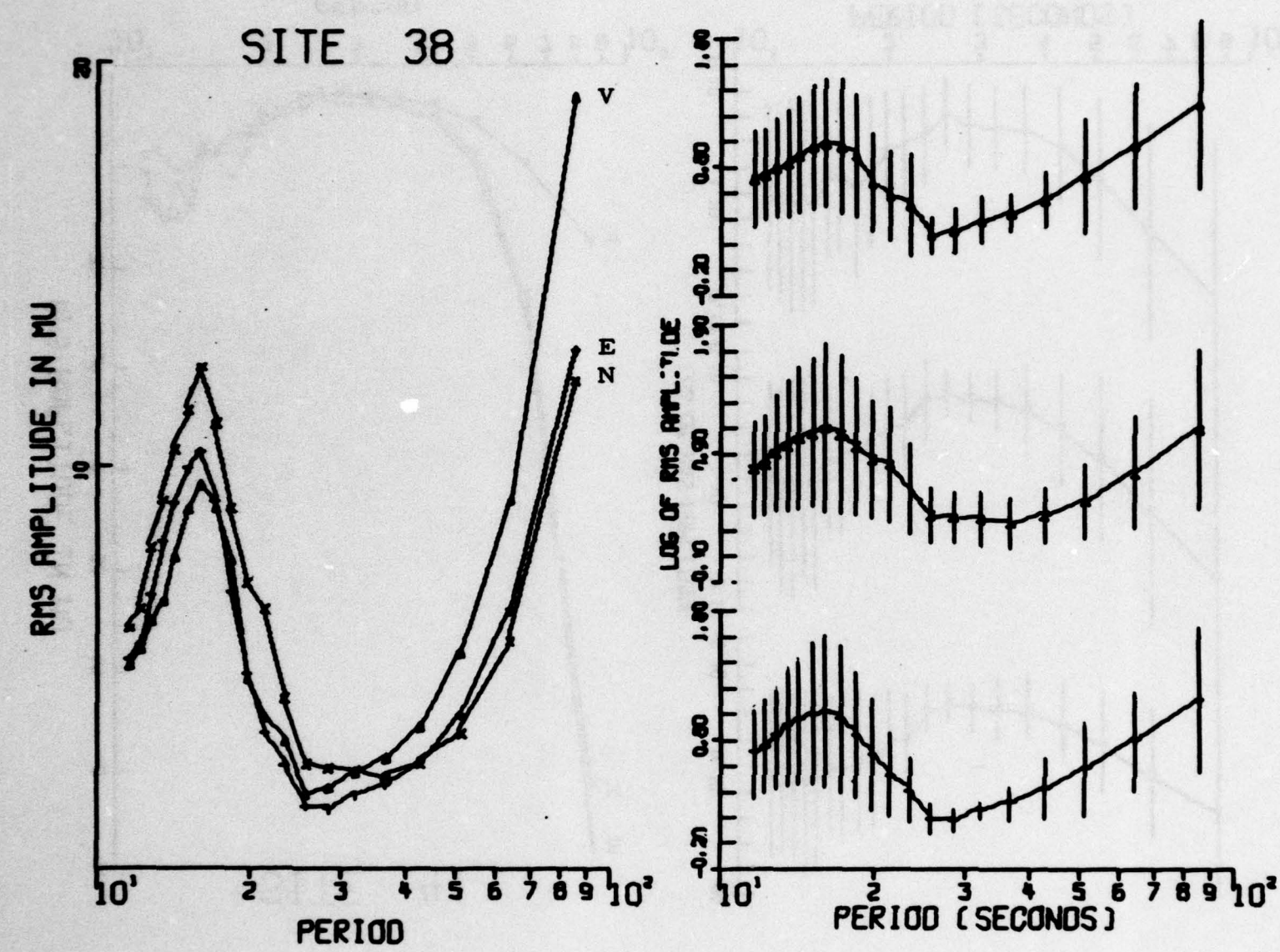

FIGURE B-17

AVERAGE RMS AMPLITUDE SPECTRA--NWAO LONG-PERIOD NOISE

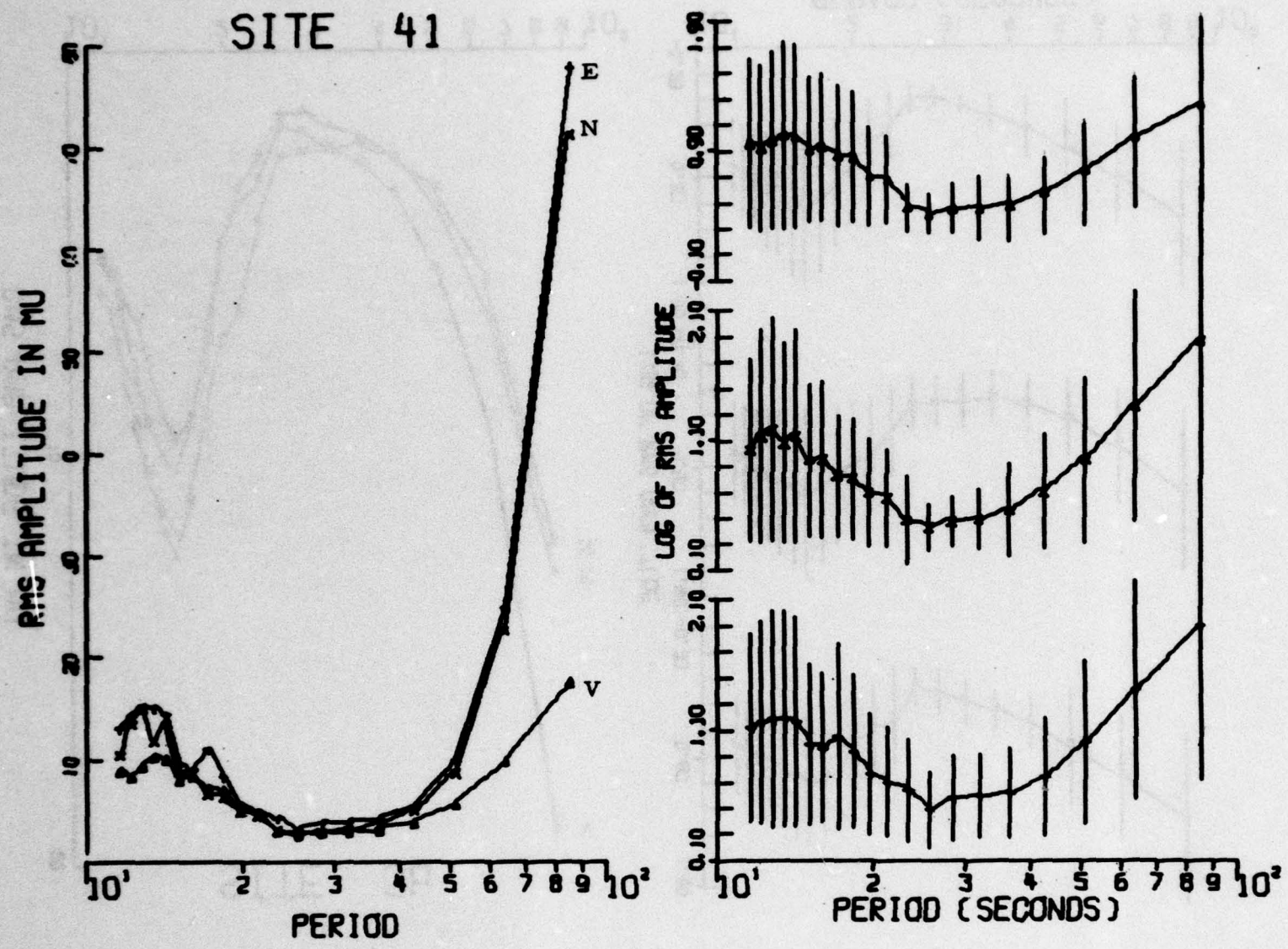

FIGURE B-18

AVERAGE RMS AMPLITUDE SPECTRA--TATO LONG-PERIOD NOISE

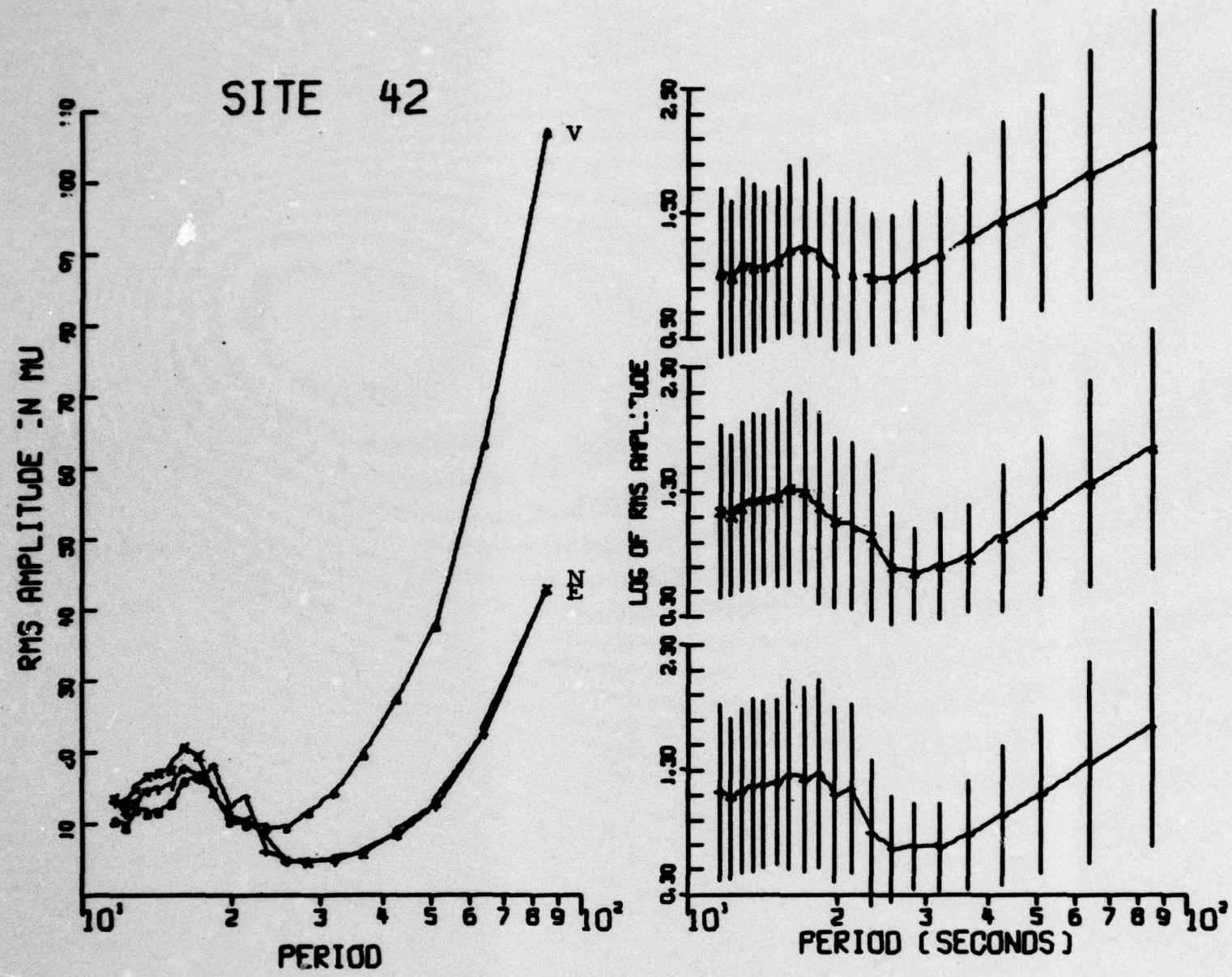

FIGURE B-19

AVERAGE RMS AMPLITUDE SPECTRA--SNZO LONG-PERIOD NOISE